

**Selective extraction of nickel(II) and copper(II) by means of
imidazole- and pyrazole-based pyridine ligands**

by

Brendan Harold Pearce

Thesis presented in fulfilment of the requirements for the degree of
Master of Science in the Faculty of Science at Stellenbosch University



Supervisor: Dr Robert C. Luckay

March 2017

Declaration

By submitting this thesis electronically, I declare that the entirety of the work contained therein is my own, original work, that I am the sole author thereof (save to the extent explicitly otherwise stated), that reproduction and publication thereof by Stellenbosch University will not infringe any third party rights and that I have not previously in its entirety or in part submitted it for obtaining any qualification.

March 2017

Copyright © 2017 Stellenbosch University

All rights reserved

Acknowledgements

Firstly, I must express my deep sense of gratitude to Dr RC Luckay. It has been a privilege and a great honour for me to have you as my supervisor. You were always more than willing to help, answer any questions I might have and challenge me to constantly deliver high-quality work. Thank you for your continued support, encouragement and all the informal chats about the Springboks and Proteas!

A special thanks should go to Hezron Ogutu (crystal structure elucidation) and the Central Analytical Facilities (CAF) at Stellenbosch University. In particular I would like to thank Riana Rossouw (ICP analyses) and Elsa Malherbe (NMR spectra) for the numerous samples I submitted to them. Special mention should also be given to the Mass Spectrometry Laboratory at the University of KwaZulu-Natal (Pietermaritzburg) for all the elemental analyses.

Without doubt, I have to thank our technical officers, Peta Steyn and Jabu Lukhele, for ensuring that we work safely and securely in a potentially dangerous environment. Thank you for maintaining impeccable safety standards and for having our best interests at heart. Thanks to all our staff members for making my studies as bump-free as possible and for quickly sourcing solvents and glassware whenever I needed them. You have spared me many a headache regarding broken glassware and faulty instruments. Thank you very much!

To my group members: you made me feel right at home from day one. Thank you for helping me out throughout my studies and for all your sound practical advice. I appreciate it very much! I would especially like to thank Gerbrandt Kotzé and Laura Leckie for their kind friendship and the countless hours we spent talking and laughing! Without you, my studies would most certainly not have been as fun!

I am deeply grateful for the financial support from the National Research Foundation's (NRF) Scarce Skills Development Fund (SSDF) and the Department of Chemistry and Polymer Science at Stellenbosch University. This study would not have been possible if it weren't for your assistance.

To my family who stood by me through every high and low: thank you for your unconditional love and support. Your timeous encouragement and kind words often lifted my spirit when I needed it most. Thank you for believing in my abilities and dreams, even when I didn't.

Lastly, I would like to thank my Heavenly Father! You have poured out innumerable blessings upon my life, none of which I ever deserved. Thank you, Daddy, for the great honour of obtaining my MSc degree *cum laude*.

Abstract

In this study, imidazolyl- and pyrazolylpyridine ligands, along with sodium dodecylbenzenesulfonate (SDBS) as synergist, was investigated as potential selective extractants of nickel(II) and copper(II) from base metal ions in a solvent extraction system.

The synthesis of the imidazolyl ligands, 2-(1*H*-imidazol-2-yl)pyridine (**1**), 2-(1-methyl-1*H*-imidazol-2-yl)pyridine (**2**), 2-(1-butyl-1*H*-imidazol-2-yl)pyridine (**3**) and 2-(1-octyl-1*H*-imidazol-2-yl)pyridine (**4**), followed the classic Debus-Radziszewski synthetic approach for imidazoles. The methylpyrazolyl ligands, 2-[(1*H*-pyrazol-1-yl)methyl]pyridine (**5**), 2-[(3,5-dimethyl-1*H*-pyrazol-1-yl)methyl]pyridine (**6**) and 2-[(3-methyl-1*H*-pyrazol-1-yl)methyl]pyridine / 2-[(5-methyl-1*H*-pyrazol-1-yl)methyl]pyridine (**7/7'**), were synthesised via simple nucleophilic substitution reactions (S_N2 mechanism), while the pyrazolyl ligands, 2-(3-butyl-1*H*-pyrazol-5-yl)pyridine (**8**), 2-[3-(*tert*-butyl)-1*H*-pyrazol-5-yl]pyridine (**9**) and 2-(3-octyl-1*H*-pyrazol-5-yl)pyridine (**10**) were obtained by the Claisen condensation of ethyl 2-picolinate with the appropriate alkyl ketones, followed by the classic Knorr synthesis for pyrazoles. Ligands **1–7/7'** were obtained in yields which ranged from 42.0–89.7%. Ligands **8–10** were obtained in particularly low yields (29.6, 26.1 and 26.3% respectively) due to the formation of unwanted side-products and the rigorous subsequent purification procedures. All ligands were characterised by ^1H and ^{13}C NMR, IR, mass spectrometry and elemental analysis.

The extraction of nickel(II) and copper(II) from borderline hard/soft metal ions; Cd^{2+} , Co^{2+} , Pb^{2+} and Zn^{2+} was carried out at $\text{pH} \approx 5$, using minute quantities of concentrated nitric acid and sodium hydroxide to adjust the pH when necessary. The optimum synergist concentration was found to be 0.05 M (5 times that of ligand and individual metal ion) after a range of optimisation studies were conducted. Nickel(II) extraction yielded results in the low to mid-70% range when ligands **1–10** were used in conjunction with SDBS, while extremely poor results were obtained in the absence of SDBS (most were $< 10\%$). Time-dependent studies were conducted to prove that extraction equilibrium was reached well before the 24-hour mark. This was followed by a comprehensive competitive extraction study using ligands **1–10**, whereby imidazolyl ligands, **1–3**, displayed significant synergistic gains for copper(II) extraction, with $32.2 (\pm 1.0)$, $35.1 (\pm 0.9)$ and $54.1 (\pm 0.9)\%$ respectively. Methylpyrazolyl ligands, **5–7/7'**, also yielded good synergistic gains of $34.1 (\pm 0.5)$, $43.2 (\pm 0.3)$ and $39.0 (\pm 0.8)\%$ respectively, while pyrazolyl ligands, **8–10**, on the other hand, had negative synergistic interactions, with copper(II) being extracted in the mid-40% range. Ligands **8** and **10**, however, exhibited impeccable copper(II) extractions in a mixed base metal ion environment, without the use of SDBS. Ligands **8** and **10** extracted $83.2 (\pm 0.6)$ and $90.2 (\pm 0.1)\%$ copper(II) respectively, with selectivity studies corroborating these findings. Metal stripping studies of ligands **8–10**, were somewhat underwhelming, with $46.7 (\pm 2.7)$, $55.0 (\pm 3.4)$ and $14.1 (\pm 1.8)\%$ copper(II) being stripped at pH 1, respectively. Ligands **8–10** were also used for nickel(II) and copper(II) pH isotherm studies, whereby the optimum extraction and stripping ranges were established. Across the board, both nickel(II) and copper(II) were optimally extracted in the 4–6 pH range, while stripping occurred at $\text{pH} < 3$.

Finally, we managed to grow single crystals of the aqua-2-[3-(*tert*-butyl)-1*H*-pyrazol-5-yl]-pyridine di(nitrato) copper(II) complex and solved the structure using single crystal X-ray diffraction. Coordination around the copper(II) centre is pseudo square pyramidal and indications are that the extraction stoichiometry is 1:1.

Opsomming

Hierdie studie stel ondersoek in aangaande die selektiewe ekstraksie van nikkell(II) en koper(II) deur middel van imidasool- en pirasoolpiridienligande in samewerking met natriumdodesielbenseensulfonaat (NDBS).

Die sintese van die imidasoolligande, 2-(1*H*-imidazol-2-iel)piridien (**1**), 2-(1-metiel-1*H*-imidazol-2-iel)piridien (**2**), 2-(1-butiel-1*H*-imidazol-2-iel)piridien (**3**) en 2-(1-oktiel-1*H*-imidazol-2-iel)piridien (**4**), was volgens die klassieke Debus-Radziszewski metode uitgevoer met goeie welslae. Die metielpirasoolligande, 2-[(1*H*-pirasol-1-iel)metiel]piridien (**5**), 2-[(3,5-dimetiel-1*H*-pirasol-1-iel)metiel]piridien (**6**) en 2-[(3-metiel-1*H*-pirasol-1-iel)metiel]piridien / 2-[(5-metiel-1*H*-pirasol-1-iel)metiel]piridien (**7/7'**), is gesintetiseer deur middel van eenvoudige nukleofiliese substitusiereaksies (S_N2 meganisme), terwyl die pirasoolligande, 2-(3-butiel-1*H*-pirasol-5-iel)piridien (**8**), 2-[3-(*ters*-butiel)-1*H*-pirasol-5-iel]piridien (**9**) en 2-(3-oktiel-1*H*-pirasol-5-iel)piridien (**10**), verkry is deur die Claisen-kondensasie van etielpiridien-2-karboksilaat met die gepaste alkielketone, gevolg deur die klassieke Knorr-pirasoolsintese. Die opbrengste van ligande **1–7/7'** het gewissel tussen 42.0 en 89.7%, terwyl die ooglopende lae opbrengste van ligande **8–10** (29.6, 26.1 en 26.3% onderskeidelik) hoofsaaklik toegeskryf kon word aan die oplewering van ongewenste neweprodukte en die gepaardgaande suiweringsprosesse. Alle ligande is suksesvol gekarakteriseer deur ^1H en ^{13}C KMR, IR, massa spektrometrie en elementele analise.

Die ekstraksie van nikkell(II) en koper(II) vanuit 'n mengsel semi-hard en -sag metaalione (Cd^{2+} , Co^{2+} , Pb^{2+} en Zn^{2+}) is by pH 5 uitgevoer, waartydens gekonsentreerde salpetersuur en natriumhidroksied met tye in klein maat gebruik is om die pH te reguleer. Die optimale sinergiskonsentrasie van 0.05 M (5 keer meer as die ligand en individuele metaalione) is aanvanklik bepaal en deurgaans as sulks gebruik. Nikkell(II)-ekstraksiestudies het goeie ekstraksieresultate opgelewer (70–78%) wanneer ligande **1–10** in die teenwoordigheid van NDBS gebruik is, terwyl beroerde resultate in die afwesigheid van NDBS verkry is (< 10%). Derhalwelik, is tydafhanklike studies ook uitgevoer om te verseker dat ekstraksie-ekwilibrium bereik is binne die 24-uurmerk. Dit was opgevolg deur 'n omvattende mededingende-ekstraksiestudies deur gebruik te maak van ligande **1–10**, waarbenewens imidasoolligande, **1–3**, duidelike sinergiswinste vir koper(II)-ekstraksies getoon het (32.2 ± 1.0 , 35.1 ± 0.9 en $54.1 \pm 0.9\%$ onderskeidelik). Die metielpirasoolligande, **5–7/7'**, het op sigself ook goeie sinergiswinste van $34.1 (\pm 0.5)$, $43.2 (\pm 0.3)$ en $39.0 (\pm 0.8)\%$ getoon, terwyl pirasoolligande, **8–10**, negatiewe sinergistiese interaksies tydens koper(II)-ekstraksies opgelewer het (40–50%). Aan die ander kant, het ligande **8** en **10** uitstekende koper(II)-ekstraksieresultate opgelewer in die afwesigheid van NDBS. Hierdie twee ligande het koper(II) teen $83.2 (\pm 0.6)$ en $90.2 (\pm 0.1)\%$ geëkstraheer, waarbenewens die selektiwiteitsstudies ook hierdie bevindinge gestaaf het. Ligande **8–10** is ondermeer ook gebruik vir metaalstropingsstudies by pH 1, maar ietwat teleurstellende resultate is verkry vanaf die koper(II)-stropingstudies (46.7 ± 2.7 , 55.0 ± 3.4 en $14.1 \pm 1.8\%$). Verder, was ligande **8–10** ook vir pH-isotermstudies gebruik, waartydens die optimale pH-gebiede vir ekstraksies en stropings bepaal is. Daar was bevind dat bykans alle nikkell(II)- en koper(II)-ekstraksies optimaal gefunksioneer het by pH 4–6, terwyl stroping optimaal by pH < 3 gefunksioneer het.

Die kristal- en molekulêre struktuur van akwa-2-[3-(*ters*-butiel)-1*H*-pirasol-5-iel]piridien di(nitrato) koper(II) is verkry deur middel van enkelkristal-X-straaldiffraksie-ontleding. Hiermee het ons bepaal dat 'n pseudo vierkantig-piramidale kompleks gevorm is, met sekere trigonaal-bipiramidale eienskappe. Die mees belangrikste brokkie inligting wat hieruit verkry is, was die feit dat ligand **9** en die koper(II)-ioon in 'n 1:1 stoigiometrieuse verhouding verkeer het.

Table of contents

Declaration	i		
Acknowledgements	ii		
Abstract	iii		
Opsomming	v		
Table of contents	vii		
List of tables	xii		
List of figures	xiii		
List of schemes	xviii		
List of abbreviations	xx		
Chapter 1: Introduction			
1.1	Historic overview of extractive metallurgy	1	
1.2	General introduction to nickel	2	
	1.2.1	Nickel properties and applications	2
	1.2.2	Sources of nickel	3
1.3	Hydrometallurgical routes for the separation of base metals	3	
	1.3.1	Crystallisation	4
	1.3.2	Ionic precipitation	4
	1.3.3	Electrochemical reduction	5
	1.3.4	Reduction with gas	5
	1.3.5	Carbon adsorption	5
	1.3.6	Ion exchange	6
	1.3.7	Electrolytic process	6
	1.3.8	Solvent extraction (also known as liquid-liquid extraction)	7
1.4	Types of extractants	9	
	1.4.1	Cationic extractants (acidic)	9
	1.4.2	Anionic extractants (basic)	11
			vii

1.4.3	Solvating extractants (neutral)	13
1.4.4	Additives in solvent extraction systems	14
1.4.5	Synergistic extraction	15
1.5	Ligand-metal compatibility	16
1.5.1	Donor atoms	16
1.6	Chelating ligands	19
1.6.1	The chelate effect	19
1.6.2	The standard reference state and the chelate effect	20
1.7	Metal ion selectivity of nitrogen donor atoms	22
1.7.1	The chelate ring geometry and preferred metal ion sizes	22
1.8	Steric and inductive effects in nitrogenous chelating ligands	24
1.9	Concluding factors to consider in ligand design	25
1.10	Pyridinyl imidazole and -pyrazole background	25
1.10.1	Relevant literature on pyridinyl imidazole and -pyrazole ligands	26
1.11	Aims of this study	26
1.11.1	Additional objectives	27
1.12	References	28
 Chapter 2: Synthesis and characterisation of imidazole- and pyrazole-based pyridine ligands		
2.1	Introduction	32
2.2	Materials and methods	33
2.2.1	Chemicals and reagents	33
2.2.2	Instrumentation	34
2.3	Experimental	35
2.3.1	Synthesis of 2-(1 <i>H</i> -imidazol-2-yl)pyridine (1)	35
2.3.2	Synthesis of 2-(1-methyl-imidazol-2-yl)pyridine (2)	37

2.3.3	Synthesis of 2-(1-butyl-imidazol-2-yl)pyridine (3)	37
2.3.4	Synthesis of 2-(1-octyl-imidazol-2-yl)pyridine (4)	38
2.3.5	Synthesis of 2-(1'-pyrazolyl)-methylpyridine (5)	39
2.3.6	Synthesis of 2-(3,5-dimethyl-pyrazol-1-yl)-methylpyridine (6)	40
2.3.7	Synthesis of an isomeric mixture of 2-(3-methyl-pyrazol-1-yl)-methylpyridine (7) and 2-(5-methyl-pyrazol-1-yl)-methylpyridine (7')	41
2.3.8	Synthesis of 2-(3-butyl-pyrazol-5-yl)pyridine (8)	42
2.3.9	Synthesis of 2-[3-(<i>tert</i> -butyl)-pyrazol-5-yl]pyridine (9)	43
2.3.10	Synthesis of 2-(3-octyl-pyrazol-5-yl)pyridine (10)	44
2.4	Results and discussion	45
2.5	Conclusions	63
2.6	References	64

Chapter 3: Solvent extraction of nickel(II) and copper(II) by means of imidazole- and pyrazole-based pyridine ligands

3.1	Introduction	66
3.1.1	Synergism	66
3.2	Materials and methods	69
3.2.1	Chemicals and reagents	69
3.2.2	Instrumentation	70
3.2.3	Preparation of acidic and basic solutions	70
3.2.4	Solvent extraction procedure and conditions	70
3.3	Results and discussion	71
3.3.1	Determining the optimum synergist concentration for nickel(II) extractions	72
3.3.2	Solvent extraction of nickel(II)	75
3.3.3	Time-dependent extraction study of nickel(II)	78
3.3.4	Competitive extraction studies	80
3.3.5	Selectivity studies	89

3.3.6	Metal stripping studies	91
3.3.7	Time-dependent extraction study of copper(II)	93
3.3.8	pH isotherm studies	93
3.3.9	Possible theory as to what mechanistic role the synergist plays	95
3.3.10	Unsuccessful attempt to explain the role of the synergist	97
3.4	Conclusions	97
3.5	References	99

Chapter 4: Crystal and molecular structure of aqua[2-[3-(*tert*-butyl)-pyrazol-5-yl]pyridine] dinitrato copper(II)

4.1	Introduction	102
4.2	Materials and methods	103
4.2.1	Chemicals and reagents	103
4.2.2	Techniques for growing quality crystals	103
4.2.3	Instrumentation and determination of crystal structure	104
4.2.4	Preparation of the crystalline $[\text{Cu}(\text{H}_2\text{O})(\text{C}_{12}\text{H}_{15}\text{N}_3)(\text{NO}_3)_2]$ complex	105
4.3	Results and discussion	105
4.3.1	Crystal and molecular structure of the $[\text{Cu}(\text{H}_2\text{O})(\text{C}_{12}\text{H}_{15}\text{N}_3)(\text{NO}_3)_2]$ complex	105
4.4	Conclusions	112
4.5	References	113

Chapter 5: Chapter summaries, concluding remarks and future work

5.1	Chapter summaries and concluding remarks	114
5.2	Future work	115
5.2.1	Structural modifications to enhance metal ion extractability	115
5.2.2	Modifications to the solvent extraction setup	116
5.2.3	Extraction of nickel(II) and copper(II) using imidazolyl- and pyrazolyl ligands on resin, silica-based and nanofibrous polymeric supports	117

5.2.4	Computational modelling methods	117
5.3	References	118

List of tables

Chapter 1

Table 1.1	Commercial cationic (acidic) extractants and their uses in industry.	10
Table 1.2	Commercial anionic (basic) extractants and their uses in industry.	12
Table 1.3	Commercial solvating (neutral) extractants and their uses in industry.	14
Table 1.4	List of common diluents for extractants.	14
Table 1.5	List of commonly used modifiers in industry.	15
Table 1.6	The hard and soft acids (metal ions) proposed by Pearson.	17
Table 1.7	The hard soft organic (non-metal) bases proposed by Pearson and Songstad.	17
Table 1.8	The formation constants of polyamine Ni(II) complexes compared with analogous ammonia complexes.	19
Table 1.9	A comparison of the observed formation constant, $\log K_1$, with the calculated formation constant derived from Equations 31 and 32 . Equation 31 only considers the asymmetry of the standard state, while Equation 32 corrects for inductive effects.	21
Table 1.10	Various ethylenediamine examples where steric effects outweigh inductive effects.	24
Table 1.11	Examples of <i>N</i> -alkyl ligands where inductive effects outweigh steric effects.	24

Chapter 2

Table 2.1	List of chemicals used.	33
------------------	-------------------------	----

Chapter 3

Table 3.1	Extraction of nickel by dinonylnaphthalene sulfonic acid.	68
Table 3.2	List of chemicals used.	69

Chapter 4

Table 4.1	Selected bond lengths and angles for the $[\text{Cu}(\text{H}_2\text{O})(\text{C}_{12}\text{H}_{15}\text{N}_3)(\text{NO}_3)_2]$ complex.	108
Table 4.2	Detailed information regarding the symmetry elements and operators of the crystal structure of the $[\text{Cu}(\text{H}_2\text{O})(\text{C}_{12}\text{H}_{15}\text{N}_3)(\text{NO}_3)_2]$ complex.	110
Table 4.3	Crystallographic data and structure refinement of the $[\text{Cu}(\text{H}_2\text{O})(\text{C}_{12}\text{H}_{15}\text{N}_3)(\text{NO}_3)_2]$ complex.	112

List of figures

Chapter 1

Figure 1.1	The solvent extraction process incorporated into a hydrometallurgical process.	4
Figure 1.2	A schematic representation of the solvent extraction process. The organic layer is depicted at the bottom of the container. This, however, is dependent on the density of the organic solvent used.	7
Figure 1.3	The hard/soft acid base trend of non-metals.	17
Figure 1.4	A diagram illustrating the Schwarzenbach ¹ model of the chelate effect where the chelating ligand (ethylenediamine) is constrained to move in a sphere, whose radius is prescribed by the length of the bridge connecting the two donor atoms.	20
Figure 1.5	Cyclohexane in its chair conformation. Additionally, the bite sizes of five- and six-membered chelate rings are shown.	22
Figure 1.6	The ideal bond angles and bond lengths of a) six-membered (1,3-diaminopropane) and b) five-membered (ethylenediamine) chelate rings.	23
Figure 1.7	The ideal bond angles and bond lengths of a) six-membered (1,3-propanediol) and b) five-membered (1,2-ethanediol) chelate rings.	23
Figure 1.8	Chemical structures of aromatic amines along with their respective pK _a values: a) pyridine, b) imidazole and c) pyrazole.	26

Chapter 2

Figure 2.1	A schematic summary of ligands 1–10 .	33
Figure 2.2	A zoomed in ¹ H NMR spectrum of 2-(1 <i>H</i> -imidazol-2-yl)pyridine (1), that highlights the singlet at 7.17 ppm of protons <i>H9</i> and <i>H10</i> .	47
Figure 2.3	A zoomed in ¹³ C NMR spectrum of 2-(1 <i>H</i> -imidazol-2-yl)pyridine (1), indicating the broad signal of carbons <i>C9</i> and <i>C10</i> .	47
Figure 2.4	A zoomed in ¹ H NMR of 2-(1-methyl-imidazol-2-yl)pyridine (2) clearly showing two distinct signals for protons <i>H9</i> and <i>H10</i> .	49
Figure 2.5	A zoomed in ¹³ C NMR of 2-(1-methyl-imidazol-2-yl)pyridine (2) clearly showing two distinct signals for carbons <i>C9</i> and <i>C10</i> .	50
Figure 2.6	Zoomed in ¹ H NMR spectra of the alkylated ligands: (a) 2-(1-methyl-imidazol-2-yl)pyridine (2); (b) 2-(1-butyl-imidazol-2-yl)pyridine (3) and (c) 2-(1-octyl-imidazol-2-yl)pyridine (4).	51
Figure 2.7	The ¹ H NMR of 2-(1'-pyrazolyl)-methylpyridine (5).	54
Figure 2.8	The ¹ H NMR of 2-(3,5-dimethyl-pyrazol-1-yl)-methylpyridine (6).	54
Figure 2.9	A zoomed in ¹ H NMR of 2-(3-methyl-pyrazol-1-yl)-methylpyridine (7) and 2-(5-methyl-pyrazol-1-yl)-methylpyridine (7').	57

Figure 2.10	¹ H NMR of the alkyl region of isomers 2-(3-methyl-pyrazol-1-yl)-methylpyridine (7) and 2-(5-methyl-pyrazol-1-yl)-methylpyridine (7').	57
Figure 2.11	A zoomed in ¹³ C NMR of the downfield region of isomers 2-(3-methyl-pyrazol-1-yl)-methylpyridine (7) and 2-(5-methyl-pyrazol-1-yl)-methylpyridine (7').	58
Figure 2.12	A zoomed in ¹³ C NMR of the upfield region of isomers 2-(3-methyl-pyrazol-1-yl)-methylpyridine (7) and 2-(5-methyl-pyrazol-1-yl)-methylpyridine (7').	58
Figure 2.13	The ¹ H NMR spectrum of 2-(3-butyl-pyrazol-5-yl)pyridine (8).	61
Figure 2.14	The ¹ H NMR spectrum of 2-[3-(<i>tert</i> -butyl)-pyrazol-5-yl]pyridine (9).	62
Figure 2.15	The ¹ H NMR spectrum of 2-(3-octyl-pyrazol-5-yl)pyridine (10).	62

Chapter 3

Figure 3.1	The neutral complex [UO ₂ (DEHPA) ₂ (TBP) ₂]. This complex is extremely hydrophobic due to the alkyl chains present on the periphery. This forces the complex to be insoluble in the aqueous phase and highly soluble in the organic phase.	67
Figure 3.2	Schematic representation of sulfonic acid extractants: a) DNNSA, b) DDNSA and c) DEHSS.	68
Figure 3.3	The synergist used in this study – sodium dodecylbenzenesulfonate.	69
Figure 3.4	General scheme of the solvent extraction procedure.	71
Figure 3.5	Percentage extraction of nickel(II) using varying concentrations of synergist (SDBS).	72
Figure 3.6	An example of a reversed SDBS micelle in a non-polar organic solvent.	73
Figure 3.7	Percentage extraction of nickel(II) using 2-(1-octyl-imidazol-2-yl)pyridine (4) and varying concentrations of synergist (SDBS).	73
Figure 3.8	Percentage extraction of nickel(II) using 2-(1'-pyrazolyl)-methylpyridine (5) and varying concentrations of synergist (SDBS).	74
Figure 3.9	Percentage extraction of nickel(II) using 2-(3-butyl-pyrazol-5-yl)pyridine (8) and varying concentrations of synergist (SDBS).	74
Figure 3.10	A comparison of the percentage extraction of nickel(II) using 2-(1 <i>H</i> -imidazol-2-yl)pyridine (1), 2-(1-methyl-imidazol-2-yl)pyridine (2), 2-(1-butyl-imidazol-2-yl)pyridine (3) and 2-(1-octyl-imidazol-2-yl)pyridine (4).	75
Figure 3.11	A comparison of the percentage extraction of nickel(II) using 2-(1'-pyrazolyl)-methylpyridine (5), 2-(3,5-dimethyl-pyrazol-1-yl)-methylpyridine (6), 2-(3-methyl-pyrazol-1-yl)-methylpyridine / 2-(5-methyl-pyrazol-1-yl)-methylpyridine (7/7').	76

Figure 3.12	A comparison of the percentage extraction of nickel(II) using 2-(3-butyl-pyrazol-5-yl)pyridine (8), 2-[3-(<i>tert</i> -butyl)-pyrazol-5-yl]pyridine (9) and 2-(3-octyl-pyrazol-5-yl)pyridine (10).	77
Figure 3.13	Percentage extraction of nickel(II) over a 24-hour period using 2-(1-octyl-imidazol-2-yl)pyridine (4) and SDBS.	79
Figure 3.14	Percentage extraction of nickel(II) over a 24-hour period using 2-(1'-pyrazolyl)-methylpyridine (5) and SDBS.	79
Figure 3.15	Percentage extraction of nickel(II) over a 24-hour period using 2-(3-butyl-pyrazol-5-yl)pyridine (8) and SDBS.	80
Figure 3.16	Competitive extraction of base metal ions in the presence of the synergist, sodium dodecylbenzenesulfonate (SDBS).	81
Figure 3.17	Varying colours of the aqueous (top layers) and organic phases (bottom layers) during competitive extraction studies using a) ligand 1 , b) ligand 2 , c) ligand 3 and d) ligand 4 .	82
Figure 3.18	Competitive extraction of various base metal ions using 2-(1 <i>H</i> -imidazol-2-yl)pyridine (1), both in the presence and absence of SDBS.	82
Figure 3.19	Competitive extraction of various base metal ions using 2-(1-methyl-imidazol-2-yl)pyridine (2), both in the presence and absence of SDBS.	83
Figure 3.20	Competitive extraction of various base metal ions using 2-(1-butyl-imidazol-2-yl)pyridine (3), both in the presence and absence of SDBS.	83
Figure 3.21	Competitive extraction of various base metal ions using 2-(1-octyl-imidazol-2-yl)pyridine (4), both in the presence and absence of SDBS.	84
Figure 3.22	Varying colours of the aqueous (top layers) and organic phases (bottom layers) during competitive extraction studies using a) ligand 5 , b) ligand 6 and c) ligand 7/7' .	85
Figure 3.23	Competitive extraction of various base metal ions using 2-(1'-pyrazolyl)-methylpyridine (5), both in the presence and absence of SDBS.	85
Figure 3.24	Competitive extraction of various base metal ions using 2-(3,5-dimethyl-pyrazol-1-yl)-methylpyridine (6), both in the presence and absence of SDBS.	86
Figure 3.25	Competitive extraction of various base metal ions using 2-(3-methyl-pyrazol-1-yl)-methylpyridine / 2-(5-methyl-pyrazol-1-yl)-methylpyridine (7/7'), both in the presence and absence of SDBS.	86
Figure 3.26	Varying colours of the aqueous (top layers) and organic phases (bottom layers) during competitive extraction studies using a) ligand 8 , b) ligand 9 and c) ligand 10 .	88
Figure 3.27	Competitive extraction of various base metal ions using 2-(3-butyl-pyrazol-5-yl)pyridine (8), both in the presence and absence of SDBS.	88

Figure 3.28	Competitive extraction of various base metal ions using 2-[3-(<i>tert</i> -butyl)-pyrazol-5-yl]pyridine (9), both in the presence and absence of SDBS.	89
Figure 3.29	Competitive extraction of various base metal ions using 2-(3-octyl-pyrazol-5-yl)pyridine (10), both in the presence and absence of SDBS.	89
Figure 3.30	Copper selectivity study using 2-(3-butyl-pyrazol-5-yl)pyridine (8), 2-[3-(<i>tert</i> -butyl)-pyrazol-5-yl]pyridine (9) and 2-(3-octyl-pyrazol-5-yl)pyridine (10). Copper concentration was decreased tenfold.	90
Figure 3.31	Copper selectivity study using 2-(3-butyl-pyrazol-5-yl)pyridine (8), 2-[3-(<i>tert</i> -butyl)-pyrazol-5-yl]pyridine (9) and 2-(3-octyl-pyrazol-5-yl)pyridine (10). Copper concentration was decreased hundredfold.	91
Figure 3.32	Percentage copper(II) and nickel(II) stripped from 2-(3-butyl-pyrazol-5-yl)pyridine (8), 2-[3-(<i>tert</i> -butyl)-pyrazol-5-yl]pyridine (9) and 2-(3-octyl-pyrazol-5-yl)pyridine (10) at pH \approx 1.	92
Figure 3.33	Percentage extraction of copper(II) over a 24-hour period using 2-(3-butyl-pyrazol-5-yl)pyridine (8), 2-[3-(<i>tert</i> -butyl)-pyrazol-5-yl]pyridine (9) and 2-(3-octyl-pyrazol-5-yl)pyridine (10).	93
Figure 3.34	pH isotherm graph: the percentage extraction of nickel(II) over an acidic pH range (0–7), using 2-(3-butyl-pyrazol-5-yl)pyridine (8), 2-[3-(<i>tert</i> -butyl)-pyrazol-5-yl]pyridine (9) and 2-(3-octyl-pyrazol-5-yl)pyridine (10).	94
Figure 3.35	pH isotherm graph: the percentage extraction of copper(II) over an acidic pH range (0–7), using 2-(3-butyl-pyrazol-5-yl)pyridine (8), 2-[3-(<i>tert</i> -butyl)-pyrazol-5-yl]pyridine (9) and 2-(3-octyl-pyrazol-5-yl)pyridine (10).	95
Figure 3.36	Sodium dodecylbenzenesulfonate (SDBS) micelle containing a nickel-rich aqueous core, with ligands (L) concentrated on its hydrophobic periphery.	96

Chapter 4

Figure 4.1	Schematic diagram representing various crystal growth techniques: a) slow evaporation b) slow cooling c) vapour diffusion and d) liquid-liquid diffusion methods.	104
Figure 4.2	Asymmetric unit cell diagram of the $[\text{Cu}(\text{H}_2\text{O})(\text{C}_{12}\text{H}_{15}\text{N}_3)(\text{NO}_3)_2]$ complex (50% thermal ellipsoids).	107
Figure 4.3	ORTEP diagram of the $[\text{Cu}(\text{H}_2\text{O})(\text{C}_{12}\text{H}_{15}\text{N}_3)(\text{NO}_3)_2]$ complex. Hydrogen atoms have been omitted the sake for clarity (50% thermal ellipsoids).	107
Figure 4.4	The bond lengths and angles of the five-membered chelate ring for a) $[\text{Cu}(\text{H}_2\text{O})(\text{C}_{12}\text{H}_{15}\text{N}_3)(\text{NO}_3)_2]$ compared to the idealised bond lengths and angles of b) ethylenediamine.	108
Figure 4.5	Symmetry elements present in an asymmetric unit cell along the a-axis.	109

Figure 4.6	ORTEP diagram of the $[\text{Cu}(\text{H}_2\text{O})(\text{C}_{12}\text{H}_{15}\text{N}_3)(\text{NO}_3)_2]$ complex (50% thermal ellipsoids) showing a network of hydrogen bonds.	110
Figure 4.7	The packing diagram of the $[\text{Cu}(\text{H}_2\text{O})(\text{C}_{12}\text{H}_{15}\text{N}_3)(\text{NO}_3)_2]$ complex (50% thermal ellipsoids) along the a-axis.	111
Figure 4.8	The packing diagram of the $[\text{Cu}(\text{H}_2\text{O})(\text{C}_{12}\text{H}_{15}\text{N}_3)(\text{NO}_3)_2]$ complex (50% thermal ellipsoids) along the b-axis.	111

List of schemes

Chapter 1

Scheme 1.1	The complexation reaction of copper(II) with a hydroxyoxime reagent.	18
-------------------	--	----

Chapter 2

Scheme 2.1	Synthetic route to 2-(1 <i>H</i> -imidazol-2-yl)pyridine (1).	35
Scheme 2.2	Synthetic route to 2-(1-methyl-imidazol-2-yl)pyridine (2).	37
Scheme 2.3	Synthetic route to 2-(1-butyl-imidazol-2-yl)pyridine (3).	37
Scheme 2.4	Synthetic route to 2-(1-octyl-imidazol-2-yl)pyridine (4).	38
Scheme 2.5	Synthetic route to 2-(1'-pyrazolyl)-methylpyridine (5).	39
Scheme 2.6	Synthetic route to 2-(3,5-dimethyl-pyrazol-1-yl)-methylpyridine (6).	40
Scheme 2.7	Synthetic route to the isomeric mixture of 2-(3-methyl-pyrazol-1-yl)-methylpyridine (7) and 2-(5-methyl-pyrazol-1-yl)-methylpyridine (7').	41
Scheme 2.8	Synthetic route to 2-(3-butyl-pyrazol-5-yl)pyridine (8).	42
Scheme 2.9	Synthetic route to 2-[3-(<i>tert</i> -butyl)-pyrazol-5-yl]pyridine (9).	43
Scheme 2.10	Synthetic route to 2-(3-octyl-pyrazol-5-yl)pyridine (10).	44
Scheme 2.11	The formation of the ethane-1,2-diimine from glyoxal and ammonia.	45
Scheme 2.12	The formation of 2-(1 <i>H</i> -imidazol-2-yl)pyridine (1) from ethane-1,2-diimine and pyridine-2-carboxaldehyde.	46
Scheme 2.13	The rapid transition between the two tautomers of 2-(1 <i>H</i> -imidazol-2-yl)pyridine (1).	46
Scheme 2.14	Nucleophilic substitution (S_N2) mechanism by which ligands 2 , 3 and 4 are formed.	48
Scheme 2.15	The synthesis of 2,6-bis[(1'-pyrazolyl)-methylpyridine as reported by Watson <i>et al.</i>	52
Scheme 2.16	The proposed synthesis of 2-(1'-pyrazolyl)-methylpyridine (5), 2-(3,5-dimethyl-pyrazol-1-yl)-methylpyridine (6) and 2-(3-methyl-pyrazol-1-yl)-methylpyridine (7).	52
Scheme 2.17	The nucleophilic substitution (S_N2) mechanism by which ligands 5 , 6 and 7 were formed.	53
Scheme 2.18	The formation of an isomeric mixture of 2-(3-methyl-pyrazol-1-yl)-methylpyridine (7) and 2-(5-methyl-pyrazol-1-yl)-methylpyridine (7') via tautomerism.	55
Scheme 2.19	The plane of symmetry present in (a) pyrazole and (b) 3,5-dimethylpyrazole that prevents isomers from being formed.	56

Scheme 2.20	A general outline of the synthesis of 2-(3-butyl-pyrazol-5-yl)pyridine (8), 2-[3-(<i>tert</i> -butyl)-pyrazol-5-yl]pyridine (9) and 2-(3-octyl-pyrazol-5-yl)pyridine (10).	59
Scheme 2.21	The formation of the unwanted secondary intermediates and final products as a result of secondary carbanion (highlighted with dotted circle) nucleophilic attack.	60
Scheme 2.22	Tautomeric forms of ligands 8–10 present in solution.	63

Chapter 5

Scheme 5.1	Modification of ligands 1–7/7' to include an acidic proton to strengthen the coordination bond to nickel(II) and copper(II).	115
Scheme 5.2	The suggested methylpyrazolyl tripodal extractant with possible electron donating R-groups.	116

List of abbreviations

%E	percentage extraction
(M)Hz	(mega) Hertz
(m)mol	(milli)mole
∫	integral
°C	degrees Celsius
1°, 2°, 3°, 4°	primary, secondary, tertiary, quaternary
¹³ C NMR	carbon 13 nuclear magnetic resonance
¹ H NMR	proton nuclear magnetic resonance
Å	Ångström
aq	aqueous
ATR	attenuated total reflectance
CDCl ₃	deuterated chloroform
cm ⁻¹	reciprocal centimetres (or wavenumber)
CMC	critical micelle concentration
d	doublet (NMR)
DDNSA	didodecyl naphthalene sulfonic acid
DEHSS	di-2-ethylhexyl sodium sulfosuccinate
DEPHA	di-2-ethylhexyl phosphoric acid
DFT	density functional theory
DIEN	diethylenetriamine
DMF	<i>N,N</i> -dimethylformamide
DNNSA	dinonyl naphthalene disulfonic acid
DNNSA	dinonyl naphthalene sulfonic acid
EA	elemental analysis

EMF	electromotive force
EN	ethylenediamine
ESI+	positive electrospray ionisation
F	ratio of molar activity coefficient
g	grams
h	hours
HSAB	hard/soft acid and base
ICP-AES	inductively coupled plasma atomic emission spectroscopy
<i>in vacuo</i>	in a vacuum
IR	infrared
<i>J</i>	coupling constant
K_D	distribution coefficient
K_{ex}°	thermodynamic extractive equilibrium constant
L	litre/ligand
M	molar/metal
m	multiplet (NMR)
m.p.	melting point
<i>m/z</i>	mass to charge ratio
MIBK	methyl isobutyl ketone
min	minutes
mL	millilitres
MS	mass spectrometry
OPIM	1-octyl-2-(2'-pyridyl)imidazole
org	organic
p	pentet (NMR)

PENTEN	pentaethylenehexamine
PGM	platinum group metal
pimH	2-(2'pyridyl)imidazole
pimMe	2-(2'pyridyl)-1-methylimidazole
pK _a	acid dissociation constant
q	quartet (NMR)
r ⁺	metal ion radius
R _f	ratio of the distance moved by the solvent and solute
rpm	revolutions per minute
s	singlet (NMR)
SDBS	sodium dodecylbenzenesulfonate
S _N 2	nucleophilic substitution
t	triplet (NMR)
TBAOH	tetrabutylammonium hydroxide
TBP	tributylphosphate
TETREN	tetraethylenepentamine
THF	tetrahydrofuran
TOF	time of flight
TOPO	trioctylphosphine oxide
TRIEN	triethylenetetramine
β _n	formation constant
δ	chemical shift (ppm)
ΔH	enthalpy
ΔS	entropy
ΔU _b	binding energy

Chapter 1

Introduction

1.1 Historic overview of extractive metallurgy

The extraction of metals from ore can be divided into two subclasses of metallurgy: pyrometallurgy and hydrometallurgy. Pyrometallurgy involves the centuries-old tradition of high-temperature roasting, smelting, converting and refining.¹ Thousands of years ago, people developed furnaces in which they would melt rocks and extract metals. These metals would typically be iron or copper, which they used to forge simple weapons and tools. Hydrometallurgy, compared to pyrometallurgy, is a relatively recent development. “Hydro” means water and “metallurgy” is the study of metal production and purification. Therefore, “hydrometallurgy” is the study of metal purification by means of aqueous systems.² Hydrometallurgy came much later when water and aqueous solutions were used instead of the well-known dry and high temperature processing of ores.¹

The roots of hydrometallurgy can be linked to a time when alchemists tried to “convert” base metals into pure gold.² A good example of base metal “conversion” was when alchemists, by chance, submerged an iron plate into a solution of blue vitriol, *i.e.*, copper sulfate, and found that the outer layer of the iron plate was covered by metallic copper.² The alchemists, at the time, didn’t understand that blue vitriol contained copper and were perplexed by the “conversion” of iron into copper.² Today we know that the apparent “conversion” can be attributed to **Equation 1**:



A big question at that time still remained, however: how can base metals be “converted” into gold, the most sought after metal? It was known that mercury dissolved gold, forming a metal mixture (amalgam), however, gold was insoluble in all known acids and bases at the time.² Jabir Ibn Hayyan (720–813 A.D.), the Arab alchemist, was the first known person who dissolved gold by means of aqua regia.² Aqua regia, known as royal water in Latin, is a mixture of one part nitric acid and three parts hydrochloric acid. It readily dissolves gold, but these acids on their own do not. The discovery of this “magical” solution is widely regarded as a pivotal milestone in the development of hydrometallurgy.² Aqua regia was extensively used in the refining of gold in the 1890s, with chlorine as one of its key ingredients (**Equation 2**):



In the 1500s, the extraction of copper gained appeal as it was done by relatively underdeveloped wet methods.² Heap leaching was practiced in the Río Tinto mines in Spain as well as in the Harz mountains, Germany.² Heap leaching was an operation where pyrite, containing tiny amounts of copper sulfide minerals, was piled out in the open, allowing months of rain to instigate the oxidation and dissolution of the copper.² The copper containing solution was subsequently drained from the heap and collected. This led to a process known as the

“cementation process”, whereby scrap iron was used to precipitate metallic copper.² This crude and relatively inefficient process is still in operation today.

Modern hydrometallurgy can be traced back to 1887, a year in which two processes were invented – the cyanidation- and Bayer processes.² The cyanidation process, a process for treating gold ore, in reality had its origins in the 1700s with the Swedish chemist Carl Wilhelm Scheele (1742–1786) who observed the dissolution of gold in a cyanide solution.³ Later, in 1846, Elsner studied this reaction and noted the important role that oxygen played in the dissolution of gold.⁴ Today, this well-known reaction can be described by the famous Elsner equation (**Equation 3**):



This important knowledge was used in the extraction of gold from its ores and patented in England by John Stewart McArthur, Robert Forrest and William Forrest in 1887.⁴ Today this patented process is known as the cyanidation process. The implementation of this process was the sole contributing factor that led to the booming production of gold during the period 1900–1910.²

The Bayer process was another important hydrometallurgical process and was invented by Karl Josef Bayer (1847–1904) for the production of pure alumina (Al_2O_3).⁵ This process entails the leaching of bauxite, an aluminium ore, with boiling sodium hydroxide solution in a pressure reactor.² The insoluble material was removed and the solution was cooled to allow pure crystalline aluminium hydroxide to precipitate.² The precipitate was filtered, washed and dried to yield pure Al_2O_3 .²

Solvent extraction is a sub-category of hydrometallurgy. It is an interphase transport process/technique whereby the applicable metal is purified. In the nineteenth century, the solvent extraction of inorganic compounds was experimented with. The first of which was reported by Peligot⁶ in 1842, when he reported the extraction of uranyl nitrate into diethyl ether. The second noteworthy mention was the extraction of iron in hydrochloric acid into diethyl ether, reported by Rothe⁷ and Hanroit⁸ in 1892. In 1900, Langmuir⁹ used the method proposed by Rothe and Hanroit to separate iron from various other metal ions. The first general understanding of liquid-liquid distribution equilibria was experimentally introduced in 1872 by French scientists Berthelot and Ungfleisch,¹⁰ and derived thermodynamically in 1891 by the German scientist Nernst.¹¹

1.2 General introduction to nickel

1.2.1 Nickel properties and applications

Nickel is a first-row transition element, known as a base metal due to its relative abundance. Along with iron, cobalt and gadolinium, nickel is ferromagnetic under ambient conditions. It also displays considerable resistance to corrosion and mechanical strain. Nickel, according to Pearson's¹² hard/soft acids and bases (HSAB) theory, can be classified as a borderline hard-soft metal ion. This is significant, because ligands with soft donor atoms preferentially coordinate to soft metal ions while ligands with hard donor atoms prefer to

coordinate to hard metal ions. We might assume that both oxygen (harder) and nitrogen (softer) could theoretically coordinate to nickel(II), since nickel(II) is a borderline hard-soft metal ion. This, however, is comprehensively covered in section 1.5.

Nickel(II) has an electron configuration of $[\text{Ar}]3d^8$. It is known to form a large number of complexes with coordination numbers of 4, 5 and 6. The typical geometries include octahedral, trigonal bipyramidal, square planar, square pyramidal and tetrahedral. Nickel(II) is a paramagnetic species since this d^8 ion has two unpaired electrons in its valence shell.

By far, the majority of uses for nickel arise from its alloys, most notably stainless steel.¹³ However, other nickel containing alloys have special high-end applications such as a nickel alloy created by Kim and co-workers¹⁴ that has a thermal expansion coefficient of zero. Miller and co-workers¹⁵ on the other hand created a nickel-titanium alloy that displays shape memory characteristics. Other modern-day applications include materials for aviation,¹⁶ rechargeable batteries,¹⁷ electroplating¹³ and catalysis.¹⁸

1.2.2 Sources of nickel

Nickel is considered to be one of the most abundant elements in the universe but forms a mere 0.016% of the earth's crust, making it the 24th most abundant element known to man.¹⁹ The total amount of nickel in the earth's crust is more than copper, zinc and lead combined but large nickel deposits are extremely rare and in most cases the economic viability in mining it is absent.¹⁹ Nickel is mostly found in the presence of magnesium- and iron-rich rocks. This is because nickel has a similar ionic radius (0.69 Å) to that of magnesium (0.65 Å) and iron (0.75 Å) and often displaces the iron and magnesium ions in some crystal lattices, especially silicates.¹⁹ In nickel-rich peridotite rock nickel is almost always found in the mineral olivine, which is an orthosilicate with the general formula $M_2\text{SiO}_4$, with M being a divalent metal ion such as Mg, Fe or Mn.¹⁹ Nickel mining is only viable when the nickel content of rocks containing the metal has been concentrated, as in the case of silicate ores or where the nickel in the magma was precipitated as sulphides.¹⁹ The silicate ores were formed by the continual weathering of peridotite rocks under special chemical conditions which usually only occurs in the tropics.¹⁹ The metals continually dissolve and precipitate in a process known as laterisation.¹⁹ From this process laterite ores have its origin of which bauxite is an example.

The largest deposits of nickel sulphide ores are found in Canada, Russia, South Africa and more recently Australia.¹⁹ The South African deposits are particularly rich in platinum group metals (Ru, Rh, Pd, Os, Ir and Pt) and the production of these are the main reason for treating the ore.¹⁹ The total world nickel reserves are estimated to be 54.5 million tonnes of which 45% is in sulphide ores and 55% in laterite ores.²⁰ Today, Canada accounts for 20–30% of the world's nickel production.¹⁹

1.3 Hydrometallurgical routes for the separation of base metals

Before we introduce the various routes for the separation of base metals, we need to ensure that we know and understand the overall hydrometallurgical process from start to finish (**Figure 1.1**). The hydrometallurgical

process that includes solvent extraction starts off with the mining of ore from metal rich sources. The metals in the ore are leached (dissolved) by using a chemical solution that dissolves the appropriate metal or metal mix. The “pregnant leach solution” is contacted with the solvent extractant which selectively extracts the metals into the organic water-immiscible phase. From here, the pH is drastically lowered to strip the metals from the extractant to afford a metal-rich aqueous solution. A reducing agent is subsequently used to reduce the metals. The stripped organic phase as well as the aqueous solution from electrolysis is reused. The metals that were not extracted during the solvent extraction process (raffinate) is recycled back to the leaching process. After the stripping phase, the extractants are recycled as well and reused in the extraction process.²¹

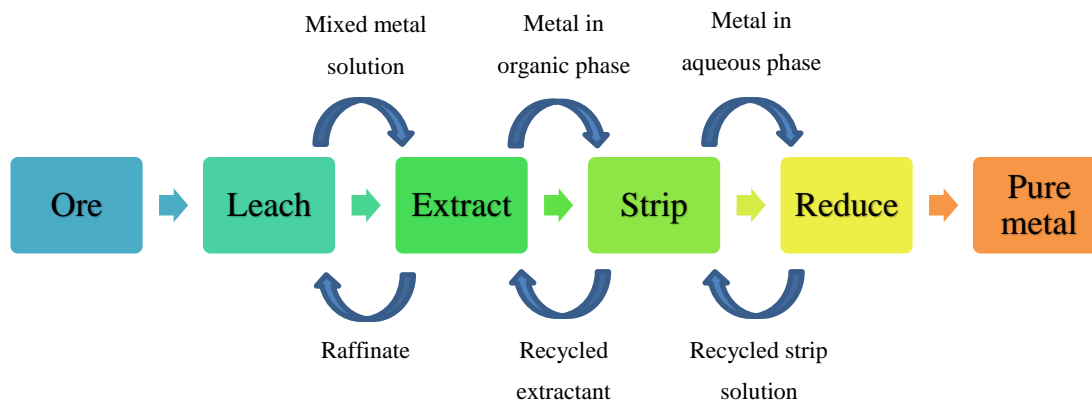


Figure 1.1: The solvent extraction process incorporated into a hydrometallurgical process. [Adapted from Wilson *et al.*²¹]

Additional purification systems, other than solvent extraction, are also used, but to lesser extents. These systems include crystallisation, ionic precipitation, electrochemical reduction, reduction with gas, carbon adsorption and ion exchange.

1.3.1 Crystallisation

Crystallisation is a centuries-old technique that is still widely used to purify compounds. It is, however, a technique that is seldom used in the recovery of metals. Crystallisation of a metal salt out of an aqueous solution occurs when the solution is evaporated and the solute goes beyond the point of saturation. Knowing that the solubility of metal salts decreases considerably beyond 200 °C, industry can effect crystallisation by implementing high temperatures and pressures. A noteworthy aspect of crystallisation is the separation of two or more chemically similar metals if they differ in their solubilities in aqueous solutions.¹

1.3.2 Ionic precipitation

Similar to crystallisation, metals can be recovered as insoluble compounds by an ionic precipitation technique. Hydroxides and sulfides are compounds that are readily precipitated and has found extensive applications in industry. In this process, an anionic reagent is added to the solution to form a metal salt which is insoluble in the present solution. This is a rapid process, because the metal salt formed has an extremely low solubility.¹

An example of this is the precipitation of copper as CuS from an acidic solution by passing H₂S gas through it, as illustrated in **Equation 4** below:



Hydrolytic reactions are also used for ionic precipitation. The precipitation of titanium hydroxide is a prime example of this, as seen below in **Equation 5**:



1.3.3 Electrochemical reduction

As mentioned in section **1.1**, a common method for the precipitation of metals can be achieved by a process called cementation, which is an electrochemical reduction process. This process involves the fact that a higher metal in the electromotive force (EMF) series, *i.e.*, a less noble metal, can be added to displace a lower metal (more noble metal) from solution.¹ An example of this was already shown where metallic iron is added to a copper solution (**Equation 1**). The copper precipitates while the iron goes into solution. Similarly, copper can displace silver from a solution of silver nitrate (**Equation 6**), a reaction often used to determine the metallic copper content of ore samples.¹ Zinc can displace cadmium from cadmium sulfate solutions (**Equation 7**), which is currently the standard procedure for recovering cadmium from leach solutions.¹ Another familiar example is the recovery of gold by precipitation on zinc metal (not shown).



1.3.4 Reduction with gas

In modern hydrometallurgy, hydrogen plays a very important role in metal recovery. Interestingly, hydrogen appears to have a dual nature. Sometimes it behaves as a metal (formation at the cathode in the hydrolysis of water) and other times more like a non-metal (formation of metal hydrides).¹ It can be displaced by sodium from water or displaced by zinc from dilute acid. Most notably, it can also displace copper and nickel from sulfate solutions.¹

1.3.5 Carbon adsorption

The use of activated carbon in the recovery of gold from cyanide leach solutions can be flagged as a major advancement in hydrometallurgy.¹ The gold cyanide anion present in the leach liquor is adsorbed onto pseudo-cationic sites on the activated carbon according to the following chemical reaction (**Equation 8**):



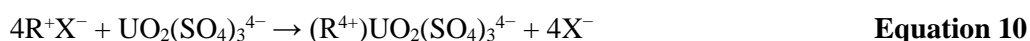
Furthermore, the loaded carbon is stripped of the gold cyanide by reversing **Equation 8** with the help of a hot caustic solution (**Equation 9**):²²



Adsorption on activated carbon can also be used for turbid solutions or pulps, thereby saving on expensive filtration processes.²

1.3.6 Ion exchange

Ion exchange is mainly used as a purification process in the recovery of uranium from low-grade uranium ores.¹ For the removal of uranium, one must add an anionic exchanger because of its complex anions such as $\text{UO}_2(\text{SO}_4)_2^{2-}$ and $\text{UO}_2(\text{SO}_4)_3^{4-}$.¹ This is a significant advantage, since cationic impurities in the leach solution (Al^{3+} , Co^{2+} , Ni^{2+} , etc.) cannot participate in the following ion exchange reaction (**Equation 10**):



where R represents the fixed ion exchange sites of the resin and $\text{X}^- = \text{NO}_3^-$, Cl^- or HSO_4^- .¹

1.3.7 Electrolytic process

The electrowinning and electrorefining processes have been the foremost processes implemented by industry in the past few decades.¹ Electrolysis can broadly be described as two equivalent reactions that occur simultaneously, *i.e.*, oxidation and reduction reactions. Oxidation takes place at the anode while reduction occurs at the cathode.

In electrorefining, the oxidation of a metal at the anode, proportional to the current passing through, is directly accompanied by the reduction of the same equivalent amount of metal ion at the reductive cathode.¹ The electrolyte composition remains unchanged and the net cell reaction is equal to the simultaneous corrosion of the metal at the anode and metal deposition at the cathode.¹ The voltage required is only needed to overcome the ohmic resistance of the electrolyte, since no decomposition potential is involved.¹

In electrowinning, the net cell reactions are also equivalent oxidation and reduction reactions, but the presence of insoluble anodes prevent the oxidation and reduction of equivalent amounts of the same metal.¹ The electrowinning of nickel can be used as a good example to illustrate this phenomenon. Nickel from an acidic sulfate solution undergoes the oxidation-reduction reaction, where NiSO_4 is oxidised at the anode into Ni^{2+} ions.¹ The reduction reaction at the cathode is can be seen in **Equation 11**:



This reaction at the cathode is similar to the electrorefining process, but the oxidation reaction at the anode discharges the sulfate ion.¹ The sulfate radical formed, however, is extremely unstable and reacts with water instantaneously to form sulfuric acid according to the following reaction (**Equation 12**):¹



1.3.8 Solvent extraction (also known as liquid-liquid extraction)

Solvent extraction is a two-phase system whereby metal ions can be efficiently and selectively transported from the metal-rich aqueous phase to the metal receiving organic (or water-immiscible) phase. The metal of interest is often at low concentrations or mixed with various other metals and the aim of the organic reagent/extractant is to selectively coordinate to the appropriate metal ion in solution. Once the organic extractant coordinates to the metal ion of interest, the complex moves into the organic phase because of its low solubility in the aqueous phase (**Figure 1.2**).

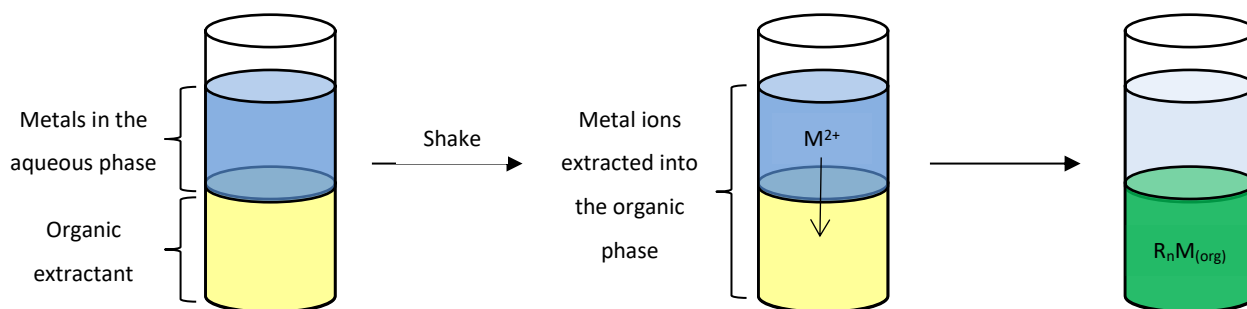


Figure 1.2: A schematic representation of the solvent extraction process. The organic layer is depicted at the bottom of the container. This, however, is dependent on the density of the organic solvent used.

It often occurs that, once the metal is extracted into the organic layer, the layer becomes brightly coloured. This is due to the complexation of the metal ion with the organic extractant. On the other hand, the aqueous phase loses its bright colour due to the depletion of metal ions in solution. At the end of the extraction procedure the organic solvent is physically separated and brought into contact with another clean aqueous solution. This process, called scrubbing, removes the unwanted impurities that was co-extracted with the metal of interest.²² This process is usually done either by a solution of acid or alkali salt that has a pH favouring the extraction procedure.²² In industry, a solution of the metal itself is used to rid the organic phase of impurities.²²

In order to recover the extracted metal, the scrubbed organic phase is mixed with a highly acidic aqueous solution ($\text{pH} < 2$) to release the metal into the aqueous phase. The high concentration of protons competes for binding sites (donor sites) on the extractant. Alternatively, the organic extractant can be reacted with another reagent that will cleave the extractant and subsequently release the metal into the new aqueous phase. The release of the metal into the aqueous phase is termed “stripping”.²² Once the metal has been retrieved, the organic solvent is reused either immediately or after it has been cleansed of impurities.¹

In solvent extraction, net electrical neutrality is preserved. This is done by the transfer of neutral molecules from one phase to another, the transfer of ion pairs or by the exchange of ions between the two liquid phases.¹ The driving force for the transfer process depends on the way the metal is associated with the extractant in the organic phase. The extractant could form a chemically neutral complex with the metal by coordination, including chelate formation, or by ion association.¹ A reversible chemical reaction is shown below to illustrate the overall solvent extraction procedure (**Equation 13**):



The thermodynamic derivations of solvent extraction are explained in great detail by Sekine and Hasegawa.²³ They derived a set of equations to determine the optimum extractant concentration as well as the optimum pH for solvent extractions. For a chelating reagent, HR, the extraction reaction for a metal ion, M^{n+} , is represented by **Equation 13** above. The thermodynamic extractive equilibrium constant (K_{ex}°) is given by **Equation 14**:

$$K_{\text{ex}}^{\circ} = \frac{[\text{MR}_n]_{\text{org}} [\text{H}^{+}]_{\text{aq}}^n}{[\text{M}^{n+}]_{\text{aq}} [\text{HR}]_{\text{org}}^n} \cdot F \quad \text{Equation 14}$$

where F is the ratio of molar activity coefficient. Usually F is unknown and is combined with K to give the extraction constant K_{ex} , as seen in **Equation 15**:²³

$$K_{\text{ex}} = \frac{K_{\text{ex}}^{\circ}}{F} = \frac{[\text{MR}_n]_{\text{org}} [\text{H}^{+}]_{\text{aq}}^n}{[\text{M}^{n+}]_{\text{aq}} [\text{HR}]_{\text{org}}^n} \quad \text{Equation 15}$$

At this stage, we should introduce the distribution coefficient, also known as the distribution ratio (K_{D}). K_{D} is defined as the ratio of total analytical concentration of the solute in the solvent to that in the aqueous phase (**Equation 16**):²³

$$K_{\text{D}} = \frac{[\text{MR}_n]_{\text{org}}}{[\text{M}^{n+}]_{\text{aq}}} \quad \text{Equation 16}$$

Now, the expression for K_{ex} can be written as (**Equation 17**):²³

$$K_{\text{ex}} = \frac{K_{\text{D}} \cdot [\text{H}^{+}]_{\text{aq}}^n}{[\text{HR}]_{\text{org}}^n} \quad \text{Equation 17}$$

From **Equation 17** we can derive **Equation 18**:

$$\log K_{\text{D}} = \log K_{\text{ex}} + n \text{pH} + n \log [\text{HR}]_{\text{org}} \quad \text{Equation 18}$$

It is quite obvious that for any solvent extraction system, a high value for K_{D} is extremely desirable for achieving satisfactory extraction results. This, according to **Equation 18**, is achieved at a high concentration of extractant and at a high pH of the aqueous solution containing the metal ion mix.²³

In the hydrometallurgical application of solvent extraction, the purpose is to transfer the metal ions from the aqueous phase to the extractant-rich organic phase. Therefore, in industry the term percentage extraction (%E) is used to determine the amount of metal extracted by the extractant.²² The %E can be calculated as follows (**Equation 19**):

$$\%E = \frac{w_i - w_f}{w_i} \times 100 \quad \text{Equation 19}$$

where w_i is the original weight of the solute in the aqueous solution before extraction, and w_f is the weight of the solute left in the aqueous solution after the extraction process.

1.4 Types of extractants

For analytical laboratory solvent extraction systems, the rate of extraction and stripping is of relatively low importance. This, however, is certainly not the case for industry, where large-scale solvent extraction processes are performed on a daily basis. For an extractant to be used successfully in industry, it has to meet several important criteria: (1) it has to be relatively cheap, (2) be highly soluble in the organic phase and highly insoluble in the aqueous phase, (3) be able to selectively form a metal complex with the desired metal and have high solubility of the organic metal species in the organic phase, (4) be easy to recover the metal from the organic phase and regenerate the extractant to be recycled and reused, (5) have suitable physical properties such as low viscosity, low flash point, non-toxicity and non-volatility.²² These factors are of less importance in an analytical environment, therefore, only a few extractants have ever made it out of the laboratory and into industry. Only a small percentage of extractants that have been synthesised in an analytical laboratory have been found to be commercially viable.²²

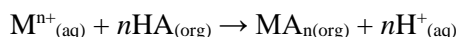
Most metal salts are ionic in character and easily dissolve in water due to the high dielectric constant of water and the well-known tendency of water to solvate ions.²² The coordination number of the metal (4 or 6) primarily dictates the number of water molecules that are bonded to the metal ion. Such metal ions, are generally not expected to be transported to the organic phase, which is mostly non-polar and have an extremely low dielectric constant.²² Therein lies the challenge of solvent extraction scientists worldwide – to ensure that these metal ions are efficiently transferred to the organic phase. This is primarily done by the reaction of suitable organic compounds with the metal ions that form neutral species soluble in the organic phase.

Most organic extractants today can be categorised into three main groups according to their mode of extraction: (1) cationic, (2) anionic and (3) solvating (neutral) extractants.

1.4.1 Cationic extractants (acidic)

In the cationic liquid-liquid extraction process, as the name suggests, cations are exchanged between the aqueous and organic phases. The formation of the extractable neutral complex can be attributed to the removal of one acidic proton on the extractant for every positive charge on the metal ion.²² Two sub-divisions within the cationic extraction process exist, namely chelate and acid extraction.

In chelate extraction, the metal ion is only transferred into the organic phase once an electrically neutral metal chelate is formed through the help of a chelating agent that satisfies both the valence and coordination number requirements of the metal ion.²² There are cases where organic solvents such as diketones, oximes and oxines contain both acidic and basic functionalities that combine with a metal ion. In such cases chelate salts are formed where both functional groups are operative.²² Overall, the chelate extraction process can be summed up by **Equation 20**:

**Equation 20**

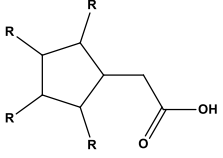
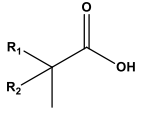
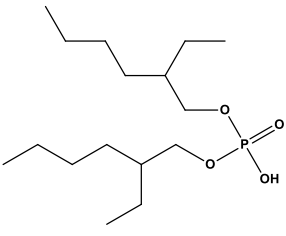
From **Equation 20**, it is clear that the hydrogen ion increases in the aqueous phase, therefore, it is imperative to control and counter this acid formation. A well-known industrial acidic chelating extractant, LIX 64 N, is successfully used in industry for the extraction of copper from dilute acidic solutions.²²

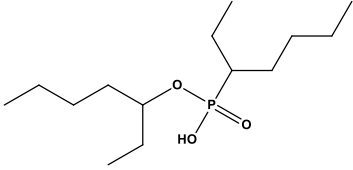
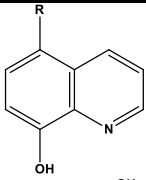
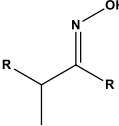
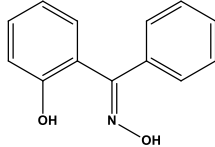
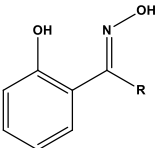
The second subgroup in cationic extraction, namely acid extraction, use acids such as alkyl carboxylic, phosphoric and sulfonic acids. Unlike chelating extractions, mechanisms in cationic extractions are far more intricate because they are affected by solvent-phase properties.²² It is known that organophosphorous and carboxylic acids form dimers, and even polymers, in the organic phase due to hydrogen bonding, which ultimately affects their extractive abilities.²² For example, di-2-ethylhexyl phosphoric acid forms dimers in most non-polar organic solvents. In such cases, the extraction reaction can be represented as follows (**Equation 21**):²³

**Equation 21**

where H_2A_2 represents the dimeric form of the extractant and m the total number of extractant molecules in the extracted species. Extraction of metal ions is improved when extractants are more basic.²² An increase of the charge on a metal cation also increases its extractability. In cases where metal ions have the same charge, the degree of extraction will depend inversely on their ionic radii, *i.e.*, smaller cations will preferentially be extracted over larger cations.²² The degree to which metal ions are extracted by means of carboxylic acid extractants and extractants similar to it, are pH dependent.²² A close eye should always be kept on this parameter for the separation of different metal ions.

Table 1.1: Commercial cationic (acidic) extractants and their uses in industry. [Adapted from Gupta and Mukherjee²²]

Type of extractant	Commercial name	Chemical structure	Manufacturer	Typical uses
Carboxylic acid	Napthenic acid		Shell Chemical Co.	Cu/Ni separation
	Versatic acid		Shell Chemical Co.	Cu/Ni separation
Phosphoric acid	Di-2-ethylhexyl phosphoric acid (DEPHA)		Mobile Chemicals (USA)	Co/Ni separation; U extraction from phosphoric acid

Type of extractant	Commercial name	Chemical structure	Manufacturer	Typical uses
Phosphonic acid	PC-88 A		Daihachi Chemical Industries (Japan)	Co/Ni separation
	Cyanex 272	Unknown (trade secret)	American Cyanamid	Co/Ni separation
Chelating type 8-hydroxy-quinoline based hydroxime	Kelex-100		Sherex Chemicals Co. (USA)	Cu extraction
	LIX 63		Cognis Inc. formerly Henkel Corp. (USA)	Cu extraction
	LIX 64		Cognis Inc. formerly Henkel Corp. (USA)	Cu, Ni and Co from NH ₃ solutions; Cu from acid solutions
	P-5000 series		Acorga Ltd. (Bermuda)	Cu extraction

1.4.2 Anionic extractants (basic)

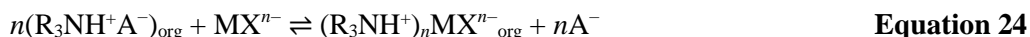
For basic extractants to be used, the metal should form an anionic complex in the aqueous solution.²⁴ It is a fact that certain metals can form anionic complexes, provided that certain conditions are met. Because of this, however, anionic extractants can selectively extract metals and yield very pure solutions.²⁴ In industry, long-chain alkylamines are the most common basic extractants (see **Table 1.2**). The acid-binding property of amines with high molecular weights depend on the fact that acid salts of these bases are insoluble in water and highly soluble in organic solvents like benzene or kerosene.²⁴ This extraction can be thought of as an ion pair formation (**Equation 22**):



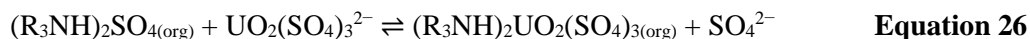
In acidic solutions the metal can be extracted due to anion exchange with an anion present in the aqueous phase. This cannot happen in basic solutions, since metal extraction will be halted (**Equation 23**):²⁴



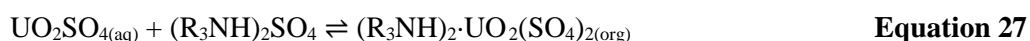
A metal can now be extracted if it can form an anionic complex (**Equation 24**):



A good example of such extractions are of anionic uranium species present in a sulfate solution, as seen in **Equations 25 and 26**:²²



The uranium, however, can also be extracted through a neutral uranyl sulfate species, instead of going via anionic metal species formation, as **Equation 27** shows:²²



The alkali amine extractants used in hydrometallurgy can be divided into three groups: primary (1°, RNH₂), secondary (2°, R₂NH) and tertiary (3°, R₃N) amines. Of course, quaternary amines (4°, R₄N⁺) also exist, but these have only found limited niche applications in industrial solvent extraction processes.²² Amines have specific trends and properties that make them unique. (1) Firstly, they can be arranged in the following pattern according to their solubility in water: primary > secondary > tertiary, where tertiary amines with long alkyl chains are effectively insoluble in water. (2) Amines are generally soluble in non-polar hydrocarbon solvents. (3) The extraction of anionic metal complexes by amines, where the complexing anion is chloride, is primarily governed by the rule: tertiary > secondary > primary. If extractions of sulfate complexes are performed, the order is exactly reversed. (4) The extraction of singly-charged anions is more effective than that of doubly- or multi-charged ones. (5) Finally, chloroanions of multivalent metals are more efficiently extracted than oxyanions.²² See **Table 1.2** for examples of anionic extractants used in industry.

Table 1.2: Commercial anionic (basic) extractants and their uses in industry. [Adapted from Gupta and Mukherjee²²]

Type of extractant	Commercial name	Chemical structure	Manufacturer	Typical uses
Primary amine (1°)	Primene JM-T	R-NH ₂	Rohm & Haas	Fe extraction from sulfate solutions
Secondary amine (2°)	LA-1 and LA-2	R ₂ -NH(<i>n</i> -laurylalkyl-methylamine)	Rohm & Haas	U extraction from sulfate solutions and Co extraction from chloride solutions
	Adogen 283	Di-tridecylamine	Sherex Chemicals Co.	Unknown
Tertiary amine (3°)	Alamine-336	R ₃ N	Cognis Inc. formerly Henkel Corp.	U, V, Mo and W extraction from sulfate solutions
	Hostarex-A 327	R ₃ N, where R = C ₈ -C ₁₀	Hoechst A.G.	Co and Cu extraction from chloride solutions; Separation of Zr from Hf
	Adogen 364	Tri-iso-octyl amine	Sherex Chemicals Co.	Platinum group metal (PGM) extraction from chloride solutions

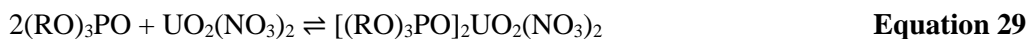
Type of extractant	Commercial name	Chemical structure	Manufacturer	Typical uses
Quaternary amine (4°)	Aliquat-336	$(R_3N^+CH_3)Cl^-$	Cognis Inc. formerly Henkel Corp.	Extraction of V, Cr, W and Cu
	Adogen 464	$(R_3N^+CH_3)Cl^-$, where R = C ₈ –C ₁₀	Sherex Chemicals Co.	Extraction of V, Cr, W and Cu

1.4.3 Solvating extractants (neutral)

Neutral extractants have various neutral solvating agents which facilitate extraction by coordinating with the metal, while simultaneously water molecules are displaced.²² This leads to the formation of neutral complexes through ion association. The extraction reaction can be formulated as follows (**Equation 28**):



where MA = metal ion pair and S = solvent. There are wide varieties of organic reagents like alcohols, ethers, ketones, alkyl phosphates, etc., with oxygen atoms as an electron donor, that can solvate metal ions and resultantly be used as solvating extractants.²² Tributylphosphate (TBP) as well as methyl isobutyl ketone (MIBK) are two well-known examples in this group. TBP especially, has found niche application in nuclear materials processing technology.²² It can extract uranium from uranyl nitrate solutions in the following way (**Equation 29**):



Furthermore, TBP can extract a number of non-ferrous metals such as Zn, Cu and Co from hydrochloric acid solutions. An interesting fact about TBP is that it can extract mineral acids from effluents and acid nickel liquors produced in metallurgical industries. The mechanism lies in the ability to solvate the proton. The order of extraction is as follows: $H_3PO_4 > HNO_3 \geq HF > HCl > H_2SO_4$.²² Other than nitric acid media, TBP can also extract metals from hydrochloric acid solutions as $MCl_2(TBP)_n$ by solvating the metal ion and as $HMCl_3(TBP)_n$ by solvating the proton.²² However, TBP cannot extract metals from H_2SO_4 or H_3PO_4 solutions.

In general, the degree of solvation and extraction is determined by four factors: (1) the elution donor property of the solvent molecule, (2) the length and molecular structure of the hydrocarbon chain, (3) the nature of the associate anion, (4) the charge as well as (5) the ionic radius (size) of the metal ion.²² As far as phosphorous-containing compounds go, the extractability increases with the number of C–P bonds in the extractant, *i.e.*, phosphine oxides > phosphonates > phosphates.²² The order is exactly reversed concerning the aqueous solubility of the solvent. The selectivity in extraction by solvating agents mainly depend on the change in solvation energy that takes place upon the displacement of water of hydration by the solvent.²⁴ See **Table 1.3** for commonly used solvating extractants.

Table 1.3: Commercial solvating (neutral) extractants and their uses in industry. [Adapted from Gupta and Mukherjee²²]

Type of extractant	Commercial name	Chemical structure	Manufacturer	Typical uses
Phosphoric acid ester	T.B.P.	$(\text{CH}_3\text{CH}_2\text{CH}_2\text{CH}_2\text{O})_3\text{PO}$	Union Carbide (USA); Albright & Wilson (UK); Daihachi (Japan)	Fe extraction from chloride solutions; Separation of Zr and Hf; Uranium purification for nuclear fuel processing
Phosphine oxide	TOPO	R_3PO , where $\text{R} = \text{C}_8\text{H}_{17}$	American Cyanamid (USA); Albright & Wilson (UK); Hokko Chemical Ind. (Japan)	Extraction of U^{6+} from H_3PO_4 in combination with DEPHA
Methyl-isobutyl ketone	MIBK	Unknown (trade secret)	Unknown	Separation of Hf from Zr; Extraction of Au from chloride solutions
Alkyl sulfides	Di- <i>n</i> -hexyl sulfides	R_2S , where $\text{R} = \text{C}_8\text{H}_{17}$	Unknown	Pd extraction from chloride solutions

1.4.4 Additives in solvent extraction systems

Besides the extractant, the organic phase often includes other organic additives too, like diluents and modifiers.

1.4.4.1 Diluents

At times, diluents are needed to dissolve or dilute the extractant so that its physical properties like viscosity and density become more favourable to enhance the mixing and consequent separation of the two phases.² These diluents are hydrocarbons and can be aliphatic, aromatic or a mixture of the two. It is important to note that diluents are inert, *i.e.*, they have no extractive power on their own, but they can affect the extraction, scrubbing, stripping and phase separation processes significantly. See **Table 1.4** for the most common diluents used in industry today.

Table 1.4: List of common diluents for extractants. [Adapted from Gupta and Mukherjee²²]

Diluent	Specific gravity (20 °C)	Boiling point (°C)
Aromatic	Benzene	0.833
	Toluene	0.873
	Xylene	0.870
	Solvesso 100	0.876
	Solvesso 150	0.931
Medium aromatic	Escaid 100	0.797
Low aromatic	Escaid 100	0.767
	Naptha 140 Flash	0.785
Aliphatic	Mineral Spirits	0.785
	Odorless 360	0.761

Diluent	Specific gravity (20 °C)	Boiling point (°C)
Aliphatic with naphthenes	Isoparo L	0.767
	Shell 140	0.790
	Kermac 470 B	0.810

1.4.4.2 Modifiers

Modifiers are only used to prevent the formation of a third phase and to improve the solubility of the metal complex in the organic layer.²² Usually, they tend to be long-chain alkyl alcohols (like isodecanol) or other neutral extractants. Like diluents, modifiers are also known to influence the extraction, scrubbing and stripping properties of the extractant, therefore, they should be chosen with caution.²² See **Table 1.5** for a list of commonly used modifiers in industry.

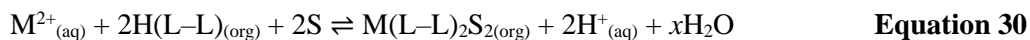
Table 1.5: List of commonly used modifiers in industry. [Adapted from Gupta and Mukherjee²²]

Modifier	Specific gravity (20 °C)	Flash point (°C)
2-Ethylhexanol	0.833	85
Isodecanol	0.841	104
Nonylphenol	0.950	140
Tri- <i>n</i> -butyl phosphate	0.973	193

1.4.5 Synergistic extraction

The word *synergism* is derived from the Greek words “συν” (together) and “εργον” (to work); hence, *synergism* means “to work together” or “to work as a unit”.² Occasionally, the mixture of two extractants (from the same class or not) will enhance the extraction of a metal above the mere summed extractions of the individual extractants.²⁵ In other words, to put it mathematically: $%E_{AB} > %E_A + %E_B$, where %E = percentage extraction, A = extractant A and B = extractant B. This phenomenon is known as the synergistic effect. The component which exhibits lower extraction ability for the metal of interest is said to be the “synergist” and enhances the extraction ability of the second component, which is known as the “extractant”.²²

There are numerous examples of synergists in literature, although very few of them were ever commercialised for industrial purposes. The principal reason for this is due to the difficulty in ensuring the optimum extractant/synergist ratio in the organic phase remains constant. This optimum ratio can easily be altered through the evaporation of the extractant, poor water solubility and/or entrainment.²⁵ The synergistic system most common today is a mixture of a solvating and acidic extractant that acts upon a metal ion where the preferred coordination number cannot satisfactorily be met by the acidic extractant alone.²⁵ For example, a divalent metal ion (M^{2+}) with a preferred coordination number of six would form a complex with a bidentate acidic extractant, $M(L-L)_2(H_2O)_2$, where HL-L is the extractant.²⁵ The displacement of the water molecules of the extracted complex with a solvating extractant (S) will ensure that the complex is soluble in the organic phase, *i.e.*, the complex will become more lipophilic, $M(L-L)_2S_2$.²⁵ When the solvating extractant is unlikely to extract the metal ion by itself, the synergistic system can be generalised as follows (**Equation 30**):



There are a few examples of synergistic systems applicable to the separation of nickel from cobalt. Varying degrees of synergism can be achieved by adduct formation of octanol, tributyl phosphate (TBP) or trioctylphosphine oxide (TOPO) for the separation of nickel from cobalt.¹⁹ This is not ideal, therefore, the addition of di-(2-ethylhexyl)phosphoric acid to LIX 63 greatly enhances the extraction of nickel and increases the separation factor for nickel from cobalt,²⁶ but even greater separation factors are achieved when carboxylic acids are used instead of the phosphoric acid.²⁷ Weak nickel extraction has been reported when a mixture of versatic acid and LIX 64N was used,²⁸ but this was greatly enhanced upon the addition of dinonylnaphthalene sulfonic acid (DNNSA) to the organic phase. Presumably the DNNSA acts as a phase transfer catalyst,²⁸ but this has by no means been verified. Selective cobalt/nickel extraction has also been reported by varying the LIX 63/DNNSA ratios so that, depending on the metal ion sought after, either cobalt or nickel could be selectively extracted above the other.²⁹

1.5 Ligand-metal compatibility

The coordination chemistry of metal ions naturally plays a major role in the separation of base metal ions. When a metal ion specific ligand is designed, it is critical to explore the properties of the metal ion of interest, as well as the properties of the metal ions from which it is separated. The following aspects are important in such a study: (1) nature of the metal ion, (2) hydrogen ion concentration, (3) thermodynamics and kinetics of complexation and (4) coordination ability of the anion.^{30,31}

Over the past decade studies have been conducted where the anion selectivity in the transport of metal salts were investigated.^{21,32-35} These studies focused on both the inner- (metal ions and immediate anions) and outer sphere coordination chemistry (solvents or anions not directly coordinated to the metal ion). Furthermore, ligand pre-organisation has also been investigated as an approach for metal ion recognition.^{36,37} This study will focus on the inner sphere coordination chemistry of ligand design. We will specifically investigate the various factors influencing the ligand-metal compatibility.

An important aspect to the design of a ligand lies in the selection of the most appropriate donor atoms.

1.5.1 Donor atoms

It is important that ligands should be structurally simple to limit the cost of synthetic procedures. Moreover, if ligands contain oxygen, nitrogen and/or sulphur donor atoms, they are much easier to synthesise compared to more exotic donor atoms.³⁸

In 1963, Pearson¹² authored an article in which he explained the hard/soft properties of acids and bases (metals only). In 1966, Pearson and Songstad³⁹ expanded this list to include organic (non-metal) species. It is of great interest to know which metal ions would preferentially be extracted by organic ligands based on the hard/soft acid base (HSAB) theory. Hard non-metals preferentially form complexes with hard metal ions, while soft non-metals preferentially complexes to soft metal ions (**Tables 1.6 and 1.7**).

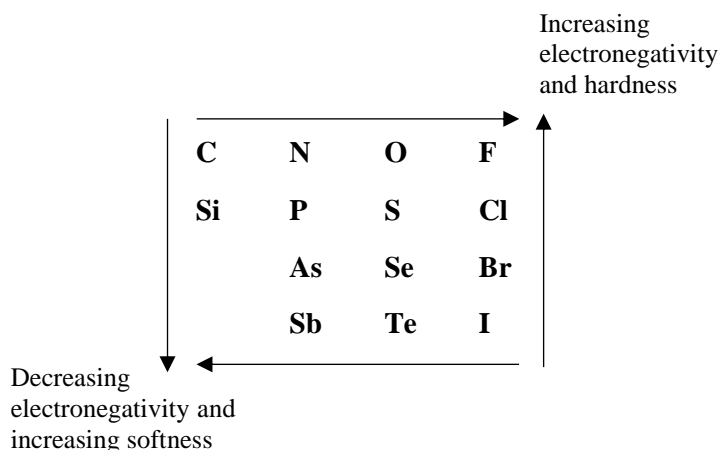
Table 1.6: The hard and soft acids (metal ions) proposed by Pearson.¹² [This table is only a partial representation.]

Hard	Soft	Borderline
H ⁺ , Li ⁺ , Na ⁺ , K ⁺ , Be ²⁺ , Mg ²⁺ , Ca ²⁺ , Sr ²⁺ , Sn ²⁺ , Al ³⁺ , Sc ³⁺ , Ga ³⁺ , In ³⁺ , La ³⁺ , Cr ³⁺ , Co ³⁺ , Fe ³⁺ , As ³⁺ , Ir ³⁺ , Si ⁴⁺ , Ti ⁴⁺ , Zr ⁴⁺ ,	Cu ⁺ , Ag ⁺ , Au ⁺ , Tl ⁺ , Hg ⁺ , Cs ⁺ , Pd ²⁺ , Cd ²⁺ , Pt ²⁺ , Hg ²⁺	Fe ²⁺ , Co ²⁺ , Ni ²⁺ , Cu ²⁺ , Zn ²⁺ , Pb ²⁺

Table 1.7: The hard and soft organic (non-metal) bases proposed by Pearson and Songstad.³⁹ [This table is only a partial representation.]

Hard	Soft	Borderline
H ₂ O, OH ⁻ , F ⁻ , CH ₃ CO ₂ ⁻ , PO ₄ ³⁻ , SO ₄ ²⁻ , CO ₃ ²⁻ , ClO ₄ ⁻ , NO ₃ ⁻ , ROH, RO ⁻ , R ₂ O, NH ₃ , RNH ₂ , N ₂ H ₄	R ₂ S, RSH, RS ⁻ , I ⁻ , SCN ⁻ , S ₂ O ₃ ²⁻ , Br ⁻ , R ₃ P, R ₃ As, (RO) ₃ P, CN ⁻ , RNC, CO, C ₂ H ₄ , C ₆ H ₆ , H ⁻ , R ⁻	C ₅ H ₅ NH ₂ , C ₅ H ₅ N, Cl ⁻ , NO ₂ ⁻ , SO ₃ ²⁻

As a general rule, the hardness of a donor atom increases with an increase in electronegativity (for example F⁻ and H₂O), while less electronegative elements such as P and I⁻ are softer donor atoms. See **Figure 1.3** for the hard/soft distribution of non-metals.

**Figure 1.3:** The hard/soft acid base trend of non-metals. [Adapted from Martell and Hancock⁴⁰]

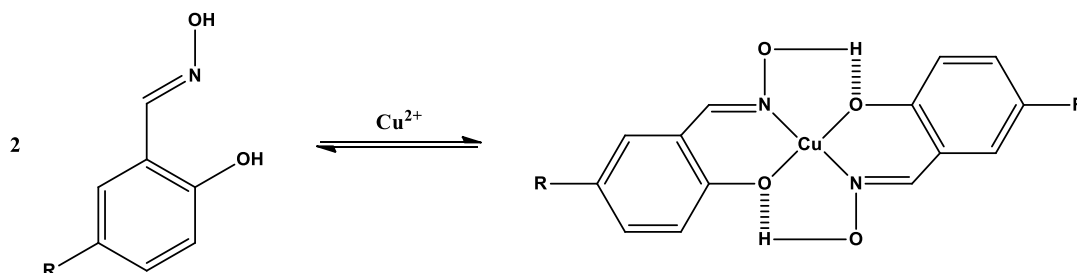
1.5.1.1 Oxygen donor atoms

It is known that oxygen donor ligands form more stable complexes with harder acids (metal ions).³⁹ This can be attributed to the fact that they possess strong σ -donor properties and no π -acceptor ability. Therefore, oxygen donor ligands will theoretically coordinate to hard metal ions and to a lesser extent later 3d transition metal ions (borderline hard/soft metal ions), of which nickel(II) is one.

The separation of cobalt from nickel in the presence of other base metal ions using organophosphorous extractants (CYANEX reagents), has been studied extensively.⁴¹ However, the reverse extraction of nickel from cobalt has not yet satisfactorily been achieved. The organophosphorous extractants preferentially extract

cobalt(II) from nickel(II) in aqueous solutions with a pH 4–6. One significant drawback of organophosphorous extractants is their high affinity towards hard metal ions, such as Fe^{3+} . This necessitates the precipitation of iron(III) salts prior to cobalt/nickel separation.⁴²

Hydroxyoxime extractants (commercialised as LIX reagents) have been used extensively for the extraction of copper(II). Szymanowski⁴³ reported the interaction of copper(II) and a hydroxyoxime, shown in **Scheme 1.1**. During the extraction of copper(II) two acidic phenolic protons are removed to form a 2:1 complex with copper(II). This complex is stabilised by the formation of five-membered chelate rings through hydrogen bonding of the hydroxyl groups.



Scheme 1.1: The complexation reaction of copper(II) with a hydroxyoxime reagent. [Adapted from Szymanowski⁴³]

Taking the above information into account, we decided that oxygen donor ligands were not the best suited donor atom for the selective extraction of nickel(II).

1.5.1.2 Sulphur donor atoms

Sulphur donor atoms are known to be softer than oxygen donor atoms.³⁹ Because of this fact, sulphur containing ligands are able to form more stable complexes with divalent 3d transition metal ions such as cobalt(II) and nickel(II). It has been reported that sulphur derivatives of di-2-ethylhexyl phosphoric acid (DEHPA) are excellent extractants of cobalt(II), but only at low pH values. This is somewhat of a concern since extremely low pH values (perhaps even negative pH values) will be needed to strip the cobalt from the ligand in the recycling process. A study by Chia *et al.*⁴⁴ showed that alkylthiomethylpyridine derivatives formed octahedral complexes with both nickel(II) and cobalt(II), but a slight preference for nickel(II) was reported. An important advantage of sulphur containing ligands is the fact that they hardly ever interact with iron(III), unlike oxygen donor atoms. A strong disadvantage lies in the synthesis of sulphur containing ligands. The reagents in the synthesis of thiol ligands can be quite harmful and are known to give off foul odours.

1.5.1.3 Nitrogen donor atoms

Nitrogen donor atoms are slightly softer in nature compared to oxygen donor atoms.³⁹ Relatively stable complexes are formed with later 3d transition metal ions (Co^{2+} , Ni^{2+} , Cu^{2+} and Zn^{2+}) compared with early and

middle 3d transition metal ions (Ti^{2+} , V^{2+} , Cr^{3+} , Mn^{2+} and Fe^{3+}). In the past twenty years an upsurge in the use of amine extractants were observed. Nitrogen donor extractants are very useful in the formation of six-coordinated Ni(II) complexes. Since nickel is known to form the most stable high spin octahedral complex of all the base metal ions, their selection as extractants in the development of nickel specific extractants is a well guided decision. Equally, copper(II) also forms stable complexes with nitrogen containing ligands and often form four-coordinated complexes, *i.e.*, tetrahedral or square-planar.⁴²

There has been a deliberate shift towards aromatic amine extractants because of their favourable properties compared with their oxygen counterparts.³¹ Aliphatic amine extractants ($R-NH_2$, where R is an alkyl moiety) tend to form complexes at relatively high pH values due to their high protonation constants which led to the hydrolysis of metal ions even under slightly acidic conditions. These aliphatic ligands with only σ -donor character show lack of metal ion selectivity, however, this can be improved if chelating ligands are used instead.³¹ An example of this would be the alkylated derivatives of ethylenediamine. Aromatic nitrogenous ligands, on the other hand, have excellent metal ion selectivity, possibly due to their σ and π bonding character. Additionally, these ligands can form complexes even in strongly acidic solution due to their lower pK_a values.^{30,31}

1.6 Chelating ligands

1.6.1 The chelate effect

In the mid-twentieth century, Bjerrum⁴⁵ and Schwarzenbach⁴⁶ ushered in a bloom period of coordination chemistry with extensive studies of equilibria in solution. Of particular importance and relevance was the recognition of the chelate effect.⁴⁷ The chelate effect can broadly be defined as polydentate ligands (ligands with more than one donor atom) forming thermodynamically more stable complexes than analogous complexes containing monodentate ligands (ligands with only one donor atom).⁴⁰ To phrase it another way: it produces increased stability for complexes of chelating ligands compared with analogous monodentate ligands.⁴⁰ An example of this can be seen in **Table 1.8** where the formation constants of Ni(II) complexes with n -dentate polyamines are compared with the analogous complexes with ammonia.

Table 1.8: The formation constants of polyamine Ni(II) complexes compared with analogous ammonia complexes. [Data from Martell and Smith⁴⁸]

Polyamine	Denticity	$\log \beta_n (NH_3)$	$\log K_1$ (polyamine)
EN ^a	2	5.08	7.47
DIEN ^b	3	6.85	10.7
TRIEN ^c	4	8.12	14.4
TETREN ^d	5	8.93	17.4
PENTEN ^e	6	9.08	19.1

^aEN = $NH_2(CH_2)_2NH_2$; ^bDIEN = $NH_2(CH_2)_2NH(CH_2)_2NH_2$; ^cTRIEN = $NH_2(CH_2)_2NH(CH_2)_2NH(CH_2)_2NH_2$;

^dTETREN = $NH_2(CH_2)_2NH(CH_2)_2NH(CH_2)_2NH(CH_2)_2NH_2$; ^ePENTEN = $(NH_2(CH_2)_2)_2N(CH_2)_2N((CH_2)_2NH_2)_2$.

Schwarzenbach⁴⁷, in explaining the chelate effect, promulgated the idea that once the first donor atom had attached itself to the metal ion, the second and subsequent donor atoms could not move freely around in solution, *i.e.*, it was restricted to a specific volume around the metal ion (**Figure 1.4**).⁴⁰ This volume was determined by the length of the chelating ligand. In effect this meant that the entropy (ΔS) of the second and subsequent donor atoms was significantly reduced as compared with an equal number of monodentate ligands.

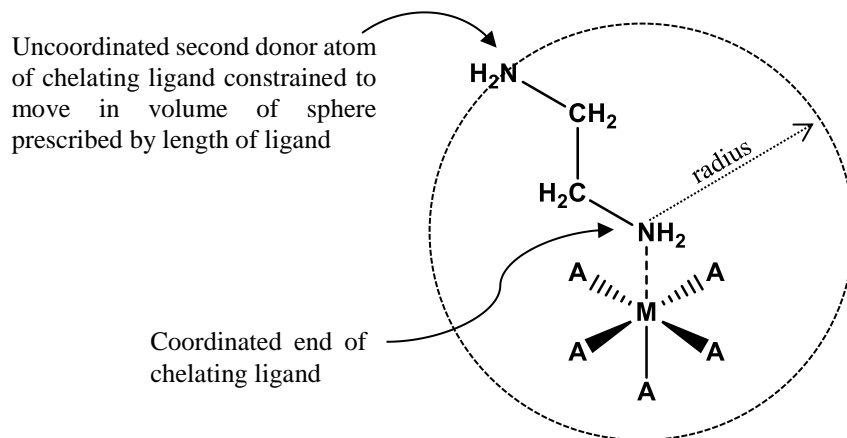


Figure 1.4: A diagram illustrating the Schwarzenbach⁴⁷ model of the chelate effect where the chelating ligand (ethylenediamine) is constrained to move in a sphere, whose radius is prescribed by the length of the bridge connecting the two donor atoms. [Adapted from Martell and Hancock⁴⁰]

This model, however, does have its shortcomings. It predicted that larger chelate rings (six-membered and larger) would exhibit lower complex stability compared with five-membered chelate rings. This was theorised because of the longer bridge connecting the two donor atoms forcing the uncoordinated donor atom to move in a larger volume of sphere around the metal ion centre.⁴⁰ In general, this seems to be valid reasoning and logic, but this model does not agree with common observations. This model predicts that the decrease in formation constants as chelate ring sizes are increased should be an entropic (ΔS) effect, but for seven-membered chelate rings and smaller, it seems to be predominantly an enthalpic (ΔH) effect instead.⁴⁹

In contrast to the explanation of the chelate effect by Schwarzenbach⁴⁷, was another proposed model. This model is commonly known as the standard reference state model.⁴⁰

1.6.2 The standard reference state and the chelate effect

In 1954, Adamson⁵⁰ noted that the units used for the concentration of the species involved in the formation constants were such that the formation constant β_n would have units of 1^n mol^{-n} , which was attributed the asymmetry of the standard reference state. This is as a result of the solvent being given an activity of unity, whereas all other species in the equilibrium are expressed as mol.dm^{-3} .⁵⁰ This means that monodentate and chelating ligands with equal number of donor atoms coordinated to the metal ion have different values of n , for β_n , with different units.⁵⁰ Therefore, the constants presented in **Table 1.8** are rendered erroneous. In fact,

the chelate effect is actually reversed,⁵⁰ when instead of mol.dm⁻³, concentrations are expressed in mol.cm⁻³ with complexes of monodentate ligands seeming to be more stable. Adamson⁵⁰ proposed that mole fractions should be used to express concentrations instead, which subsequently forces the formation constants to be dimensionless. Only now, according to Adamson, true and valid comparisons in **Table 1.8** can be made. Adamson's proposal resulted in the fact that, at low concentrations, the total number of moles present in the solution is effectively the molarity of pure water (55.5 M at 25 °C).⁵⁰ This is a major mathematical finding and effectively means that each species in the equilibrium can divide its molarity by 55.5 and obtain their individual mole fractions. Now, it is required that $n \cdot \log 55.5$ must be added to all $\log \beta_n$ values to ensure that they are comparable.⁵⁰ This principally deals with the chelate effect in a detailed mathematical way, something the Schwarzenbach model doesn't address adequately.

Adamson's proposal leads to **Equation 31**,⁵¹ for relating the formation constant of a polydentate chelating ligand to that of the analogous complex containing monodentate ligands:

$$\log K_1 (\text{polydentate}) = \log \beta_n (\text{monodentate}) + (n - 1) \log 55.5 \quad \text{Equation 31}$$

This equation predicts lower values for polyamine complexes than observed, as seen in **Table 1.9**. The main reason for this is that the nitrogen donor atoms of the polyamines are more basic ($pK_a = 10.6$) than the zero order nitrogen of ammonia ($pK_a = 9.2$).⁴⁰ This can be corrected by taking inductive effects into consideration. We can add an inductive effect factor of 1.152 ($= 10.6 \div 9.2$) to **Equation 31**, to give **Equation 32**:⁴⁰

$$\log K_1 (\text{polyamine}) = 1.152 \cdot \log \beta_n (\text{ammonia}) + (n - 1) \log 55.5 \quad \text{Equation 32}$$

Now, the predicted (calculated) values of $\log K_1$ are in accord with the observed values of $\log K_1$, as shown in **Table 1.9**.

Table 1.9: A comparison of the observed formation constant, $\log K_1$, with the calculated formation constant derived from **Equations 31** and **32**. **Equation 31** only considers the asymmetry of the standard state, while **Equation 32** corrects for inductive effects. [Data from Martell and Smith⁴⁸]

Polyamine ^a	Denticity	$\log K_1$ calculated by Equation 31	$\log K_1$ calculated by Equation 32	Observed $\log K_1$
EN	2	6.82	7.58	7.47
DIEN	3	10.33	11.37	10.96
TRIEN	4	13.34	14.67	14.4
TETREN	5	15.89	17.25	17.4
PENTEN	6	17.78	19.16	19.1

^a Polyamine abbreviations can be found in **Table 1.8**.

From the results in **Table 1.9**, we see that the formation constants of polyamine complexes are dependent on two thermodynamic contributions: (1) the entropy (ΔS) contribution from the asymmetry of the standard reference state, and (2) an enthalpy (ΔH) driven inductive effect contribution from the ethylene bridges of polyamine ligands.⁴⁰ At the core of Adamson's model is the suggestion that the chelate effect should mainly be considered as a strong entropic effect from (1), with a minor, yet vital, enthalpic contribution from (2).⁴⁰

One question still remains, however, and needs to be resolved – which model (Adamson or Schwarzenbach's) describes the chelate effect more accurately? Adamson⁵⁰ and Schwarzenbach's⁴⁷ individual proposals on the origin of the chelate effect are, at their cores, very similar. The Schwarzenbach model sets the translational entropy of the second monodentate ligand close to zero by making it move in a limited spherical volume, while the Adamson model sets the translational entropy of the second monodentate ligand to exactly zero by making each reactant completely fill the space of the standard reference state once the constants are expressed as mole fractions.⁴⁰ This means that Adamson's model appears more accurate and reliable, since it doesn't make any assumptions regarding the ligand geometry or the length of the carbon bridge connecting the donor atoms.⁴⁰

1.7 Metal ion selectivity of nitrogen donor ligands

It is known that smaller metal ions are more likely to form complexes with six-membered chelate rings than five-membered ones.⁴⁰ Conversely, five-membered chelate rings preferentially coordinate to larger metal ions. This, by far, is one of the most powerful ligand design tools and can be used to extract specific metal ions. Metal ion sizes, in terms of the ionic radius (r^+), can be categorised as follows: $r^+ \geq 1.2 \text{ \AA}$ (very large), $1.2 > r^+ > 1.0 \text{ \AA}$ (large), $1.0 > r^+ > 0.8 \text{ \AA}$ (medium), $0.8 > r^+ > 0.7 \text{ \AA}$ (medium-small), $0.7 > r^+ > 0.5 \text{ \AA}$ (small) and $r^+ < 0.5 \text{ \AA}$ (very small).⁵²

1.7.1 The chelate ring geometry and preferred metal ion sizes

It is quite easily understood why five-membered chelate rings form more stable complexes with larger metal ions, while six-membered chelate rings predominantly form stable complexes with smaller metal ions, when the relatively low-strain form of cyclohexane is referenced.^{53,54} Cyclohexane, seen in **Figure 1.5**, has the minimum strain possible for a cyclohexane in its chair conformation. The torsion angles are 60° and the C–C–C bond angles are all 109.5° .

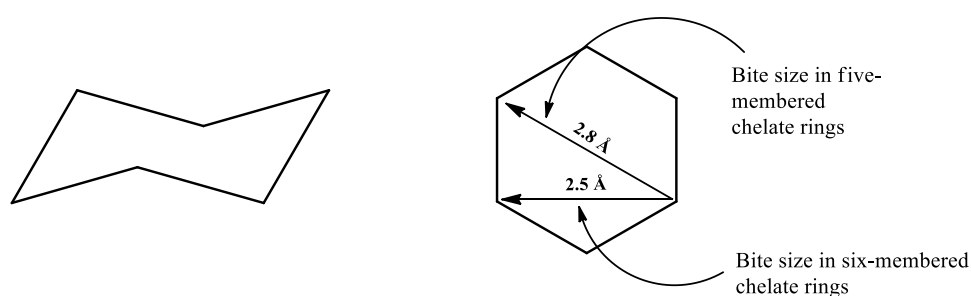


Figure 1.5: Cyclohexane in its chair conformation. Additionally, the bite sizes of five- and six-membered chelate rings are shown. [Adapted from Martell and Hancock⁴⁰]

The six-membered chelate ring of 1,3-diaminopropane containing two nitrogen donor atoms and a metal ion in place of three carbon atoms of cyclohexane will also exhibit very low strain energy.⁴⁰ This is obviously pre-conditional to the metal ion having roughly the same size and geometry as an sp^3 hybridised carbon atom. The ideal metal ion for coordination to 1,3-diaminopropane has a N–M–N bond angle of 109.5° , and a short M–N bond length of 1.6 \AA (**Figure 1.6a**).⁴⁰ This conformation is better suited for smaller metal ions.

The ideal metal ion size for a five-membered chelate ring can also be derived by considering the aforementioned cyclohexane ring. One can envisage a minimally strained ethylenediamine ring by removing two adjacent carbon atoms and converting the next two to nitrogen donor atoms. The two lone pairs on the nitrogens are extrapolated to focus them about 2.5 Å away from the metal ion. This was necessary to ensure that the lone pairs are in the same plane.⁴⁰ This simple pictorial diagram (**Figure 1.6b**) shows that when ethylenediamine is in its least strained conformation, the M–N bond lengths are 2.5 Å and the N–M–N bond angles are 69°. Because of these specific dimensions, this conformation is better suited to form complexes with larger metal ions.

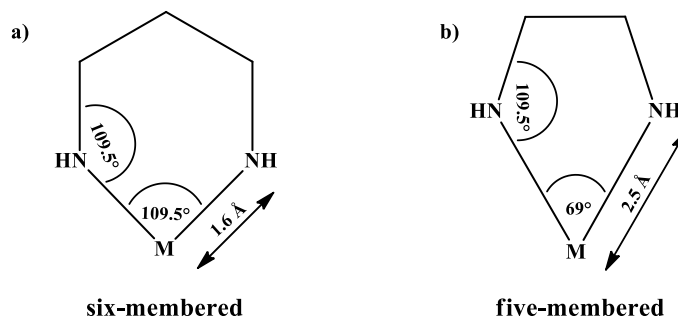


Figure 1.6: The ideal bond angles and bond lengths of **a**) six-membered (1,3-diaminopropane) and **b**) five-membered (ethylenediamine) chelate rings. [Adapted from Martell and Hancock⁴⁰]

The relation of complex stability to chelate ring sizes is readily understood in terms of the best-fit size of the metal ion for complexing with five- and six-membered chelate rings. In particular, smaller metal ions tend to have lower coordination numbers, and also, as the M–N bond lengths become smaller, the N–M–N bond angles become larger.⁴⁰

When the nitrogen donor atoms are replaced with oxygen donor atoms, the six-membered chelate ring's O–M–O bond angle becomes 95°, while the C–O–C bond angle becomes 126°. Moreover, the M–O bond length stretches to 1.9 Å (**Figure 1.7a**).⁵⁵ The five-membered oxygen chelate ring's O–M–O bond angle becomes 58°, while the C–O–C bond angle remains 126°. The M–O bond length stretches to more than 3.2 Å (**Figure 1.7b**).⁵⁵

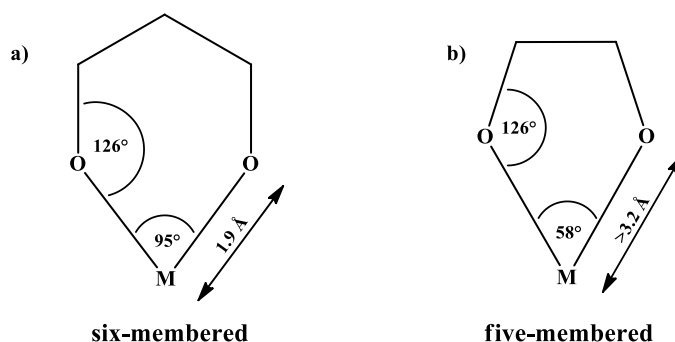






Figure 1.7: The ideal bond angles and bond lengths of **a**) six-membered (1,3-propanediol) and **b**) five-membered (1,2-ethanediol) chelate rings. [Adapted from Martell and Hancock⁴⁰]

It is quite obvious from **Figures 1.6** and **1.7** that there are big variations in the bond lengths and angles of the nitrogen and oxygen chelate rings. These differences can be attributed to the fact that neutral nitrogen donor atoms form tetrahedral geometries, while neutral oxygen donor atoms form trigonal planar geometries.⁴⁰

1.8 Steric and inductive effects in nitrogenous chelating ligands

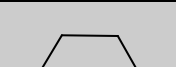
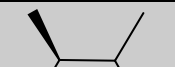

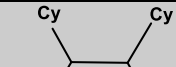
Two of the most important structural factors in chelate formation are steric and inductive effects. The tendency of donor strength increases along the following series: $\text{NH}_3 < \text{NH}_2\text{CH}_3 < \text{NH}(\text{CH}_3)_2 < \text{N}(\text{CH}_3)_3$, but also increases the possibility of steric hindrance.⁴⁰ The inductive effects are often overshadowed by the steric hindrance of large alkyl moieties. Therefore, inductive effects are often ignored or overlooked, and when they do manifest themselves, they are misunderstood and attributed to “other effects”.⁴⁰ These inductive effects have consequently been coined as “hidden” inductive effects.⁵⁶ An example of inductive effects outweighed by steric effects can be seen in **Table 1.10**, where ethylenediamines have different *N*-methyl moieties.

Table 1.10: Various ethylenediamine examples where steric effects outweigh inductive effects. [Data from Martell and Smith⁴⁸]

$\log K_1 [\text{M}^{2+}]$				
$\log K_1 [\text{Cu(II)}]$	10.48	10.33	10.02	7.20
$\log K_1 [\text{Ni(II)}]$	7.35	7.17	6.89	3.57
$\log K_1 [\text{Cd(II)}]$	5.4	5.47	5.20	3.87

It would appear from literature⁴⁸ that *N*-alkyl substitution usually leads to a decrease in complex stability, but several examples of nitrogenous ligands with *C*-substitution, where the inductive effect dominates, exist (**Table 1.11**).

Table 1.11: Examples of *N*-alkyl ligands where inductive effects outweigh steric effects. [Data from Martell and Smith⁴⁸]

$\log K_1$ and $\log \beta_2$ [M^{2+}]				
$\log K_1 [\text{Cu(II)}]$	10.48	11.27	11.63	12.20
$\log \beta_2 [\text{Ni(II)}]$	13.54	14.01	14.56	14.90

Observations for monodentate amines follow this exact pattern of behaviour as well, where *C*-methyl substitution is found to produce less serious effects than *N*-methyl substitution, *i.e.*, inductive effects can be observed with little or no impact by steric effects.⁵⁷ In general, the basicity of the nitrogen donor atoms increase with an increase in alkyl substitution: primary < secondary < tertiary. This is due to alkyl moieties pushing

electron density (inductive effect) onto the nitrogen donor atoms. Tertiary carbons (highly substituted) have a greater inductive effect than secondary and subsequently primary carbons.

1.9 Concluding factors to consider in ligand design

Factors to consider when designing novel ligands are:

1. The hard/soft character of both the metal ion and the relevant donor atoms. From the hard and soft acids and bases (HSAB) theory proposed by Pearson¹², we know that soft metal ions (for example Ag(I)) prefer to form complexes with ligands containing soft donor atoms (less electronegative) such as iodide. Hard metal ions (for example In(III)) prefer to form complexes with harder (more electronegative) donor atoms such as fluoride. Borderline metal ions show no real preference for specific donor atoms.
2. The size of the metal ion (metal ion radius, r^+). The metal ion radius roughly matching the bite size of an appropriate chelating ligand will have increased its thermodynamic odds of forming a complex.
3. The size of the chelate ring. This is complimentary to (2), where five- and six-membered chelate rings preferentially form complexes with large and small metal ions respectively.
4. The coordination number and geometry of the metal ion. Some metal ions, for example, prefer tetrahedral geometry as opposed to octahedral geometry because of the valence electrons present in specific orbitals. Metal ions and donor atoms can only form complexes when both their outer shell orbitals overlap correctly.
5. The denticity of the donor atoms. This is somewhat akin to (3), where the correct geometry and number of the donor atoms seriously need to be considered before a ligand is used for metal ion coordination.
6. The induction and steric effects. Alkyl moieties (or any electron donating moiety) on carbons adjacent to the donor atoms can increase the electron density on the donor atoms and therefore making it better suited for metal ion coordination. One should, however, be somewhat cautious to build too much steric bulk on the donor atoms themselves. We do know that they add positive induction effects, but this is often overshadowed or “hidden” by the steric hindrance of bulky groups.

1.10 Pyridyl imidazole and -pyrazole background

The solvent extraction chemistry using imidazole- and pyrazole-based pyridine ligands are of great interest, since we know that complexes with these ligands, according to literature, are readily formed. Aromatic nitrogenous ligands show relative preference for metal ions because of their σ -donor and π -acceptor abilities. Imidazole extractants also show high formation constants with later 3d transition metal ions resulting in high extraction efficiencies.⁴² These extractants can also coordinate with metal ions in slightly acidic media due to their mild pK_a values. Pyridine derivatives have low protonation constants and are known to interact strongly with metal ions in strongly acidic media (**Figure 1.8a**).⁴² This very fact can work against it in industry because

of the difficulty involved in the stripping process. Pyrazole derivatives have lower protonation constants and should be combined, either with pyridine or imidazole moieties, for successful extractions.⁴²

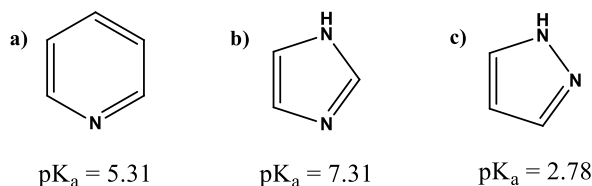


Figure 1.8: Chemical structures of aromatic amines along with their respective pK_a values: **a)** pyridine, **b)** imidazole and **c)** pyrazole.

1.10.1 Relevant literature on pyridyl imidazole and -pyrazole ligands

Gerber *et al.*⁵⁸ reported the use of 2-(2'-pyridyl)imidazole (pimH) in the synthesis of the rhenium(III) salt $[\text{ReCl}_2(\text{pimH})(\text{PPh}_3)_2](\text{ReO}_4)$ and 2-(2'-pyridyl)-1-methylimidazole (pimMe) in the synthesis of the rhenium(III) complex, $[\text{ReCl}_3(\text{pimMe})(\text{PPh}_3)]$. The monooxorhenium(V) complexes $[\text{ReOCl}_3(\text{pimR})]$ (where R = H or Me) were also reported. All of the complexes were characterised by X-ray crystallography, ^1H NMR and IR spectroscopy.

Okewole *et al.*⁵⁹ investigated 1-octyl-2-(2'-pyridyl)imidazole (OPIM), along with dinonylnaphthalene sulfonic acid (DNNSA) as a synergist as a potential selective extractant of Ni(II) from base metals in a solvent extraction system using 2-octanol/ShellSol 2325 as a diluent and modifier respectively. They were successful in the separation of Ni(II) from the other base metal ions at a pH range of 0.5–3.5 in sulfate media. The interesting fact about this study was that the extraction of Ni(II) was extremely poor without the use of the synergist, DNNSA. Once DNNSA was used, the extraction of Ni(II) increased considerably.

Watson *et al.*⁶⁰ intensely studied chiral heterocyclic ligands. In particular, they focused on the synthesis of 2,6-bis(pyrazol-1-ylmethyl)pyridine metal complexes and their chiral derivatives. They managed to prepare complexes with several divalent transition metal ions (Fe^{2+} , Ni^{2+} , Cu^{2+} , Ru^{2+} and Pd^{2+}).

Satake and Nakata⁶¹ synthesised novel cationic η^3 -allylpalladium-pyridinylpyrazole complexes from 3-alkyl-5-(2-pyridinyl)pyrazole and η^3 -allylpalladium chloride dimer in the presence of AgBF_4 . They converted cationic complexes into neutral complexes under basic conditions. These complexes were characterised by ^1H , ^{13}C and ^{15}N NMR studies. Comparisons of the cationic and neutral complexes and the reaction mechanism of cyclopropanation were discussed in depth.

1.11 Aims of this study

The main objective of this study was to selectively extract Ni(II) from a base metal ion mix (Co^{2+} , Zn^{2+} , Cu^{2+} , Pb^{2+} and Cd^{2+}) using various imidazole- and pyrazole-based pyridine ligands. These ligands, based on information gathered from literature, were 2-(1*H*-imidazol-2-yl)pyridine (**1**), 2-(1-methyl-imidazol-2-yl)pyridine (**2**), 2-(1-butyl-imidazol-2-yl)pyridine (**3**), 2-(1-octyl-imidazol-2-yl)pyridine (**4**), 2-(1'-pyrazolyl)-

methylpyridine (5), 2-(3,5-dimethyl-pyrazol-1-yl)-methylpyridine (6), 2-(3-methyl-pyrazol-1-yl)-methylpyridine (7), 2-(3-butyl-pyrazol-5-yl)pyridine (8), 2-[3-(*tert*-butyl)-pyrazol-5-yl]pyridine (9) and 2-(3-octyl-pyrazol-5-yl)pyridine (10).

1.11.1 Additional objectives

1. Synthesise and fully characterise all the ligands (1–10). These ligands are separated into three groups: imidazole ligands (1–4), pyrazole-methyl ligands (5–7) and pyrazole ligands (8–10). Characterisation of these ligands will be done by ^1H and ^{13}C nuclear magnetic resonance (NMR), infrared (IR) spectroscopy, mass spectrometry (MS), elemental analysis (EA) and melting point (mp) analysis, if applicable.
2. Extract Ni(II) only (no other metal ions present) using ligands 1–10, with and without the presence the synergist, sodium dodecylbenzenesulfonate. Firstly, the optimum synergist concentration for extraction purposes will be determined. This optimum concentration will be used throughout the study.
3. Competitively extract Ni(II) and Cu(II) (in the presence of other base metal ions) using ligands 1–10. This too will be performed with and without the synergist mentioned above.
4. Perform selectivity studies, where the appropriate metal ion's concentration is ten and one hundred times less compared to the concentrations of the other base metal ions. This will show us how selective a particular ligand is for a specific metal ion. This, at its core, is another competitive extraction study, with the exception of the varying concentration of the appropriate metal ion.
5. Study the metal stripping of certain ligands, to determine the stripping capability for industrial purposes. This is an important step in the overall hydrometallurgical process for the recovery of metals.
6. Perform time-dependent studies to ensure that metal ion extraction equilibrium is reached well within a twenty-four-hour time frame. This is critical, since all extraction studies are performed over a twenty-four-hour period.
7. Perform extensive pH isotherm studies to determine the optimum pH at which certain ligands extract Ni(II) and Cu(II). Furthermore, these isotherms will indicate at which pH values metal stripping can occur.
8. Grow crystals of Ni(II) and Cu(II) complexes for single crystal X-ray diffraction analysis. Crystal structures give valuable information about bond lengths and angles. Such an investigation additionally provides information on the coordination number and geometry around the central metal ion.

Objective 1 will be dealt with in great detail in **Chapter 2**, while objectives 2–7 will fully be explored in **Chapter 3**. Furthermore, **Chapter 4** will cover objective 8, while finally, overall conclusions of this study and future work will be discussed in **Chapter 5**.

1.12 References

1. Gupta, C. K.; Mukherjee, T. K. *Hydrometallurgy in Extraction Processes*; CRC Press: Boca Raton, Florida, 1990; Vol. 1, pp 225.
2. Habashi, F. *A Textbook of Hydrometallurgy*; Métallurgie Extractive Quebec: Sainte-Foy, 1999; pp 739.
3. Habashi, F. One hundred years of cyanidation. *Bull. Can. Inst. Min. Metall.* **1987**, *80*, 108.
4. Habashi, F. A short history of hydrometallurgy. *Hydrometallurgy* **2005**, *79*, 15-22.
5. Habashi, F. Bayer's process for alumina production: a historical perspective. *Bull. Hist. Chem.* **1995**, *17/18*, 15.
6. Peligot, E. Recherches sur l'uranium. *Ann. Chim. Phys.* **1842**, *5*, 7.
7. Rothe, J. W. Separation of iron from the elements by a new process. *Chem. News* **1892**, *66*, 182.
8. Hanroît, M. *Bull. Soc. Chim. Fr.* **1892**, *7*, 171.
9. Langmuir, A. C. The determination of sulphur in bitumens. *J. Am. Chem. Soc.* **1900**, *22*, 99-102.
10. Berthelot, M.; Ungfleisch, J. Sur les lois qui président au partage d'un corps entre deux dissolvants. *Ann. Chim. Phys.* **1872**, *26*, 396.
11. Nernst, W. Z. *Phys. Chem.* **1891**, *8*, 110.
12. Pearson, R. G. Hard and soft acids and bases. *J. Am. Chem. Soc.* **1963**, *85*, 3533-3539.
13. Mudd, G. M. Global trends and environmental issues in nickel mining: Sulfides versus laterites. *Ore Geol. Rev.* **2010**, *38*, 9-26.
14. Kim, B.; Yoo, K.; Kim, B.; Lee, H. Effect of carbon on the coefficient of thermal expansion of as-cast Fe-30wt.%Ni-12.5wt.%Co-xC Invar alloys. *Met. Mater. Int.* **2002**, *8*, 247-252.
15. Miller, D. J.; Fahnstock, L. A.; Eatherton, M. R. Development and experimental validation of a nickel-titanium shape memory alloy self-centering buckling-restrained brace. *Eng. Struct.* **2012**, *40*, 288-298.
16. Furrer, D.; Fecht, H. Ni-based superalloys for turbine discs. *JOM* **1999**, *51*, 14-17.
17. Parsons, D. The environmental impact of disposable versus re-chargeable batteries for consumer use. *Int. J. Life Cycle Assess.* **2007**, *12*, 197-203.
18. Akiyama, M.; Oki, Y.; Nagai, M. Steam reforming of ethanol over carburized alkali-doped nickel on zirconia and various supports for hydrogen production. *Catal Today* **2012**, *181*, 4-13.
19. Burkin, A. R. *Extractive Metallurgy of Nickel*; Critical Reports on Applied Chemistry; Published on behalf of the Society of Chemical Industry by Wiley: Chichester; New York, 1987; Vol. 17, pp 150.
20. Ozberk, E.; Davenport, W. G.; Gibson, N. FUTURE OF THE NICKEL INDUSTRY IN CANADA. *CIM Bull.* **1983**, *76*, 99-106.
21. Wilson, A. M.; Bailey, P. J.; Tasker, P. A.; Turkington, J. R.; Grant, R. A.; Love, J. B. Solvent extraction: The coordination chemistry behind extractive metallurgy. *Chem. Soc. Rev.* **2014**, *43*, 123-134.

22. Gupta, C. K.; Mukherjee, T. K. *Hydrometallurgy in Extraction Processes*; CRC Press: Boca Raton, Florida, 1990; Vol. 2, pp 262.
23. Sekine, T.; Hasegawa, Y. *Solvent extraction chemistry: fundamentals and applications*; M. Dekker: New York, 1977.
24. De, A. K.; Khopkar, S. M.; Chalmers, R. A. *Solvent Extraction of Metals*; Van Nostrand Reinhold Co.: London; New York, 1970, pp 259.
25. Aguilar, M.; Cortina, J. L. *SOLVENT EXTRACTION and LIQUID MEMBRANES: Fundamentals and Applications in New Materials*; CRC Press: Boca Raton, 2008, pp 344.
26. Schaufelberger, F. A. US Patent 2695843, 1954.
27. Van Hare, G.; Allen, L. N. US Patent 2733990, 1956.
28. Van Hare, G. US Patent 2813020, 1957.
29. Schaufelberger, F. A.; Roy, T. K. Separation of copper, nickel and cobalt by selective reduction from aqueous solution. *Trans. Inst. mining Metall.* **1955**, *64*, 375.
30. Okewole, A. I.; Antunes, E.; Nyokong, T.; Tshentu, Z. R. The development of novel nickel selective amine extractants: 2,20'-pyridylimidazole functionalised chelating resin. *Minerals Eng* **2013**, *54*, 88-93.
31. Du Preez, J. G. H. Recent advances in amines as separating agents for metal ions. *Solvent Extr. Ion Exch.* **2000**, *18*, 679-701.
32. Bates, G. W.; Davidson, J. E.; Forgan, R. S.; Gale, P. A.; Henderson, D. K.; King, M. G.; Light, M. E.; Moore, S. J.; Tasker, P. A.; Tong, C. C. A dual host approach to NiSO₄ extraction. *Supramol. Chem.* **2012**, *24*, 117-126.
33. Tasker, P. A.; Tong, C. C.; Westra, A. N. Co-extraction of cations and anions in base metal recovery. *Coord. Chem. Rev.* **2007**, *251*, 1868-1877.
34. Galbraith, S. G.; Tasker, P. A. The design of ligands for the transport of metal salts in extractive metallurgy. *Supramol. Chem.* **2005**, *17*, 191-207.
35. Forgan, R. S.; Davidson, J. E.; Galbraith, S. G.; Henderson, D. K.; Parsons, S.; Tasker, P. A.; White, F. J. Transport of metal salts by zwitterionic ligands; simple but highly efficient salicylaldoxime extractants. *Chem. Commun.* **2008**, 4049-4051.
36. Williams, N. J.; Gephart Iii, R. T.; Hames, A. E.; Reibenspies, J. H.; Luckay, R. C.; De Sousa, A. S.; Hancock, R. D. Affinity of two highly preorganized ligands for the base metal ions Co(II), Ni(II) and Cu(II): A thermodynamic, crystallographic and fluorometric study. *Polyhedron* **2012**, *46*, 139-148.
37. Hancock, R. D.; Melton, D. L.; Harrington, J. M.; McDonald, F. C.; Gephart, R. T.; Boone, L. L.; Jones, S. B.; Dean, N. E.; Whitehead, J. R.; Cockrell, G. M. Metal ion recognition in aqueous solution by highly preorganized non-macrocyclic ligands. *Coord. Chem. Rev.* **2007**, *251*, 1678-1689.
38. Hancock, R. D.; Martell, A. E. Ligand design for selective complexation of metal ions in aqueous solution. *Chem. Rev.* **1989**, *89*, 1875-1914.
39. Pearson, R. G.; Songstad, J. Application of the principle of hard and soft acids and bases to organic chemistry. *J. Am. Chem. Soc.* **1967**, *89*, 1827-1836.

40. Martell, A. E.; Hancock, R. D. *Metal Complexes in Aqueous Solutions*; Modern Inorganic Chemistry; Plenum Press: New York, 1996, pp 253.
41. Rickelton, W. A.; Flett, D. S.; West, D. W. Cobalt-Nickel Separation by Solvent Extraction with bis(2,4,4-trimethylpentyl)phosphinic acid. *Solvent Extr. Ion Exch.* **1984**, 2, 815-838.
42. Du Preez, J. G. H.; Postma, J.; Ravindran, S.; Van Brecht, B. J. A. M. Nitrogen reagents in metal ion separation. Part 6. 2-(1'-octylthiomethyl)pyridine as extractant for later 3d transition metal ions. *Solvent Extr. Ion Exch.* **1997**, 15, 79-96.
43. Szymanowski, J. *Hydroxyoximes and Copper Hydrometallurgy*; CRC Press: Boca Raton, 1993, pp 59.
44. Chia, P. S. K.; Livingstone, S. E.; Lookyer, T. N. Sulphur-Nitrogen Chelating Agents: II. Metal Complexes of 2-Methylthiomethylpyridine. *Aust. J. Chem.* **1967**, 20, 239-250.
45. Bjerrum, J.; Christensen, E. Metal Ammine Formation in Aqueous Solution: Theory of the Reversible Step Reactions, Haase, Copenhagen, 1941.
46. Schwarzenbach, G. The General, Selective, and Specific Formation of Complexes by Metallic Cations. *Adv. Inorg. Chem. Radiochem.* **1961**, 3, 257-285.
47. Schwarzenbach, G. The chelate effect. *Helv. Chim. Acta* **1952**, 35, 2344-59.
48. Martell, A. E.; Smith, R. M. *Critical Stability Constants*; Plenum: New York, 1974, 1975, 1977, 1977, 1982 and 1986; Vols. 1-6.
49. Hancock, R. D.; Martell, A. E. The Chelate, Cryptate and Macrocyclic Effects. *Comments Inorg. Chem.* **1988**, 6, 237-284.
50. Adamson, A. W. A proposed approach to the chelate effect. *J. Am. Chem. Soc.* **1954**, 76, 1578-1579.
51. Hancock, R. D.; Marsicano, F. The chelate effect: A simple quantitative approach. *Journal of the Chemical Society, Dalton Transactions* **1976**, 1096-1098.
52. Shannon, R. D. Revised effective ionic radii and systematic studies of interatomic distances in halides and chalcogenides. *Acta Crystallogr. Sect. A Found. Crystallogr.* **1976**, 32, 751-767.
53. Hancock, R. D.; Bhavan, R.; Wade, P. W.; Boeyens, J. C. A.; Dobson, S. M. Ligand design for complexation in aqueous solution. 1. Neutral oxygen donor bearing groups as a means of controlling size-based selectivity for metal ions. *Inorg. Chem.* **1989**, 28, 187-194.
54. Hancock, R. D. Molecular mechanics calculations and metal ion recognition. *Acc. Chem. Res.* **1990**, 23, 253-257.
55. Hay, B. P.; Rustad, J. R.; Hostetler, C. J. Quantitative structure-stability relationship for potassium ion complexation by crown ethers. A molecular mechanics and ab Initio study. *J. Am. Chem. Soc.* **1993**, 115, 11158-11164.
56. Hancock, R. D.; Nakani, B. S.; Marsicano, F. Relationship between Lewis acid-base behavior in the gas phase and in aqueous solution. 1. Role of inductive, polarizability, and steric effects in amine ligands. *Inorg. Chem.* **1983**, 22, 2531-2535.
57. Hancock, R. D. Polar and steric effects in the stability of silver complexes of primary amines. *Journal of the Chemical Society, Dalton Transactions* **1980**, 416-418.

58. Gerber, T. I. A.; Hosten, E.; Mayer, P.; Tshentu, Z. R. Synthesis and characterization of rhenium(III) and (V) pyridylimidazole complexes. *Journal of Coordination Chemistry* **2006**, *59*, 243-253.
59. Okewole, A. I.; Magwa, N. P.; Tshentu, Z. R. The separation of nickel(II) from base metal ions using 1-octyl-2-(2'-pyridyl)imidazole as extractant in a highly acidic sulfate medium. *Hydrometallurgy* **2012**, *121-124*, 81-89.
60. Watson, A. A.; House, D. A.; Steel, P. J. Chiral heterocyclic ligands. Part IV. Synthesis and metal complexes of 2,6-Bis(pyrazol-1-ylmethyl)pyridine and chiral derivatives. *Inorg. Chim. Acta* **1987**, *130*, 167-176.
61. Satake, A.; Nakata, T. Novel η^3 -allylpalladium-pyridinylpyrazole complex: Synthesis, reactivity, and catalytic activity for cyclopropanation of ketene silyl acetal with allylic acetates. *Journal of the American Chemical Society* **1998**, *120*, 10391-10396.

Chapter 2

Synthesis and characterisation of imidazole- and pyrazole-based pyridine ligands

2.1 Introduction

The use of amines as extractants and separating agents have been common for almost eighty years.¹ These molecules were extensively researched and developed in the early years of ion exchange resins and solvent extraction reagents (1940s–1960s).¹ The main drive for the development of these molecules lied in the pursuit to obtain ever purer metals through hydrometallurgical means.¹ Notable contributions were made by researchers like Gray *et al.*² and Vidal³ who reported on the synthesis of amines. Furthermore, in 1969 Marcus and Kertes,⁴ compiled a comprehensive review textbook on amines as separating agents. However, amine extractants in their neutral form have not been widely studied as separating agents for base metal ions.¹ Nitrogenous ligands can be difficult to work with in the field of solvent extraction since they are easily protonated. This in conjunction with the hydrolysis of metal ions at pH > 5, means that there are fine pH boundaries to work within. On the one hand the pH has to be kept high enough to prevent the protonation of the ligands, while on the other hand the pH has to be kept low enough to prevent metal ion hydrolysis. This gum-like metal hydroxide precipitate, due to hydrolysis, is extremely difficult to filter and is a major drawback for industrial purposes.¹

Early progress on amine ligands was largely made on ligands of the form RNH₂, where R can either be an alkyl or an aryl moiety. These amines are only able to bond, via sigma donicity, to a hydrogen or metal ion. However, the protonation constants of these ligands are so high that there is no real preference for the metal ion over the hydrogen.¹ This can be somewhat improved if chelates are used instead.¹ In the last twenty years, large strides were made in the use of aromatic ligands in the extraction of metal ions through their *N*-donor capabilities. Monodentate amine ligands are known to have larger protonation constants than their bidentate counterparts, which means that bidentate ligands can extract at lower pH values. It is also known that monodentate aromatic ligands are not as stable as bidentate aromatic ligands when bound to a metal ion.¹

During the last two decades imidazole- and pyrazole-based pyridine ligands were developed and studied as solvent extractants. Examples would include ligands like *N,N,N',N'*-tetraoctylethylenediamine, *N,N'*-di-*n*-octyl- α -aminopicoline and derivatives thereof.⁵ Du Preez *et al.*^{6,7} reported on the stability and wide pH range at which imidazole- and pyrazole-based ligands can extract metal ions. This is the first reason as to why we will investigate imidazole- and pyrazole-based pyridine ligands, with the second being that later 3d transition metal ions like, Cu²⁺, Zn²⁺, Ni²⁺ and Co²⁺, have appreciably high affinities for amines.¹

Therefore, taking all of the above into account, we set out to synthesise 2-(1*H*-imidazol-2-yl)pyridine (**1**), 2-(1-methyl-imidazol-2-yl)pyridine (**2**), 2-(1-butyl-imidazol-2-yl)pyridine (**3**), 2-(1-octyl-imidazol-2-yl)pyridine (**4**), 2-(1'-pyrazolyl)-methylpyridine (**5**), 2-(3,5-dimethyl-pyrazol-1-yl)-methylpyridine (**6**), 2-(3-methyl-pyrazol-1-yl)-methylpyridine (**7**), 2-(3-butyl-pyrazol-5-yl)pyridine (**8**), 2-[3-(*tert*-butyl)-pyrazol-5-yl]pyridine (**9**) and 2-(3-octyl-pyrazol-5-yl)pyridine (**10**). See **Figure 2.1** below for a schematic summary of ligands **1–10**.

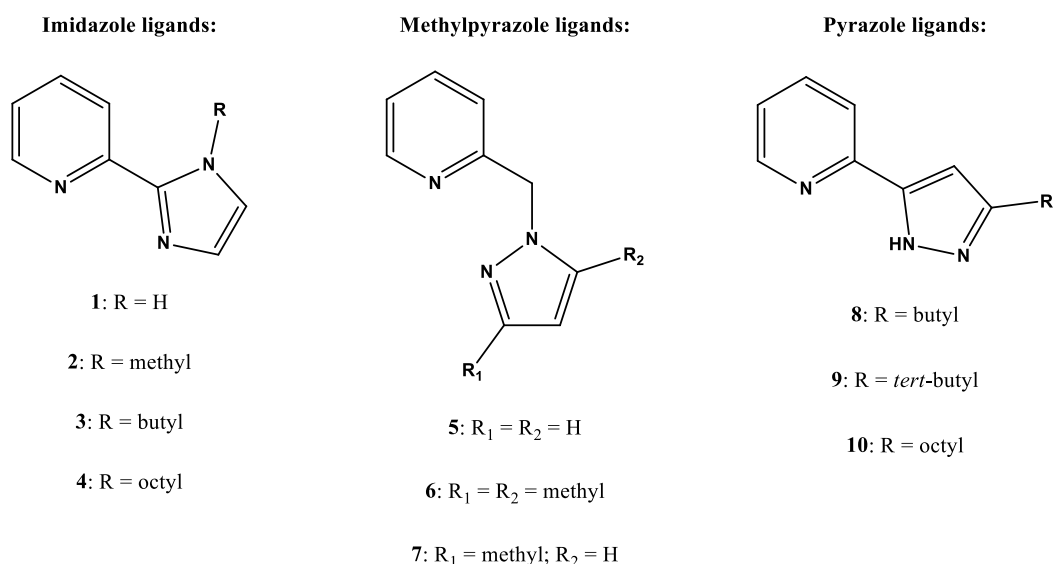


Figure 2.1: A schematic summary of ligands **1–10**.

2.2 Materials and methods

2.2.1 Chemicals and reagents

The chemicals listed in **Table 2.1** were all bought from reputable suppliers and used without further purification.

Table 2.1: List of chemicals used.

Chemical/Reagent	% Purity/Concentration	Supplier
1-Bromobutane	98	BDH Chemicals
1-Bromooctane	99	Sigma-Aldrich
2-(Chloromethyl)pyridine hydrochloride	98	Sigma-Aldrich
2-Decanone	98	Merck
2-Hexanone	98	Sigma-Aldrich
3,3-Dimethyl-2-butanone	97	Merck
3,5-Dimethylpyrazole	99	Sigma-Aldrich
3-Methylpyrazole	97	Sigma-Aldrich

Chemical/Reagent	% Purity/Concentration	Supplier
Ammonia	25 wt. % in H ₂ O	Merck
Benzene	99	Sigma-Aldrich
Diethyl ether	99	Alfa Aesar
Ethanol (absolute)	≥ 99.8	Kimix Chemicals
Ethyl 2-pyridinecarboxylate	99	Merck
Ethyl acetate (anhydrous)	99.8	Sigma-Aldrich
Glyoxal solution	40 wt. % in H ₂ O	Sigma-Aldrich
Hydrazine monohydrate	98	Sigma-Aldrich
Iodomethane	99	Merck
Magnesium sulfate (anhydrous)	≥ 99	Sigma-Aldrich
Pyrazole	98	Merck
Pyridine-2-carboxaldehyde	99	Alfa Aesar
Sodium hydride	60 wt. % in mineral oil	Sigma-Aldrich
Sodium hydroxide	≥ 97	Sigma-Aldrich
Sodium sulfate (anhydrous)	≥ 99	Sigma-Aldrich
Tetrabutylammonium hydroxide solution	40 wt. % in H ₂ O	Sigma-Aldrich
Tetrahydrofuran (anhydrous)	≥ 99	Sigma-Aldrich
Toluene	99	Sigma-Aldrich

2.2.2 Instrumentation

2.2.2.1 Nuclear magnetic resonance spectroscopy

Nuclear magnetic resonance (NMR) spectra were recorded at room temperature by using various NMR spectrometers. These would include the *Varian UnityInova 600 Liquid State NMR Spectrometer*, *Varian UnityInova 400 Liquid State NMR Spectrometer* and the *Varian VNMRS 300 Liquid State NMR Spectrometer*. All fid/propcar files were processed using *MestReNova*, Version 6.0.2-5475. All chemical shifts (δ) are given in ppm and are relative to chloroform (CDCl₃, δ 7.26).

2.2.2.2 Infrared spectroscopy

All ligands were partially characterised by infrared (IR) spectroscopy. This was done using a *Nicolet Avatar 330 FT-IR Spectrometer* in the mid-IR range (4000–500 cm⁻¹).

2.2.2.3 Mass spectrometry

Time of flight (TOF) positive electrospray ionisation (ESI+) mass spectrometry (MS) was carried out on a *Waters Synapt G2 High Resolution Mass Spectrometer*, with a cone voltage of 15 V. The ESI probe was injected into a stream of acetonitrile. All signals were recorded as a mass over charge (m/z) ratio, with the molecular ion typically observed as an (M+H)⁺ ion.

2.2.2.4 Elemental analysis

All elemental analyses were done using a *PerkinElmer 2400 Series II CHNS/O Elemental Analyzer* at the University of KwaZulu-Natal's (UKZN) mass spectrometry laboratory, Pietermaritzburg.

2.2.2.5 Melting point analysis

The melting points of solid ligands and complexes were determined using a *Stuart™ melting point apparatus, SMP3*.

2.2.2.6 pH determinations

The pH measurements were performed on a *Thermo Orion 420A+ pH meter*, using standards (pH 4, 7 and 10) to calibrate the system before every set of measurements.

2.2.2.7 Rotary evaporation

A *BÜCHI Rotavapor R-200* was used to remove excess solvent from crude products.

2.2.2.8 Short path distillation

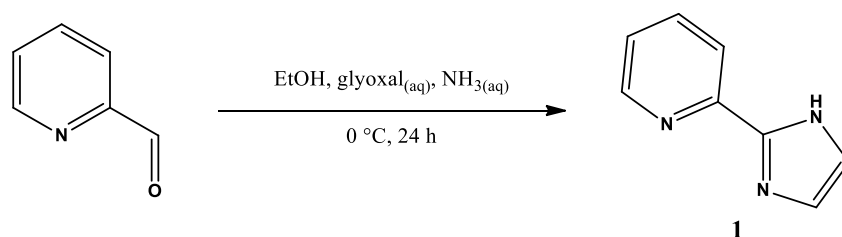
Vacuum distillation was performed using a *BÜCHI Glass oven B-585 kugelrohr* short path distillation apparatus to rid the sample of trace amounts of solvent and/or reagent.

2.2.2.9 Balances

The *Precisa XB 320M* and *Precisa XB 220A* balances were used to weigh off accurate amounts of reagent.

2.3 Experimental

2.3.1 Synthesis of 2-(1*H*-imidazol-2-yl)pyridine (1)



Scheme 2.1: Synthetic route to 2-(1*H*-imidazol-2-yl)pyridine (1). [Adapted from Gerber *et al.*⁸]

Method 1

A 250 mL round-bottom flask was charged with pyridine-2-carboxaldehyde (5.39 g, 50.0 mmol), ethanol (8.00 mL) and 40% aqueous glyoxal solution (10.0 mL). After the solution was cooled to 0 °C, ice-cold 25% aqueous ammonia solution (12.5 mL) was added and the dark brown solution was stirred for 30 minutes at 0 °C. The solution was allowed to reach room temperature and stirred overnight. The ethanol was removed by rotary evaporation and the brown residue was extracted with 100 mL aliquots of diethyl ether until the

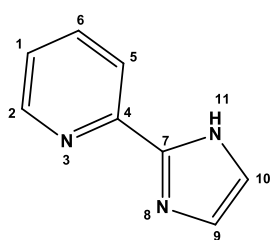
ether layer remained clear. The yellow liquid was concentrated *in vacuo*. The yellow-brown oil was dried under vacuum and yellow prisms formed on the side of the round-bottom flask. Recrystallisation was done from ethyl acetate to yield ligand **1** (1.93 g, 26.4%) as yellow-orange crystals.

Method 2

A 250 mL round-bottom flask was charged with pyridine-2-carboxaldehyde (5.39 g, 50.0 mmol), ethanol (8.00 mL) and 40% aqueous glyoxal solution (10.0 mL). After the solution was cooled to 0 °C, ice cold 25% aqueous ammonia solution (12.5 mL) was added and the dark brown solution was stirred under nitrogen for 30 minutes at 0 °C. The round-bottom flask was sealed with a rubber stopper and left to stir at room temperature overnight. The ethanol was removed by rotary evaporation and the brown residue was extracted with 100 mL aliquots of diethyl ether until the ether layer remained clear. The yellow liquid was concentrated *in vacuo*. The yellow-brown oil was dried under vacuum and yellow prisms formed on the side of the round-bottom flask. Recrystallisation was done from ethyl acetate to yield ligand **1** (1.62 g, 22.1%) as yellow-orange crystals.

Method 3

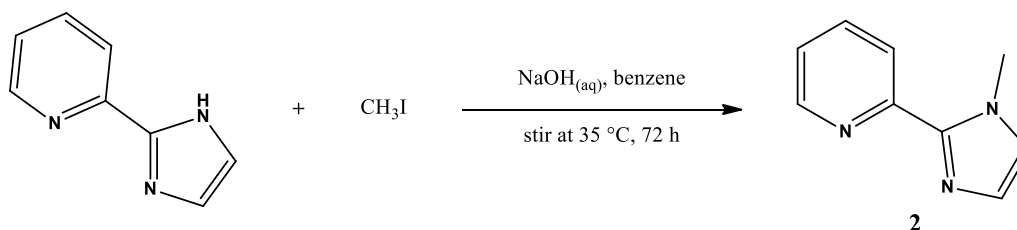
A 250 mL round-bottom flask was charged with 40% aqueous glyoxal solution (10.0 mL) and ethanol (8.00 mL). After the solution was cooled to 0 °C, ice cold 25% aqueous ammonia solution (12.5 mL) was added and stirred for 30 minutes. Cold pyridine-2-carboxaldehyde (5.39 g, 50.0 mmol) was slowly added and the dark brown solution was stirred for 30 minutes at 0 °C and left to stir at room temperature overnight. The ethanol was removed by rotary evaporation and the brown residue was extracted with 100 mL aliquots of diethyl ether until the ether layer remained clear. The yellow liquid was concentrated *in vacuo*. The yellow-brown oil was subjected to vacuum distillation using a kugelrohr short path distillation apparatus. This resulted in the formation of ligand **1** as yellow-orange crystals (3.07 g, 42.0%).



IR (ATR, cm^{-1}) 2888 (br C–H str), 1593 (pyridine C=N str), 1567 (imidazole C=N str). **^1H NMR (300 MHz, CDCl_3)** δ 8.49 (ddd, $J = 4.9, 1.7, 1.0$ Hz, H_2 , 1H), 8.22 (dt, $J = 8.0, 1.1$ Hz, H_5 , 1H), 7.78 (td, $J = 7.6, 1.7$ Hz, H_1 , 1H), 7.26 (ddd, $J = 7.5, 4.9, 1.2$ Hz, H_6 , 1H), 7.17 (s, H_{9-10} , 2H). **^{13}C NMR (300 MHz, CDCl_3)** δ 148.8 (C_7), 148.6 (C_2), 146.4 (C_4), 137.5 (C_6), 130.4 (C_{9-10}), 123.3 (C_1), 120.3 (C_5).

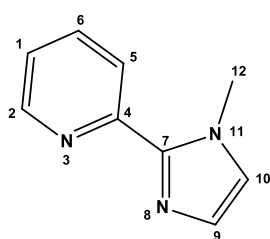
Expected mass ($\text{g}\cdot\text{mol}^{-1}$) 145.1643. **ESI-MS m/z** 146.0718 ($\text{M} + \text{H}^+$). **EA calculated (%)** C, 66.19; H, 4.86; N, 28.95. **EA found (%)** C, 66.13; H, 4.71; N, 28.10. **m.p.** 132–133 °C. See the full range of spectra on the CD supplied with this thesis.

2.3.2 Synthesis of 2-(1-methyl-imidazol-2-yl)pyridine (2)



Scheme 2.2: Synthetic route to 2-(1-methyl-imidazol-2-yl)pyridine (2). [Adapted from Wang *et al.*⁹]

A 250 mL round-bottom flask was charged with 2-(1*H*-imidazol-2-yl)pyridine (4.04 g, 27.8 mmol), 40% aqueous NaOH (20.0 mL) and benzene (50.0 mL) and stirred for 1 hour at ambient temperature. Iodomethane (7.10 g, 50.0 mmol) was added dropwise and the mixture was stirred at 35 °C for 72 hours. After the mixture was allowed to cool to room temperature, the organic layer was separated from the aqueous layer and dried over Na₂SO₄ overnight. The Na₂SO₄ was filtered off and the solvent was removed under reduced pressure yielding ligand **2** (3.51 g, 79.2%) as yellow-brown oil. No further purification was necessary.

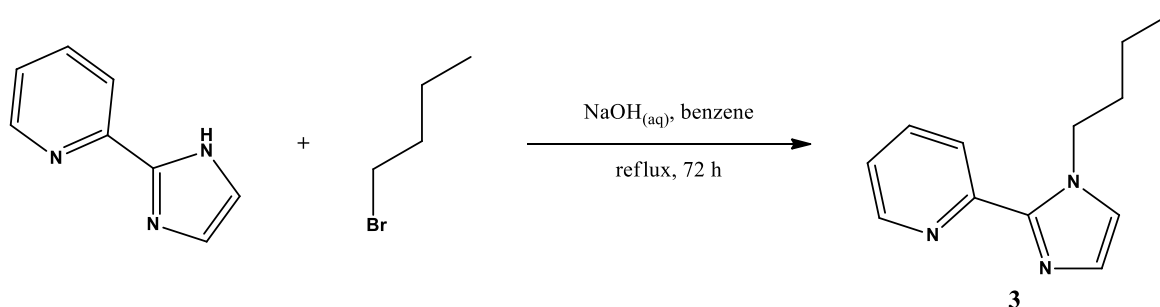


IR (ATR, cm⁻¹) 3103 (aromatic C–H str), 2953 (aliphatic C–H str), 1587 (pyridine C=N str), 1565 (imidazole C=N str). **¹H NMR (300 MHz, CDCl₃)** δ 8.55 (ddd, *J* = 4.9, 1.8, 0.9 Hz, *H*₂, 1H), 8.15 (dt, *J* = 8.0, 0.9 Hz, *H*₅, 1H), 7.72 (td, *J* = 7.7, 2.0 Hz, *H*₁, 1H), 7.19 (ddd, *J* = 6.2, 4.9, 1.2 Hz, *H*₆, 1H), 7.10 (d, *J* = 1.1 Hz, *H*₉, 1H), 6.95 (d, *J* = 1.1 Hz, *H*₁₀, 1H), 4.10 (s, *H*₁₂, 3H). **¹³C NMR (300 MHz, CDCl₃)** δ

150.9 (*C*₇), 148.3 (*C*₂), 145.1 (*C*₄), 136.6 (*C*₆), 128.3 (*C*₉), 124.5 (*C*₁₀), 122.7 (*C*₁), 122.4 (*C*₅), 36.4 (*C*₁₂).

Expected mass (g.mol⁻¹) 159.1911. **ESI-MS *m/z*** 160.0871 (M + H)⁺. **EA calculated (%)** C, 67.90; H, 5.70; N, 26.40. **EA found (%)** C, 68.12; H, 5.49; N, 26.08. See the full range of spectra on the CD supplied with this thesis.

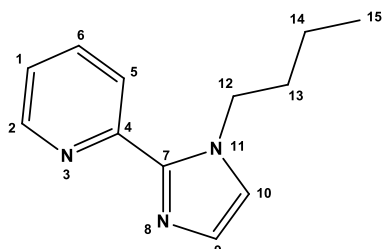
2.3.3 Synthesis of 2-(1-butyl-imidazol-2-yl)pyridine (3)



Scheme 2.3: Synthetic route to 2-(1-butyl-imidazol-2-yl)pyridine (3). [Adapted from Wang *et al.*⁹]

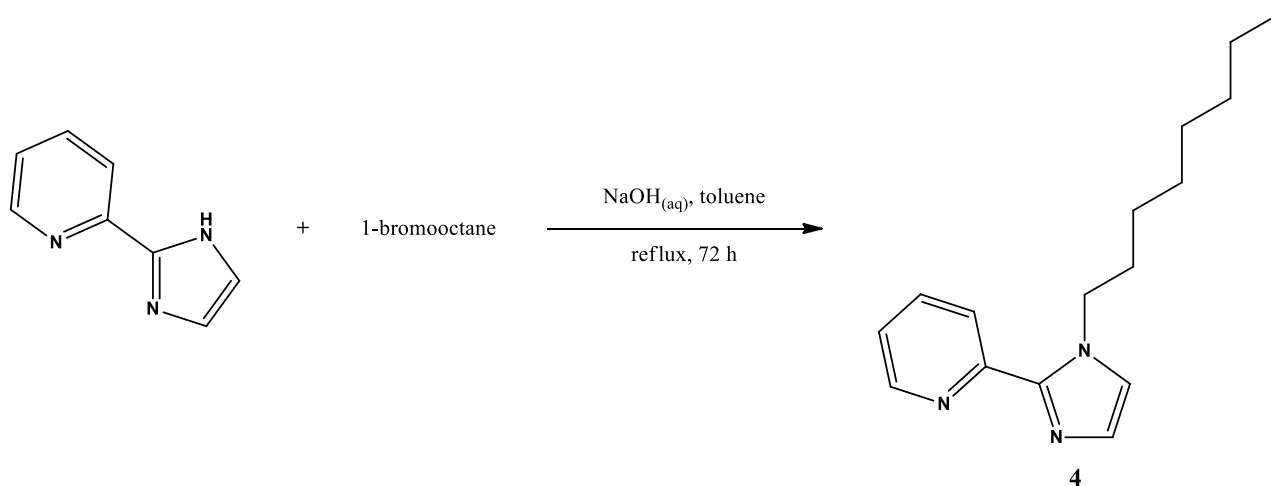
A mixture of 2-(1*H*-imidazol-2-yl)pyridine (1.00 g, 6.89 mmol) and 40% aqueous NaOH (5.00 mL) in benzene (20.0 mL) was stirred for 1 hour at room temperature. Excess 1-bromobutane (1.89 g, 13.8 mmol)

was slowly added and the resulting mixture was refluxed for 72 hours. Once the reflux period concluded, the mixture was allowed to cool to room temperature. The orange-brown organic layer was separated from the aqueous layer and dried over Na₂SO₄. The Na₂SO₄ was filtered off and the solvent was removed under reduced pressure on a rotary evaporator. Further removal of trace amounts of solvent and excess 1-bromobutane was removed by using a high vacuum system. This led to the yield of ligand **3** (1.10 g, 79.4%) as clear brown oil with no additional purification needed.



IR (ATR, cm⁻¹) 3101 (aromatic C–H str), 2956 (aliphatic C–H str), 1587 (pyridine C=N str), 1565 (imidazole C=N str), 1458 (–CH₂– bend), 1378 (–CH₃ bend). **¹H NMR (600 MHz, CDCl₃)** δ 8.55 (ddd, *J* = 4.8, 1.7, 0.9 Hz, *H*₂, 1H), 8.15 (dt, *J* = 8.0, 0.9 Hz, *H*₅, 1H), 7.72 (td, *J* = 7.7, 2.0 Hz, *H*₁, 1H), 7.19 (ddd, *J* = 6.8, 4.9, 1.6 Hz, *H*₆, 1H), 7.10 (d, *J* = 1.0 Hz, *H*₉, 1H), 6.99 (d, *J* = 1.0 Hz, *H*₁₀, 1H), 4.59 (t, *J* = 7.4 Hz, *H*₁₂, 2H), 1.76 (p, *J* = 7.4 Hz, *H*₁₃, 2H), 1.33 (sex, *J* = 7.4 Hz, *H*₁₄, 2H), 0.90 (t, *J* = 7.4 Hz, *H*₁₅, 3H). **¹³C NMR (600 MHz, CDCl₃)** δ 151.0 (*C*₇), 148.3 (*C*₂), 144.5 (*C*₄), 136.6 (*C*₆), 128.3 (*C*₉), 123.3 (*C*₁₀), 122.9 (*C*₅), 122.4 (*C*₁), 48.2 (*C*₁₂), 33.5 (*C*₁₃), 19.9 (*C*₁₄), 13.8 (*C*₁₅). **Expected mass (g.mol⁻¹)** 201.2715. **ESI-MS *m/z*** 202.1335 (*M* + *H*)⁺. **EA calculated (%)** C, 71.61; H, 7.51; N, 20.88. **EA found (%)** C, 71.64; H, 7.43; N, 20.57. See the full range of spectra on the CD supplied with this thesis.

2.3.4 Synthesis of 2-(1-octyl-imidazol-2-yl)pyridine (4)



Scheme 2.4: Synthetic route to 2-(1-octyl-imidazol-2-yl)pyridine (**4**). [Adapted from Wang *et al.*⁹]

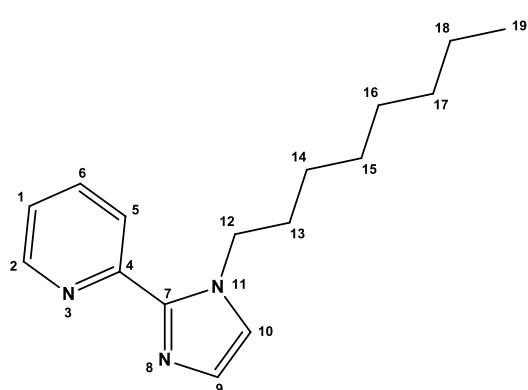
Method 1

A mixture of 2-(1*H*-imidazol-2-yl)pyridine (1.00 g, 6.89 mmol) and 40% aqueous NaOH (6.00 mL) in toluene (30.0 mL) was stirred for 1 hour at room temperature. A slight excess of 1-bromooctane (1.50 g, 7.77 mmol) was slowly added and the mixture was refluxed for 72 hours. After the resulting mixture was allowed to cool to room temperature, the yellow-brown organic layer was separated from the aqueous layer and dried over Na₂SO₄. After the drying agent was filtered off, the solvent was removed under reduced

pressure on a rotary evaporator. Purification was achieved by vacuum distillation using a kugelrohr short path distillation apparatus, yielding ligand **4** (1.41 g, 79.6%) as pale yellow oil.

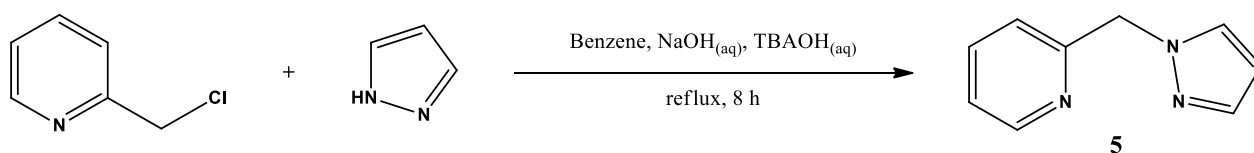
Method 2

A mixture of 2-(1*H*-imidazol-2-yl)pyridine (1.00 g, 6.89 mmol) and 40% aqueous NaOH (6.00 mL) in toluene (30.0 mL) was stirred for 1 hour at room temperature. A slight excess of 1-bromooctane (1.50 g, 7.77 mmol) was slowly added and the mixture was refluxed for 72 hours. After the resulting mixture was allowed to cool to room temperature, the yellow-brown organic layer was separated from the aqueous layer and dried over Na₂SO₄. After the drying agent was filtered off, the solvent was removed under reduced pressure on a rotary evaporator. Purification was done by column chromatography on silica gel using ethyl acetate as eluent, yielding ligand **4** (1.50 g, 84.6%, R_f = 0.70) as pale yellow oil.



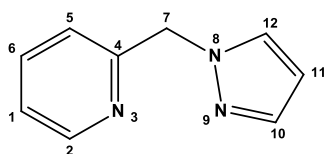
IR (ATR, cm⁻¹) 3044 (aromatic C–H str), 2922 (aliphatic C–H str), 1588 (pyridine C=N str), 1565 (imidazole C=N str), 1459 (–CH₂– bend), 1376 (–CH₃ bend). **¹H NMR (600 MHz, CDCl₃)** δ 8.55 (ddd, *J* = 4.8, 1.7, 0.9 Hz, *H*₂, 1H), 8.16 (dt, *J* = 8.0, 0.9 Hz, *H*₅, 1H), 7.72 (td, *J* = 7.7, 2.0 Hz, *H*₁, 1H), 7.19 (ddd, *J* = 6.8, 4.9, 1.6 Hz, *H*₆, 1H), 7.11 (d, *J* = 1.1 Hz, *H*₉, 1H), 6.99 (d, *J* = 1.1 Hz, *H*₁₀, 1H), 4.58 (t, *J* = 7.4 Hz, *H*₁₂, 2H), 1.78 (p, *J* = 7.4 Hz, *H*₁₃, 2H), 1.29 – 1.20 (m, *H*₁₄–18, 10H), 0.85 (t, *J* = 7.1 Hz, *H*₁₉, 3H). **¹³C NMR (400 MHz, CDCl₃)** δ 150.9 (*C*₇), 148.4 (*C*₂), 144.5 (*C*₄), 136.6 (*C*₆), 128.2 (*C*₉), 123.3 (*C*₁₀), 122.9 (*C*₅), 122.4 (*C*₁), 48.5 (*C*₁₂), 31.9 (*C*₁₃), 31.4 (*C*₁₄), 29.2 (*C*₁₅), 29.2 (*C*₁₆), 26.7 (*C*₁₇), 22.7 (*C*₁₈), 14.2 (*C*₁₉). **Expected mass (g.mol⁻¹)** 257.3787. **ESI-MS *m/z*** 258.1973 (*M* + *H*)⁺. **EA calculated (%)** C, 74.67; H, 9.01; N, 16.33. **EA found (%)** C, 75.31; H, 8.87; N, 16.41. See the full range of spectra on the CD supplied with this thesis.

2.3.5 Synthesis of 2-(1'-pyrazolyl)-methylpyridine (**5**)



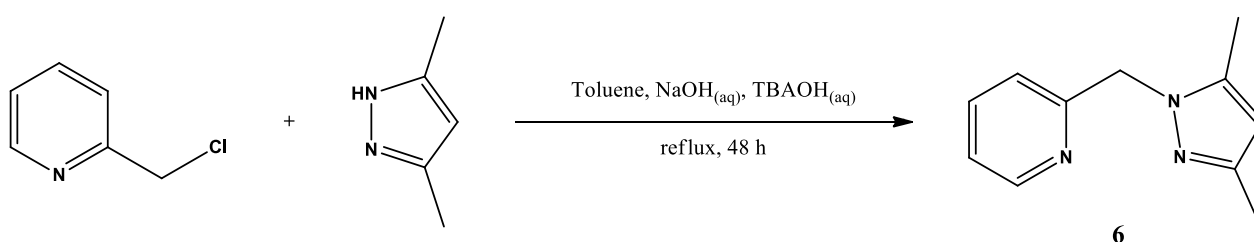
Scheme 2.5: Synthetic route to 2-(1'-pyrazolyl)-methylpyridine (**5**). [Adapted from Watson *et al.*¹⁰]

Tetrabutylammonium hydroxide (18 drops) and 40% aqueous NaOH (54.0 mL) was added to a 250 mL round-bottom flask containing a mixture of 2-(chloromethyl)pyridine hydrochloride (3.00 g, 18.3 mmol) and pyrazole (1.25 g, 18.3 mmol) in benzene (80.0 mL). The solution was refluxed for 8 hours and left to stir at room temperature overnight. The yellow organic layer was separated from the clear aqueous layer, dried over anhydrous Na₂SO₄ and concentrated *in vacuo* to yield ligand **5** (2.61 g, 89.7%) as yellow oil. No further purification was necessary.



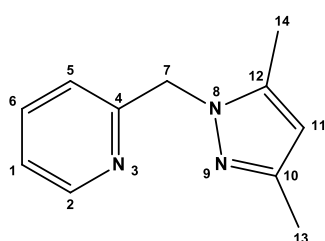
IR (ATR, cm^{-1}) 3104 (aromatic C–H str), 2937 (aliphatic C–H str), 1593 (pyridine C=N str), 1571 (pyrazole C=N str), 1475 ($-\text{CH}_2-$ bend). **^1H NMR (600 MHz, CDCl_3)** δ 8.54 (ddd, $J = 4.9, 1.6, 0.9$ Hz, H_2 , 1H), 7.61 (td, $J = 7.7, 1.8$ Hz, H_1 , 1H), 7.55 (d, $J = 1.6$ Hz, H_{10} , 1H), 7.51 (d, $J = 2.3$ Hz, H_{12} , 1H), 7.20 – 7.16 (m, H_6 , 1H), 6.95 (d, $J = 7.9$ Hz, H_5 , 1H), 6.29 (t, $J = 2.1$ Hz, H_{11} , 1H), 5.43 (s, H_7 , 2H). **^{13}C NMR (400 MHz, CDCl_3)** δ 156.8 (C_4), 149.5 (C_2), 140.0 (C_{10}), 137.2 (C_6), 130.0 (C_{12}), 122.8 (C_1), 121.8 (C_5), 106.3 (C_{11}), 57.6 (C_7). **Expected mass ($\text{g}\cdot\text{mol}^{-1}$)** 159.1911. **ESI-MS m/z** 160.0876 ($\text{M} + \text{H}^+$). **EA calculated (%)** C, 67.90; H, 5.70; N, 26.40. **EA found (%)** C, 67.63; H, 5.75; N, 25.42. See the full range of spectra on the CD supplied with this thesis.

2.3.6 Synthesis of 2-(3,5-dimethyl-pyrazol-1-yl)-methylpyridine (6) (6)



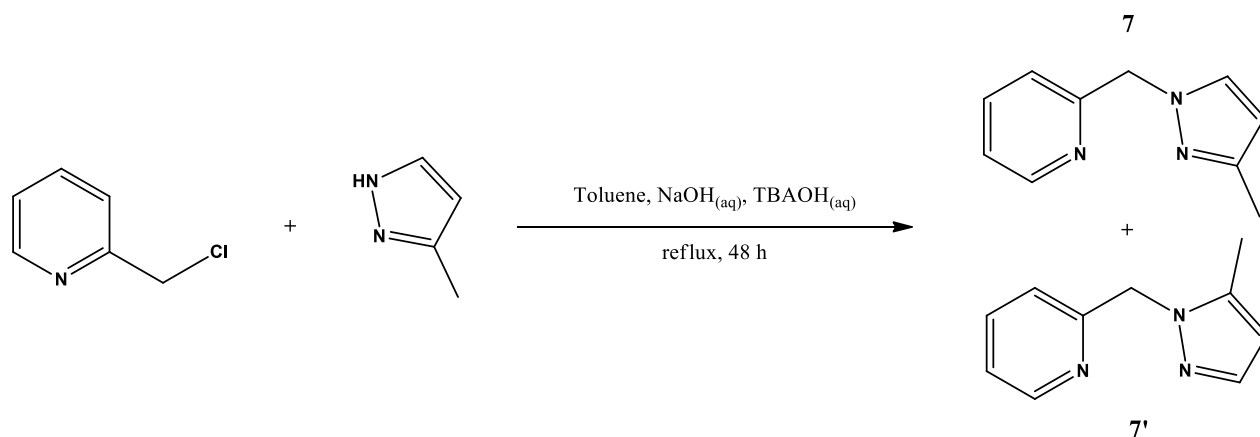
Scheme 2.6: Synthetic route to 2-(3,5-dimethyl-pyrazol-1-yl)-methylpyridine (6). [Adapted from Watson *et al.*¹⁰]

A mixture of 2-(chloromethyl)pyridine hydrochloride (3.00 g, 18.3 mmol), 3,5-dimethylpyrazole (1.76 g, 18.3 mmol), toluene (80.0 mL), 40% aqueous NaOH (50.0 mL) and tetrabutylammonium hydroxide (18 drops) was refluxed for 48 hours. After allowing the mixture to cool to room temperature, the yellow organic layer was separated from the aqueous layer, dried over anhydrous Na_2SO_4 , filtered and concentrated *in vacuo* to yield ligand **6** (2.44 g, 71.3%) as yellow-brown oil. No further purification was required.



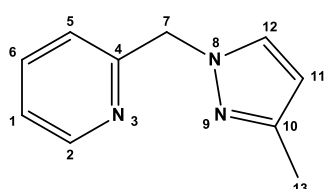
IR (ATR, cm^{-1}) 3200 (aromatic C–H str), 2919 (aliphatic C–H str), 1592 (pyridine C=N str), 1570 (pyrazole C=N str), 1462 ($-\text{CH}_2-$ bend), 1383 ($-\text{CH}_3$ bend), 1349 (C–N str). **^1H NMR (400 MHz, CDCl_3)** δ 8.53 (ddd, $J = 4.9, 1.6, 0.8$ Hz, H_2 , 1H), 7.58 (td, $J = 7.7, 1.8$ Hz, H_1 , 1H), 7.14 (ddd, $J = 7.1, 5.3, 0.5$ Hz, H_6 , 1H), 6.77 (d, $J = 7.9$ Hz, H_5 , 1H), 5.86 (s, H_{11} , 1H), 5.32 (s, H_7 , 2H), 2.24 (s, H_{13} , 3H), 2.16 (s, H_{14} , 3H). **^{13}C NMR (400 MHz, CDCl_3)** δ 157.4 (C_4), 149.2 (C_2), 148.0 (C_{10}), 139.7 (C_{12}), 137.1 (C_6), 122.4 (C_1), 120.9 (C_5), 105.7 (C_{11}), 54.4 (C_7), 13.6 (C_{13}), 11.1 (C_{14}). **Expected mass ($\text{g}\cdot\text{mol}^{-1}$)** 187.2447. **ESI-MS m/z** 188.1182 ($\text{M} + \text{H}^+$). **EA calculated (%)** C, 70.56; H, 7.00; N, 22.44. **EA found (%)** C, 70.18; H, 6.81; N, 22.04. See the full range of spectra on the CD supplied with this thesis.

2.3.7 Synthesis of an isomeric mixture of 2-(3-methyl-pyrazol-1-yl)-methylpyridine and 2-(5-methyl-pyrazol-1-yl)-methylpyridine (7) & (7')



Scheme 2.7: Synthetic route to the isomeric mixture of 2-(3-methyl-pyrazol-1-yl)-methylpyridine (7) and 2-(5-methyl-pyrazol-1-yl)-methylpyridine (7'). [Adapted from Watson *et al.*¹⁰]

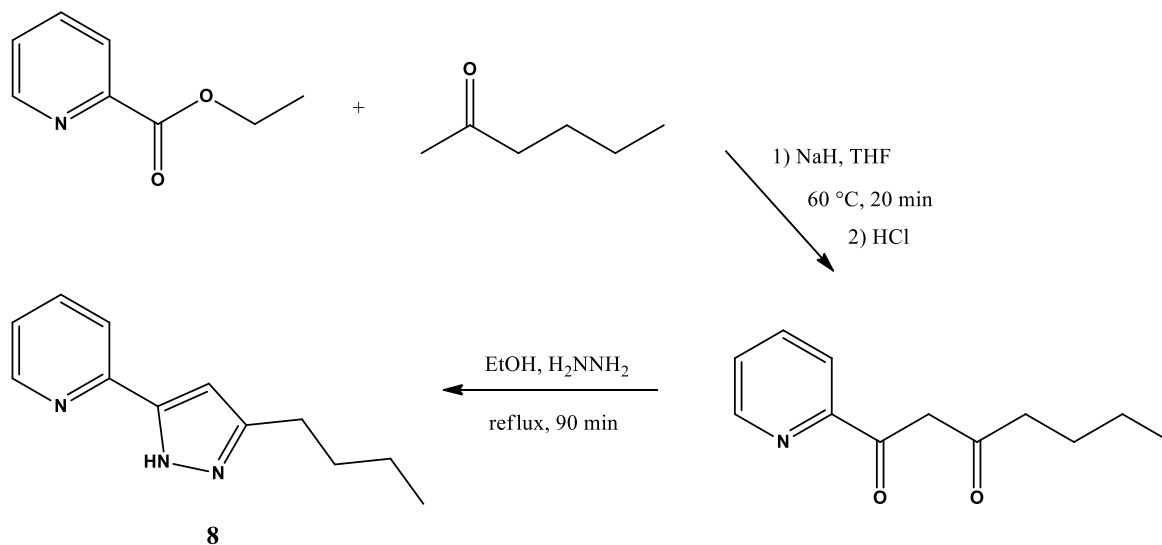
A 250 mL round-bottom flask was charged with 2-(chloromethyl)pyridine hydrochloride (3.00 g, 18.3 mmol), 3-methylpyrazole (1.50 g, 18.3 mmol), toluene (80.0 mL), 40% aqueous NaOH (50.0 mL) and tetrabutylammonium hydroxide (18 drops). While stirring, the solution was refluxed for 48 hours. Once the mixture was allowed to cool to room temperature, the yellow organic layer was separated and dried over anhydrous Na₂SO₄. The solvent was evaporated under reduced pressure to yield an isomeric mixture of ligands 7 and 7' (2.29 g, 72.3%) as yellow-brown oil.



IR (ATR, cm⁻¹) 2930 (aliphatic C–H str), 1592 (pyridine C=N str), 1570 (pyrazole C=N str), 1475 (–CH₂– bend). **Expected mass (g.mol⁻¹)** 173.2179. **ESI-MS *m/z*** 174.1031 (M + H)⁺. **EA calculated (%)** C, 69.34; H, 6.40; N, 24.26. **EA found (%)** C, 68.64; H, 6.23; N, 23.59. See **RESULTS AND**

DISCUSSION for ¹H and ¹³C NMR results. See the full range of spectra on the CD supplied with this thesis.

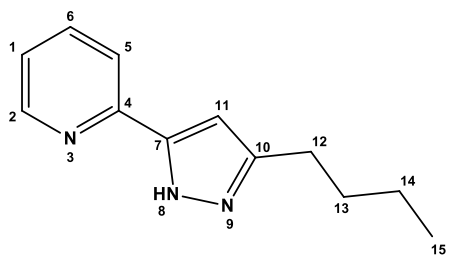
2.3.8 Synthesis of 2-(3-butyl-pyrazol-5-yl)pyridine (8) (8)



Scheme 2.8: Synthetic route to 2-(3-butyl-pyrazol-5-yl)pyridine (8). [Adapted from Satake and Nakata¹¹]

2-Hexanone was added to a suspension of NaH (60 wt% in mineral oil, 3.20 g, 80.0 mmol) in THF (40.0 mL). The resulting mixture was stirred at room temperature for 20 minutes and then heated to 60 °C. To the heated mixture, ethyl 2-picolinate (7.56 g, 50.0 mmol) in THF (40.0 mL) was added dropwise and allowed to stir at 60 °C for 20 minutes. The mixture was cooled to 0 °C and dilute HCl solution was added to the mixture until the pH was in the range 8–9. The mixture was extracted with diethyl ether (20.0 mL × 5) and the combined organic layers were washed with brine, dried over anhydrous MgSO₄ and concentrated *in vacuo* to give the crude intermediary product, 1-(pyridin-2-yl)heptane-1,3-dione, as yellow oil.

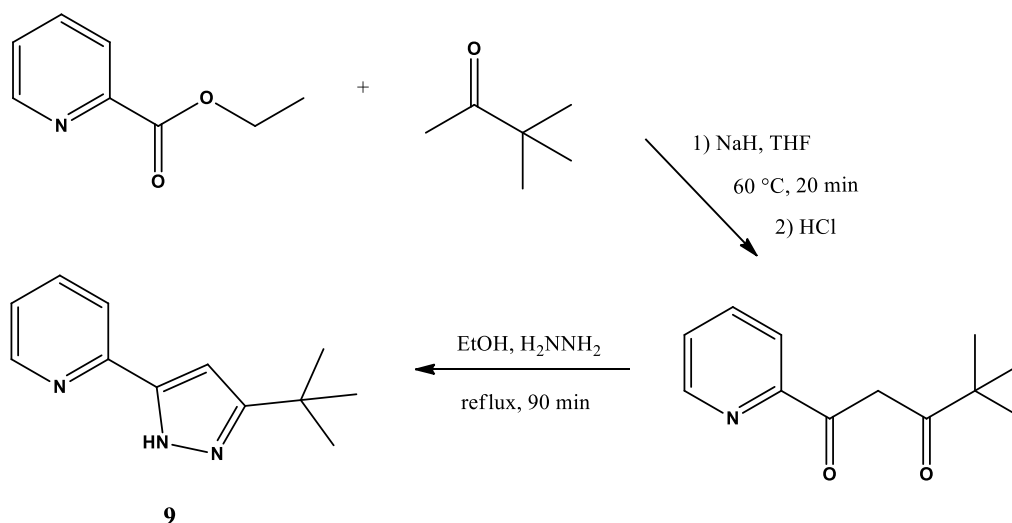
To a refluxing solution of the crude intermediary product in ethanol (100 mL) was added hydrazine monohydrate (5.51 g, 110 mmol) in ethanol (20.0 mL) over a period of 10 minutes. After the mixture was refluxed for 90 minutes, the solvent was removed under reduced pressure. Purification was done by column chromatography on silica gel, initially using toluene as eluent ($R_f = 0.211$) to rid the sample of impurities. The eluent was then changed to ethyl acetate ($R_f = 0.810$) to flush the product out of the column. The solvent was removed on a high vacuum system to yield ligand 8 (2.98 g, 29.6%) as pale yellow oil.



IR (ATR, cm⁻¹) 3180 (aromatic C–H str), 2954 (aliphatic C–H str), 1594 (pyridine C=N str), 1565 (pyrazole C=N str), 1464 (–CH₂– bend), 1149 (C–N str). **¹H NMR (600 MHz, CDCl₃)** δ 8.61 (d, $J = 4.6$ Hz, *H*₂, 1H), 7.76 (d, $J = 7.9$ Hz, *H*₅, 1H), 7.67 (td, $J = 7.8$, 1.6 Hz, *H*₁, 1H), 7.16 (dd, $J = 6.9$, 5.3 Hz, *H*₆, 1H), 6.60 (s, *H*₁₁, 1H), 2.66 (t, $J = 7.7$ Hz, *H*₁₂, 2H), 1.64 (q, $J = 7.7$ Hz, *H*₁₃, 2H), 1.36 (hex, $J = 7.7$ Hz, *H*₁₄, 2H), 0.89 (t, $J = 7.3$ Hz, *H*₁₅, 3H). **¹³C NMR (600 MHz, CDCl₃)** δ 150.8 (*C*₄), 150.3 (*C*₇), 149.3 (*C*₂), 146.7 (*C*₁₀), 136.9 (*C*₆), 122.6 (*C*₁), 120.1 (*C*₅), 102.1 (*C*₁₁), 31.6 (*C*₁₂), 26.9 (*C*₁₃), 22.4 (*C*₁₄), 13.9 (*C*₁₅). **Expected mass (g.mol⁻¹)** 201.2715. **ESI-MS *m/z*** 202.1335 (*M* + *H*)⁺. **EA**

calculated (%) for $C_{12}H_{15}N_3 \cdot 0.1 C_7H_8$ (toluene) C, 72.47; H, 7.57; N, 19.96. EA found (%) C, 72.32; H, 7.62; N, 19.83. See the full range of spectra on the CD supplied with this thesis.

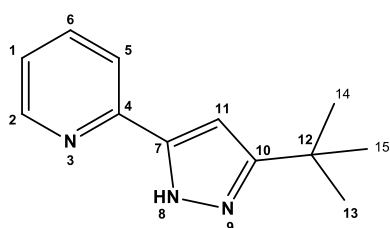
2.3.9 Synthesis of 2-[3-(*tert*-butyl)-pyrazol-5-yl]pyridine (9)



Scheme 2.9: Synthetic route to 2-[3-(*tert*-butyl)-pyrazol-5-yl]pyridine (9). [Adapted from Satake and Nakata¹¹]

3,3-Dimethyl-2-butanone was added to a suspension of NaH (60 wt% in mineral oil, 3.20 g, 80.0 mmol) in THF (40.0 mL). The resulting mixture was stirred at room temperature for 20 minutes and then heated to 60 °C. To the heated mixture, ethyl 2-picolinate (7.56 g, 50.0 mmol) in THF (40.0 mL) was added dropwise and allowed to stir at 60 °C for 20 minutes. The mixture was cooled to 0 °C and dilute HCl solution was added to the mixture until the pH was in the range 8–9. The mixture was extracted with diethyl ether (20.0 mL \times 5) and the combined organic layers were washed with brine, dried over anhydrous $MgSO_4$ and concentrated *in vacuo* to give the crude intermediary product, 4,4-dimethyl-1-(pyridin-2-yl)pentane-1,3-dione, as yellow oil.

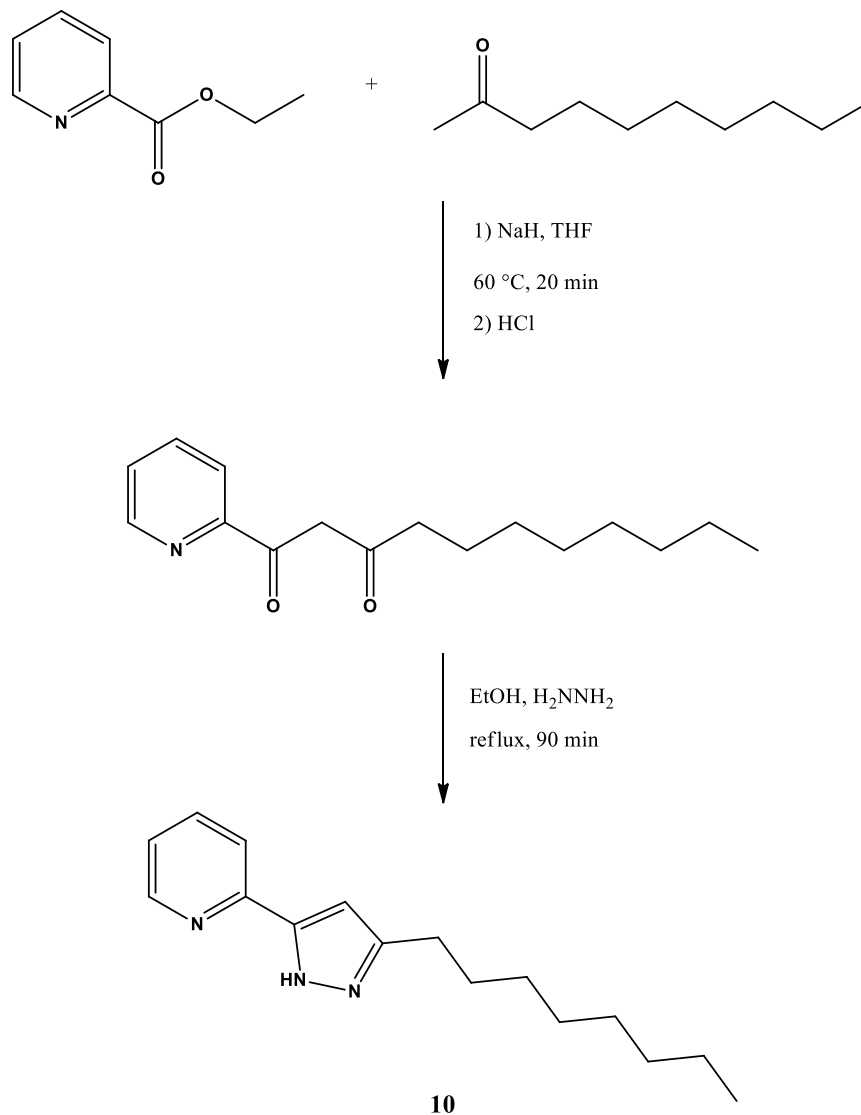
To a refluxing solution of the crude intermediary product in ethanol (100 mL) was added hydrazine monohydrate (5.51 g, 110 mmol) in ethanol (20.0 mL) over a period of 10 minutes. After the mixture was refluxed for 90 minutes, the solvent was removed under reduced pressure. Purification was done by column chromatography on silica gel, initially using toluene as eluent ($R_f = 0.202$) to flush out the impurities. The eluent was then changed to ethyl acetate ($R_f = 0.798$) to get the sample off the silica gel column. The solvent was removed on a high vacuum system to yield ligand 9 (2.63 g, 26.1%) as white solid.



IR (ATR, cm^{-1}) 3186 (aromatic C–H str), 2956 (aliphatic C–H str), 1595 (pyridine C=N str), 1566 (pyrazole C=N str), 1458 ($-CH_3$ bend). **1H NMR (400 MHz, $CDCl_3$)** δ 8.60 (d, $J = 4.6$ Hz, H_2 , 1H), 7.82 (d, $J = 7.9$ Hz, H_5 , 1H), 7.68 (td, $J = 7.7, 1.8$ Hz, H_1 , 1H), 7.16 (ddd, $J = 7.4,$

4.9, 1.0 Hz, *H*₆, 1H), 6.67 (s, *H*₁₁, 1H), 1.36 (s, *H*₁₃₋₁₅, 9H). ¹³C NMR (600 MHz, CDCl₃) δ 159.2 (*C*₄), 150.5 (*C*₇), 149.4 (*C*₂), 146.9 (*C*₁₀), 136.8 (*C*₆), 122.5 (*C*₁), 120.1 (*C*₅), 99.9 (*C*₁₁), 31.7 (*C*₁₂), 30.5 (*C*₁₃₋₁₅). **Expected mass (g.mol⁻¹)** 201.2715. **ESI-MS *m/z*** 202.1335 (M + H)⁺. **EA calculated (%) for C₁₂H₁₅N₃ · 0.25 C₇H₈ (toluene)** C, 73.63; H, 7.64; N, 18.73. **EA found (%)** C, 73.69; H, 7.49; N, 18.89. **m.p.** 104–105 °C. See the full range of spectra on the CD supplied with this thesis.

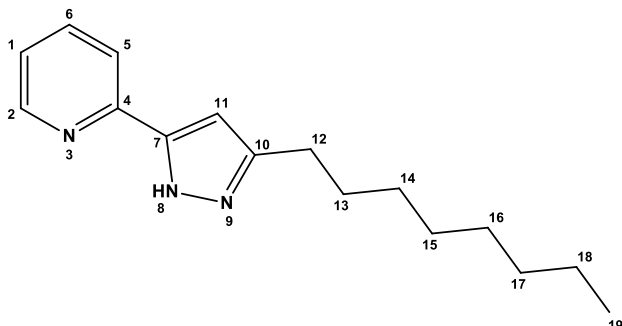
2.3.10 Synthesis of 2-(3-octyl-pyrazol-5-yl)pyridine (10) (10)



Scheme 2.10: Synthetic route to 2-(3-octyl-pyrazol-5-yl)pyridine (**10**). [Adapted from Satake and Nakata¹¹]

2-Decanone was added to a suspension of NaH (60 wt% in mineral oil, 3.20 g, 80.0 mmol) in THF (40.0 mL). The resulting mixture was stirred at room temperature for 20 minutes and then heated to 60 °C. To the heated mixture, ethyl 2-picolinate (7.56 g, 50.0 mmol) in THF (40.0 mL) was added dropwise and allowed to stir at 60 °C for 20 minutes. The mixture was cooled to 0 °C and dilute HCl solution was added to the mixture until the pH was in the range 8–9. The mixture was extracted with diethyl ether (20.0 mL × 5) and the combined organic layers were washed with brine, dried over anhydrous MgSO₄ and concentrated *in vacuo* to give the crude intermediary product, 1-(pyridin-2-yl)undecane-1,3-dione, as yellow oil.

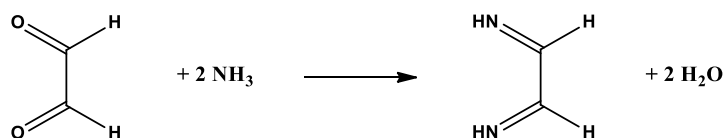
To a refluxing solution of the crude intermediary product in ethanol (100 mL) was added hydrazine monohydrate (5.51 g, 110 mmol) in ethanol (20.0 mL) over a period of 10 minutes. After the mixture was refluxed for 90 minutes, the solvent was removed under reduced pressure. Purification was done by column chromatography on silica gel, initially using toluene as eluent ($R_f = 0.111$) to flush out impurities. The eluent was then changed to ethyl acetate ($R_f = 0.742$) to get the sample off the silica gel column. The solvent was removed on a high vacuum system to yield ligand **10** (2.65 g, 26.3%) as off-white solid.



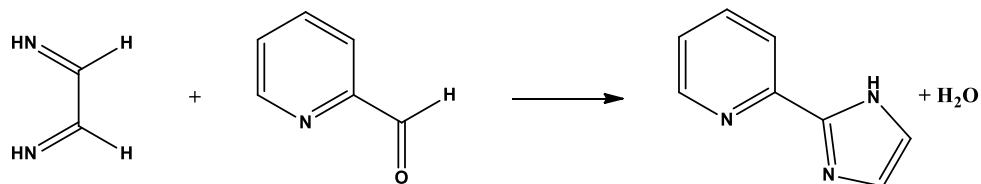
IR (ATR, cm^{-1}) 3252 (N–H str), 2916 (aliphatic C–H str), 1599 (pyridine C=N str), 1566 (pyrazole C=N str), 1473 (–CH₂– bend), 1453 (–CH₃ bend). **¹H NMR (600 MHz, CDCl₃)** δ 8.61 (d, $J = 4.7$ Hz, *H*2, 1H), 7.75 (d, $J = 7.9$ Hz, *H*5, 1H), 7.73 – 7.65 (m, *H*1, 1H), 7.23 – 7.15 (m, *H*6, 1H), 6.60 (s, *H*11, 1H), 2.68 (t, $J = 7.7$ Hz, *H*12, 2H), 1.69 (p, $J = 7.3$ Hz, *H*13, 2H), 1.42 – 1.18 (m, *H*14–18, 10H), 0.87 (t, $J = 6.9$ Hz, *H*19, 3H). **¹³C NMR (600 MHz, CDCl₃)** 151.4 (*C*4), 150.1 (*C*7), 149.4 (*C*2), 146.4 (*C*10), 136.9 (*C*6), 122.7 (*C*1), 120.1 (*C*5), 102.1 (*C*11), 32.0 (*C*12), 29.5 (*C*13), 29.5 (*C*14), 29.5 (*C*15), 29.4 (*C*16), 27.5 (*C*17), 22.8 (*C*18), 14.2 (*C*19). **Expected mass ($\text{g}\cdot\text{mol}^{-1}$)** 257.3787. **ESI-MS m/z** 258.1978 ($M + H$)⁺. **EA calculated (%)** C, 74.67; H, 9.01; N, 16.33. **EA found (%)** C, 74.89; H, 8.97; N, 16.30. **m.p.** 79–81 °C. See the full range of spectra on the CD supplied with this thesis.

2.4 Results and discussion

The synthesis of 2-(1*H*-imidazol-2-yl)pyridine (**1**) followed the classic Debus-Radziszewski synthetic approach for imidazoles.^{12,13} This synthetic pathway always includes the presence of three typical reagents: a dicarbonyl species, an aldehyde and two equivalents of ammonia. In the synthetic procedure of ligand **1**, ethanedial, or more typically known as glyoxal, acted as the dicarbonyl species, while pyridine-2-carboxaldehyde served as the source of aldehyde. Glyoxal and ammonia condensed to form ethane-1,2-diimine with two equivalents of water as the by-product (**Scheme 2.11**). Following this, the addition of pyridine-2-carboxaldehyde to the diimine species led to another condensation reaction whereby 2-(1*H*-imidazol-2-yl)pyridine (**1**) was formed (**Scheme 2.12**).



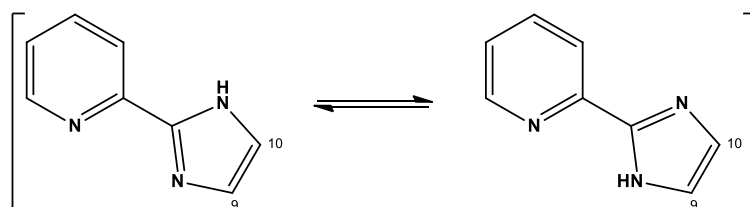
Scheme 2.11: The formation of the ethane-1,2-diimine from glyoxal and ammonia.



Scheme 2.12: The formation of 2-(1*H*-imidazol-2-yl)pyridine (**1**) from ethane-1,2-diimine and pyridine-2-carboxaldehyde.

In the synthesis of 2-(1*H*-imidazol-2-yl)pyridine (**1**), Gerber *et al.*⁸ reported a one-step reaction with a yield of 75%. This synthetic procedure (method 1) was followed to a tee, but somehow after several attempts we could never recreate such generous yields. Instead, we obtained yields of 10–26%. Since we needed several grams of this parent ligand for future alkylations, we adapted the procedure slightly in an attempt to increase the yield. We performed the synthesis under nitrogen gas, ridding the reaction flask of air (method 2). Additionally, we sealed the round-bottom flask with a rubber stopper to prevent the ammonia from escaping/leaking overnight. However, these slight modifications to the procedure did not pay off, as we obtained an even lower yield of 22%. Finally, we set out with another method adaptation (method 3) where we changed the addition order of pyridine-2-carboxaldehyde. Pyridine-2-carboxaldehyde was added after the combined mixture of glyoxal, ethanol and ammonia was stirred for 30 minutes at 0 °C. Following this, we purified the product by kugelrohr short path distillation instead of the classic recrystallisation technique. This led to needle-like crystals being formed on the inside of the kugelrohr bulb. This method proved to be somewhat successful, as our yield increased to 42%. We could still not, however, obtain yields as reported by Gerber *et al.*,⁸ but had a modified procedure that was slightly more successful in synthesising 2-(1*H*-imidazol-2-yl)pyridine (**1**), albeit extremely time consuming. It's important to note that methods 1, 2 and 3 must be done at 0 °C to limit the rate of evaporation of ammonia and the formation of unwanted side-products.

At first glance, the ¹H NMR spectrum of 2-(1*H*-imidazol-2-yl)pyridine (**1**) was slightly confusing. We expected to see six proton signals (excluding the NH proton), but only observed five. We came to the conclusion that we had a case of tautomerism, whereby the NH proton was loosely bound to the imidazolyl nitrogens with the double bond simultaneously shifting back and forth (**Scheme 2.13**).



Scheme 2.13: The rapid transition between the two tautomers of 2-(1*H*-imidazol-2-yl)pyridine (**1**).

Because of this tautomeric effect and induced quasi-symmetry, both protons *H*9 and *H*10 were in chemically equivalent environments. This meant that protons *H*9 and *H*10 would appear as a singlet instead of two distinct doublets. The singlet at 7.17 ppm integrates for two protons, indicating the merge of protons *H*9 and *H*10 (**Figure 2.2**). All other aromatic multiplet signals integrated for one, attesting to the fact that 2-(1*H*-imidazol-2-yl)pyridine (**1**) had indeed been successfully synthesised. Since protons *H*9 and *H*10 were in

chemically equivalent environments, carbons *C9* and *C10* should also theoretically be in chemically equivalent environments. This was confirmed by ^{13}C NMR, when one broad signal appeared at 130.6 ppm instead of two separate carbon signals (**Figure 2.3**).

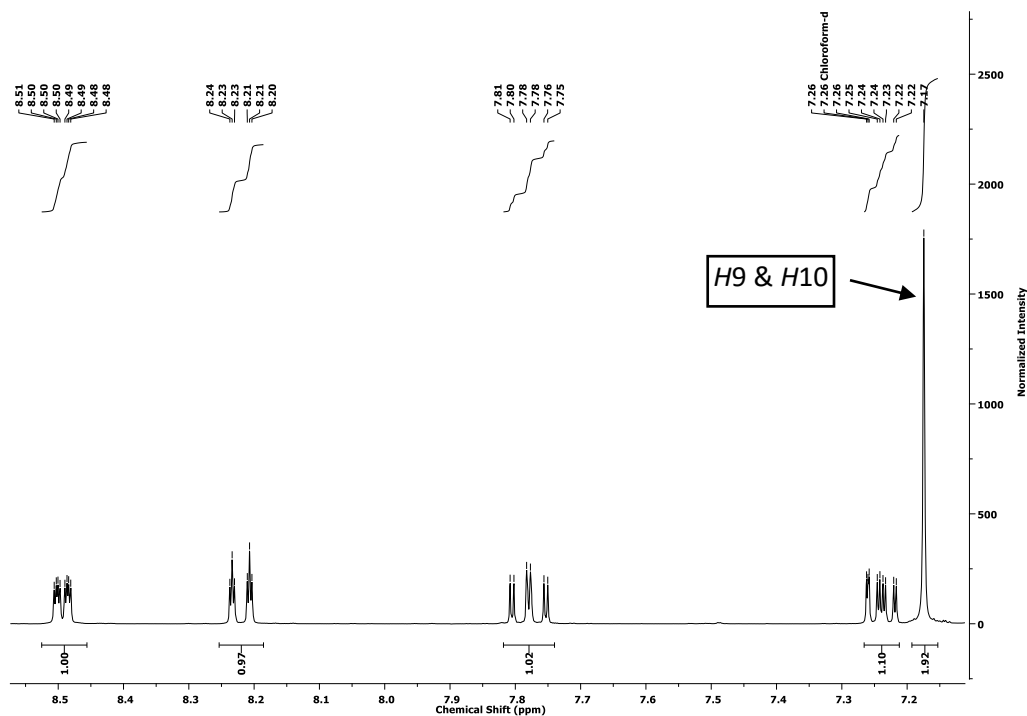


Figure 2.2: A zoomed in ^1H NMR spectrum of 2-(1*H*-imidazol-2-yl)pyridine (**1**), that highlights the singlet at 7.17 ppm of protons *H9* and *H10*.

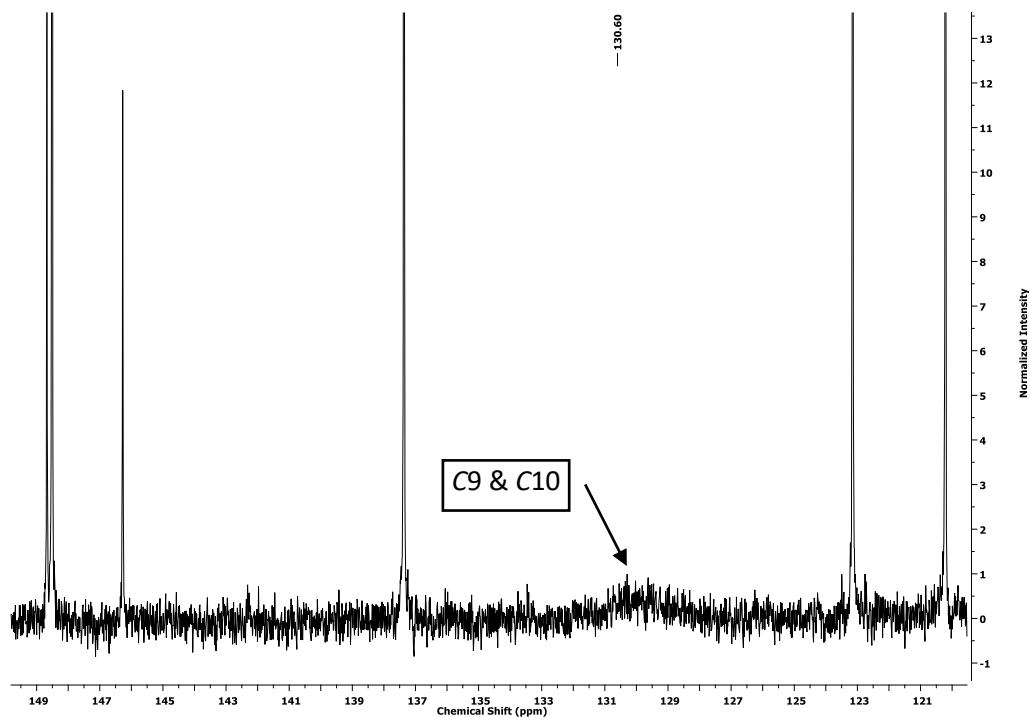
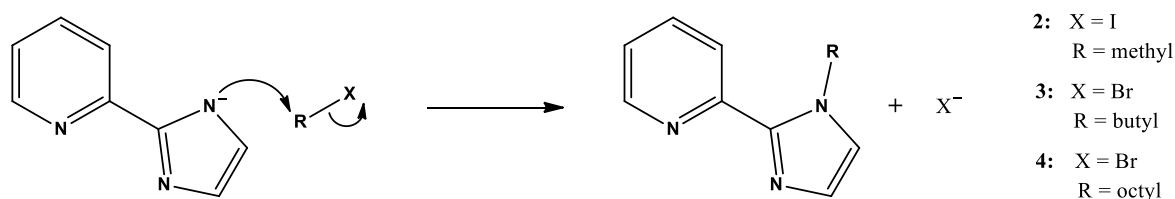


Figure 2.3: A zoomed in ^{13}C NMR spectrum of 2-(1*H*-imidazol-2-yl)pyridine (**1**), indicating the broad signal of carbons *C9* and *C10*.

The synthesis of 2-(1-methyl-imidazol-2-yl)pyridine (**2**), previously reported by Wang *et al.*,⁹ was adapted by using a different solvent and modified reaction conditions. Instead of *N,N*-dimethylformamide (DMF), benzene was used as solvent because of its lower boiling point and ease with which it can be removed by rotary evaporator. The sodium hydroxide acted as the base that deprotonated the nitrogen, resulting in a 2-(1*H*-imidazol-2-yl)pyridine sodium salt being formed. After the salt mixture was stirred for 1 hour, excess methyl iodide was slowly added and the resulting mixture was stirred at 35 °C for 72 hours. It was crucial that the temperature of the mixture remained below 42.4 °C as to avoid excessive evaporation of methyl iodide. Alternatively, a condenser could be used if higher temperatures are experimented with. After the mixture was cooled to room temperature, the organic layer was separated from the aqueous layer and dried over Na₂SO₄. The drying agent was filtered off and the solvent was removed under reduced pressure. This alkylation reaction went to completion after ± 3 days and the excess methyl iodide was easily removed under reduced pressure along with the solvent. We obtained an analytically pure yellow/brown product, that needed no further purification (79.2%). The yield was comparable to that reported by Wang *et al.*⁹ (82%).

In this simple nucleophilic substitution (S_N2) reaction, the deprotonated nitrogen acted as the nucleophile that attacked the electrophilic carbon of the methyl iodide. This was also true for all the alkylation reactions of 2-(1*H*-imidazol-2-yl)pyridine (**1**), whereby ligands **2**, **3** and **4** were formed (**Scheme 2.14**).



Scheme 2.14: Nucleophilic substitution (S_N2) mechanism by which ligands **2**, **3** and **4** were formed.

2-(1-Butyl-imidazol-2-yl)pyridine (**3**) was prepared in a similar manner to that of ligand **2**. The only difference was the removal of the excess haloalkane, 1-bromobutane, which had a higher boiling point (± 102 °C). This was easily achieved by placing the crude sample under a high vacuum system for 24 hours, ridding the product of excess haloalkane. Finally, a yellow/brown oil was retrieved in a 79.4% yield.

Like ligand **3**, 2-(1-octyl-imidazol-2-yl)pyridine (**4**) was also prepared in a similar manner to ligand **2**. Ligand **4**, however, had two distinctly different work-up procedures whereby the excess high boiling 1-bromooctane (201 °C) had to be removed. The first method (method 1) relied upon the distillation of the excess haloalkane under a high vacuum system, using a kugelrohr short path distillation apparatus. This setup includes the use of a high vacuum system as well as temperatures of up to 200 °C. The distillation process proved to be successful as a yield of 79.6% was obtained. It is important to note that a strong and effective vacuum pump should be used (pressure ≈ 0 bar) to avoid the use of high temperatures (> 120 °C), since the crude product started to decompose at ± 130 °C. In method 2 we tried to use a greener approach whereby we purified the crude product by gravitational column chromatography on silica gel with ethyl acetate as eluent. We obtained good separation between the product, 2-(1-octyl-imidazol-2-yl)pyridine, and

the starting material, 1-bromooctane. The eluent flushed out the desired product first, leaving the unwanted starting material on the column. After removing the ethyl acetate under vacuum, a pure sample of ligand **4** was obtained as a yellow/brown oil in an 84.6% yield. By using ^1H and ^{13}C NMR, we deduced that we have in fact successfully synthesised ligands **2**, **3** and **4**. This was attributed to the presence of four distinct signals in the aromatic region (7.1–8.6 ppm) and two doublet signals in the lower aromatic region (6.9–7.1 ppm). Previously we explained at length the appearance of a singlet for protons *H9* and *H10* in 2-(1*H*-imidazol-2-yl)pyridine (**1**), but since the nitrogen was alkylated, protons *H9* and *H10* were rendered chemically non-equivalent. This meant that the tautomeric form was not present and that protons *H9*/*H10* and carbons *C9*/*C10* should give rise to distinct signals (**Figure 2.4** and **Figure 2.5**). This was applicable to ligands **2**, **3** and **4** as well.

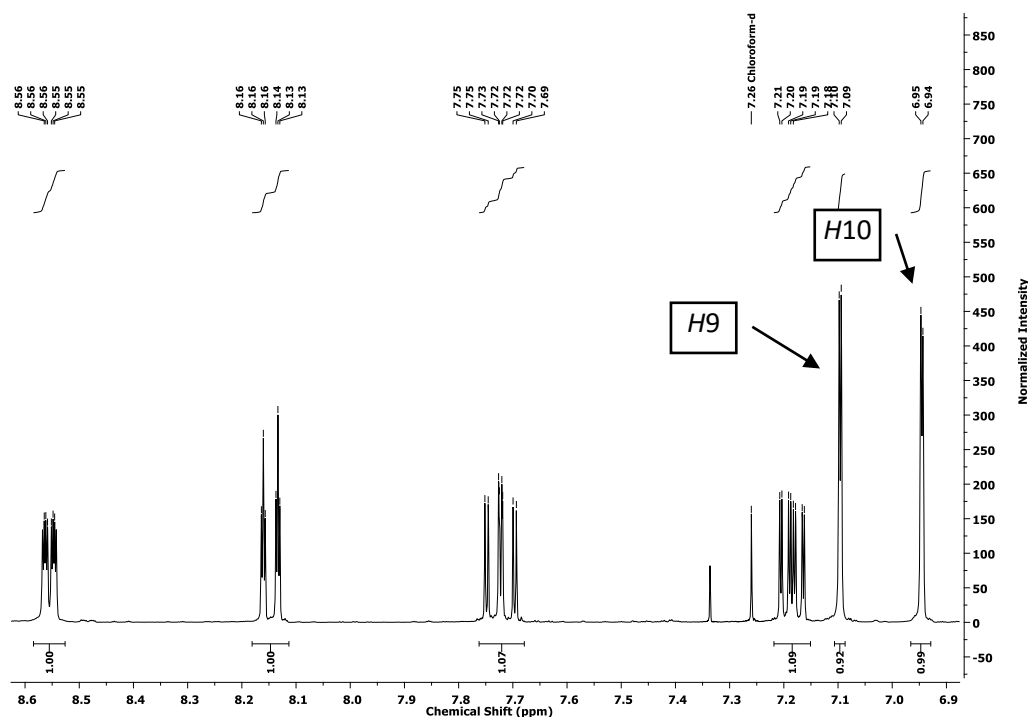


Figure 2.4: A zoomed in ^1H NMR of 2-(1-methyl-imidazol-2-yl)pyridine (**2**) clearly showing two distinct signals for protons *H9* and *H10*. This is representative of ligands **3** and **4** as well.

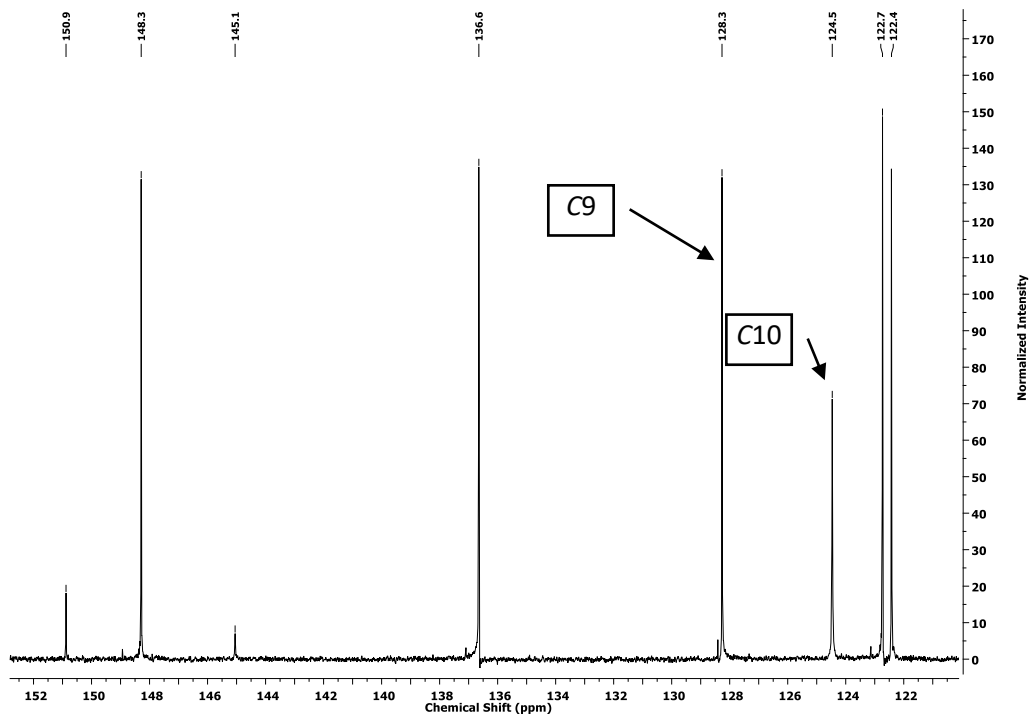


Figure 2.5: A zoomed in ^{13}C NMR of 2-(1-methyl-imidazol-2-yl)pyridine (**2**) clearly showing two distinct signals for carbons C9 and C10. This is representative of ligands **3** and **4** as well.

Furthermore, to prove that ligands **2**, **3** and **4** were successfully synthesised as a result of alkylation, we homed in on the alkyl region (0–5 ppm) of the ^1H NMR spectra for these ligands (**Figure 2.6**).

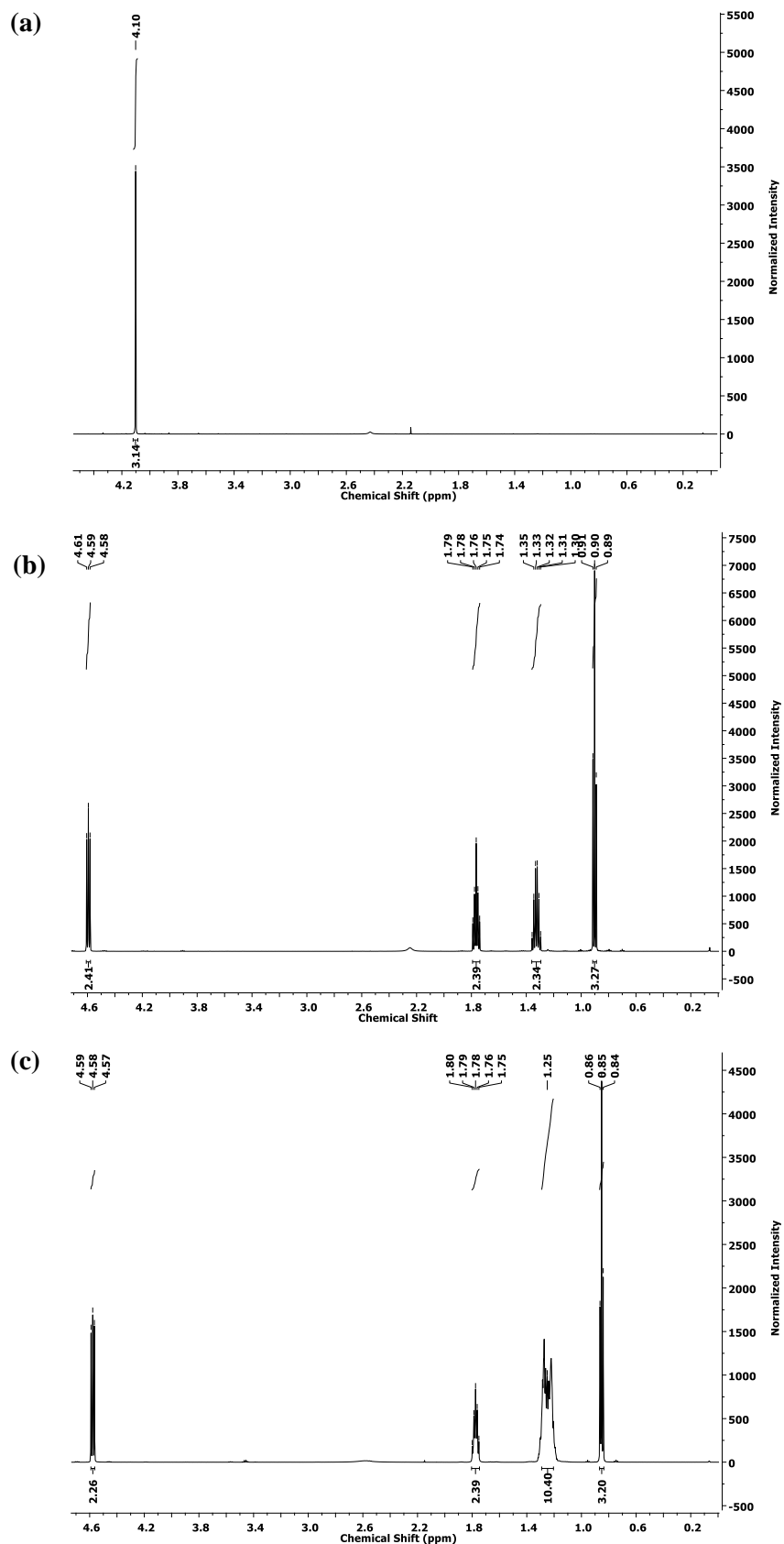


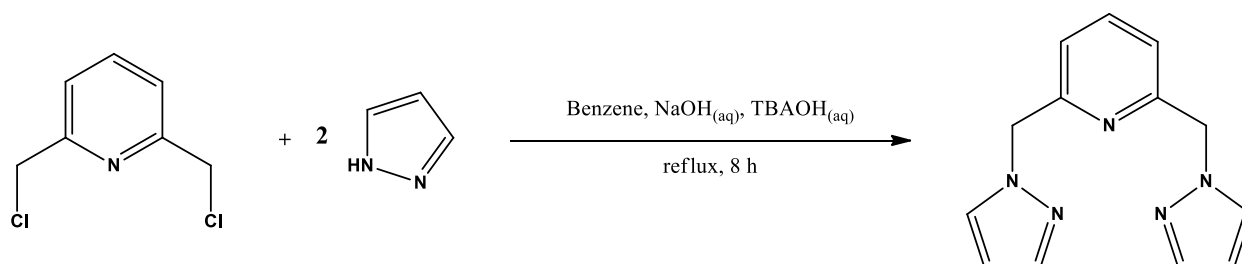
Figure 2.6: Zoomed in ^1H NMR spectra of the alkylated ligands: **(a)** 2-(1-methyl-imidazol-2-yl)pyridine (**2**); **(b)** 2-(1-butyl-imidazol-2-yl)pyridine (**3**) and **(c)** 2-(1-octyl-imidazol-2-yl)pyridine (**4**).

It was plain to see that the singlet at 4.10 ppm, which integrated for 3, represented the $-\text{CH}_3$ protons of 2-(1-methyl-imidazol-2-yl)pyridine (**2**) (**Figure 2.6a**). For 2-(1-butyl-imidazol-2-yl)pyridine (**3**), we observed

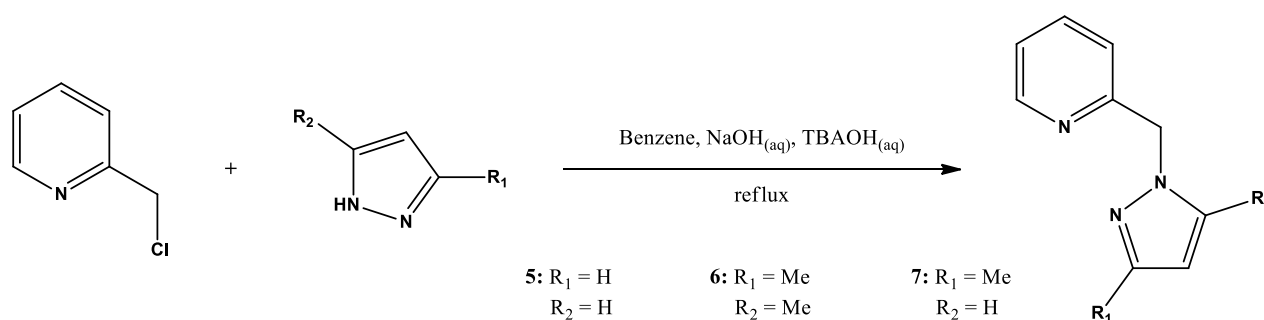
four signals (combined integration of 9), each representing the four distinctly different chemical environments of the butyl moiety (**Figure 2.6b**). Lastly, for 2-(1-octyl-imidazol-2-yl)pyridine (**4**), we saw the presence of a multiplet at 1.25 ppm. This was expected as the internal protons of a long alkyl chain species often overlap. This multiplet integrated for 10, and when it was added to the sum of the remaining integrals, we observed an expected total integration of 17 (**Figure 2.6c**).

As the discussion of imidazole based pyridine ligands are brought to a close, a new set of ligands are introduced: methylpyrazole based pyridine ligands (**5–7**).

In 1987, Watson *et al.*¹⁰ reported the synthesis of 2,6-bis(1'-pyrazolyl)-methylpyridine from 2,6-bis(chloromethyl)pyridine hydrochloride and pyrazole (**Scheme 2.15**). We, on the other hand, wanted to synthesise a series of mono substituted pyrazole tethered arms instead of the doubly substituted version outlined by Watson *et al.*¹⁰ So, we set out to synthesise 2-(1'-pyrazolyl)-methylpyridine (**5**), 2-(3,5-dimethyl-pyrazol-1-yl)-methylpyridine (**6**) and 2-[(3-methyl-pyrazol-1-yl)methyl]pyridine (**7**) from basic and readily available starting materials (**Scheme 2.16**).



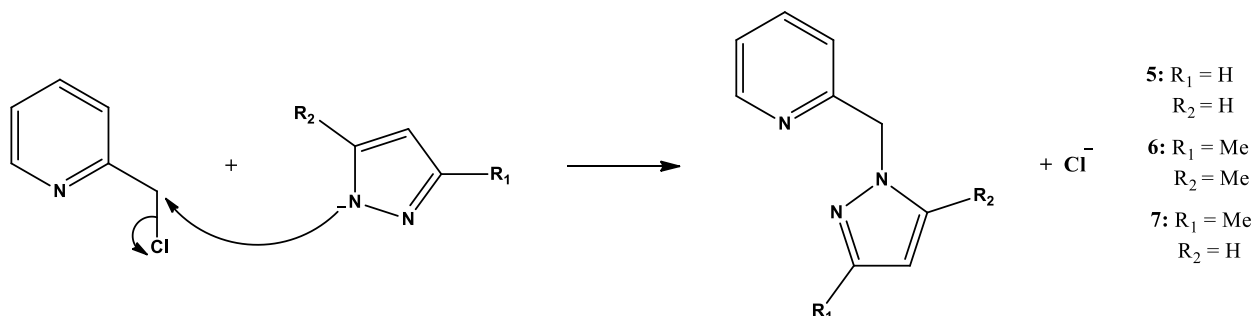
Scheme 2.15: The synthesis of 2,6-bis[(1'-pyrazolyl)-methyl]pyridine as reported by Watson *et al.*¹⁰



Scheme 2.16: The proposed synthesis of 2-(1'-pyrazolyl)-methylpyridine (**5**), 2-(3,5-dimethyl-pyrazol-1-yl)-methylpyridine (**6**) and 2-(3-methyl-pyrazol-1-yl)-methylpyridine (**7**).

The synthesis of our modified monosubstituted ligands necessitated the use of 2-(chloromethyl)pyridine hydrochloride and one equivalent of the appropriate pyrazole. The solvent, base and phase-transfer base were kept the same as reported by Watson *et al.*¹⁰ The phase-transfer base, tetrabutylammonium hydroxide (TBAOH), is commonly used to effect alkylations and deprotonations. In our case, we needed a base that was soluble in the organic phase, since all of the pyrazole reagents were only soluble in the organic phase. TBAOH was then used to deprotonate the pyrazole reagent, which in turn acted as nucleophiles that attacked

the electrophilic carbon adjacent to the chlorine atom on 2-(chloromethyl)pyridine (**Scheme 2.17**). The role of the aqueous sodium hydroxide was two-fold: it assisted in the deprotonation of pyrazole as well as mopping up the HCl that was formed during the reaction.



Scheme 2.17: The nucleophilic substitution (S_N2) mechanism by which ligands **5**, **6** and **7** were formed.

In the one-pot synthesis of 2-(1'-pyrazolyl)-methylpyridine (**5**) we refluxed the mixture for 8 hours and left it stirring at room temperature overnight to ensure that the reaction goes to completion. After the yellow organic layer was separated, dried over anhydrous Na₂SO₄ and concentrated in vacuo, we obtained a yellow oil in a 89.7% yield. In 1987, Watson *et al.*¹⁰ reported a yield of 90%, while in 1997, Bhatti *et al.*¹⁴ reported a much lower yield of 58%. We were glad to find that our results correlated to the former.

We obtained a ¹H NMR spectrum of ligand **5** and were surprised to see that we obtained an exceptionally clean spectrum without any additional purification procedures required. From the ¹H NMR spectrum (**Figure 2.7**) we concluded that all the peaks are accounted for. A telltale sign that the pyrazole was tethered to the pyridine moiety was the presence of the -CH₂ protons at 5.43 ppm (J=2). Usually, alkyl protons appear more upfield (lower chemical shifts) between 0 and 4 ppm. However, since the -CH₂ protons were adjacent to an electronegative nitrogen atom (electron withdrawing), the -CH₂ protons were deshielded and moved downfield. Since no coupling to neighbouring protons were possible we expected to see a singlet. This was confirmed by the ¹H NMR of ligand **5** (**Figure 2.7**). The presence of two doublets (7.55 and 7.51 ppm) and one triplet (6.29 ppm) was attributed to the pyrazole moiety while the other four peaks were attributed to the pyridine moiety.

2-(3,5-Dimethyl-pyrazol-1-yl)-methylpyridine (**6**) was prepared in a similar way to that of ligand **5**. The only difference in the procedure was the reflux time. At first we kept the reflux time at 8 hours, but according to a preliminary ¹H NMR spectrum of ligand **6**, the reaction had not gone to completion. We decided to leave the stirring mixture to reflux an additional 40 hours, for a total of 48 hours. ¹H NMR confirmed that ligand **6** was successfully synthesised (**Figure 2.8**). Once again this was obvious with the presence of a singlet at 5.32 ppm which correlated to the alkyl -CH₂ protons. The presence of two singlets (each integrating for 3) at 2.16 and 2.24 ppm respectively, were associated with the -CH₃ protons on the pyrazole moiety. The singlet at 5.86 ppm, which integrated for 1, was associated with the -CH proton between the two methyl groups. The other four signals in the aromatic region (6.5–8.5 ppm) correlated to the pyridine moiety. We noticed that there were tiny blips on the ¹H NMR spectrum that indicated the presence of trace amounts of starting material

(**Figure 2.8**). We speculated that the presence of two methyl groups on the reagent, 3,5-dimethylpyrazole, rendered the -NH proton less acidic by increasing the electron density within the pyrazole ring (positive inductive effect). This meant that the -NH proton was slightly harder to deprotonate. To counter this, a stronger base could be used, the reflux time could be increased or purification via column chromatography could be done. We, however, decided that these impurities were negligible and that no further purification was needed.

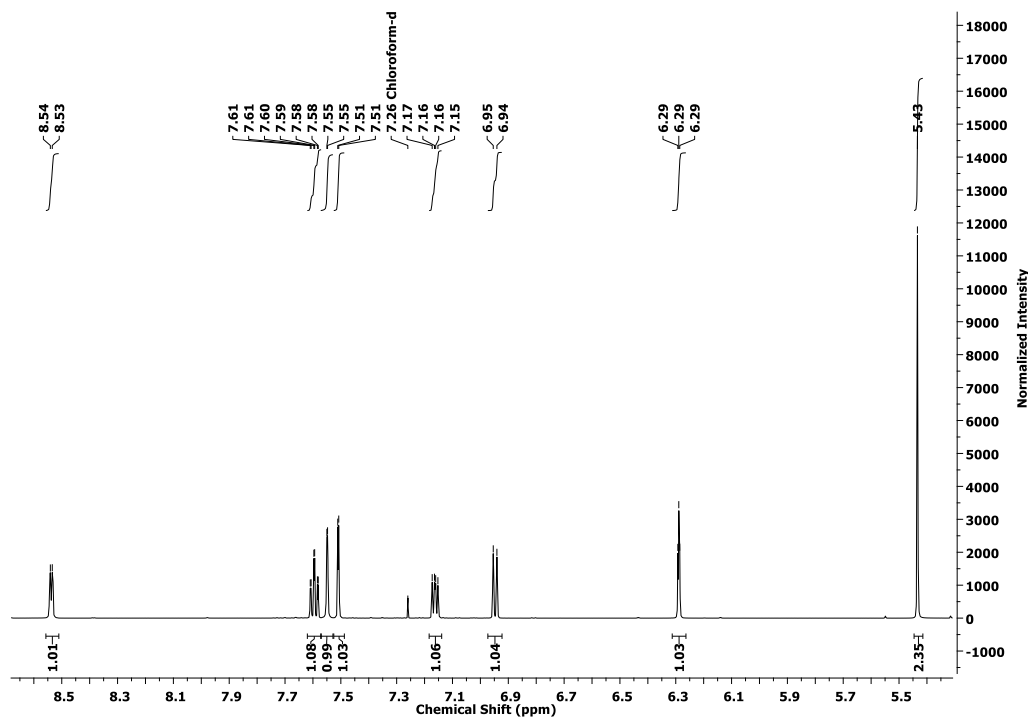


Figure 2.7: The ^1H NMR of 2-(1'-pyrazolyl)-methylpyridine (5).

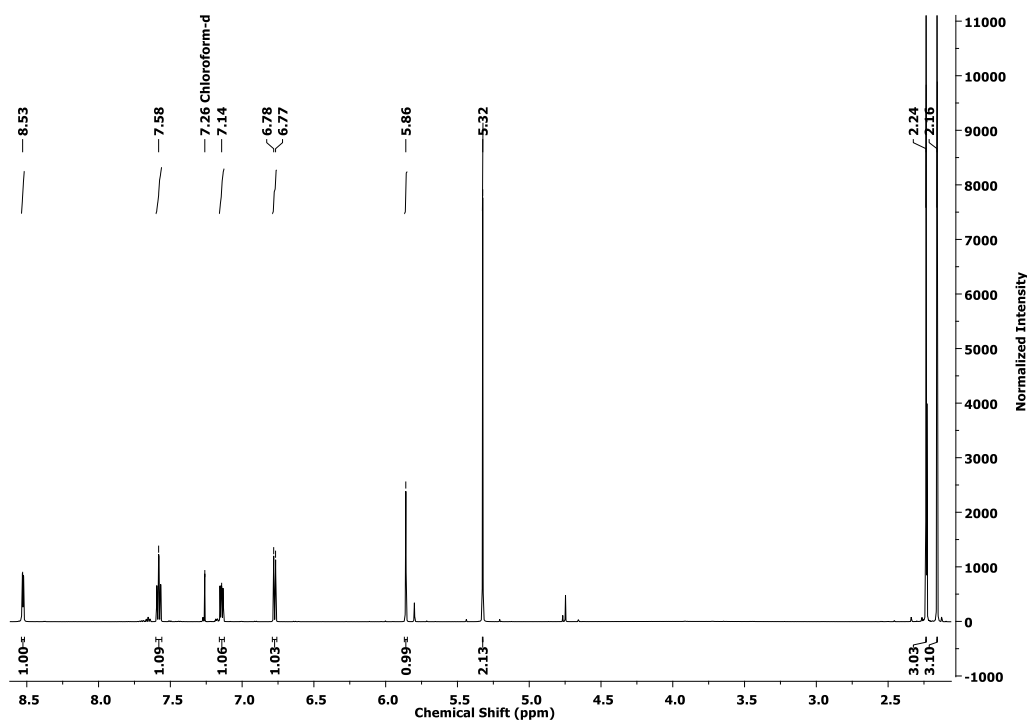
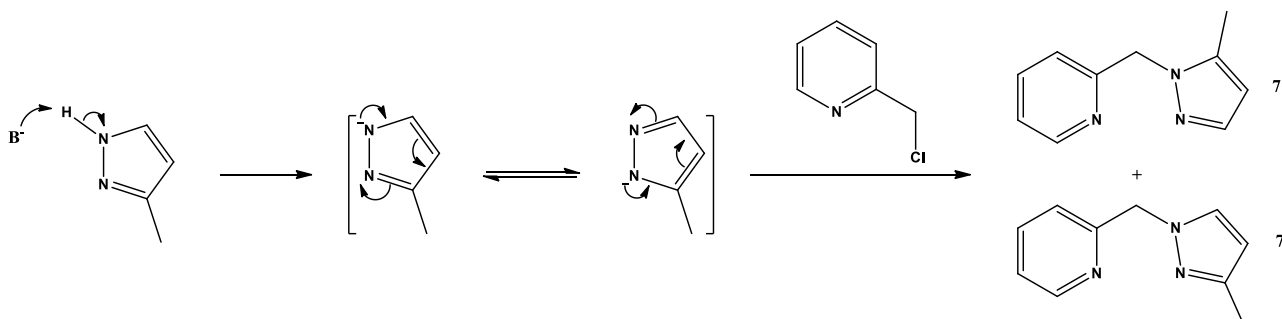


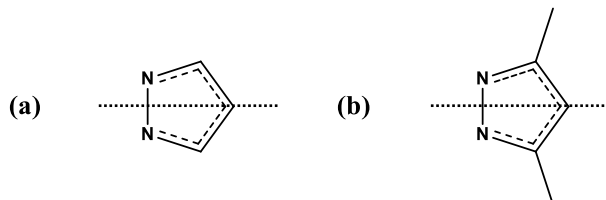
Figure 2.8: The ^1H NMR of 2-(3,5-dimethyl-pyrazol-1-yl)-methylpyridine (6).

After the synthesis of ligands **5** and **6**, we proceeded with the synthesis of 2-(3-methyl-pyrazol-1-yl)-methylpyridine (**7**). Since we successfully synthesised ligands **5** and **6**, we assumed that ligand **7** wouldn't be any different. We set out with the exact same synthetic procedure as ligand **5**. We had a one-pot reaction mixture with 2-(chloromethyl)pyridine hydrochloride and 3-methylpyrazole as reagents. After refluxing the mixture for 8 hours we performed the work-up procedure and immediately submitted the sample for NMR analysis. The ^1H NMR along with the ^{13}C NMR spectrum showed that we had considerable “impurities” in the sample (**Figures 2.9–2.12**). The ratio of “impurities” to product was roughly 1:2. This prompted us to increase the reflux time to 48 hours like we did with ligand **6**. After the 48-hour reflux period and consequent work-up procedure, we once again submitted the sample for NMR analysis. Still we found “impurities” in the sample which frustrated us, especially since ligands **5** and **6** were synthesised without a hitch. We decided to submit the sample for mass spectrometry (MS) and elemental analysis and obtained a clean spectrum with a solitary base peak at 174.1 m/z . The experimental results of the elemental analysis (C, 68.64; H, 6.23; N, 23.59) compared well with the expected calculated results (C, 69.34; H, 6.40; N, 24.26). This, along with the MS result, meant that our sample was in fact clean, although it didn't appear to be the case on the NMR spectra. This strange phenomenon warranted further investigation.

We realised we had yet another case of tautomerism. Once 3-methylpyrazole was deprotonated, the negative charge on the nitrogen kicked into the pyrazole ring, pushing the electrons around the ring and ultimately causing the adjacent nitrogen to be negatively charged. This meant that we now had two possible sites from which nucleophilic attack can occur, resulting in a mixture of two isomers being formed: 2-(3-methyl-pyrazol-1-yl)-methylpyridine (**7**) and 2-(5-methyl-pyrazol-1-yl)-methylpyridine (**7'**) (**Scheme 2.18**). This was somewhat surprising to us, since Gao *et al.*¹⁵ reported the synthesis of ligand **7**, but never mentioned the role that tautomerism might play. We also realized that we had been using similar pyrazole reagents for the synthesis of ligands **5** and **6**, but never saw any evidence of tautomerism. This was because pyrazole and 3,5-dimethylpyrazole had a plane of symmetry between the two nitrogens (**Scheme 2.19**). Even though tautomerism did occur in pyrazole and 3,5-dimethylpyrazole, we did not see it because both tautomeric forms gave rise to the same product.



Scheme 2.18: The formation of an isomeric mixture of 2-(3-methyl-pyrazol-1-yl)-methylpyridine (**7**) and 2-(5-methyl-pyrazol-1-yl)-methylpyridine (**7'**) via tautomerism.



Scheme 2.19: The plane of symmetry present in **(a)** pyrazole and **(b)** 3,5-dimethylpyrazole that prevents isomers from being formed.

After we concluded that tautomerism played a major part in what we witnessed in the NMR spectra, we could start to theorise as to why one isomer was preferably formed above the other. From the ^1H and ^{13}C NMR spectra it was clear that the peaks of the two isomers were roughly in a 1:2 ratio (**Figures 2.9–2.12**). That meant that there were factors hindering the formation of one of these isomers. Ordinarily, one would expect a 1:1 ratio between isomers, but in this case steric hindrance probably played a major role. If nucleophilic attack occurred through the nitrogen closest to the methyl substituent, one would expect the methyl to crowd and hinder that mode of nucleophilic attack. On the other hand, the nucleophilic attack through the nitrogen furthest away from the methyl, would be less sterically hindered. Therefore, we proposed that the smaller of the ^1H NMR peaks represented 2-(5-methyl-pyrazol-1-yl)-methylpyridine (**7'**) and the larger peaks represented 2-(3-methyl-pyrazol-1-yl)-methylpyridine (**7**). Inductive effects could also have played a role in the selective nucleophilic attack. We know that methyl ($-\text{CH}_3$) moieties are electron donating, resulting in the fact that electron density was pushed into the 3-methylpyrazole ring. This could mean that the tautomer with the negative charge on the nitrogen closest to the methyl group, could be rendered slightly more unstable because of repelling electron forces. This was by no means verified and is a working theory. Having said that, we are convinced that if inductive effects do contribute to the selective nucleophilic attack, they play a minor role while steric effects play the major role

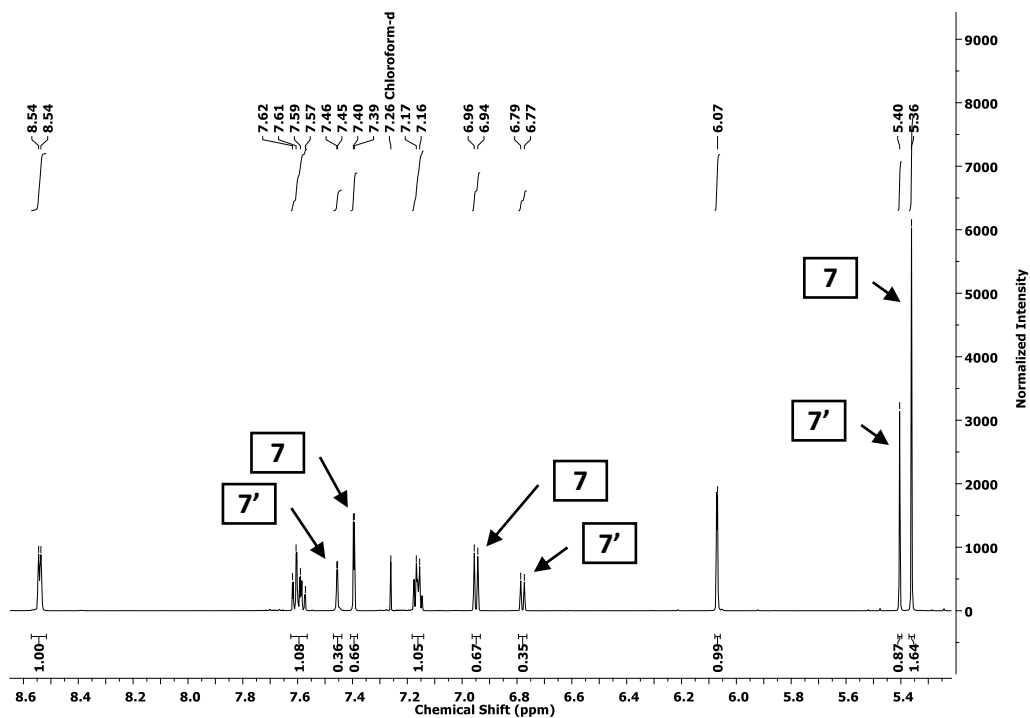


Figure 2.9: A zoomed in ^1H NMR of 2-(3-methyl-pyrazol-1-yl)-methylpyridine (**7**) and 2-(5-methyl-pyrazol-1-yl)-methylpyridine (**7'**).

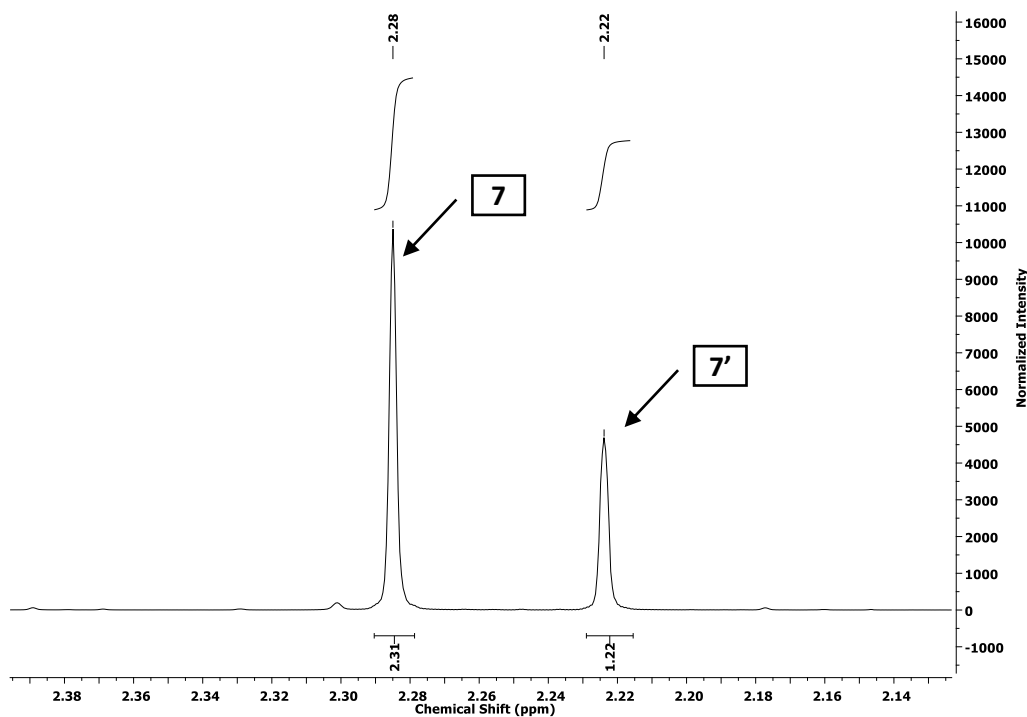


Figure 2.10: ^1H NMR of the alkyl region of isomers 2-(3-methyl-pyrazol-1-yl)-methylpyridine (**7**) and 2-(5-methyl-pyrazol-1-yl)-methylpyridine (**7'**).

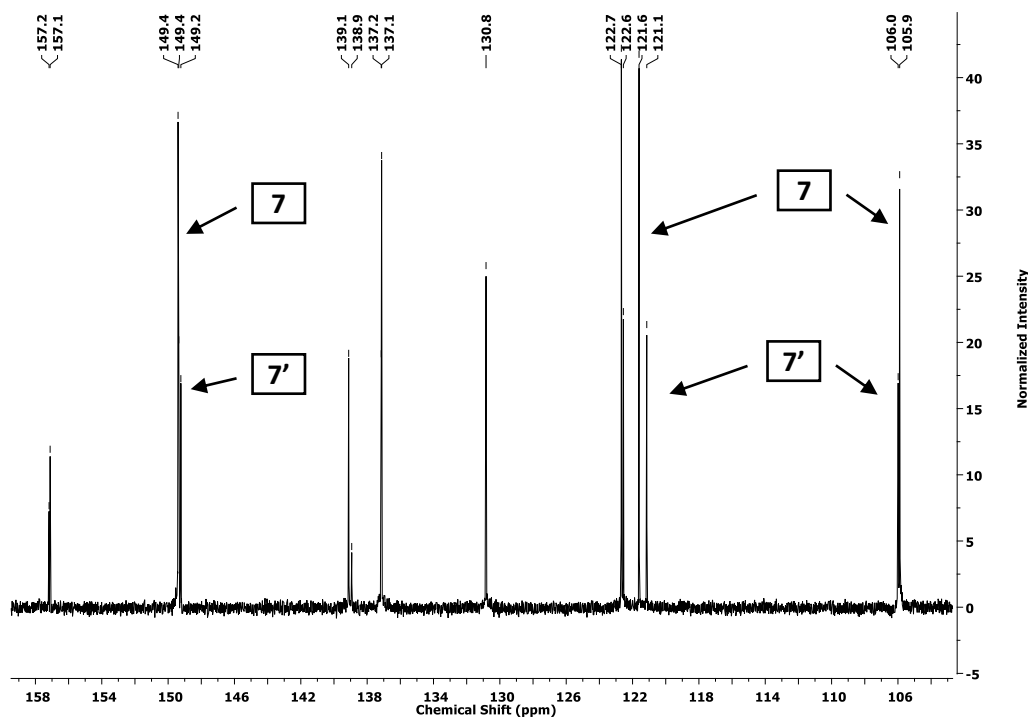


Figure 2.11: A zoomed in ^{13}C NMR of the downfield region of isomers 2-(3-methyl-pyrazol-1-yl)-methylpyridine (**7**) and 2-(5-methyl-pyrazol-1-yl)-methylpyridine (**7'**).

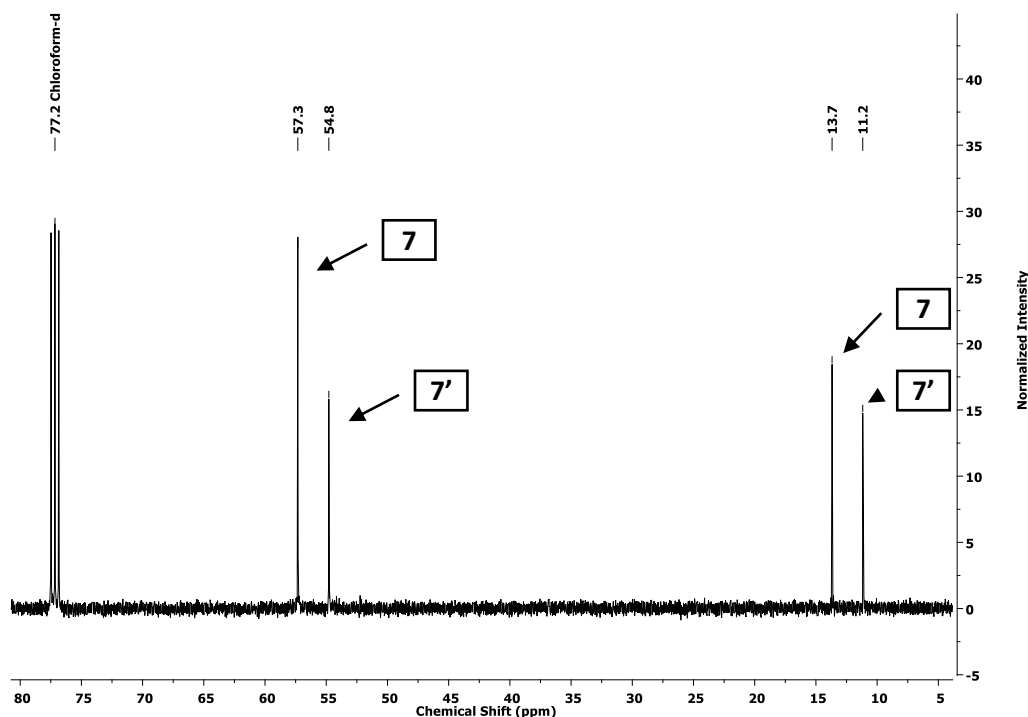
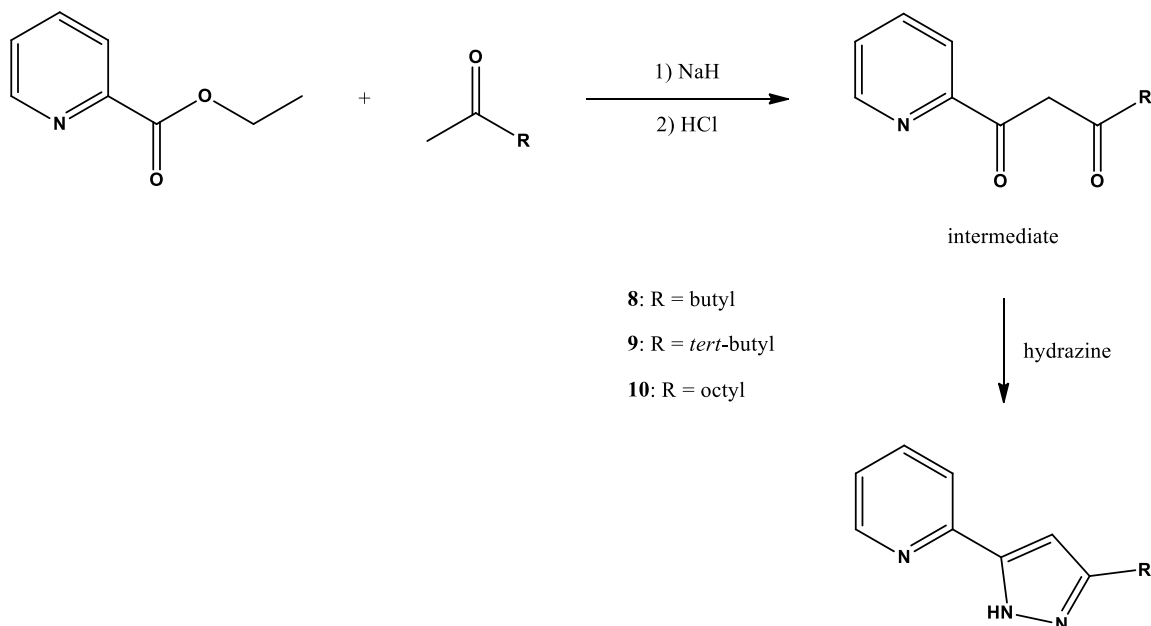


Figure 2.12: A zoomed in ^{13}C NMR of the upfield region of isomers 2-(3-methyl-pyrazol-1-yl)-methylpyridine (**7**) and 2-(5-methyl-pyrazol-1-yl)-methylpyridine (**7'**).

The last set of ligands, which were also pyrazole based, were synthesised in a two-step synthetic procedure. The synthesis of 2-(3-butyl-pyrazol-5-yl)pyridine (**8**), 2-[3-(*tert*-butyl)-pyrazol-5-yl]pyridine (**9**) and 2-(3-octyl-pyrazol-5-yl)pyridine (**10**) were virtually identical and we will discuss these ligands (**8–10**) as a unit.

The pyridylpyrazole ligands (**8–10**) were obtained via the Claisen condensation of ethyl 2-picolinate with the appropriate alkyl ketones, yielding a crude 1,3-dicarbonyl intermediary species. We used the crude intermediary product immediately without purification. Subsequently, we performed the classic Knorr pyrazole synthesis¹⁶ with hydrazine to yield the desired pyridylpyrazole products (**Scheme 2.20**).

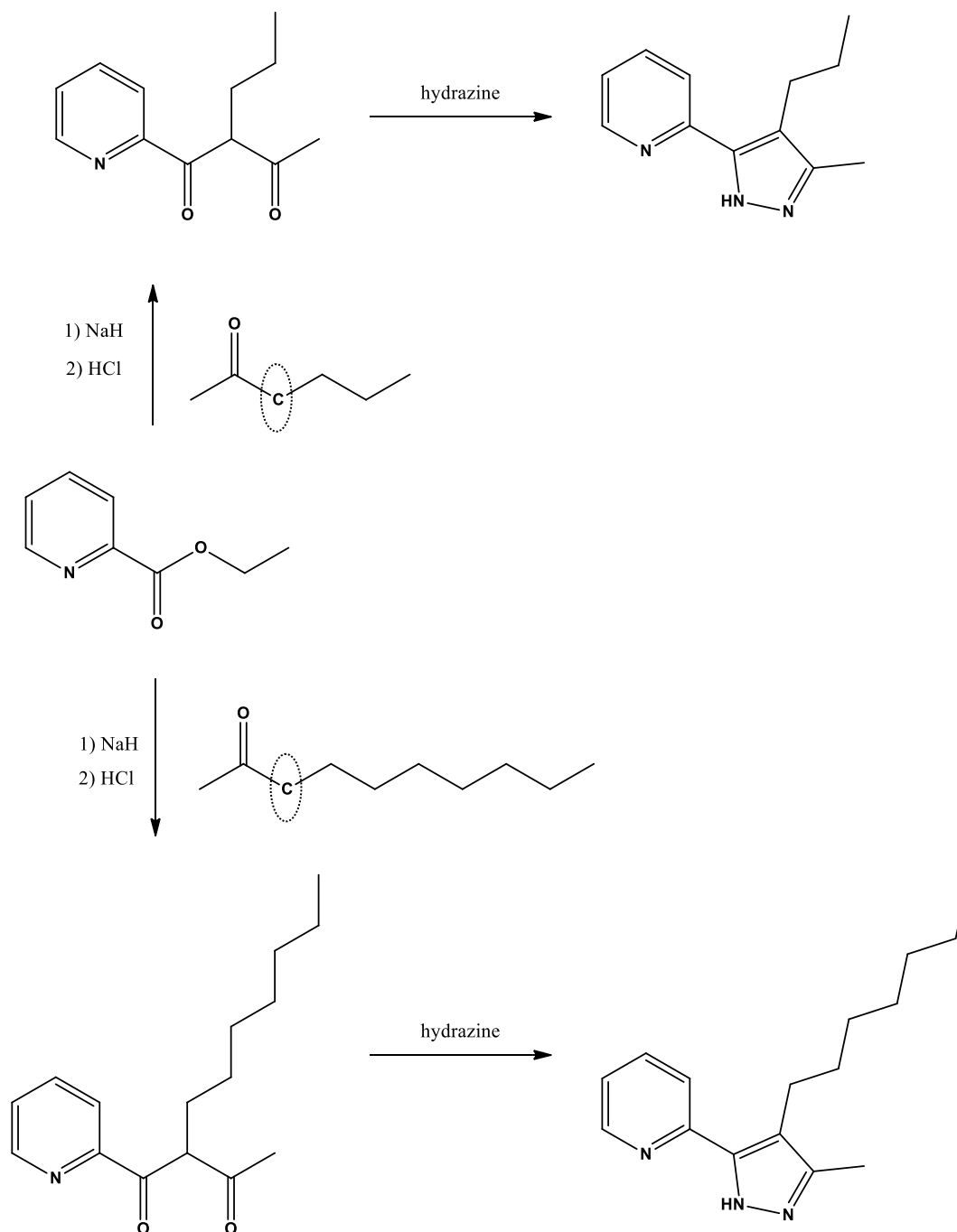


Scheme 2.20: A general outline of the synthesis of 2-(3-butyl-pyrazol-5-yl)pyridine (**8**), 2-[3-(*tert*-butyl)-pyrazol-5-yl]pyridine (**9**) and 2-(3-octyl-pyrazol-5-yl)pyridine (**10**).

In retrospect, we probably should have purified the crude intermediary products by column chromatography to rid it of impurities and secondary products. The sodium hydride deprotonated the primary carbon of the ketone reagents, resulting in a carbanion being formed. We know that primary carbanions on ketone reagents are more stable than secondary carbanions. This meant that the main product formed via Claisen condensation was in fact our desired intermediary product, but Claisen condensation could also theoretically occur via the secondary carbanion, ultimately yielding unwanted intermediary and final products (**Scheme 2.21**). This was, however, limited due to the inherent steric hindrance of secondary carbanions and the aforementioned stability factors. It was also interesting to note that the synthesis of ligand **9** did not produce these unwanted side-products, due to the lack of secondary or tertiary protons on 3,3-dimethyl-2-butanone, *i.e.*, no secondary or tertiary carbanions could be formed.

Satake and Nakata¹¹ did not perform any intense purification procedures and reported yields of 65–71%. We, on the other hand, obtained ¹H NMR spectra that were extremely dirty, forcing us to do gravitational column chromatography after attempting to purify the product using various techniques. We developed a system whereby toluene was initially used as eluent to flush out the impurities/side-products while the product remained on the silica gel column. Once the impurities were removed, we changed the eluent to ethyl acetate. This swiftly forced the product out of the column. We removed the solvent using a high vacuum pump and reported yields of 26.1–29.6%. This is considerably lower than the aforementioned authors'

yields. We suspect that we had lost product by using various purifying techniques, but still do not know exactly why our yield was substantially lower than Satake and Nakata's.¹¹ We also expected the yield of ligand **9** to be higher than ligands **8** and **10**, since no obvious side-products were able to form during the reaction. This clearly was not the case. Another interesting side-note was that ligands **9** and **10** were obtained as solids, with melting points of 104–105 and 79–81 °C respectively, while ligand **8** was obtained as an oil.



Scheme 2.21: The formation of the unwanted secondary intermediates and final products as a result of secondary carbanion (highlighted with dotted ellipse) nucleophilic attack.

The ¹H NMR spectra obtained for ligands **8–10** were clean after performing column chromatography. It was relatively easy to assign all the peaks, with no major overlapping signals. The ¹H NMR of ligand **8** had four characteristic signals between 0.8 and 2.7 ppm that was assigned to the butyl moiety. Another telling

characteristic, that indicated whether ligand **8** had been successfully characterised, was the presence of a singlet that integrated for 1, at 6.60 ppm. This singlet was attributed to the lone proton on the pyrazole ring. The last four signals in the aromatic region (7.0–9.0 ppm) were assigned to the four protons present on the pyridine ring (**Figure 2.13**). The ^{13}C NMR, IR and MS results were positive as well, although it is not shown here. The elemental analysis (EA) results were slightly off, but we realized that there were still trace amounts of toluene solvent present even after drying the sample under high vacuum for several days. For every ten molecules of ligand **8**, there was one toluene molecule present. This was evidently seen in the EA results: EA calculated (%) for $\text{C}_{12}\text{H}_{15}\text{N}_3 \cdot 0.1 \text{ C}_7\text{H}_8$ **C**, 72.47; **H**, 7.57; **N**, 19.96. EA found (%) **C**, 72.32; **H**, 7.62; **N**, 19.83.

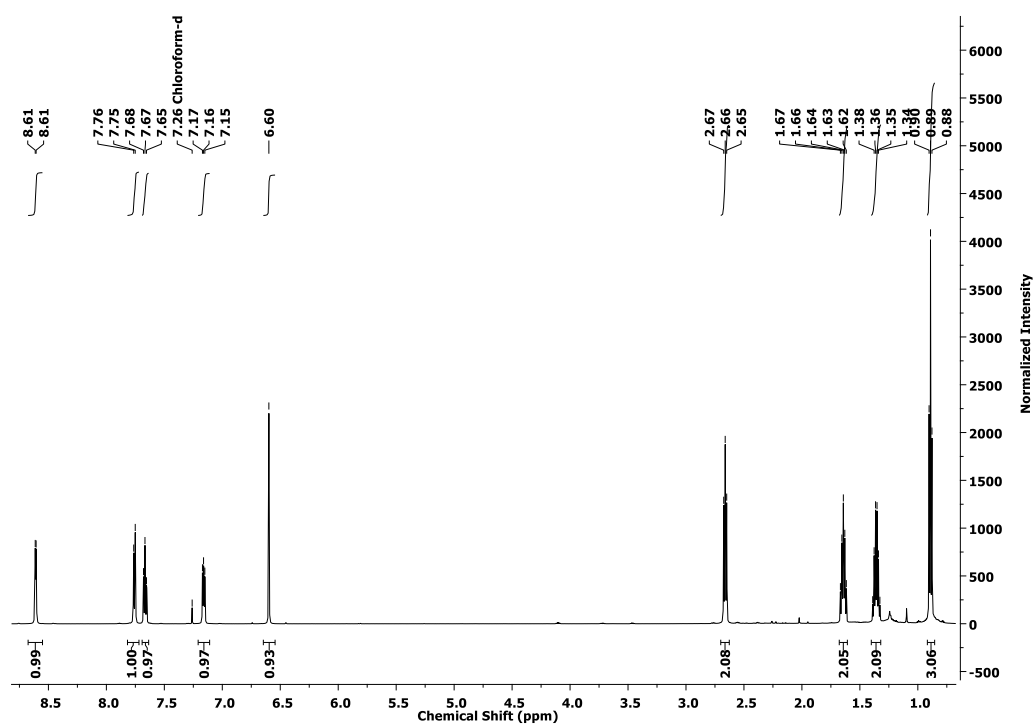


Figure 2.13: The ^1H NMR spectrum of 2-(3-butyl-pyrazol-5-yl)pyridine (**8**).

Ligand **9** also appeared to be relatively clean on the ^1H NMR spectrum, with slight impurities in the upfield alkyl region (± 1.25 ppm). The singlet at 1.36 ppm, which integrated for 9, was attributed to the protons of the *tert*-butyl moiety of ligand **9**. The presence of the singlet at 6.67 ppm once again indicated the presence of the sole proton on the pyrazole ring. The four signals in the aromatic region (6.5–9.0 ppm) were indicative of the four protons on the pyridine ring (**Figure 2.14**). Ligand **9** too had near perfect results when it came to the other characterisation techniques (IR, MS and ^{13}C NMR), but had EA results that were awry. The sample still had trace amounts of toluene and can be verified by the EA results: EA calculated (%) for $\text{C}_{12}\text{H}_{15}\text{N}_3 \cdot 0.25 \text{ C}_7\text{H}_8$ **C**, 73.63; **H**, 7.64; **N**, 18.73. EA found (%) **C**, 73.69; **H**, 7.49; **N**, 18.89. For every four molecules of ligand **9**, one molecule of toluene solvent was present.

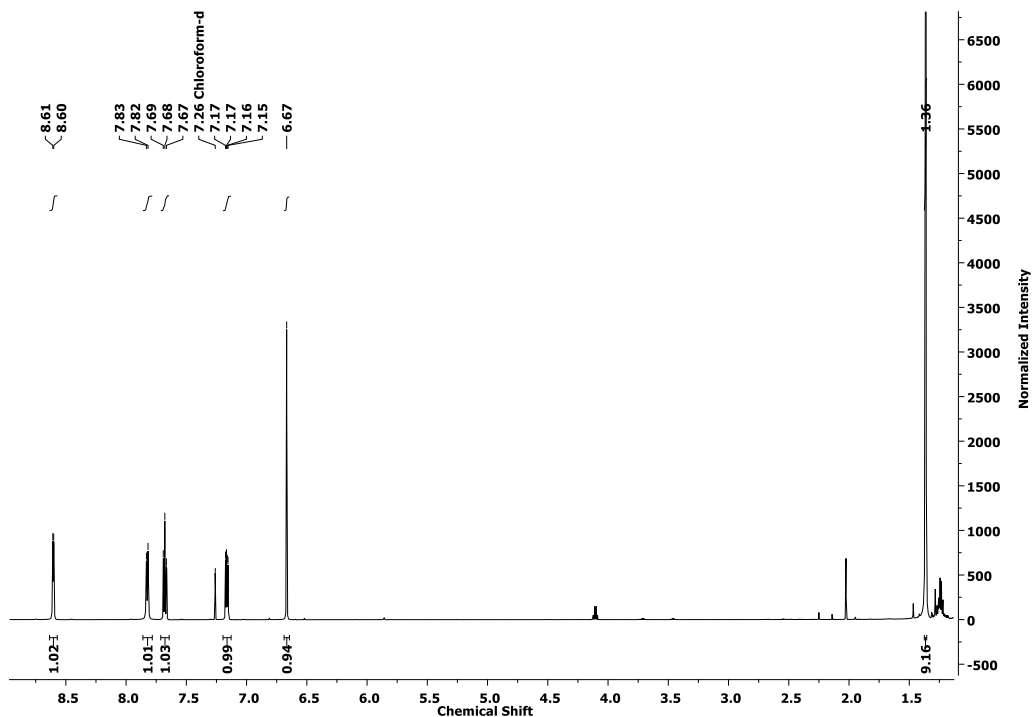


Figure 2.14: The ^1H NMR spectrum of 2-[3-(*tert*-butyl)pyrazol-5-yl]pyridine (**9**).

The ^1H NMR spectra of ligand **10**, were like ligands **8** and **9**, relatively clean. This was solely due to the purification process performed on the silica gel column. The signals between 0.5 and 3.0 ppm were representative of the alkyl protons (octyl moiety) present on ligand **10**. The summed integrals correlated exactly to what we would've expected to find, which was 17. Still, we found the characteristic solitary proton signal at 6.60 ppm that corresponded to the pyrazole proton, while the four aromatic peaks (6.5–9.0 ppm) were assigned to the pyridine protons (**Figure 2.15**).

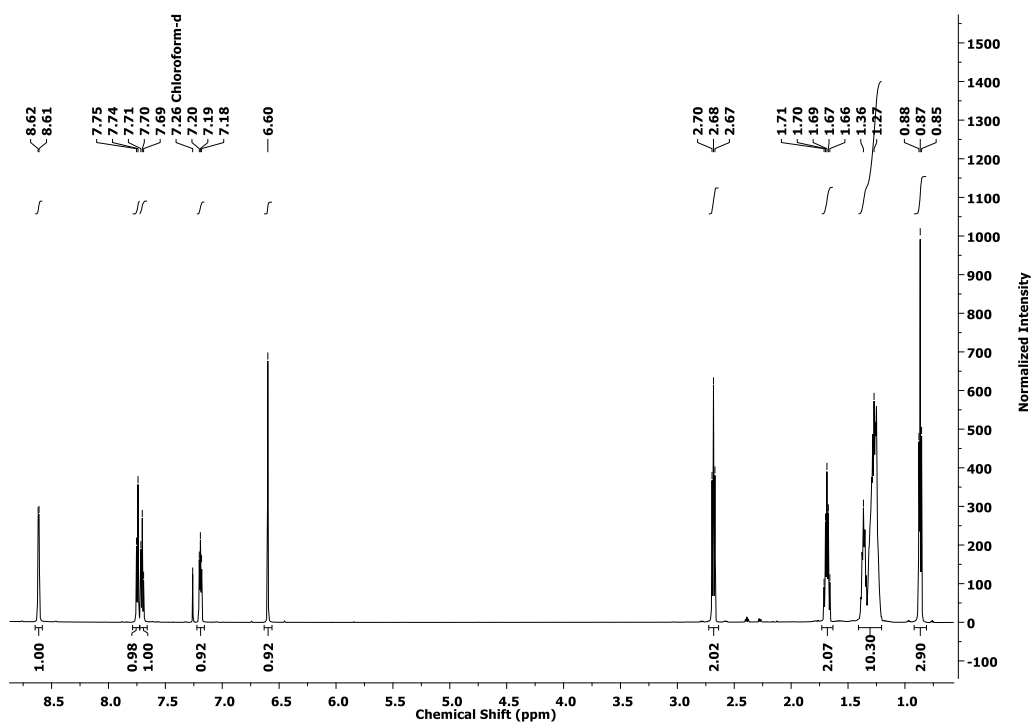
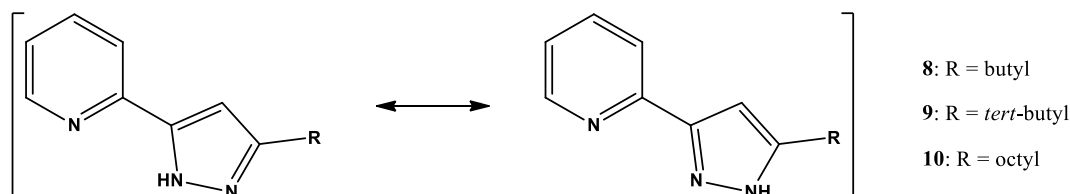


Figure 2.15: The ^1H NMR spectrum of 2-(3-octylpyrazol-5-yl)pyridine (**10**).

Interestingly, according to literature,^{11,17} ligands **8–10** also exhibit a form of tautomerism, whereby the –NH proton rapidly shifts between either of the pyrazolyl nitrogen atoms in solution (**Scheme 2.22**). This, however, is difficult to trace on ¹H NMR spectra where, occasionally, broad signals can be witnessed in the 8.5–9.5 ppm region. Unfortunately, we could not find sufficient evidence for this on either the ¹H or ¹³C NMR spectra, but crystal structure elucidation of ligand **9** coordinated to copper(II) indicated the –NH proton to be bound to the pyrazolyl nitrogen closest to the *tert*-butyl moiety (see **Section 4.3.1, Chapter 4**).



Scheme 2.22: Tautomeric forms of ligands **8–10** present in solution.

2.5 Conclusions

One of the most strenuous challenges in the synthesis of ligands **1–10** were the purification processes. It often occurred that we were confronted with an impure sample that needed to be purified, either by recrystallisation or gravitational column chromatography. Both of these techniques were extremely time consuming and cumbersome, and in certain cases took up to a month to complete. Another negative in using these techniques were the fact that a certain percentage of product was always lost during the purification process. Either the product struggled to come out of solution (recrystallisation) or the product stuck to the silica gel column (column chromatography). Therefore, an overarching difficulty in the synthesis of ligands **1–10** was the challenge of synthesising sufficient amounts of pure product, that were to be used in future solvent extraction studies. This was especially true concerning ligand **1**. Although ligand **1** was used as an extractant on its own, it was also the precursor to ligands **2, 3** and **4**. This meant that we had to spend a lot of time synthesising large amounts of this ligand. Ligands **8, 9** and **10** are also good examples of products that were extremely dirty after their respective two-step synthetic procedures. This, however, can be countered by purifying the intermediate products, but one should be mindful that a small percentage of product will be lost due to the purification process.

In this investigation we have successfully managed to synthesise and characterise a series of imidazole- (**1–4**) and pyrazole-based (**5–10**) pyridine ligands. We have largely been able to match the yields of Wang *et al.*⁹ and Watson *et al.*¹⁰ in the synthesis of ligands **2–7**, but have fallen substantially short of the yields reported by Gerber *et al.*⁸ and Satake *et al.*¹¹ for ligands **1** and **8–10** respectively. The main reason for this was the cumbersome work-up procedure for ligand **1** and the demanding purifying procedures for ligands **8–10**. All the ligands were successfully characterised by means of ¹H and ¹³C NMR, IR, MS and EA.

Finally, we report for the first time the synthesis of 2-(3-octyl-pyrazol-5-yl)pyridine (**10**), which to the best of our knowledge, is novel.

2.6 References

1. Du Preez, J. G. H. Recent advances in amines as separating agents for metal ions. *Solvent Extr. Ion Exch.* **2000**, *18*, 679-701.
2. Gray, A. P.; O'Dell, T. B. Reaction of ethylene bromide with trimethylamine and the neuromuscular blocking activity of ethylenebis(trimethylammonium) [22]. *Nature* **1958**, *181*, 634-635.
3. Vidal, F. Reaction of ethylene dibromide with triethylamine and the restoring action of some alkanebis(trimethylammonium) ions upon sodium-deficient nerve fibers. *J. Org. Chem.* **1959**, *24*, 680-683.
4. Marcus, Y.; Kertes, A. S. *Ion Exchange and Solvent Extraction of Metal Complexes*; Wiley-Interscience: London; New York, 1969, pp 1037.
5. Du Preez, J. G. H.; Schanknecht, S. B.; Shillington, D. P. Polynitrogen reagents in metal separation. Part 3. the extraction of Co^{2+} , Ni^{2+} , Cu^{2+} and Zn^{2+} using novel ditertiary-amine extractants. *Solvent Extr. Ion Exch.* **1987**, *5*, 789-809.
6. Du Preez, J. G. H.; Sumter, N.; Mattheüs, C.; Ravindran, S.; Van Brecht, B. J. Nitrogen reagents in metal ion separation. Part VII. The development of a novel copper(II) extractant. *Solvent Extr. Ion Exch.* **1997**, *15*, 1007-1021.
7. Du Preez, J. G. H.; Mattheüs, C.; Sumter, N.; Ravindran, S.; Potgieter, C.; Van Brecht, B. J. Nitrogen reagents in metal ion separation. Part VIII. Substituted imidazoles as extractants for Cu^{2+} . *Solvent Extr. Ion Exch.* **1998**, *16*, 565-586.
8. Gerber, T. I. A.; Hosten, E.; Mayer, P.; Tshentu, Z. R. Synthesis and characterization of rhenium(III) and (V) pyridylimidazole complexes. *Journal of Coordination Chemistry* **2006**, *59*, 243-253.
9. Wang, R.; Xiao, J.; Twamley, B.; Shreeve, J. M. Efficient Heck reactions catalyzed by a highly recyclable palladium(II) complex of a pyridyl-functionalized imidazolium-based ionic liquid. *Organic and Biomolecular Chemistry* **2007**, *5*, 671-678.
10. Watson, A. A.; House, D. A.; Steel, P. J. Chiral heterocyclic ligands. Part IV. Synthesis and metal complexes of 2,6-bis(pyrazol-1-ylmethyl)pyridine and chiral derivatives. *Inorg. Chim. Acta* **1987**, *130*, 167-176.
11. Satake, A.; Nakata, T. Novel η^3 -allylpalladium-pyridinylpyrazole complex: Synthesis, reactivity, and catalytic activity for cyclopropanation of ketene silyl acetal with allylic acetates. *Journal of the American Chemical Society* **1998**, *120*, 10391-10396.
12. Debus, H. Ueber die Einwirkung des Ammoniaks auf Glyoxal. *Eur. J. Org. Chem.* **1858**, *107*, 199-208.
13. Radziszewski, B. Ueber Glyoxalin und seine Homologe. *Berichte der deutschen chemischen Gesellschaft* **1882**, *15*, 2706-2708.
14. Bhatti, I. A.; Busby, R. E.; Bin Mohamed, M.; Parrick, J.; Shaw, C. J. G. Pyrolysis of 1-substituted pyrazoles and chloroform at 550 °C: Formation of α -carboline from 1-benzylpyrazoles. *Journal of the Chemical Society - Perkin Transactions 1* **1997**, 3581-3585.

15. Gao, E.; Bai, S.; Wang, C.; Yue, Y.; Yan, C. Structural and Magnetic Properties of Three One-Dimensional Azido-Bridged Copper(II) and Manganese(II) Coordination Polymers. *Inorg. Chem.* **2003**, *42*, 8456-8464.
16. Knorr, L.; Blank, A. Einwirkung substituierter Acetessigester auf Phenylhydrazin. *Berichte der deutschen chemischen Gesellschaft* **1884**, *17*, 2049-2052.
17. Henkelis, J. J.; Kilner, C. A.; Halcrow, M. A. New insights into the aggregation of silver pyrazolides using sterically hindered bidentate pyrazole ligands. *Chem. Commun.* **2011**, *47*, 5187-5189.

Chapter 3

Solvent extraction of nickel(II) and copper(II) by means of imidazole- and pyrazole-based pyridine ligands

3.1 Introduction

The application of amine extractants in nickel solvent extraction systems are generally well-known. These systems would typically include generic extractants such as Alamine 336, Alamine 308 and Alamine 300, which are all tertiary alkylamine extractants.¹ Aromatic amine extractants, on the other hand, have been studied to a much lesser extent due to their general inability to be exclusively soluble in the organic phase. This obstacle has hindered research in this field and can only be overcome with the addition of hydrophobic moieties (e.g., alkyl chains) to the aromatic amine extractants, resulting in additional time, money and effort to design ligands that meet all the prerequisites of a successful solvent extractant.

In the late 1990s, Du Preez *et al.*²⁻⁵ authored a series of articles in which they reported the use of imidazole, pyrazole and pyridine ligands for the separation of nickel, cobalt and copper from an array of base metals. The imidazole ligands were of particular interest, since they showed excellent selectivity towards Cu(II), and once these ligands were modified, they were selective towards Ni(II) and Co(II) as well. These South African workers used imidazole, pyrazole and pyridine extractants independently and never attempted to combine these moieties into a single extractant, thereby forfeiting the opportunity of using bidentate aromatic amine ligands in the selective extraction of base metal ions.

Although innumerable bidentate aromatic amine ligands have been synthesised over the past few decades, very few of them were ever used for solvent extraction purposes. They are often used in catalytic⁶ and polymeric⁷ studies, which allows us to probe their usefulness for solvent extraction purposes. To the best of our knowledge, only one publication, by Okewole *et al.*,⁸ investigates the use of pyridylimidazole as an extractant in the solvent extraction of nickel(II). Because of this, we set out to investigate a series of imidazole- and pyrazole-based pyridine ligands with regard to their extractive ability of nickel(II) and copper(II).

3.1.1 Synergism

The past few decades saw great interest being shown in the synergistic behaviour present in various solvent extraction systems. The term *synergism* was first coined by Blake *et al.*⁹ in 1958, when they reported the use of a dialkyl hydrogen phosphate, (RO)₂POOH, in conjunction with a neutral organophosphorous reagent, tributyl phosphate (TBP). They noticed that the percentage extraction of the combined reagents exceeded the sum of the individual extractions. This intermolecular phenomenon between two or more reagents, causing significantly enhanced extractions of metal ions, is called *synergism*.

Another example of synergism is illustrated in the extraction of uranium(VI) as $[\text{UO}_2]^{2+}$ from a nitric acid medium. The species initially present as $[\text{UO}_2(\text{NO}_3)_2(\text{OH}_2)_2]$ can be extracted by TBP or di-2-ethylhexyl phosphoric acid (DEHPA) as $[\text{UO}_2(\text{NO}_3)_2(\text{TBP})_2]$ and $[\text{UO}_2(\text{DEHPA})_2(\text{OH}_2)_2]$ respectively.¹⁰ If, however, TBP and DEHPA are combined, the neutral species formed is $[\text{UO}_2(\text{DEHPA})_2(\text{TBP})_2]$, which is 1000 times more extractable into the organic phase than either of the complexes containing only one of the phosphorous ligands (**Figure 3.1**).¹⁰

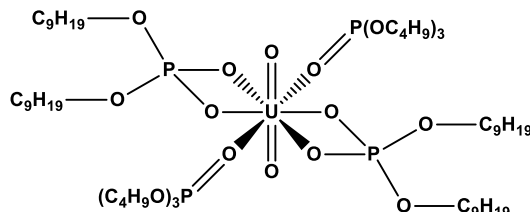


Figure 3.1: The neutral complex $[\text{UO}_2(\text{DEHPA})_2(\text{TBP})_2]$. This complex is extremely hydrophobic due to the alkyl chains present on the periphery. This forces the complex to be insoluble in the aqueous phase and highly soluble in the organic phase. [Adapted from Laing¹⁰]

3.1.1.1 Justification for using a sulfonic acid synergist

There are numerous examples in literature where authors have investigated the selective extraction of nickel(II) by means of synergistic systems, with their respective end-purposes varying greatly.^{1,11-14} Only a handful of them, however, reported the use of a sulfonic acid synergist in an attempt to increase the uptake of nickel(II).

In 1977, Flett¹⁵ reported the use of a carboxylic acid and 5,8-diethyl-7-hydroxy-6-dodecanone oxime (commercially known as LIX63) extractant system for the selective extraction of nickel over cobalt. Although reasonable separation was achieved, Flett¹⁵ recognised that the separation was not good enough to be implemented in an industrial environment. He acknowledged the work done by Finnish workers^{16,17} who showed that addition of dinonylnaphthalene sulfonic acid (DNNSA) considerably accelerated the rate of nickel extraction in such systems. To confirm the extractive ability of DNNSA, Flett¹⁵ performed a series of experiments under the experimental conditions of the Finnish workers (**Table 3.1**). Thereby, he proved that DNNSA did in fact extract nickel. As the equilibrium pH increased, the nickel concentration in the aqueous phase diminished while the nickel concentration in the organic phase increased. This indicated that DNNSA was coordinating to nickel(II) and transferring (extracting) the nickel from the aqueous phase to the organic phase.

Table 3.1: Extraction of nickel(II) using dinonylnaphthalene sulfonic acid.* [Adapted from Flett¹⁵]

Equilibrium pH	Equilibrium Ni concentration**	
	Organic phase (g.L ⁻¹)	Aqueous phase (g.L ⁻¹)
2.03	0.22	0.37
2.46	0.50	0.09
3.03	0.58	0.01

* Dinonylnaphthalene sulfonic acid concentration = 0.002 M in hexane

** Nickel concentration 1×10^{-3} M in 1 M KNO₃

In 1980, Osseo-Asare and Keeney¹⁸ compared three sulfonic acid extractants regarding their effects on the extraction of nickel with LIX63. These extractants were: dinonylnaphthalene sulfonic acid (DNNSA), didodecyl naphthalene sulfonic acid (DDNSA) and di-2-ethylhexyl sodium sulfosuccinate (DEHSS) (Figure 3.2).

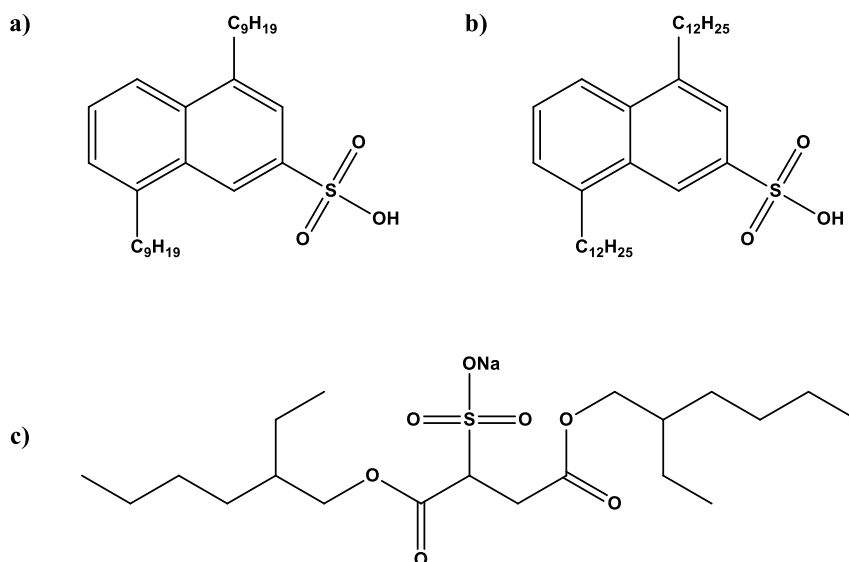


Figure 3.2: Schematic representation of sulfonic acid extractants **a)** DNNSA, **b)** DDNSA and **c)** DEHSS.

They concluded that the acidic extractants interacted synergistically with the oxime extractant. They studied the interfacial (contact point between the aqueous and organic phase) tension and demonstrated that the sulfonates form reversed micelles (alkyl chains on the periphery) in non-polar organic solvents.¹⁸ They proposed that the reversed micelles catalyse the extraction by specific solubilisation of both the metal and the extractant, resulting in an increase in the interfacial concentration of the reacting species.¹⁸

When Osseo-Asare and Keeney¹⁸ made their final comment on the use of sulfonic acids as extractants, they said the following: “*It appears therefore that the sulfonic acids have tremendous potential as catalysts for the liquid-liquid extraction of metals if used in conjunction with the appropriate secondary extractant.*”

More recently, in 2012, Okewole *et al.*⁸ studied the nickel extractive ability of 1-octyl-2-(2'-pyridyl)imidazole (OPIM) in conjunction with dinonylnaphthalene sulfonic acid (DNNSA) as synergist. Their aim was the

selective extraction of nickel(II) from a mixture of base metal ions in a solvent extraction system using 2-octanol/Shellsol 2325 (4:1) as a diluent and modifier respectively.⁸ Interestingly, without any DNNSA present, the nickel(II) extraction was extremely poor. Upon addition of DNNSA they reported the co-extraction of both nickel and cobalt. They subsequently managed to successfully separate nickel from cobalt at an optimised concentration of 0.025 M OPIM along with 0.02 M DNNSA at pH \approx 1.6.⁸

Taking all of the information above into account, we set out to use DNNSA as synergist in this study as well. That, however, could not be realised since Sigma-Aldrich discontinued this product and companies that did have it in stock were asking a mini fortune to ship it to Cape Town, South Africa. Consequently, we decided to use a reagent similar to that of DNNSA: sodium dodecylbenzenesulfonate (**Figure 3.3**). Compared to DNNSA, it too has a characteristic long alkyl tail, an aromatic body and sulfonate head.

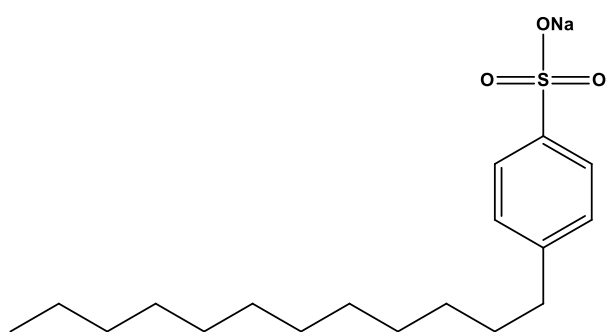


Figure 3.3: The synergist used in this study – sodium dodecylbenzenesulfonate (SDBS).

3.2 Materials and methods

3.2.1 Chemicals and reagents

The chemicals listed in **Table 3.2** were all bought from reputable suppliers and used without further purification.

Table 3.2: List of chemicals used.

Chemical/Reagent	% Purity/Concentration	Supplier
Cadmium(II) nitrate tetrahydrate	98	Fluka
Chloroform	98	Alfa Aesar
Cobalt(II) nitrate hexahydrate	\geq 98	Merck
Copper(II) nitrate trihydrate	\geq 99	Sigma-Aldrich
Lead(II) nitrate	\geq 99	Sigma-Aldrich
Nickel(II) nitrate hexahydrate	\geq 96	Merck
Nitric acid concentrate	1.0 M	Sigma-Aldrich
Sodium dodecylbenzenesulfonate	technical grade	Sigma-Aldrich
Sodium hydroxide	\geq 97	Alfa Aesar
Zinc(II) nitrate hexahydrate	\geq 98	Sigma-Aldrich

The ligands 2-(1*H*-imidazol-2-yl)pyridine (**1**), 2-(1-methyl-imidazol-2-yl)pyridine (**2**), 2-(1-butyl-imidazol-2-yl)pyridine (**3**), 2-(1-octyl-imidazol-2-yl)pyridine (**4**), 2-(1'-pyrazolyl)-methylpyridine (**5**), 2-(3,5-dimethyl-pyrazol-1-yl)-methylpyridine (**6**), 2-(3-methyl-pyrazol-1-yl)-methylpyridine / 2-(5-methyl-pyrazol-1-yl)-methylpyridine (**7/7'**), 2-(3-butyl-pyrazol-5-yl)pyridine (**8**), 2-[3-(*tert*-butyl)-pyrazol-5-yl]pyridine (**9**) and 2-(3-octyl-pyrazol-5-yl)pyridine (**10**) were synthesised according to the procedures described in **Sections 2.3.1–2.3.10** of **Chapter 2**.

3.2.2 Instrumentation

3.2.2.1 pH determinations

The pH measurements were performed on a *Thermo Orion 420A+ pH meter*, using standards (pH 4, 7 and 10) to calibrate the system before every set of measurements.

3.2.2.2 Lab shaker

The organic and aqueous phases were thoroughly mixed during extraction studies using a *SPL-MP15 Labcon linear platform shaker*.

3.2.2.3 Inductively coupled plasma

Metal concentrations in the ppm to mid-ppb range were measured on a *Thermo ICap 6300 ICP-AES*, while ultra-trace analyses were performed on an *Agilent 7900 ICP-MS* or *Agilent 8800 QQQ ICP-MS*.

3.2.2.4 Balances

Precisa XB 320M and *Precisa XB 220A* balances were used to weigh off accurate amounts of reagent.

3.2.3 Preparation of acidic and basic solutions

1.0 M HNO₃ and 1.0 M NaOH solutions were prepared to adjust the pH of the aqueous phase during extraction studies. Very small amounts were used as not to alter the metal ion concentration too much.

3.2.3.1 1.0 M HNO₃ solution

Nitric acid concentrate (1.0N) was quantitatively transferred into a 1 L volumetric flask and filled up to the mark using deionised water, yielding a 1.0 M HNO₃ solution.

3.2.3.2 1.0 M NaOH solution

A 1.0 M NaOH solution was prepared by adding NaOH pellets (40 g) into a 1 L volumetric flask and dissolving it in 0.50 L deionised water, whereafter the volumetric flask was filled up to the mark.

3.2.4 Solvent extraction procedure and conditions

All the solvent extraction experiments were carried out in a temperature controlled laboratory at 25 (± 2) °C. Equal volumes (5 mL) of 0.01 M metal nitrate solution (aqueous phase) and chloroform (containing 0.01 M of the appropriate ligand and varying concentrations of synergist) were transferred into a 30 mL glass vial (no. 8 polytop) using a Gilson pipette (**Figure 3.4**). Once the glass vials had the appropriate contents, they were

sealed with plastic tops and parafilm to ensure that no leakages occurred. These vials were placed on a *Labcon* laboratory shaker for 24 hours (in-built automatic timer) at an optimised speed of 150 rpm. After the 24-hour period, 1 mL of the aqueous phase was collected and diluted to 10 mL with 0.1 M HNO₃ and submitted for ICP analysis. The percentage extraction (%E) of the metals were calculated according to **Equation 33**:

$$\%E = \left(\frac{C_i - C_s}{C_i} \right) \times 100 \quad \text{Equation 33}$$

where C_i is the initial concentration (mg.L⁻¹) of the metal aqueous solution and C_s is the concentration (mg.L⁻¹) of the metal aqueous solution after extraction.

Generally, the pH of the aqueous phase was kept as close to ~5 as possible, except for pH isotherm and metal stripping studies. Solvent extraction experiments were performed either in duplicate (×2) or triplicate (×3) to ensure that the results were accurate and trustworthy.

Microsoft Office Excel, Version 16.0.7167.2040 was used for all calculations, extraction plots and curves.

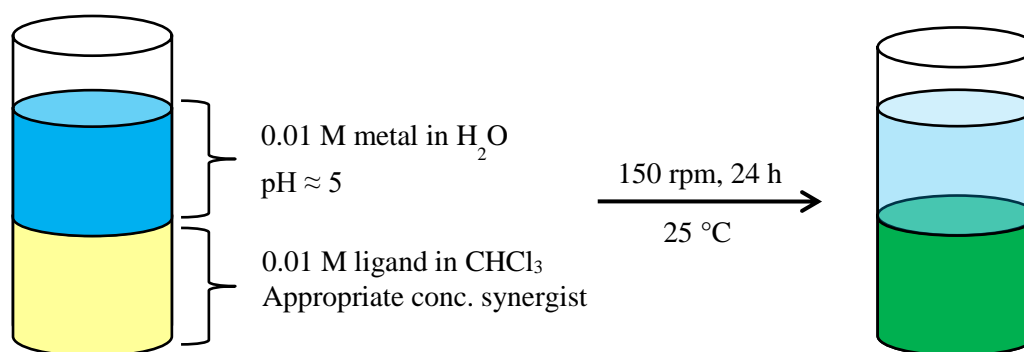


Figure 3.4: General scheme of the solvent extraction procedure.

3.3 Results and discussion

Solvent extraction studies can be challenging in the sense that it requires large quantities of extractant to successfully execute a wide range of studies. This fact was compounded by the fact that each individual extraction experiment was repeated three times to ensure that the data was reliable and to minimise the effects of experimental errors. Therefore, great care was taken with each measurement and experimental setup so as not to waste synthesised extractants unnecessarily.

We decided that the ligand concentration to be used throughout this study should be 0.01 M. This was merely done to save time in synthesising these ligands and to limit the cost of chemicals, reagents and laboratory consumables. From literature¹⁹⁻²⁴ it was clear that there were numerous examples of imidazolyl- and pyrazolyl pyridine ligands forming 1:1 complexes with Ni(II), Cu(II), Cd(II), Zn(II), etc. Therefore, we expected the metal-to-ligand (M:L) ratio to be 1:1, and subsequently led us to use a 0.01 M metal ion concentration throughout this study as well.

3.3.1 Determining the optimum synergist concentration for nickel(II) extractions

Before any extraction study can commence, it is imperative that the optimum synergist concentration be determined first. This is crucial information that is frequently omitted from literature. It is often thought that an increase in synergist concentration would lead to an increase in the percentage extraction of a metal ion. Although this seems logical, it has to be proved by performing an experiment where the synergist concentration is varied and the metal ion concentration is kept constant (**Figure 3.5**). Extractants were excluded from this experiment in order to observe the effect of the synergist concentration on the percentage extraction of nickel(II).

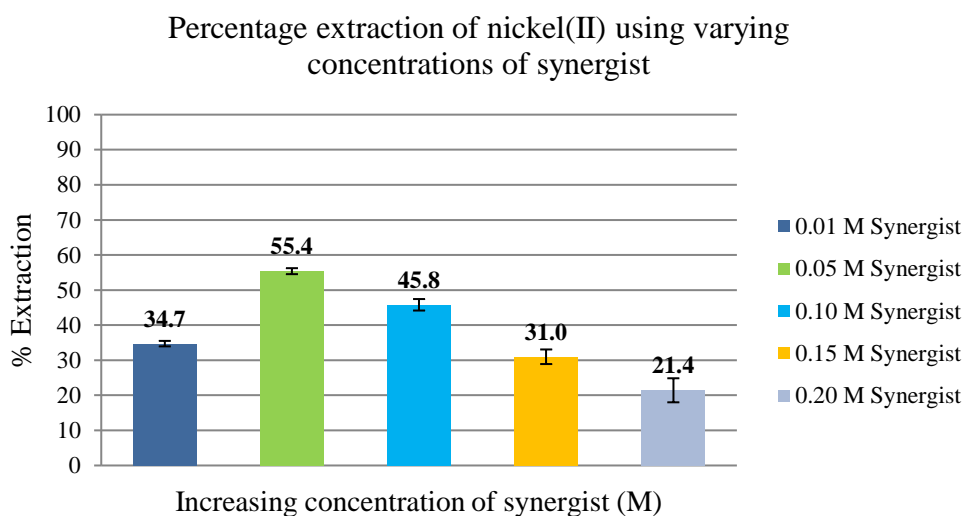


Figure 3.5: Percentage extraction of nickel(II) using varying concentrations of synergist (SDBS). [See **Table 3.5** in **Supplementary information** on CD]

From **Figure 3.5** it was clear that 0.05 M of sodium dodecylbenzenesulfonate (SDBS) gave the best extraction result. This meant that the optimum metal to synergist (M:S) ratio was 1:5. This seemed to be somewhat counter-intuitive, as one would expect an increase in nickel(II) extraction as the synergist concentration increases. From literature,²⁵⁻²⁷ SDBS is well-known as a surfactant which has an amphiphilic nature, *i.e.*, it is both hydrophilic (due to its sulfonate head) and hydrophobic (due to its long alkyl tail). This leads to the fact that SDBS can form micelles under a specific set of conditions, one of which is the critical micelle concentration (CMC): the minimum concentration needed for the formation of micelles to occur. It is also known that liquid-liquid (aqueous-organic) systems encourage the formation of reverse micelles in the less polar organic phase. This means that the aliphatic chains are pointed outward while the sulfonate heads are pointing inward (**Figure 3.6**).

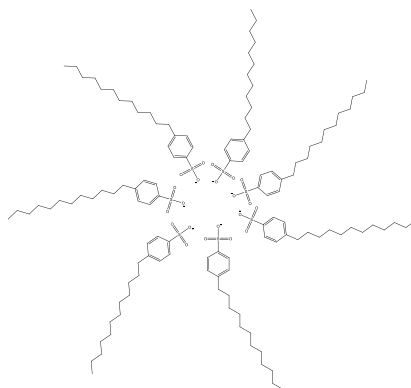


Figure 3.6: An example of a reversed SDBS micelle in a non-polar organic solvent.

Osseo-Asare and Keeney¹⁸ reported a dramatic increase in nickel(II) extraction with DDNSA at the critical micelle concentration and showed that the percentage extraction only increases past this point, albeit very slight. We, on the other hand, observed a sharp rise in extraction from a 1:1 to 1:5 ratio and then witnessed a steady decline in the extraction of nickel(II) from a 1:10 to 1:20 ratio. As yet, we could not fully explain this interesting phenomenon, although we theorise that the high concentration of sulfonate synergist may be thermodynamically more stable in forming colloids/micelles than coordinating to the nickel(II) ions. High sulfonate concentrations also make it difficult to distinguish between the effects of micelles and microemulsions.¹⁸

To further prove that the optimum synergist concentration was 0.05 M, we performed experiments similar to the one above (**Figure 3.5**), only this time in the presence of a ligand as well. Three ligands were chosen at random, one from each of the main ligand classes (see **Section 2.1** in **Chapter 2**): 2-(1-octyl-imidazol-2-yl)pyridine (**4**), 2-(1'-pyrazolyl)-methylpyridine (**5**) and 2-(3-butyl-pyrazol-5-yl)pyridine (**8**). These ligands (0.01 M) in conjunction with SDBS (varying concentrations) were used in the extraction of nickel(II) (**Figures 3.7–3.9**).

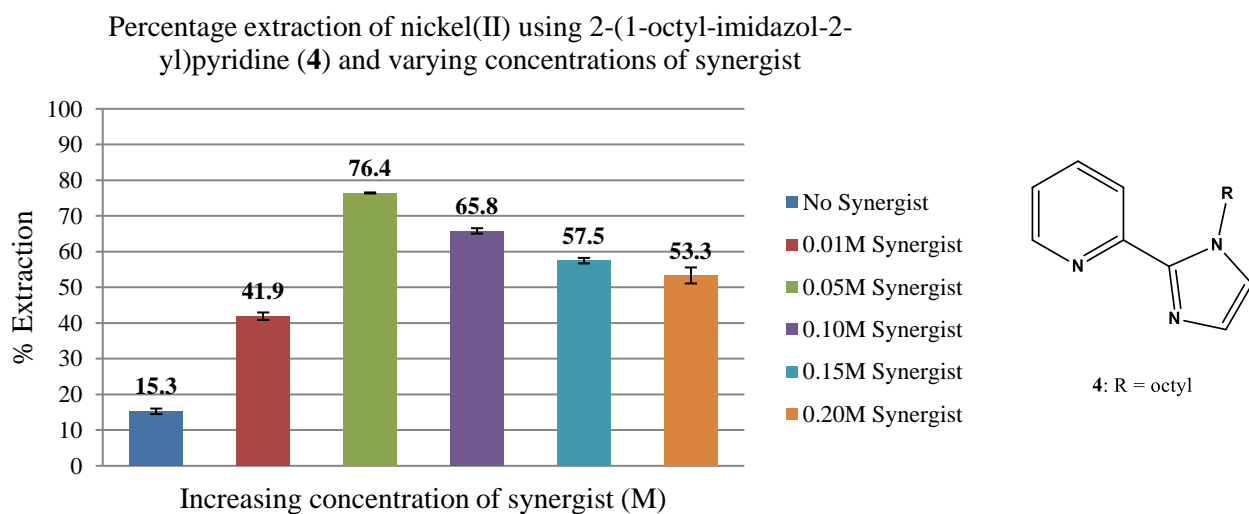


Figure 3.7: Percentage extraction of nickel(II) using 2-(1-octyl-imidazol-2-yl)pyridine (**4**) and varying concentrations of synergist (SDBS). [See **Table 3.7** in **Supplementary information** on CD]

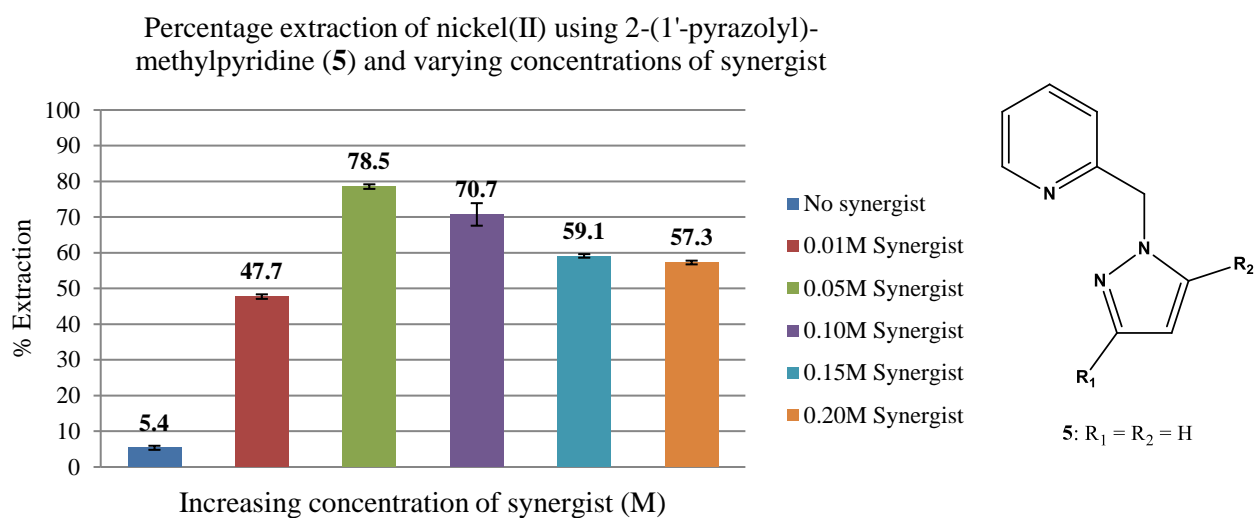


Figure 3.8: Percentage extraction of nickel(II) using 2-(1'-pyrazolyl)-methylpyridine (**5**) and varying concentrations of synergist (SDBS). [See **Table 3.8** in **Supplementary information** on CD]

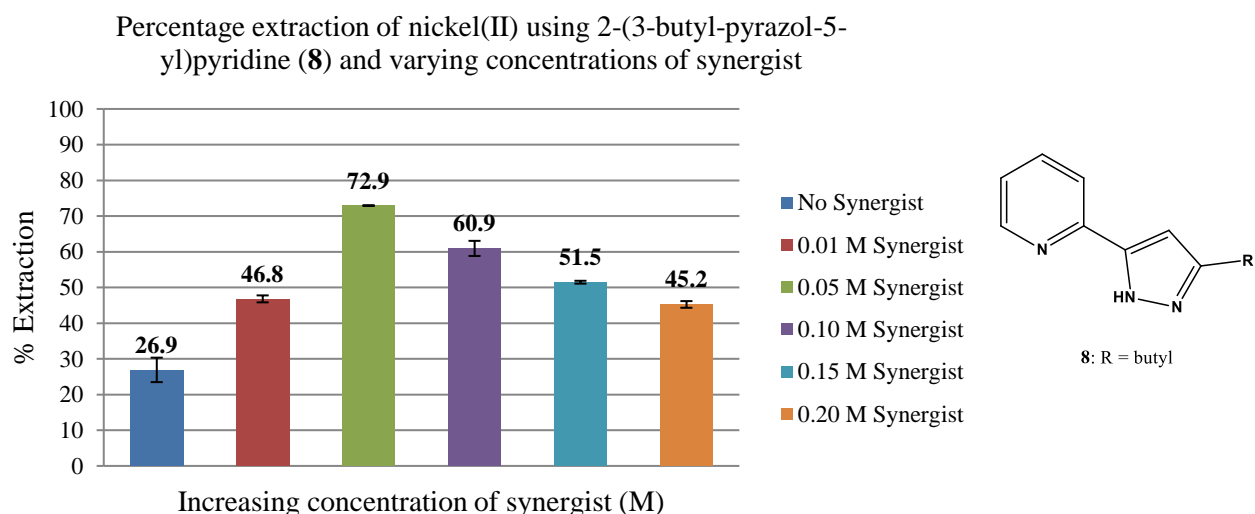


Figure 3.9: Percentage extraction of nickel(II) using 2-(3-butyl-pyrazol-5-yl)pyridine (**8**) and varying concentrations of synergist (SDBS). [See **Table 3.9** in **Supplementary information** on CD]

From **Figures 3.7–3.9** we proved without doubt that the optimum synergist concentration was in fact 0.05 M. The first sign of synergistic effects was observed from **Figures 3.7** and **3.8**. Without any synergist added, 2-(1-octyl-imidazol-2-yl)pyridine (**4**) extracted 15.3% nickel(II) while 2-(1'-pyrazolyl)-methylpyridine (**5**) extracted 5.4%. When these extraction values along with the optimum extraction value of the synergist ($55.4 \pm 0.9\%$, **Figure 3.5**) were subtracted from their individual maximum extraction values (76.4 ± 0.1 and $78.5 \pm 0.6\%$, **Figures 3.7** and **3.8**), we observed synergistic gains of $5.70 (\pm 0.85)$ and $17.7 (\pm 0.9)\%$ respectively. The opposite was true for 2-(3-butyl-pyrazol-5-yl)pyridine (**8**), where it appeared as though a negative interaction between the ligand and synergist was at play (this is discussed in greater detail in **Section 3.3.4**, **Chapter 3**).

Once again, in all three cases, we observed a steep increase in the extraction of nickel(II) from no synergist (ligand only) to a 1:5 (M:S) ratio and a steady decline from a 1:10 to 1:20 ratio. The involvement of the synergist proved to be essential to this study, in view of the fact that a lack of extraction was observed in its absence. This could possibly be rationalised on the basis that nitrate ions do not readily phase-transfer cationic complexes from the aqueous to the organic phase due to high hydration energies offered by nitrate ions.²⁸

3.3.2 Solvent extraction of nickel(II)

The extraction of nickel(II) by means of imidazolyl pyridine ligands (**1–4**) yielded good results in terms of synergistic extractions (**Figure 3.10**). All four ligands (**1–4**), in conjunction with SDBS (at optimum concentration: 0.05 M), extracted nickel(II) in the low to mid-70% range and gained 10.2 (± 0.2), 15.7 (± 0.8), 14.0 (± 0.3) and 5.70 (± 0.15)% respectively for their synergistic interactions with SDBS. Okewole *et al.*⁸ reported extraction results for nickel(II) in the mid-90% range using 2-(1-heptyl-1*H*-imidazol-2-yl)pyridine, 2-(1-octyl-imidazol-2-yl)pyridine and 2-(1-decyl-1*H*-imidazol-2-yl)pyridine in conjunction with DNNSA. In light of their results it would appear as though our extraction results don't compare as well, but it has to be noted that Okewole *et al.*⁸ used an extractant to metal ratio of 1:25 and a synergist to metal ratio of 1:15. This means that their extraction system has far greater extractive power, hence their excellent results.

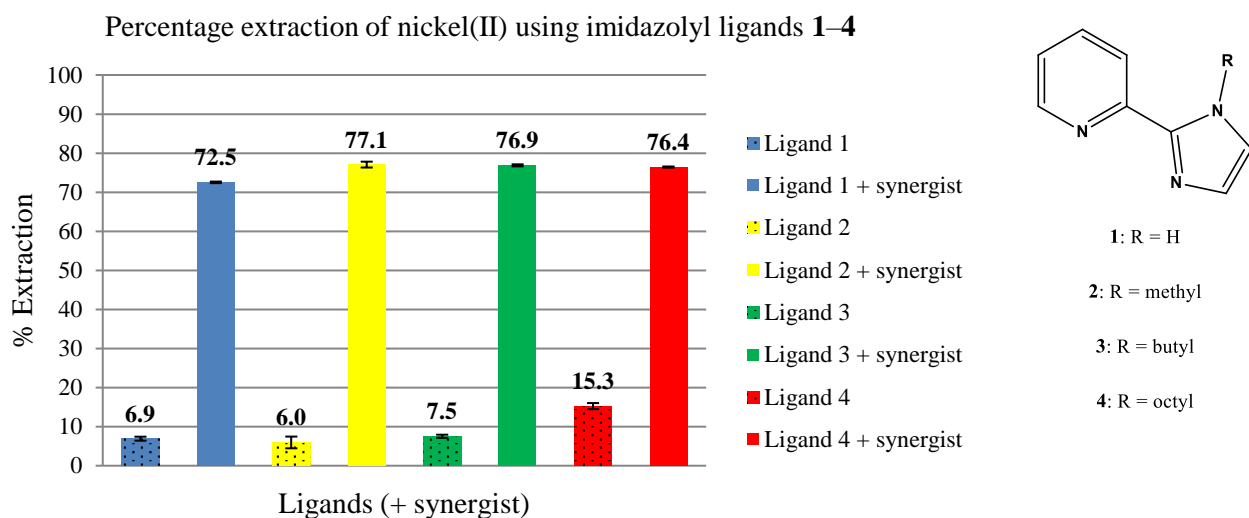


Figure 3.10: A comparison of the percentage extraction of nickel(II) using 2-(1*H*-imidazol-2-yl)pyridine (**1**), 2-(1-methyl-imidazol-2-yl)pyridine (**2**), 2-(1-butyl-imidazol-2-yl)pyridine (**3**) and 2-(1-octyl-imidazol-2-yl)pyridine (**4**). Synergist concentration = 0.05 M. [See **Table 3.10** in **Supplementary information** on CD]

From **Figure 3.10**, in the absence of synergist, we noted that ligand **4** extracted slightly more nickel(II) than ligands **1–3** and can most likely be attributed to the presence of the octyl moiety, making it more soluble in the organic phase and less soluble in the aqueous phase. Generally, it would appear as though the following extraction trend holds true (no synergist): ligand **4** > ligand **3** > ligand **2** \approx ligand **1**.

Nickel(II) extraction using methylpyrazolyl ligands (**5–7/7'**) yielded similar results to the abovementioned imidazolyl ligands (**1–4**) (**Figure 3.11**). Poor extraction results were observed for ligands **5**, **6** and **7/7'** without

the addition of synergist. This was somewhat surprising, since we expected an increase in chelate ring size (smaller bite-size) to effect an increase in their selectivity towards smaller divalent metal ions, such as nickel(II).²⁹ Upon the addition of SDBS, however, we observed a dramatic increase in nickel(II) extraction with synergistic gains of 17.7 (± 0.6), 9.80 (± 0.37) and 16.1 (± 0.4)% for ligands **5**, **6** and **7/7'** respectively.

From the data (**Figure 3.11** and **Table 3.11** in **Supplementary information**) we observed the following synergistic extraction trend: ligand **5** > ligand **7/7'** > ligand **6**. This possibly indicates that an increase in methyl groups on the pyrazole moiety leads to a slight decrease in nickel(II) extraction. The methyl group closest to the chelating nitrogen atom may hinder access to that nitrogen, resulting in slightly poorer extraction results for ligands **6** and **7/7'**. For ligand **5**, however, the absence of alkyl groups on the pyrazole moiety seems to play a significant role in its superior nickel(II) extraction results.

Due to lack of studies on the extraction of nickel(II) using similar ligands, no meaningful comparison to literature could be made.

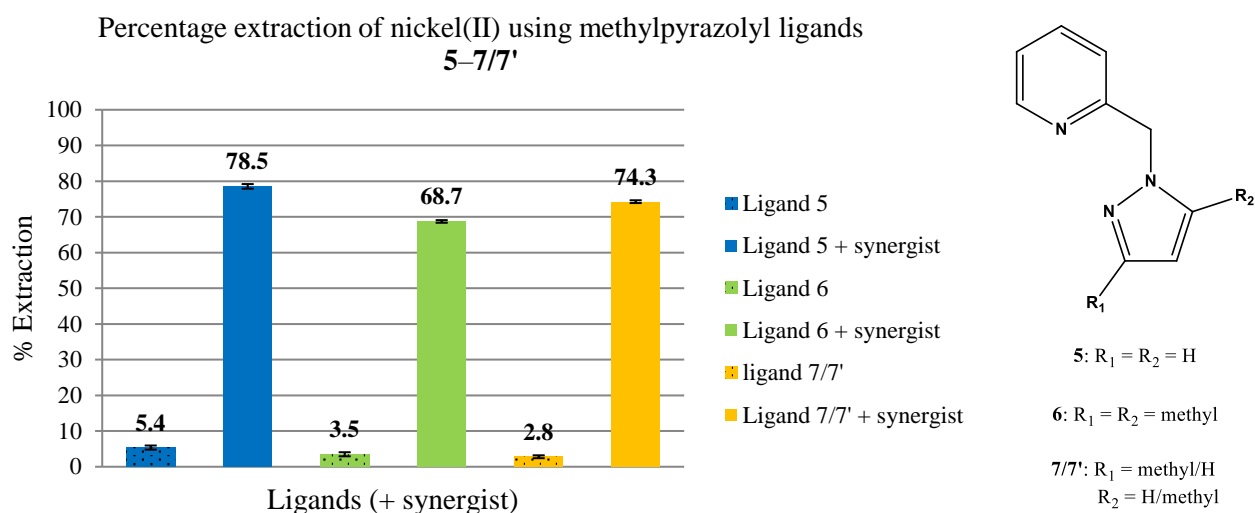


Figure 3.11: A comparison of the percentage extraction of nickel(II) using 2-(1'-pyrazolyl)-methylpyridine (**5**), 2-(3,5-dimethyl-pyrazol-1-yl)-methylpyridine (**6**), 2-(3-methyl-pyrazol-1-yl)-methylpyridine / 2-(5-methyl-pyrazol-1-yl)-methylpyridine (**7/7'**). Synergist concentration = 0.05 M. [See **Table 3.11** in **Supplementary information** on CD]

The most interesting results regarding nickel(II) extractions, were the much improved extractive ability of pyrazolyl ligands **8–10** (relative to ligands **1–7/7'**), without the use of SDBS (**Figure 3.12**). We theorise that the presence of the acidic (labile) proton on the pyrazole moiety in addition to the position of the alkyl moiety contribute greatly toward these extraction results. It was also noted from **Figure 3.12** that 2-(3-octyl-pyrazol-5-yl)pyridine (**10**) had a slightly better extractive ability due to its octyl moiety, making the Ni-complex more soluble in the organic phase. Moreover, the long alkyl chain pushes electron density into the pyrazole ring making the -NH proton more acidic (labile) and, therefore, resulting in even stronger coordination bonds. The general extractive ability of ligands **8–10** appears to be the following: ligand **10** > ligand **9** > ligand **8**. This

agrees with what we expected to observe, since we know that tertiary butyl moieties have stronger electron donating power than butyl moieties.

Upon addition of SDBS, we expected extraction results of > 80%. This did not materialise due to a negative synergistic effect. Ligands **8**, **9** and **10** showed significant decreases in nickel(II) extractions due to negative synergist-ligand interactions. Ligands **8**, **9** and **10** in conjunction with SDBS yielded the following results respectively: $-9.4 (\pm 0.1)$, $-11.8 (\pm 0.1)$ and $-18.8 (\pm 0.5)\%$. We theorise that the sodium ion (from the synergist, SDBS) acts as an electron acceptor to the anionic pyrazolyl ligand species. In essence, the sodium cation acts as an anionic dampener (or neutraliser) and withdraws electron density from the pyrazole ring, resulting in weaker coordination bonds being formed.

Once again, due to lack of studies on the extraction of nickel(II) by means of pyrazolyl-type ligands, we could not draw meaningful comparisons to previously reported studies. One would assume that ligands **8–10** would not be implemented in industry in conjunction with SDBS, due to the aforementioned negative interaction between the synergist and the ligands. However, in the absence of SDBS, the use of ligands **8–10** as extractants of other divalent base metal ions, such as copper(II), still warrants further investigation (see **Sections 3.3.4, 3.3.5 and 3.3.8, Chapter 3**).

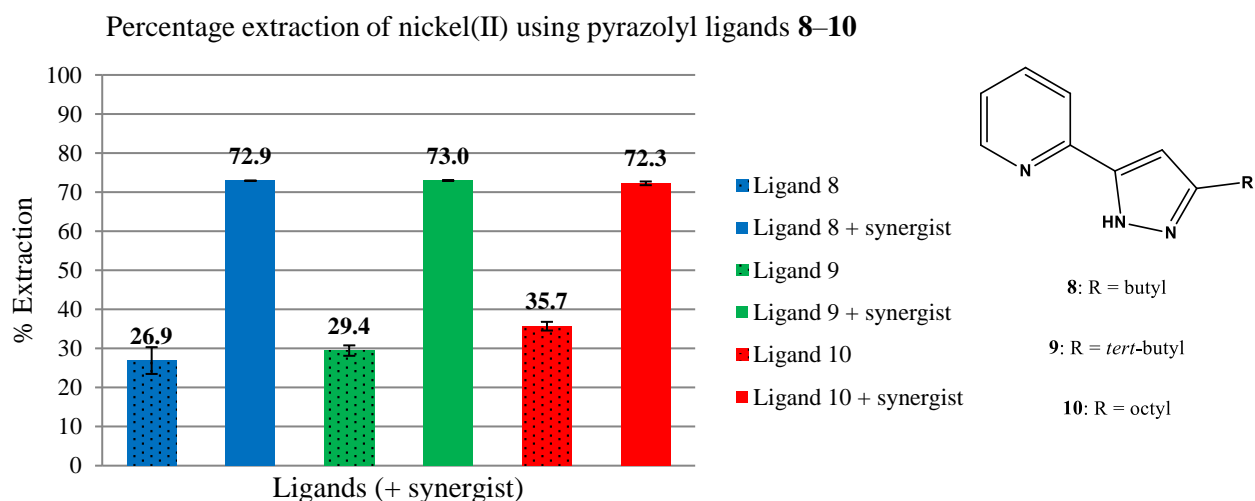


Figure 3.12: A comparison of the percentage extraction of nickel(II) using 2-(3-butyl-pyrazol-5-yl)pyridine (**8**), 2-[3-(*tert*-butyl)-pyrazol-5-yl]pyridine (**9**) and 2-(3-octyl-pyrazol-5-yl)pyridine (**10**). Synergist concentration = 0.05 M. [See **Table 3.12** in **Supplementary information** on CD]

Comparing ligands **1–10**, we clearly saw improved nickel(II) extraction results for ligands **8–10** in the absence of SDBS. The presence of an acidic proton and generally low pK_a values (0–4) for pyrazolyl ligands,² play a major role in its enhanced ability to extract nickel(II).

3.3.3 Time-dependent extraction study of nickel(II)

The extraction process is a dynamic one, meaning that it takes various extraction systems different times to reach equilibrium at $25 (\pm 2) ^\circ\text{C}$. It is essential that extraction processes are at equilibrium and not in the process of reaching equilibrium when samples are submitted for ICP analyses. When ICP analyses are performed on samples that have not yet reached equilibrium, the results would be inaccurate and misinterpreted.

Three ligands, one from each of the main classes of ligands (see **Section 2.1 in Chapter 2**), were chosen to determine whether the extraction of nickel(II) reached equilibrium within the 24-hour time frame (**Figures 3.13–3.15**). These ligands were 2-(1-octyl-imidazol-2-yl)pyridine (**4**), 2-(1'-pyrazolyl)-methylpyridine (**5**) and 2-(3-butyl-pyrazol-5-yl)pyridine (**8**).

From **Figures 3.13–3.15** it was blatantly clear that equilibrium had been reached for all three ligands well before the 24-hour mark. In fact, ligand **4** reached equilibrium after about one hour while ligands **5** and **8** reached equilibrium after approximately four hours. This agrees with observations made in the laboratory, in that upon the addition of the pale blue aqueous phase (Ni^{2+} -rich) to the pale yellow organic phase (ligand- and synergist-rich) the organic phase turned bright blue-green almost instantly. This was the first indication that the ligand/synergist combination had a high affinity for Ni^{2+} ions and that equilibrium would be reached speedily. The percentage extraction of nickel(II) after 24 hours is in good accord with the extraction results reported in **Section 3.3.2, Chapter 3 (Figures 3.10–3.12)**. There are, however, a few data points, especially from **Figures 3.13** and **3.14**, that are outliers but can generally be attributed to experimental/human error, since these studies were only performed in duplicate.

Time-dependent studies are extremely valuable in industry, where time equals money. The faster an extraction process can occur, the quicker the end-product can be obtained. This would not only save money, time and resources, but limit waste production as well.

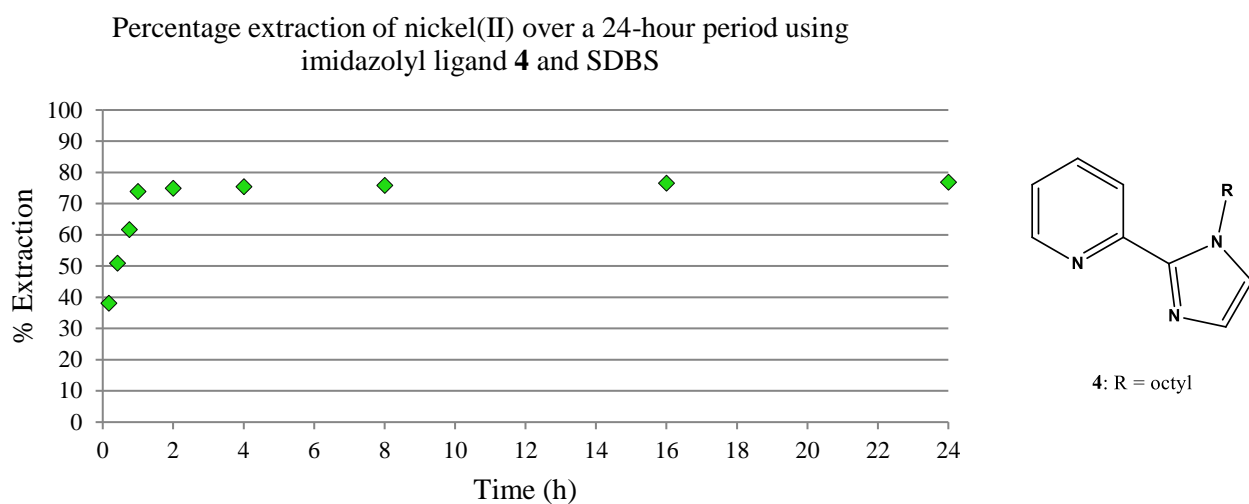


Figure 3.13: Percentage extraction of nickel(II) over a 24-hour period using 2-(1-octyl-imidazol-2-yl)pyridine (**4**) and SDBS. SDBS concentration = 0.05 M. [No error bars added to graph to prevent clutter, see **Table 3.13** in **Supplementary information** on CD]

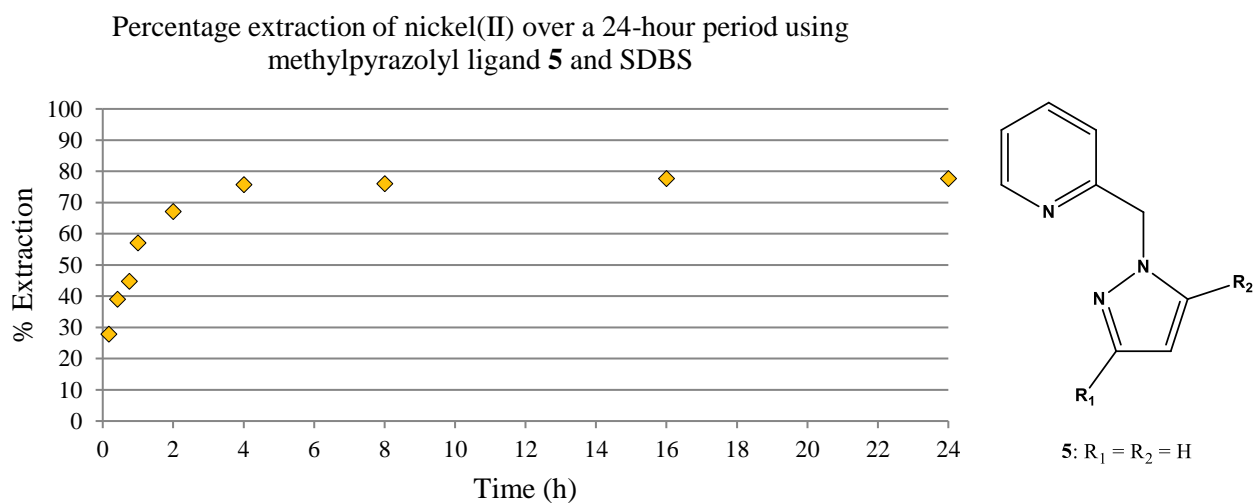


Figure 3.14: Percentage extraction of nickel(II) over a 24-hour period using 2-(1'-pyrazolyl)-methylpyridine (**5**) and SDBS. SDBS concentration = 0.05 M. [No error bars added to graph to prevent clutter, see **Table 3.14** in **Supplementary information** on CD]

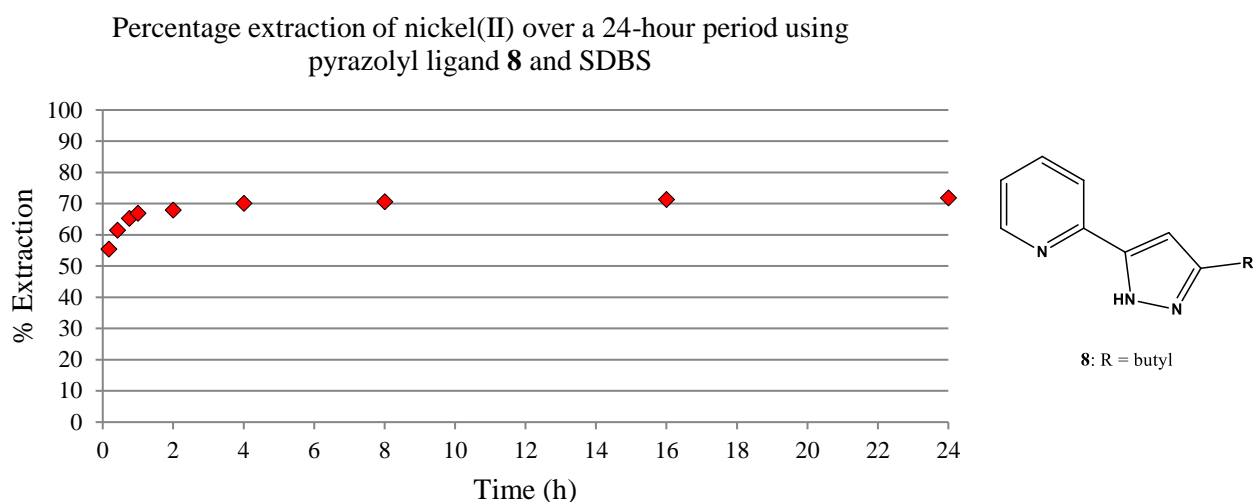


Figure 3.15:

Percentage extraction of nickel(II) over a 24-hour period using 2-(3-butyl-pyrazol-5-yl)pyridine (**8**) and SDBS. SDBS concentration = 0.05 M. [No error bars added to graph to prevent clutter, see **Table 3.15** in **Supplementary information** on CD]

3.3.4 Competitive extraction studies

The competitive (or simultaneous) extraction of six different base metal ions (Cd^{2+} , Co^{2+} , Cu^{2+} , Ni^{2+} , Pb^{2+} and Zn^{2+} , 1:1:1:1:1:1 ratio) using ligands **1–10**, were performed to determine the selectivity of these ligands for any of the aforementioned metal ions. This is a slightly better representation of real-world conditions and mimics what one would find in industry today, but only on a much smaller scale. These studies were performed both in the absence and presence of the synergist, SDBS, to determine its impact on the extraction results. Firstly, we performed a competitive extraction experiment using SDBS in the absence of ligands to measure its extractive capability in a mixed metal ion environment (**Figure 3.16**). This information could be telling in understanding what contribution SDBS makes towards the overall percentage extraction in ligand-synergist systems.

One glaringly obvious fact from **Figure 3.16** was the exceptional selectivity of SDBS towards lead(II) ions. This was not surprising, since it is traditionally known that oxygen extractants selectively extract lead(II) in high yields, especially sulfonic acids.³⁰ The competitive extraction results of lead(II) throughout this study was for all intents and purposes solely attributed to the synergist and not ligands **1–10**. Most other base metal ions were extracted in the mid-20% range, with the exception of copper(II) extraction at 13.2 (± 0.8)%.

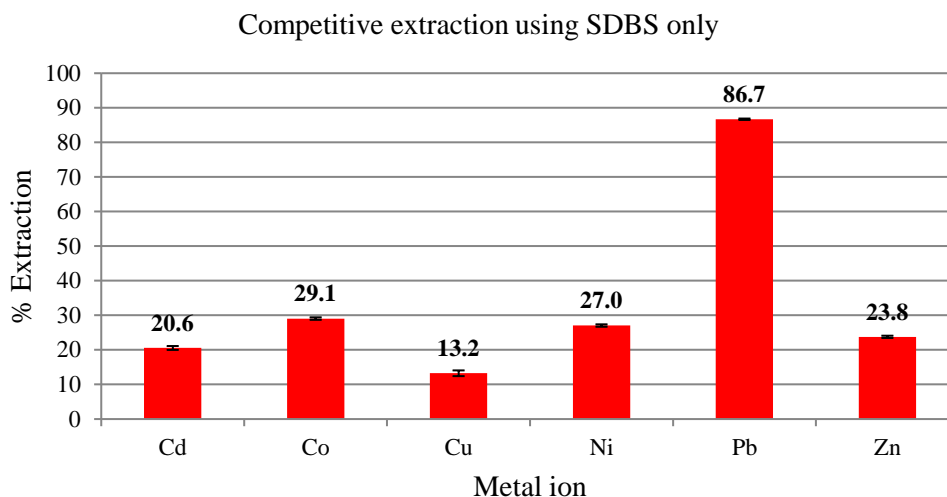


Figure 3.16: Competitive extraction of base metal ions in the presence of the synergist, sodium dodecylbenzenesulfonate (SDBS). [SDBS] = 0.05 M, $[M^{2+}] = 0.01$ M. [See **Table 3.16** in **Supplementary information** on CD]

3.3.4.1 Competitive extraction using imidazolyl ligands

Photos were taken of the competitive extraction polytops for ligands **1–4** (**Figure 3.17**). From the three polytops on the left-hand side of each mini photo (**a–d**), one can clearly see the dark blue colours present in the aqueous phase (top layer), with the exception of photo **d** (ligand **4**). These polytops indicate the extraction of the base metal ion mix without the addition of SDBS. The absence of colour from the organic phases are good visual indicators of poor metal ion extractions, since we expected to see a brightly coloured organic phase upon metal ion coordination and extraction. This fact was supported by **Figures 3.18–3.20** where we performed competitive extraction studies both in the presence and absence of SDBS. **Figures 3.18–3.20** show poor extraction results for all metal ions in the absence of SDBS, with ligand **4** being the exception to the rule. Ligand **4** clearly shows some selectivity towards nickel(II), but more so towards copper(II) (**Figure 3.21**). This follows the trend proposed by Irving and Williams³¹ in 1953, that divalent transition metal ions form stable complexes in the order $Mn < Fe < Co < Ni < Cu > Zn$. The presence of the octyl moiety in ligand **4** seems to have an important effect on extraction results. It is proposed that an increase in alkyl length enhances the solubility of the complex in the organic phase, leading to an increase in extraction. This is confirmed by **Figures 3.18–3.21** (blue bars) as we observe the following extraction trend: ligand **1** < ligand **2** < ligand **3** < ligand **4**. This trend is not only applicable to copper(II) extraction, but to nickel(II) extraction as well.

The use of SDBS in conjunction with ligands **1–4** resulted in a colour change of the organic phase (three polytops on right-hand side of each mini photo, **a–d**). These colour conversions indicate that metal ions have been transferred from the aqueous phase to the organic phase. As we expected, a significant increase in metal extraction was observed upon the addition of SDBS (**Figures 3.18–3.21**, red bars). The lead(II) extraction can solely be attributed to the extractive ability of SDBS, as the extraction values are almost identical to the results displayed in **Figure 3.16**. The most significant synergistic gains were observed for copper(II) extractions using

ligands **1**, **2** and **3**. These yielded mammoth gains of 32.2 (\pm 1.0), 35.1 (\pm 0.9) and 54.1 (\pm 0.9)% respectively. No other noteworthy synergistic gains were made.

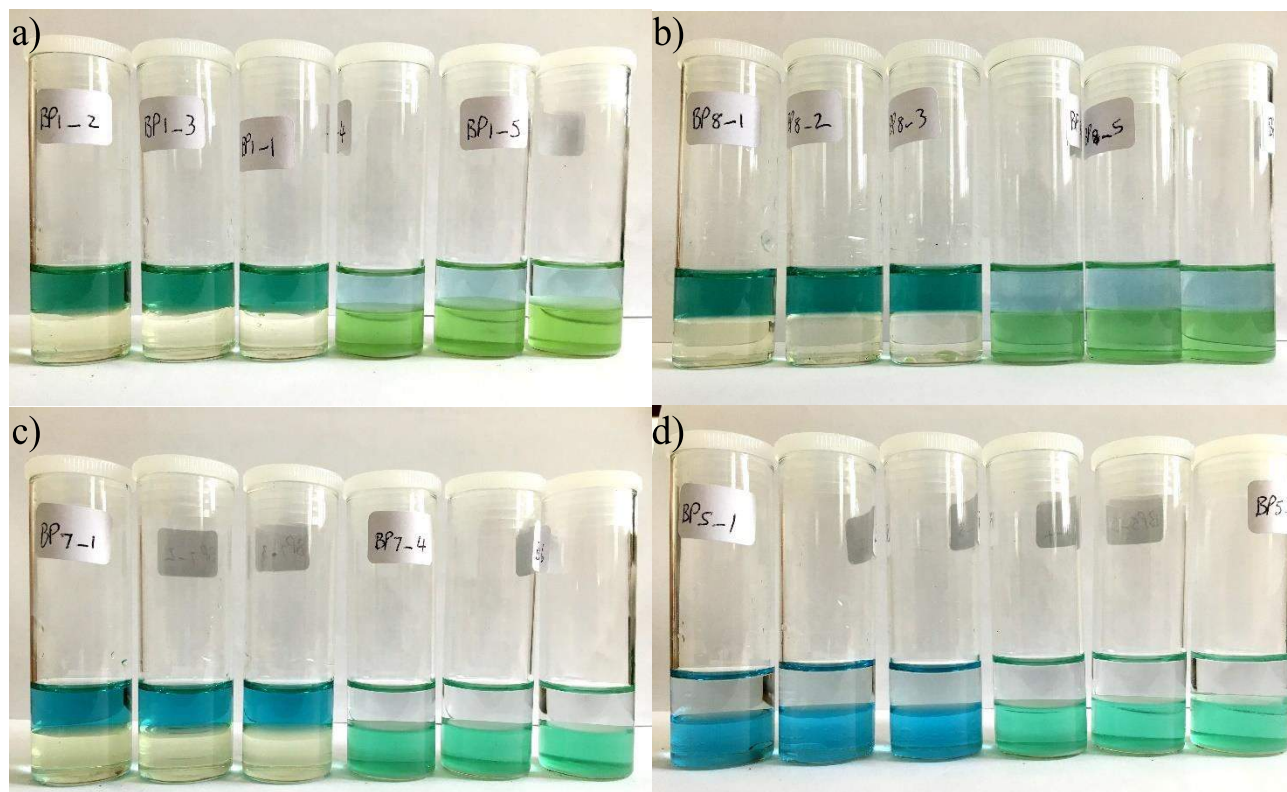


Figure 3.17: Varying colours of the aqueous (top layers) and organic phases (bottom layers) during competitive extraction studies using **a)** ligand **1**, **b)** ligand **2**, **c)** ligand **3** and **d)** ligand **4**. In each picture, the first three polytopes (left) represent competitive extractions without the use of synergist, while the following three polytopes (right) represent competitive extractions in conjunction with the synergist, SDBS.

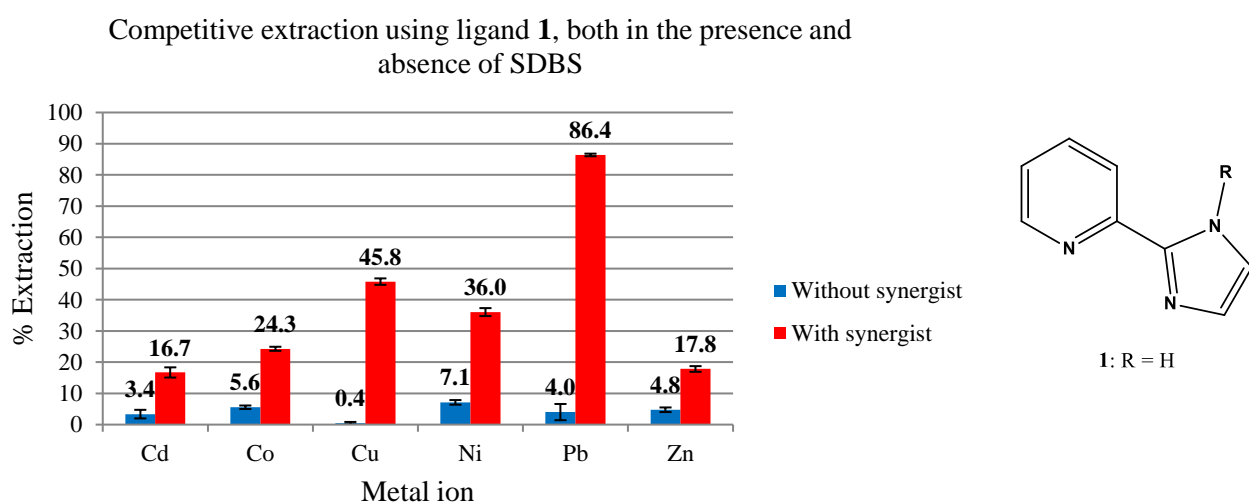


Figure 3.18: Competitive extraction of various base metal ions using 2-(1*H*-imidazol-2-yl)pyridine (**1**), both in the presence and absence of SDBS. [SDBS] = 0.05 M, [M²⁺] = 0.01 M. [See **Table 3.18** in **Supplementary information** on CD]

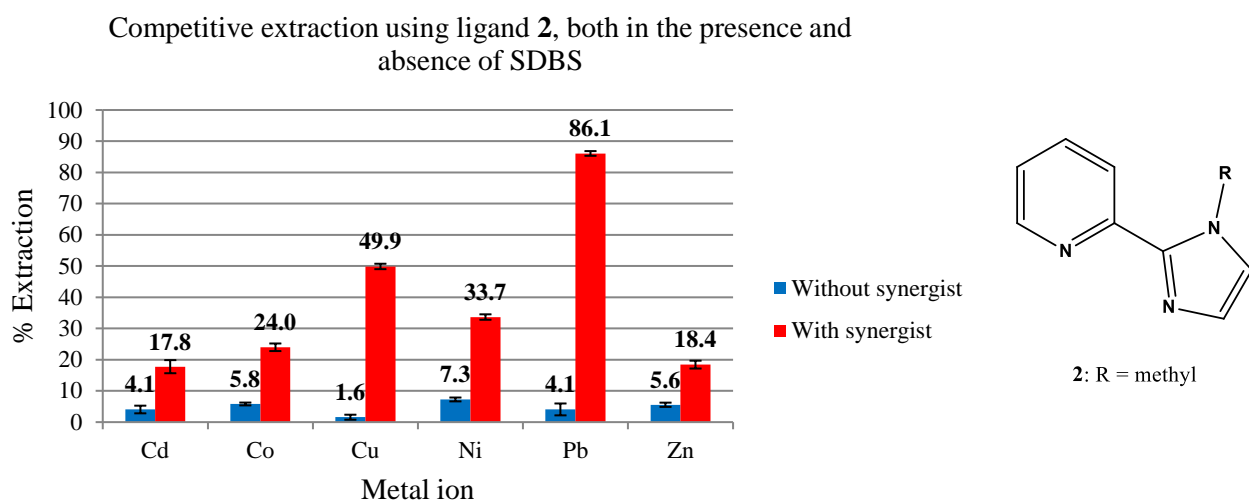


Figure 3.19: Competitive extraction of various base metal ions using 2-(1-methyl-imidazol-2-yl)pyridine (**2**), both in the presence and absence of SDBS. [SDBS] = 0.05 M, $[M^{2+}] = 0.01$ M. [See **Table 3.19** in **Supplementary information** on CD]

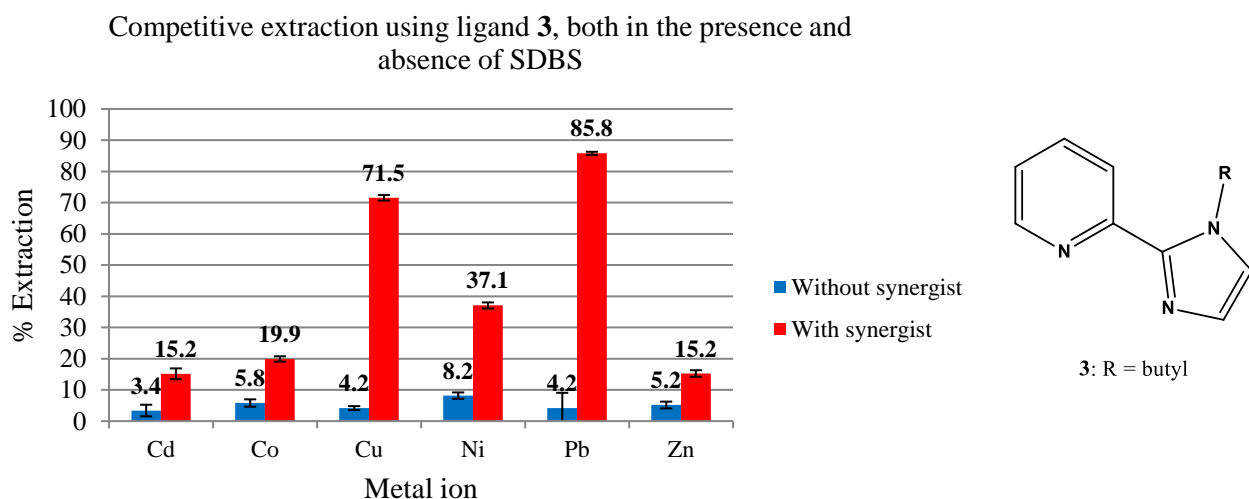


Figure 3.20: Competitive extraction of various base metal ions using 2-(1-butyl-imidazol-2-yl)pyridine (**3**), both in the presence and absence of SDBS. [SDBS] = 0.05 M, $[M^{2+}] = 0.01$ M. [See **Table 3.20** in **Supplementary information** on CD]

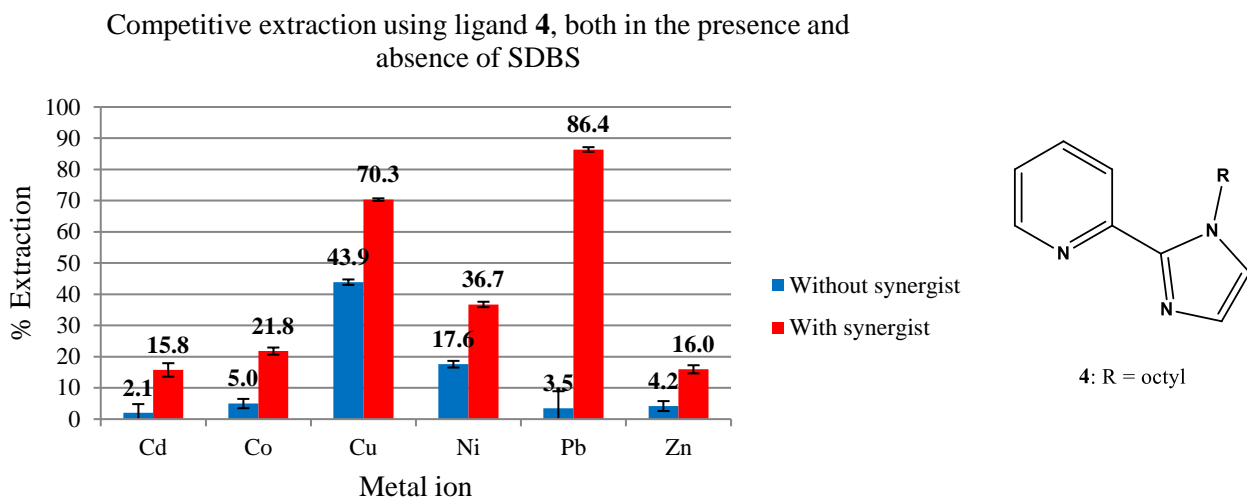


Figure 3.21: Competitive extraction of various base metal ions using 2-(1-octyl-imidazol-2-yl)pyridine (**4**), both in the presence and absence of SDBS. [SDBS] = 0.05 M, $[M^{2+}] = 0.01$ M. [See **Table 3.21** in **Supplementary information** on CD]

3.3.4.2 Competitive extraction using methylpyrazolyl ligands

From **Figure 3.22** we observed brightly coloured aqueous phases (top layers) that indicated a lack of metal ion extraction in the absence of SDBS. **Figures 3.22a** and **b** exhibited blue aqueous phases while **Figure 3.22c** exhibited green aqueous phases. Initially we thought that ligand **7/7'** had extracted a particular metal ion in great excess, thereby resulting in a green coloured aqueous phase. This, however, was not the case once we inspected **Figure 3.25**. There was no real evidence to suggest that the aqueous phase colour was due to metal extraction, therefore we proposed that the colour was due to the mixed ligand system (**7/7'**). We theorised that the combination of ligands **7** and **7'**, each with its own unique electronic properties, contributed toward the green colour we observed in **Figure 3.22c**.

Once we inspected the polytops that contained SDBS (right-hand side of the mini photos) we once again observed a colour conversion, signifying metal ion migration from the aqueous phase to the organic phase. Ligand **5**'s organic phase (bottom layer) was a light blue hue, while ligand **6** had a slightly darker blue hue, indicating that ligand **6** possibly extracted copper(II) in slight excess compared to ligand **5**. This was confirmed upon inspection of **Figures 3.23** and **3.24**, which showed that ligand **5** had extracted $47.6 (\pm 0.5)\%$ copper(II) while ligand **6** extracted $59.9 (\pm 0.3)\%$.

Substantial synergistic gains were observed for copper(II) extractions. Ligands **5–7/7'** in conjunction with SDBS exhibited gains of $34.1 (\pm 0.5)$, $43.2 (\pm 0.3)$ and $39.0 (\pm 0.8)\%$ respectively. These results can most likely be attributed to the fact that larger chelate ring sizes (in this case a six-membered chelate ring) preferentially coordinate to smaller metal ions, such as copper(II).²⁹ The presence of methyl moieties on the pyrazole rings (ligands **6** and **7/7'**) assist in the extraction of copper(II) and consequently decreases the percentage extraction of nickel(II). We theorised that an increase in the number of methyl substituents on the pyrazole ring would lead to an increase in copper(II) extraction due to increased solubility of the copper(II)

complex in the organic phase. This was substantiated after the following copper(II) extraction trend was observed from **Figures 3.23–3.25**: ligand **5** (no methyl substituents) < ligand **7/7'** (one methyl substituent) < ligand **6** (two methyl substituents).



Figure 3.22: Varying colours of the aqueous (top layers) and organic phases (bottom layers) during competitive extraction studies using **a)** ligand **5**, **b)** ligand **6** and **c)** ligand **7/7'**. In each picture, the first three polytops (left) represent competitive extractions without the use of synergist, while the following three polytops (right) represent competitive extractions in conjunction with the synergist, SDBS.

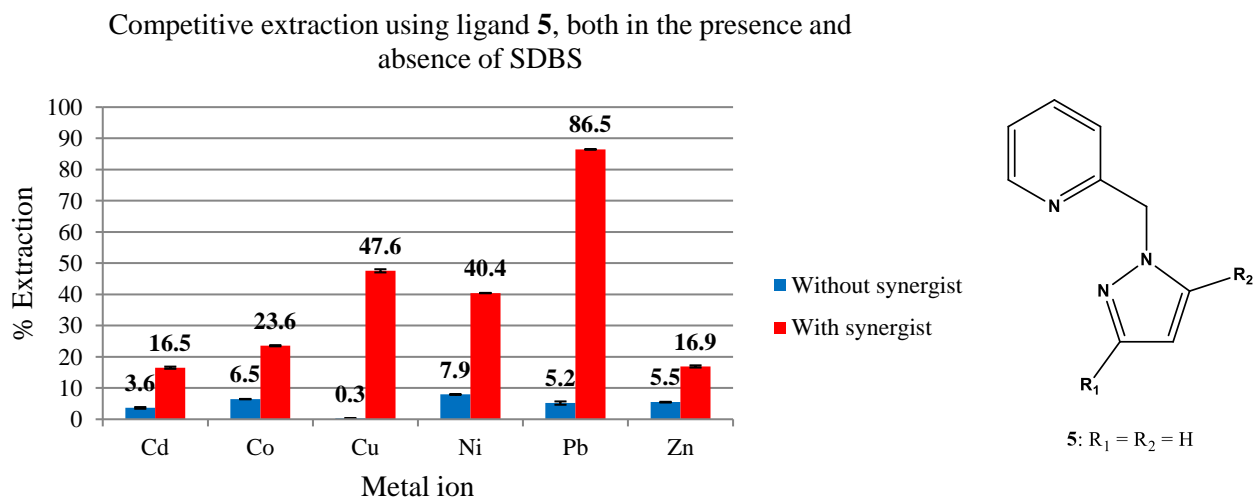


Figure 3.23: Competitive extraction of various base metal ions using 2-(1'-pyrazolyl)-methylpyridine (**5**), both in the presence and absence of SDBS. [SDBS] = 0.05 M, $[M^{2+}] = 0.01$ M. [See **Table 3.23** in **Supplementary information** on CD]

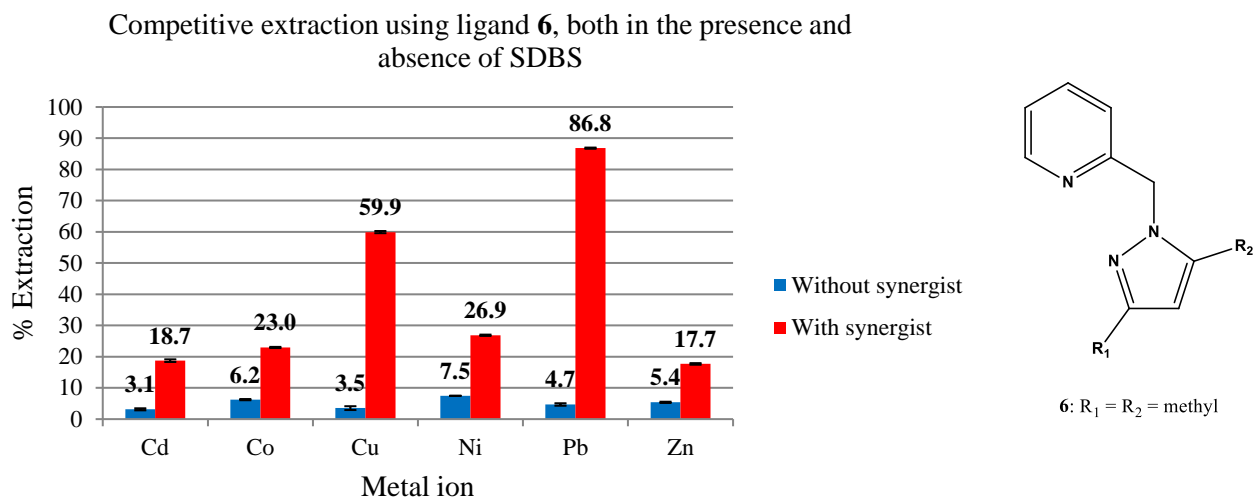


Figure 3.24: Competitive extraction of various base metal ions using 2-(3,5-dimethyl-pyrazol-1-yl)-methylpyridine (**6**), both in the presence and absence of SDBS. [SDBS] = 0.05 M, $[M^{2+}] = 0.01$ M. [See **Table 3.24** in **Supplementary information** on CD]

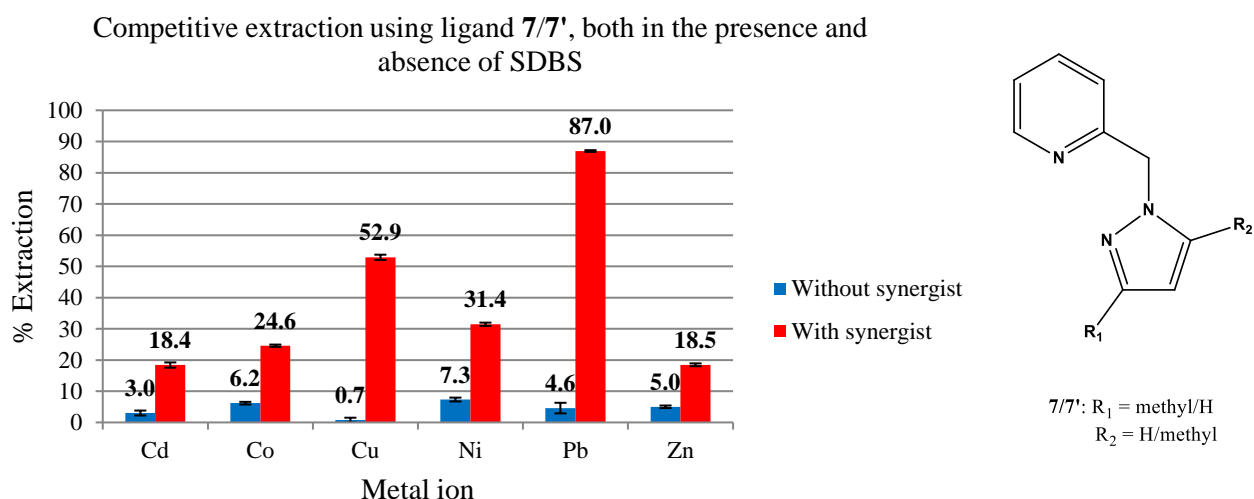


Figure 3.25: Competitive extraction of various base metal ions using 2-(3-methyl-pyrazol-1-yl)-methylpyridine / 2-(5-methyl-pyrazol-1-yl)-methylpyridine (**7/7'**), both in the presence and absence of SDBS. [SDBS] = 0.05 M, $[M^{2+}] = 0.01$ M. [See **Table 3.25** in **Supplementary information** on CD]

3.3.4.3 Competitive extraction using pyrazolyl ligands

Arguably the most interesting results were that of the pyrazole ligands in the absence of SDBS. From **Figures 3.26a** and **c** we observed emerald green organic phases (bottom layers), which was totally unexpected in light of our previous results. We knew, without question, that significant copper(II) extraction took place without SDBS present. This was obvious due to both the colour and colour intensity of the organic phase. Upon studying **Figures 3.27–3.29**, our suspicions were realised. Ligands **8**, **9** and **10** extracted a staggering 83.2 (± 0.6), 38.8 (± 1.0) and 90.2 (± 0.1)% copper(II) respectively, without the use of a synergist. It was interesting

to note that ligand **9** did not extract copper(II) as well as ligands **8** and **10**, and can most likely be attributed to the fact that longer alkyl chains (not branched) are more soluble in the organic phase than in the aqueous phase. Once again alkyl chain length played a major role in the extraction of copper(II), but the opposite seemed to be true regarding nickel(II) extraction. Ligand **9** performed the best regarding nickel(II) extraction, followed by ligands **8** and **10**. This was expected, since ligands **8** and **10** are highly selective towards copper(II) one would automatically expect lower extractions for nickel(II) as explained by the Irving-Williams series.³¹ Conversely, since ligand **9** isn't as selective toward copper(II), the nickel(II) extraction will automatically increase due to more ligand molecules being available for coordination. Generally, the following copper(II) extraction trend seems to hold true regarding extractions with varying alkyl chain length: ligand **9** (*tert*-butyl) < ligand **8** (butyl) < ligand **10** (octyl).

An important characteristic of ligands **8–10** is the presence of an acidic proton. The pyrazolyl moiety can easily be deprotonated in slightly acidic media, yielding an anionic pyrazolyl pyridine ligand that can form strong coordination bonds to copper(II). This, along with strong electron donating alkyl groups (inductive effect) leads to the fact that ligands **8** and **10** (and to a lesser extent ligand **9**) are highly selective towards copper(II) in the presence of other base metal ions.

Upon the addition of SDBS, the selectivity of ligands **8** and **10** towards copper(II) were halved, while the selective extraction of nickel(II) increased with synergistic gains of 9.5 (\pm 0.4) and 8.7 (\pm 0.4)% respectively. In this case, the addition of SDBS actually hinders the selectivity of ligands **8** and **10** towards copper(II) quite significantly, thereby resulting in copper(II) and nickel(II) being co-extracted in the mid-40% range. Although this might seem undesirable, one must keep in mind that nickel(II) and copper(II) separation could possibly occur over two separate stages of extraction: initially with SDBS and then followed by the absence thereof.

In 2006, Bouabdallah *et al.*³² reported the competitive extraction results using tripodal *N*-donor pyrazole ligands. At best, their ligands selectively extracted copper(II) at 62%, which pales in comparison to ligands **8** and **10** in this study.

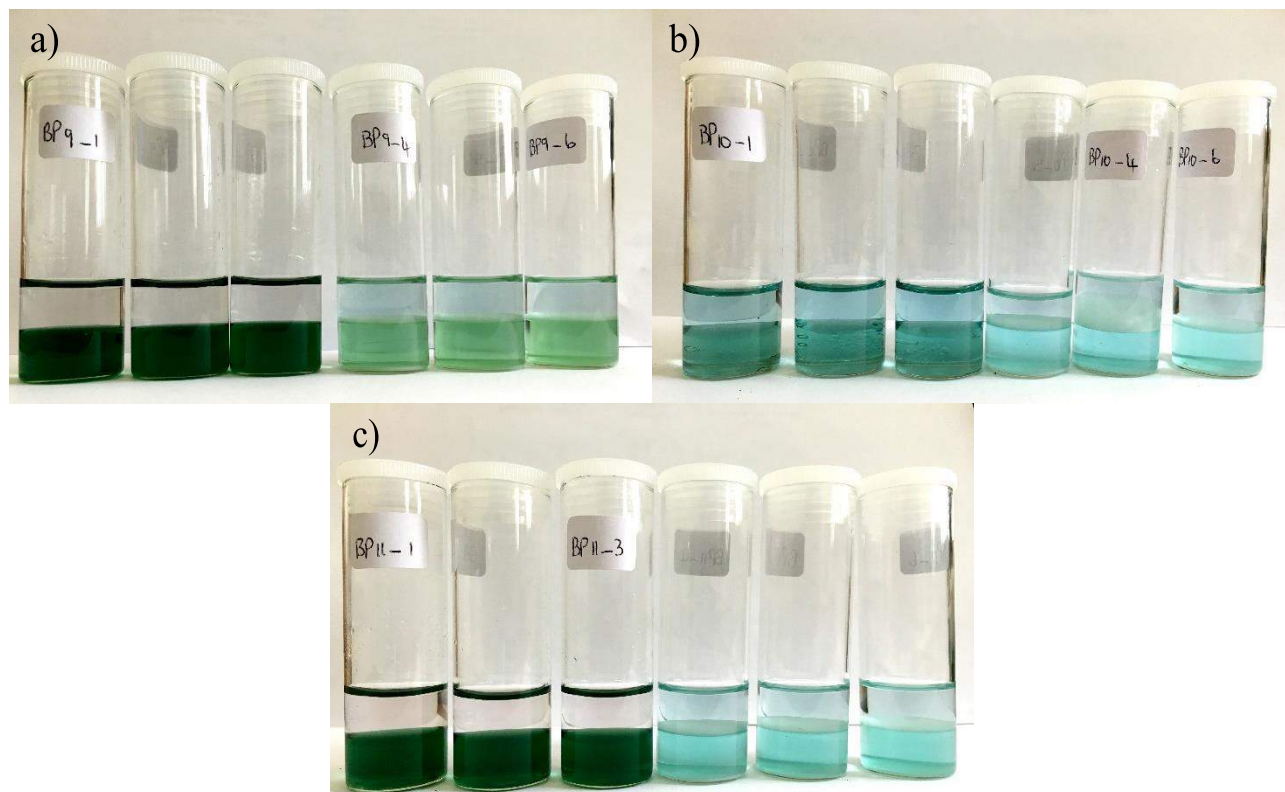


Figure 3.26: Varying colours of the aqueous (top layers) and organic phases (bottom layers) during competitive extraction studies using **a)** ligand **8**, **b)** ligand **9** and **c)** ligand **10**. In each picture, the first three polytops (left) represent competitive extractions without the use of synergist, while the following three polytops (right) represent competitive extractions in conjunction with the synergist, SDBS.

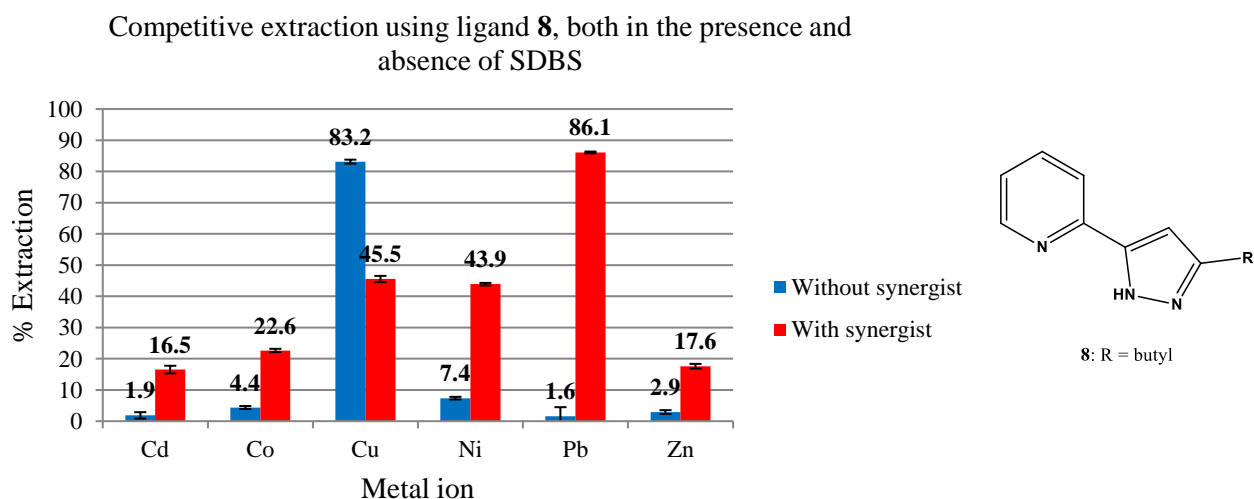


Figure 3.27: Competitive extraction of various base metal ions using 2-(3-butyl-pyrazol-5-yl)pyridine (**8**), both in the presence and absence of SDBS. [SDBS] = 0.05 M, $[M^{2+}] = 0.01$ M. [See **Table 3.27** in **Supplementary information** on CD]

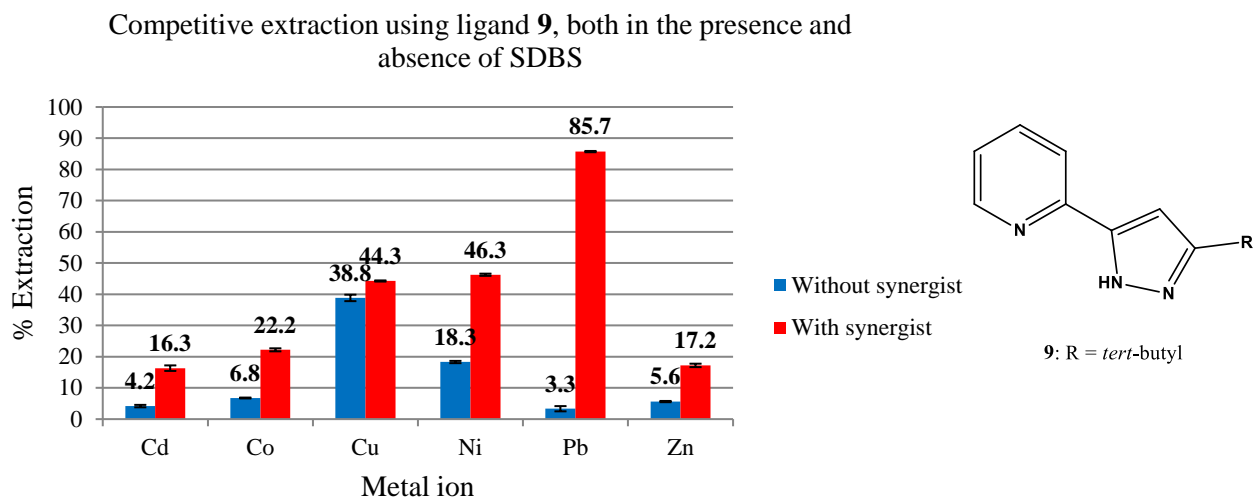


Figure 3.28: Competitive extraction of various base metal ions using 2-[3-(*tert*-butyl)-pyrazol-5-yl]pyridine (**9**), both in the presence and absence of SDBS. [SDBS] = 0.05 M, $[M^{2+}] = 0.01$ M. [See **Table 3.28** in **Supplementary information** on CD]

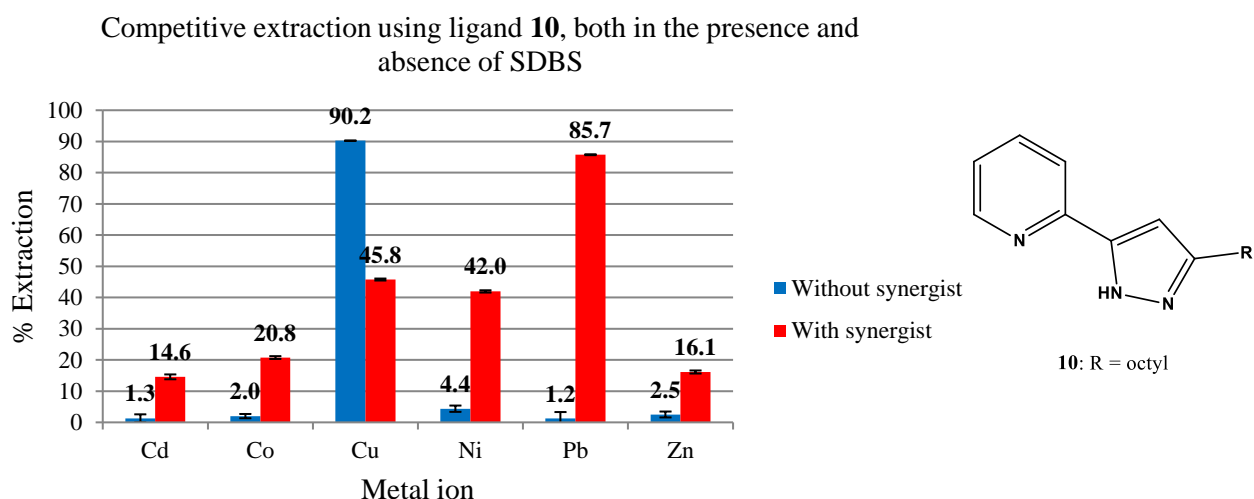


Figure 3.29: Competitive extraction of various base metal ions using 2-(3-octyl-pyrazol-5-yl)pyridine (**10**), both in the presence and absence of SDBS. [SDBS] = 0.05 M, $[M^{2+}] = 0.01$ M. [See **Table 3.29** in **Supplementary information** on CD]

3.3.5 Selectivity studies

After ligands **8–10** exhibited successful competitive extraction results for copper(II), we decided to perform selectivity studies for copper(II) using these ligands. Selectivity studies are similar to competitive extraction studies, with the main focus on decreasing the metal ion of interest's concentration (usually by a factor of 10 or 100). This will give a good indication whether a ligand is still selective for a particular metal ion.

In this study, we had the same selection of base metal ions present (Cd^{2+} , Co^{2+} , Cu^{2+} , Ni^{2+} , Pb^{2+} and Zn^{2+}) in a 1:1:0.1:1:1:1 ratio ($[M^{2+}] = 0.01$ M, $[Cu^{2+}] = 0.001$ M). With the decrease in copper(II) concentration we

expected to see an increase in extraction results for the other base metal ions present, especially nickel(II). This was confirmed upon closer inspection of **Figure 3.30**, when we observed noteworthy increases for nickel(II) and to lesser extents cobalt(II). Still we witnessed excellent copper(II) extraction results for ligand **10** at 85.9 (± 0.9)%, with ligand **8** dropping its selectivity towards copper(II) to 57.6 (± 2.0)%. These results reinforced the fact that ligands **8** and **10** are truly selective toward copper(II), with ligand **10** topping the chart.

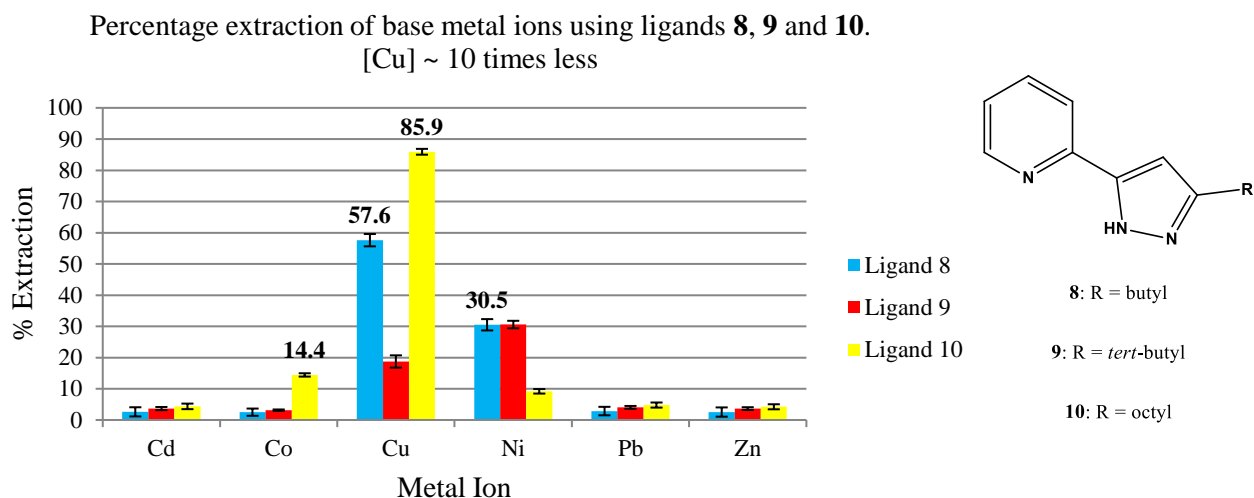


Figure 3.30: Copper selectivity study using 2-(3-butyl-pyrazol-5-yl)pyridine (**8**), 2-[3-(*tert*-butyl)-pyrazol-5-yl]pyridine (**9**) and 2-(3-octyl-pyrazol-5-yl)pyridine (**10**). Copper concentration was decreased tenfold. [See **Table 3.30** in **Supplementary information** on CD]

The following selectivity study (**Figure 3.31**) was similar to the aforementioned study, only this time the copper(II) concentration was decreased hundredfold (0.0001 M). This led to a base metal ion ratio of 1:1:0.01:1:1:1 for Cd²⁺, Co²⁺, Cu²⁺, Ni²⁺, Pb²⁺ and Zn²⁺ respectively.

Like the aforementioned selectivity study, ligand **10** once again yielded an exceptional copper(II) extraction percentage of 90.0 (± 0.4)%. A markedly strong improvement towards cobalt(II) extraction was also noted at 30.0 (± 0.2)%. Ligand **8** showed a slight decrease in copper(II) extraction at 52.4 (± 1.5)% with no real improvement in extraction results for any of the other base metal ions. Throughout this study, ligand **9** showed no concrete preference for any of the base metal ions, with nickel(II) extraction peaking at 34.7 (± 0.1)%.

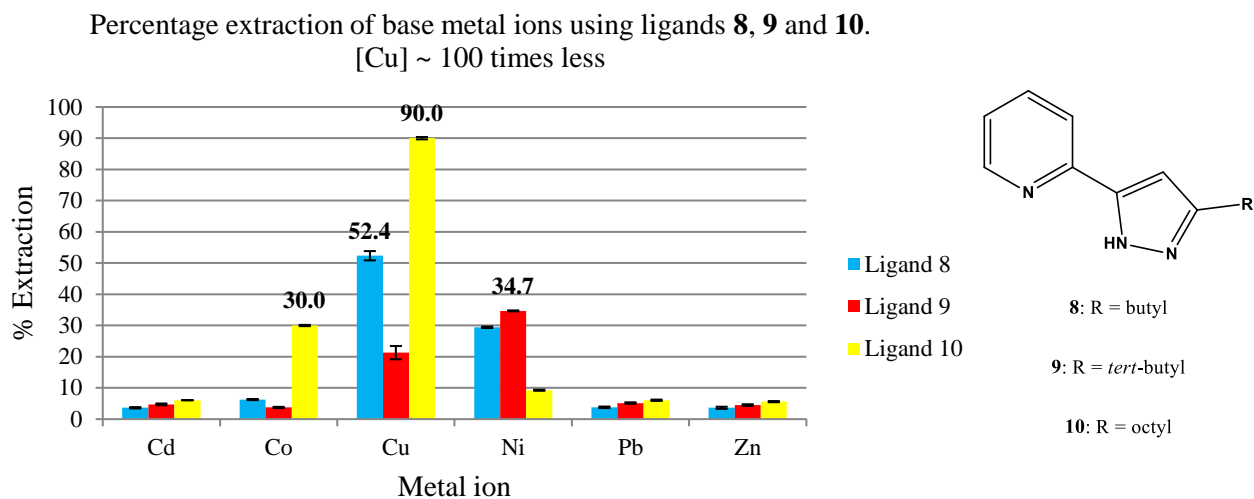


Figure 3.31: Copper selectivity study using 2-(3-butyl-pyrazol-5-yl)pyridine (**8**), 2-[3-(*tert*-butyl)-pyrazol-5-yl]pyridine (**9**) and 2-(3-octyl-pyrazol-5-yl)pyridine (**10**). Copper concentration was decreased hundredfold. [See Table 3.31 in Supplementary information on CD]

3.3.6 Metal stripping studies

The art of designing ligands with the sole purpose of extracting metal ions is a feasible one, but the true test lies in the recovery of those metal ions. A successful industrial extractant should have the ability to extract metal ions as well as release those metal ions in an acidic aqueous medium ($\text{pH} < 2$), without being hydrolysed (destroyed).

Before we continued with metal stripping studies, we had to prove that ligands **8–10** were stable at $\text{pH} = 1$. We transferred 2 mL of each ligand into a polytop with 5 mL of 0.1 M HNO_3 solution ($\text{pH} \approx 1$). These polytops were sealed and put on the laboratory shaker for 24 hours at 150 rpm. After the 24-hour period, the oily ligand (floating) was decanted off and dried overnight *in vacuo*. We resubmitted these ligands for ^1H NMR analysis and found that no structural differences were present. No additional peaks or peak shifting were observed either.

Now, the metal stripping of ligands **8–10** could commence. A 0.1 M HNO_3 aqueous solution ($\text{pH} \approx 1$) was used as the aqueous phase. The extracted nickel(II) and copper(II) in chloroform solutions (present as complexes) were brought into contact with the HNO_3 aqueous solution in polytops. The polytops were sealed and placed on the laboratory shaker for 24 hours, after which the aqueous phase was analysed via ICP-AES. It has to be mentioned that the percentage metal stripped was calculated based on the percentage metal originally extracted. It was not as a percentage of the original stock solution concentration. Mathematically, it can be expressed as follows (**Equation 34**):

$$\%S = \frac{C_{\text{strip}}}{\%E} \times 100$$

Equation 34

where %S is the percentage metal ion stripped, C_{strip} is the concentration of the applicable metal ion after stripping and %E is the original percentage metal ion extracted which can be calculated according to **Equation 33 (Section 3.2.4, Chapter 3)**.

From **Figure 3.32** it is apparent that both nickel(II) and copper(II) stripping follows the following basic trend: ligand **10** < ligand **8** < ligand **9**. Ligand **10** exhibits the least amount of stripping at 22.4 (± 2.7)% for nickel(II) and 14.1 (± 1.8)% for copper(II), followed by ligands **8** (Ni^{2+} : 38.0 \pm 5.8; Cu^{2+} : 46.7 \pm 2.7) and **9** (Ni^{2+} : 62.1 \pm 3.6; Cu^{2+} : 55.0 \pm 3.4) respectively. This makes complete sense since we know that ligand **10** was observed to be the best nickel(II) and copper(II) extractant, followed by ligands **8** and **9**. The best extractant (**10**) forms the most stable coordination bonds with nickel(II) and copper(II), and in turn, holds on to the metal ions more strongly, *i.e.*, it is less prone to be stripped in an acidic medium. Conversely, the ligand that was stripped with the most ease (**9**), is the ligand that forms the weakest coordination bonds to nickel(II) and copper(II), *i.e.*, the least favoured extractant. This is a catch-22 situation whereby the pros and cons are weighing on each side of the coin. The user (or implementer) of ligands **8**, **9** and **10** should ask themselves the following question: “Do we need an excellent extractant that perhaps cannot be stripped proficiently, or do we need an extractant that doesn’t extract as well, but strips extremely efficiently?” Perhaps the answer lies with ligand **8** - the golden middle. Ligand **8** extracts quite efficiently (not as good as ligand **10**, but better than ligand **9**) and strips reasonably good as well (better than ligand **10**, but worse than ligand **9**).

Stripping results can drastically be improved upon lowering the pH closer to 0. This was the case when Okewole *et al.*⁸ reported the quantitative stripping of Ni^{2+} at pH 0.32, using similar ligands. The only drawback is the possible hydrolysis of the extractants, which for obvious reasons should be avoided at all times.

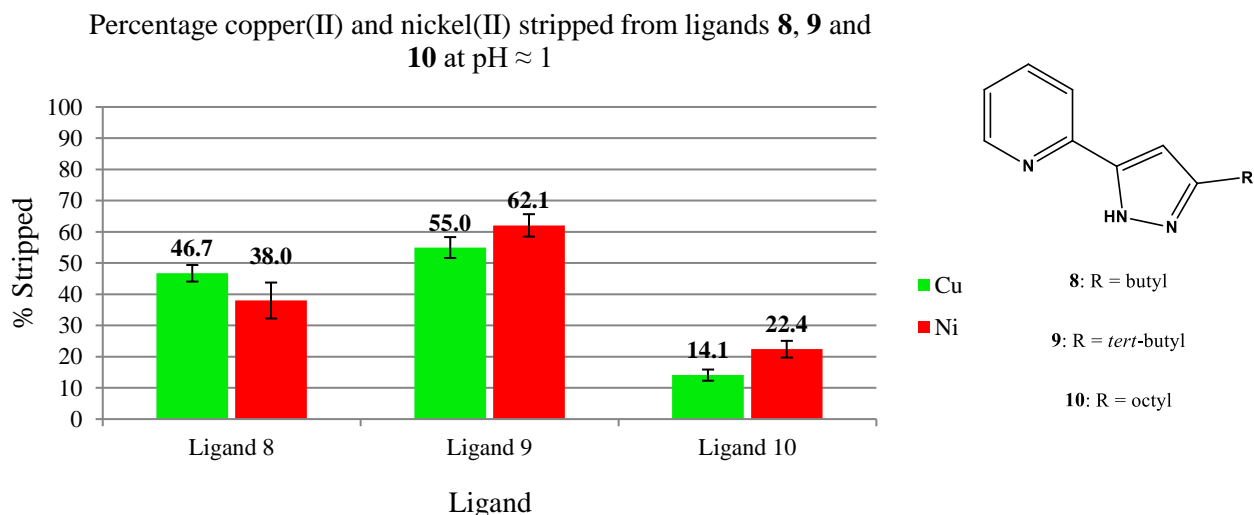


Figure 3.32: Percentage copper(II) and nickel(II) stripped from 2-(3-butyl-pyrazol-5-yl)pyridine (**8**), 2-[3-(*tert*-butyl)-pyrazol-5-yl]pyridine (**9**) and 2-(3-octyl-pyrazol-5-yl)pyridine (**10**) at pH \approx 1. [See **Table 3.32** in **Supplementary information** on CD]

3.3.7 Time-dependent extraction study of copper(II)

To ensure that the abovementioned copper(II) extraction and stripping studies are accurate and trustworthy, we performed 24-hour time dependent studies (similar to **Section 3.3.5, Chapter 3**). These studies give an indication as to whether the extraction of copper(II) has reached equilibrium before the 24-hour mark or not. This is a tedious and cumbersome experiment to perform, but equally important and necessary.

Figure 3.33 represents a time dependent extraction study over a 24-hour period using ligands **8–10**. It was well noted that all three ligands reach extraction equilibrium well before the 24-hour mark, with ligand **10** reaching equilibrium after about 1 hour, while ligands **8** and **9** reached equilibrium after 4 and 8 hours respectively. Outliers do exist (**Figure 3.33**), but can readily be attributed to human/experimental error. These studies were only performed in duplicate, thereby contributing to the odd outlier.

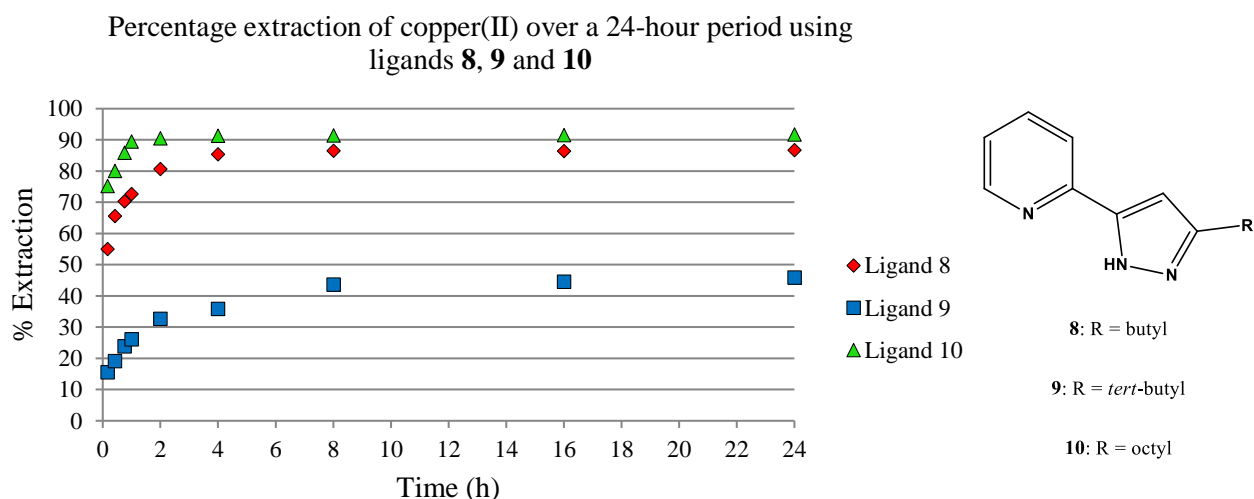


Figure 3.33: Percentage extraction of copper(II) over a 24-hour period using 2-(3-butyl-pyrazol-5-yl)pyridine (**8**), 2-[3-(*tert*-butyl)-pyrazol-5-yl]pyridine (**9**) and 2-(3-octyl-pyrazol-5-yl)pyridine (**10**). [No error bars added to graph to prevent clutter, see **Table 3.33** in **Supplementary information** on CD]

3.3.8 pH isotherm studies

In these studies, the conditions for the extraction of nickel(II) and copper(II) were altered by varying the pH of the aqueous solution. The pH of the aqueous metal ion solutions was adapted by adding small amounts of 1 M HNO₃ or 1 M NaOH. The metal (0.01 M) to ligand (0.01 M) ratio was kept at 1:1 throughout this study. Note that no synergist was used in these studies, since ligands **8–10** extracted copper(II) in high yields on their own.

Figure 3.34 represents the percentage extraction of nickel(II) over a pH range of 0–7, using ligands **8–10**. These ligands yielded broad S-curve type plots with maximum %E in the 20–40% range, which isn't ideal for metal ion separation. A steep curve is often desired to effect metal ion separation based on a small window of varying pH. Okewole *et al.*⁸ reported steep nickel(II) pH isotherm curves whereby the difference between the

minimum and maximum extraction values stretched from pH 1 to pH 2. This means that stripping can be effected at $\text{pH} < 1$, while extractions can be performed at $\text{pH} > 2$.

Ligands **8** and **10** have oddly shaped *S*-curves, which can be attributed to human error and irregular equipment malfunction (pH meter). Having said that, one could still see from **Figure 3.34** that stripping could possibly be done at $\text{pH} < 1.5$ while optimum extraction studies can be performed at $4 < \text{pH} < 7$ (at $\text{pH} > 7$ metal salts start to precipitate out).

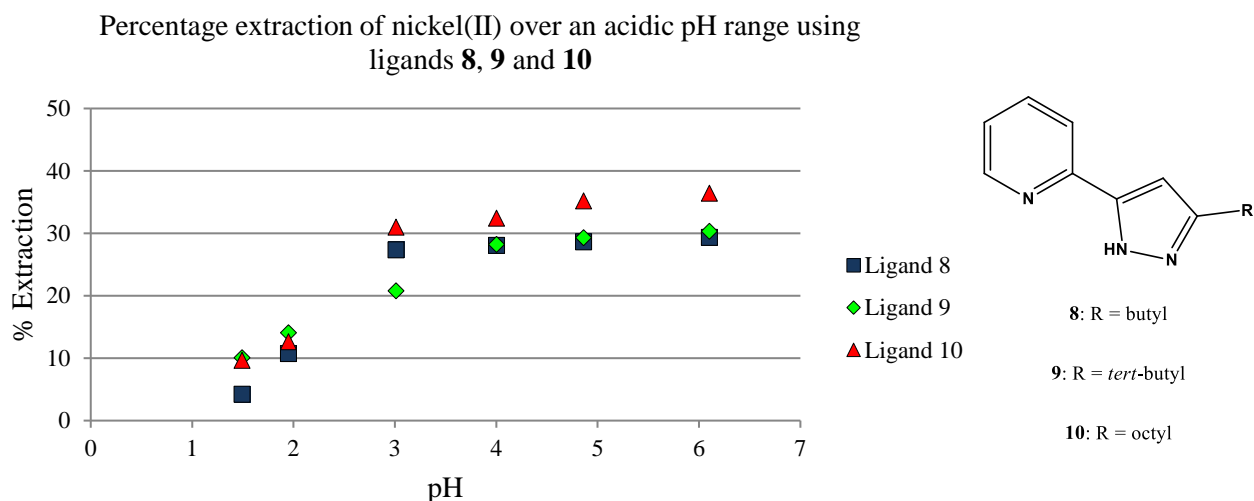


Figure 3.34: pH isotherm graph: the percentage extraction of nickel(II) over an acidic pH range (0–7), using 2-(3-butyl-pyrazol-5-yl)pyridine (**8**), 2-[3-(*tert*-butyl)-pyrazol-5-yl]pyridine (**9**) and 2-(3-octyl-pyrazol-5-yl)pyridine (**10**). [No error bars added to graph to prevent clutter, see **Table 3.34** in **Supplementary information** on CD]

The copper(II) pH isotherm studies (**Figure 3.35**) yielded much better results in terms of curve steepness. Ligand **10** exhibits a particular steep *S*-curve in the pH region of 2–3, which could lead to excellent copper(II) separation in a competitive extraction environment. Ligands **8** and **9** have slightly broader pseudo *S*-curves which renders it somewhat inappropriate for copper(II) separation. These results are similar to those reported by Okewole *et al.*,⁸ in that they too reported broad *S*-curves for copper(II) pH isotherm studies, using imidazolyl-type ligands.

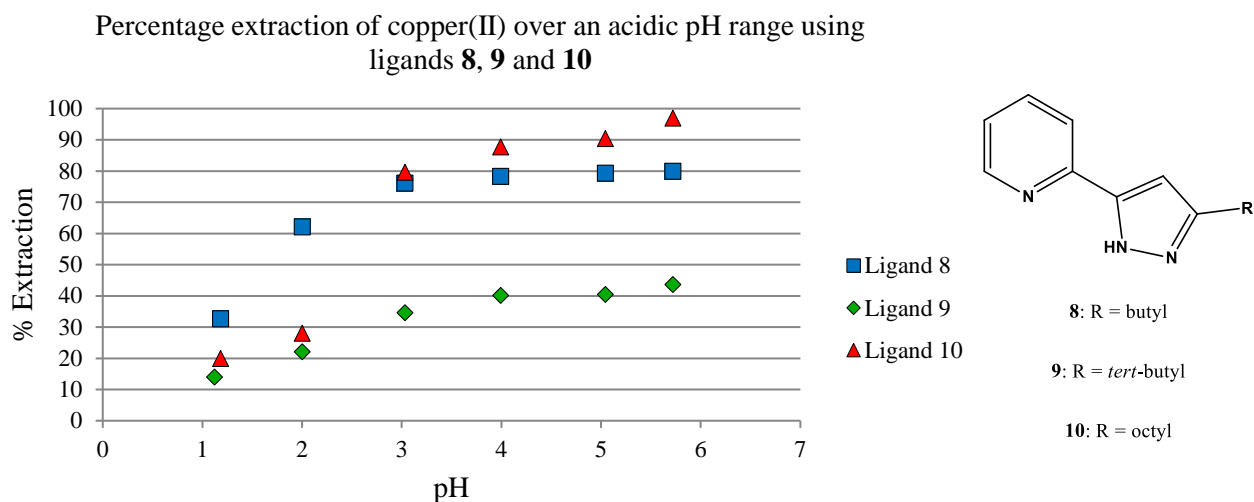


Figure 3.35: pH isotherm graph: the percentage extraction of copper(II) over an acidic pH range (0–7), using 2-(3-butyl-pyrazol-5-yl)pyridine (**8**), 2-[3-(*tert*-butyl)-pyrazol-5-yl]pyridine (**9**) and 2-(3-octyl-pyrazol-5-yl)pyridine (**10**). [No error bars added to graph to prevent clutter, see **Table 3.35** in **Supplementary information** on CD]

3.3.9 Possible theory as to what mechanistic role the synergist plays

The role of the synergist, SDBS, in nickel(II) extraction systems is somewhat unclear and difficult to unravel. In 1980, Osseo-Asare and Keeney¹⁸ reported the use of DDNSA (see **Figures 3.2** and **3.3** for comparison) as a synergist in nickel(II) extractions. They claimed that DDNSA formed micelles and contained large aqueous cores with solubilised nickel(II).¹⁸ In view of the low aqueous solubility of all our synthesised ligands (**1–10**), it is unlikely that ligands **1–10** would be solubilised in the aqueous core.¹⁸ It was proposed that the ligands are concentrated on the hydrophobic periphery of the sulfonate micelles, which means that the sulfonate micelles appears to provide a concentrative effect (**Figure 3.36**).¹⁸ In other words, concentrations of both the ligands and aqueous (solubilised) nickel(II) ions are high in the micellar region, therefore, reaction rates are also expected to be high.¹⁸

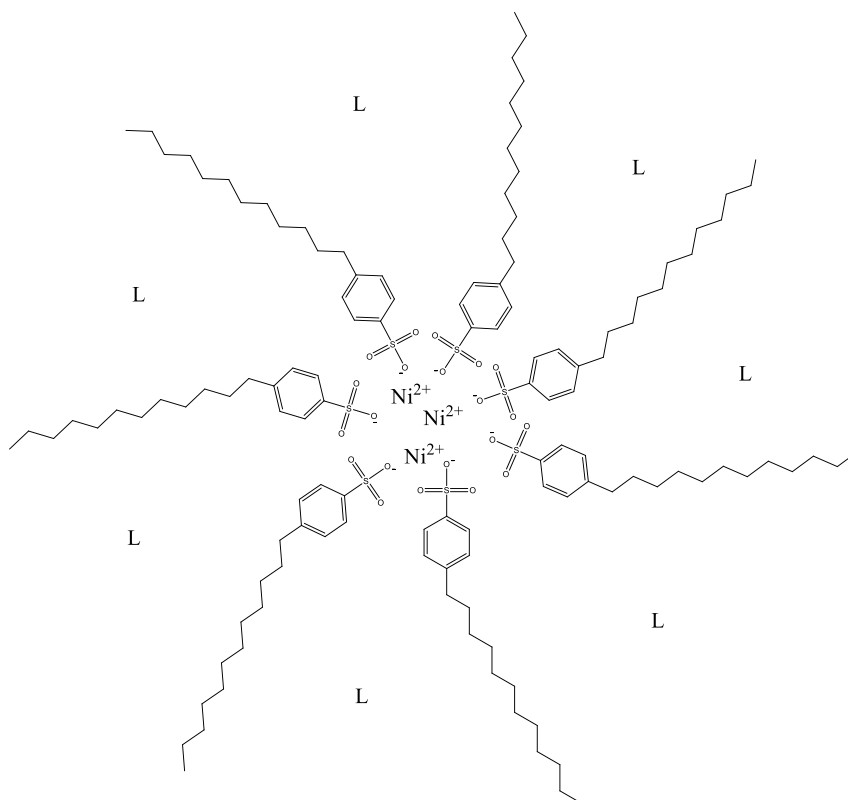


Figure 3.36: Sodium dodecylbenzenesulfonate (SDBS) micelle containing a nickel-rich aqueous core, with ligands (L) concentrated on its hydrophobic periphery.

The micellar catalysed extraction mechanism may be summarised by the following simplified steps:¹⁸

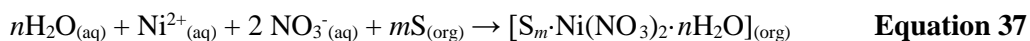
1. Chelation reaction at the micellar interface (**Equation 35**):



2. Collapse of the micelle, *i.e.*, loss of aqueous phase (**Equation 36**):



3. Formation of a new micelle with a new aqueous core (**Equation 37**):



where L = bidentate amine ligands (**1–10**), S = synergist, n and m = arbitrary values.

The mechanism above is by no means 100% accurate or complete, but gives an idea of the mechanistic role that the synergist might play. In future, additional steps need to be included in the mechanism, such as diffusional and interfacial area considerations.¹⁸

3.3.10 Unsuccessful attempt to explain the role of the synergist

Before we even set out to conduct this study, we knew that the synergist (in this case, SDBS) would play a major role in the various extraction studies of both nickel(II) and copper(II). The following experiments/studies were proposed to help us understand what the role of the synergist might be:

IR study:

- Obtain a spectrum of the ligand
- Obtain a spectrum of the synergist
- Obtain a combined spectrum of the ligand and synergist (1:1 ratio)
- Obtain a combined spectrum of the ligand and synergist (1:5 ratio)
- Obtain a combined spectrum of the ligand, synergist and $\text{Ni}(\text{NO}_3)_2 \cdot 6\text{H}_2\text{O}$ (1:1:1 ratio)
- Obtain a combined spectrum of the ligand, synergist and $\text{Ni}(\text{NO}_3)_2 \cdot 6\text{H}_2\text{O}$ (1:5:1 ratio)

^1H NMR study:

- Obtain a spectrum of the ligand
- Obtain a spectrum of the synergist
- Obtain a combined spectrum of the ligand and synergist (1:1 ratio)
- Obtain a combined spectrum of the ligand, synergist and $\text{Ni}(\text{NO}_3)_2 \cdot 6\text{H}_2\text{O}$ (1:1:1 ratio)

Our main goal was to observe any peak shifts in the IR and ^1H NMR studies. This would give us an inkling regarding the role of the synergist, however, this was not a plausible study.

The main obstacle with the abovementioned list of proposed experiments was the fact that the synergist, SDBS, was only soluble in CHCl_3 (IR) and CDCl_3 (^1H NMR) at low concentrations. This meant that concentrated solutions for IR and ^1H NMR analyses were not obtainable. When the synergist eventually became soluble in H_2O (IR) and D_2O (^1H NMR) upon heating, the ligand on the other hand proved to be insoluble. Most common laboratory deuterated solvents were tested (CDCl_3 , D_2O , $(\text{CD}_3)_2\text{SO}$ and CD_3OD), but alas, none were satisfactory. This halted our inquiry into a possible ligand/synergist mechanism.

3.4 Conclusions

Amine extractants are widely used in industry today for the selective extraction of various metal ions, however, very little work is done on the design, synthesis and optimisation of aromatic amine extractants. That was the gap we tried to narrow with tailor-made ligands designed for the sole purpose of extracting nickel(II) and copper(II).

The role of the synergist, sodium dodecylbenzenesulfonate (SDBS), played a particularly important role in nickel(II) extraction studies, whereby it contributed significantly to the overall extraction results. The exact

mechanism by which SDBS extracts base metal ions, in conjunction with ligands **1–10**, is still in question and warrants further investigation. Allen²⁸ proposed that dinonylnaphthalene disulfonic acid (DNNDISA), a similar synergist to SDBS, acts as an ion-pairing agent with the cationic complex species in the organic phase due to its bulky presence and low pK_a value (0.6–0.7). Although it seems sensible, the micellar and colloidal mechanism described by Osseo-Asare and Keeney¹⁸ appears to be the more reasonable and feasible option. Upon studying and researching this phenomenon one will also be able to reason as to why the optimum synergist concentration peaked at 0.05 M, followed by a steady decline thereafter. This was something we were unable to derive.

Ligands **1–10** in conjunction with SDBS yielded reasonable nickel(II) extraction results, all of which extracted nickel(II) in the low to high 70% range. In view of the imidazolyl and methylpyrazolyl ligands (**1–7/7'**), the pyrazolyl ligands (**8–10**) extracted both nickel(II) and copper(II) in very high percentages, which can most likely be attributed to the presence of an acidic proton on the pyrazole moiety as well as alkyl substituted pyrazole moieties. It was evident that alkyl chain length played a significant role in ensuring that complexes stayed solubilised in the organic phase.

One of the most interesting and exciting revelations of this study came to light upon performing competitive extraction studies using pyrazolyl ligands, **8–10**. These ligands were highly selective towards copper(II) in a mixed base metal ion solution. Extractions in the 80 to 90% range indicated the preference these ligands showed toward copper(II). This was not totally surprising, though, as we expected more stable copper complexes to be formed with ligands **8–10**, according to the Irving-Williams series.³¹ These ligands would perform well in an industrial setting, but the synthesis and purification of these ligands are tedious, cumbersome and time-consuming, unless automated systems are put in place to alleviate the need for human hands.

Metal stripping results are somewhat inadequate for future industrial purposes and need to be optimised by perhaps lowering the pH from 1 to 0. Without question, this would increase the recovery potential of metal ions, but would also increase the need for more concentrated strong acids. This could, not only be a major financial drawback in an industrial setting, but also cause the industrial plant to be an environmental liability.

The nickel(II) pH isotherms for ligands **8–10** yielded broad pseudo *S*-curve plots, which are unsuitable for industrial implementation, especially in light of previous results reported by Okewole *et al.*⁸ These authors reported steep *S*-curves with complimenting extraction yields in the mid-90% range, while our results fall short of the mark at roughly 30%. Our reported copper(II) pH isotherms had a much better *S*-curve “steepness” with complimenting maximum extraction values of 80–90%, which is comparable to literature.⁸

3.5 References

1. Wang, L.; Lee, M. S. Solvent extraction of cobalt and nickel from chloride solution by mixtures of acidic organophosphorous extractants and amines. *Geosystem Eng.* **2016**, 1-5.
2. Du Preez, J. G. H.; Postma, J.; Ravindran, S.; Van Brecht, B. J. A. M. Nitrogen reagents in metal ion separation. Part 6. 2-(1'-octylthiomethyl)pyridine as extractant for later 3d transition metal ions. *Solvent Extr. Ion Exch.* **1997**, *15*, 79-96.
3. Du Preez, J. G. H.; Sumter, N.; Mattheüs, C.; Ravindran, S.; Van Brecht, B. J. Nitrogen reagents in metal ion separation. Part VII. The development of a novel copper(II) extractant. *Solvent Extr. Ion Exch.* **1997**, *15*, 1007-1021.
4. Du Preez, J. G. H.; Mattheüs, C.; Sumter, N.; Ravindran, S.; Potgieter, C.; Van Brecht, B. J. Nitrogen reagents in metal ion separation. Part VIII. Substituted imidazoles as extractants for Cu²⁺. *Solvent Extr. Ion Exch.* **1998**, *16*, 565-586.
5. Du Preez, J. G. H.; Mattheüs, C.; Sumter, N.; Edge, W.; Potgieter, C.; Van Brecht, B. J. Nitrogen reagents in metal ion separation. Part IX. Extraction of cobalt and nickel using imidazole derivatives. *Solvent Extr. Ion Exch.* **1998**, *16*, 1033-1046.
6. Wei, Y.; Wang, S.; Zhou, S.; Feng, Z.; Guo, L.; Zhu, X.; Mu, X.; Yao, F. Aluminum alkyl complexes supported by bidentate N,N ligands: Synthesis, structure, and catalytic activity for guanylation of amines. *Organometallics* **2015**, *34*, 1882-1889.
7. Wang, Y.; Ma, H. Aluminum complexes of bidentate phenoxy-amine ligands: Synthesis, characterization and catalysis in ring-opening polymerization of cyclic esters. *J. Organomet. Chem.* **2013**, *731*, 23-28.
8. Okewole, A. I.; Magwa, N. P.; Tshentu, Z. R. The separation of nickel(II) from base metal ions using 1-octyl-2-(2'-pyridyl)imidazole as extractant in a highly acidic sulfate medium. *Hydrometallurgy* **2012**, *121-124*, 81-89.
9. Blake, C.; Baes, C.; Brown, K. Solvent Extraction with Alkyl Phosphoric Compounds. *Ind. Eng. Chem.* **1958**, *50*, 1763-1767.
10. Laing, M. Solvent Extraction of Metals *Is* Coordination Chemistry. In American Chemical Society: 1994; Vol. 565, pp 382-394.
11. Joo, S.; Shin, D. J.; Oh, C.; Wang, J.; Senanayake, G.; Shin, S. M. Selective extraction and separation of nickel from cobalt, manganese and lithium in pre-treated leach liquors of ternary cathode material of spent lithium-ion batteries using synergism caused by Versatic 10 acid and LIX 84-I. *Hydrometallurgy* **2016**, *159*, 65-74.
12. Guimarães, A. S.; Da Silva, P. S.; Mansur, M. B. Purification of nickel from multicomponent aqueous sulfuric solutions by synergistic solvent extraction using Cyanex 272 and Versatic 10. *Hydrometallurgy* **2014**, *150*, 173-177.
13. Fouad, E. A. Extraction of nickel by bis(2,4,4-trimethylpentyl) dithiophosphinic acid synergism. *J. Eng. Appl. Sci.* **2009**, *56*, 661-677.
14. Du Preez, A. C.; Preston, J. S. Separation of nickel and cobalt from calcium, magnesium and manganese by solvent extraction with synergistic mixtures of carboxylic acids. *J. S. Afr. Inst. Min. Metall.* **2004**, *104*, 333-338.
15. Flett, D. S. SOLVENT EXTRACTION. *Chem Ind (London)* **1977**, 223-224.

16. Nyman, B. G.; Hummelstedt, L. *Use of liquid cation exchange for separation of nickel(II) and cobalt(II) with simultaneous concentration of nickel sulphate*; Proc. ISEC 74; SCI: London, 1974; Vol. 1, pp 669-684.
17. Hummelstedt, L.; Lund, H.; Karjaluo, J.; Berts, L.; Nyman, B. G. *Use of extractant mixtures containing Kelex 100 for separation of nickel(II) and cobalt(II)*; Proc. ISEC 74; SCI: London, 1974; Vol. 1, pp 829-849.
18. Osseo-Asare, K.; Keeney, M. E. Sulfonic acids: Catalysts for the liquid-liquid extraction of metals. *Sep. Sci. Technol.* **1980**, *15*, 999-1011.
19. Ndayambaje, G.; Laatikainen, K.; Laatikainen, M.; Beukes, E.; Fatoba, O.; van der Walt, N.; Petrik, L.; Sainio, T. Adsorption of nickel(II) on polyacrylonitrile nanofiber modified with 2-(2'-pyridyl)imidazole. *Chem. Eng. J.* **2016**, *284*, 1106-1116.
20. Magubane, M. N.; Nyamoto, G. S.; Ojwach, S. O.; Munro, O. Q. Structural, kinetic, and DFT studies of the transfer hydrogenation of ketones mediated by (pyrazole)pyridine iron(II) and nickel(II) complexes. *RSC Adv.* **2016**, *6*, 65205-65221.
21. Nyamoto, G. S.; Alam, M. G.; Ojwach, S. O.; Akerman, M. P. Nickel(II) complexes bearing pyrazolylpyridines: Synthesis, structures and ethylene oligomerization reactions. *Appl. Organomet. Chem.* **2016**, *30*, 89-94.
22. Ojwach, S. O.; Guzei, I. A.; Benade, L. L.; Mapolie, S. F.; Darkwa, J. (Pyrazol-1-ylmethyl)pyridine nickel complexes: Ethylene oligomerization and unusual Friedel-Crafts alkylation catalysts. *Organometallics* **2009**, *28*, 2127-2133.
23. Ojwach, S. O.; Nyamoto, G. S.; Omondi, B.; Darkwa, J. Chelating (pyrazolylmethyl)pyridine ligands: Coordination chemistry and binding properties with zinc(II) and cadmium(II) cations. *Inorg. Chim. Acta* **2012**, *392*, 141-147.
24. Ojwach, S. O.; Okemwa, T. T.; Attandoh, N. W.; Omondi, B. Structural and kinetic studies of the polymerization reactions of ϵ -caprolactone catalyzed by (pyrazol-1-ylmethyl)pyridine Cu(II) and Zn(II) complexes. *Dalton Trans.* **2013**, *42*, 10735-10745.
25. Zhang, X. L.; Taylor, D. J. F.; Thomas, R. K.; Penfold, J. The role of electrolyte and polyelectrolyte on the adsorption of the anionic surfactant, sodium dodecylbenzenesulfonate, at the air-water interface. *J. Colloid Interface Sci.* **2011**, *356*, 656-664.
26. Mohsenpour, A.; Eisazadeh, H. Preparation and Characterization of Polythiophene Containing Al₂O₃ Nanoparticles Using Sodium Dodecylbenzenesulfonate as a Surfactant. *Polym. -Plast. Technol. Eng.* **2015**, *54*, 57-60.
27. Chabba, S.; Kumar, S.; Aswal, V. K.; Kang, T. S.; Mahajan, R. K. Interfacial and aggregation behavior of aqueous mixtures of imidazolium based surface active ionic liquids and anionic surfactant sodium dodecylbenzenesulfonate. *Colloids Surf. A Physicochem. Eng. Asp.* **2015**, *472*, 9-20.
28. Allen, K. A. The equilibria between di-n-decylamine and sulfuric acid. *J. Phys. Chem.* **1956**, *60*, 943-946.
29. Martell, A. E.; Hancock, R. D. *Metal Complexes in Aqueous Solutions*; Modern Inorganic Chemistry; Plenum Press: New York, 1996, pp 253.
30. Fassbender, S.; Dreisinger, D.; Wu, Z. US Patent 20140131220 A1, 2014.

31. Irving, H.; Williams, R. J. P. The stability of transition-metal complexes. *Journal of the Chemical Society (Resumed)* **1953**, 3192-3210.
32. Bouabdallah, I.; Zidane, I.; Hacht, B.; Touzani, R.; Ramdani, A. Liquid-liquid extraction of copper(II), cadmium(II) and lead(II) using tripodal N-donor pyrazole ligands. *Arkivoc* **2006**, 2006, 59-65.

Chapter 4

Crystal and molecular structure of aqua[2-[3-(*tert*-butyl)-pyrazol-5-yl]pyridine] dinitrato copper(II)

4.1 Introduction

The formation of metal complexes of bidentate aromatic amine ligands is a research field that is widely considered to be in its blooming years, with major advancements made in the past decade. The interest in this field originates from the idea that supramolecular architectures can be designed and tailored to satisfy specific needs. From this idea, the field of crystal engineering was born. The term *crystal engineering* was first coined in 1971 by Schmidt,¹ when he studied photodimerisation reactions in crystalline cinnamic acids. Later, in 1989, Desiraju² defined *crystal engineering* as “the understanding of intermolecular interactions in the context of crystal packing and the utilisation of such understanding in the design of new solids with desired physical and chemical properties.” Systems that are self-assembled by weak intermolecular forces are vital in crystal engineering. One such example would include molecular materials assembled by means of hydrogen bond interactions.³ The objective to design new materials with an array of different physical and chemical properties, however, can only be achieved once the properties of the individual units, their response to chemical substitutions, as well as their interactions are quantitatively understood.⁴

For synthetic chemists, it can be a significant challenge in trying to understand the main factors that govern the wide variety of supramolecular crystal packing organisations. The study of single-crystal structures of metal ion complexes greatly increases the level of understanding of the factors that govern complex formation processes.⁴ This has allowed synthetic chemists to design ligands that exhibit unique complexing properties in a much-improved manner. The bite-size and chelate ring size of a bidentate aromatic amine ligand is of prime interest in understanding their selectivity for metal ions. According to Martell and Hancock,⁵ metal complexes show increased stability when five-membered chelate rings are formed with larger metal ions. This, in addition to bond lengths, bond angles, torsion angles, overall geometry, packing efficiency, *etc.*, can be visualised with crystal and molecular structure determinations. Naturally, these crystal determinations can also give an account of deformed bond angles and bond length distortions, of which the Jahn-Teller effect is the most common.⁶ The Jahn-Teller effect results in the compression, or more commonly, the elongation of axial bonds.

The crystal structure was mainly derived to understand the solution chemistry of bidentate aromatic amine metal complexes. However, intramolecular interactions in a supramolecular context were also of interest and are pointed out where relevant.

4.2 Materials and methods

4.2.1 Chemicals and reagents

The ligand 2-[3-(*tert*-butyl)-pyrazol-5-yl]pyridine (**9**) was synthesised according to the procedure described in **Section 2.3.9** of **Chapter 2**. Copper(II) nitrate trihydrate, $\text{Cu}(\text{NO}_3)_2 \cdot 3\text{H}_2\text{O}$, was purchased from Sigma-Aldrich, while absolute ethanol was purchased from Kimix Chemicals.

4.2.2 Techniques for growing quality crystals

There are numerous techniques for growing crystals suitable for X-ray analysis. It is vitally important, however, that time and effort be put in to grow quality crystals to ensure that high-quality crystal and molecular determinations can be made. The following crystallisation techniques are the most common among synthetic chemists:

4.2.2.1 Slow evaporation method

This crystal growing method is probably the simplest to execute, yet most time-consuming dependent on the solvent used (**Figure 4.1a**). A near-saturated solution of the applicable compound in a suitable solvent is placed into a clean container with a large surface area. The container can be covered with aluminium foil or parafilm and punched with tiny holes to allow slow evaporation over a few days. Set the container to one side and prevent stirring or swirling the solution at all costs. This method can be extremely time-consuming and requires large amounts of material to ensure that the solution is near its saturation point.

4.2.2.2 Slow cooling method

A nearly saturated solution of the compound should be prepared at the boiling point of the solvent of your choice. The hot solution should then be transferred to a clean container and allowed to cool to room temperature (**Figure 4.1b**). Another alternative to this method is to prepare a near-saturated solution at room temperature and place the container in a fridge or freezer to cool the solution down to encourage crystal growth.

4.2.2.3 Vapour diffusion method

This method requires a dual solvent system that mixes well (**Figure 4.1c**). The compound should be relatively soluble in the solvent with the highest boiling point and near-insoluble in the solvent with the lower boiling point. A solution of the compound should be prepared in a small open-top container and placed in a slightly larger container containing the low boiling solvent. The outer container should be tightly sealed to avoid vapour from escaping. Over time the low boiling solvent in the outer container will vaporise and diffuse into the high boiling solvent, leading to oversaturation, nucleation and possibly crystallisation. If need be, the speed of vaporisation can be controlled by regulating the temperature.

4.2.2.4 Liquid-liquid diffusion method

As with the vapour diffusion method, this method also requires a dual solvent system (**Figure 4.1d**). In this case the boiling points of the solvents do not matter, but their respective specific densities do. A saturated solution of your compound should be prepared and the solvent with the highest specific density should be placed in a small container (perhaps a polytop). Use a syringe and hypodermic needle to layer the remaining liquid in the polytop. Over time, the liquids will mix and hopefully yield high-quality crystals. A variation to this method is to freeze the lower layer before adding the remaining liquid. This will ensure that a clean separation between the two layers is achieved.

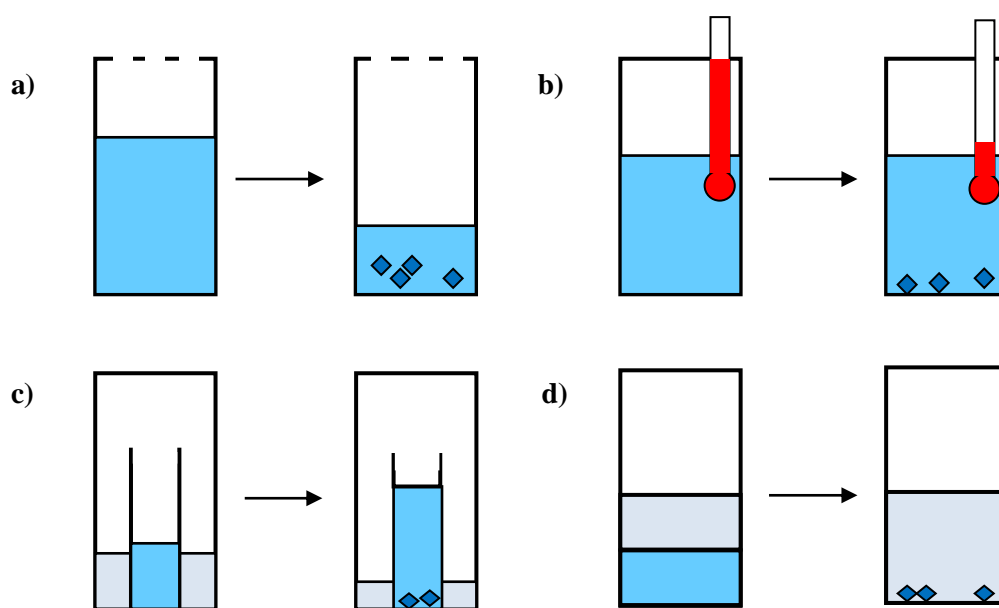


Figure 4.1: Schematic diagram representing various crystal growth techniques: **a)** slow evaporation **b)** slow cooling **c)** vapour diffusion and **d)** liquid-liquid diffusion methods.

4.2.3 Instrumentation and determination of crystal structure

A suitable crystal was mounted on a thin glass fiber, while data was collected using a *Bruker APEX-II CCD* diffractometer with graphite monochromated Mo-K α radiation ($\lambda = 0.71073 \text{ \AA}$) (Bruker 2012). Data reduction was performed using *SAINT* (Bruker 2012). A cryostat: *Oxford Cryogenics (700 Series Cryostream Plus)* was used to cool the crystal to 100 K. Empirical corrections were performed with *SADABS* (Bruker 2001). The structure was solved by direct methods, while the remainder of the atomic positions were found using difference Fourier methods. All non-hydrogen atoms were refined anisotropically (with appropriate restraints using *SIMU* and *ISOR*) by blocked full-matrix least squares calculations on F^2 using *SHELXL-97* (Sheldrick 1997) within the *X-SEED* environment (Barbour 2001; Atwood and Barbour 2003). Hydrogen atoms were added to the structure model on calculated positions and were refined as rigid atoms. *Mercury V.3.8* for Windows was used to generate figures.

4.2.4 Preparation of the crystalline $[\text{Cu}(\text{H}_2\text{O})(\text{C}_{12}\text{H}_{15}\text{N}_3)(\text{NO}_3)_2]$ complex

A mixture of copper(II) nitrate trihydrate (0.300 g, 0.124 mmol) and 2-[3-(*tert*-butyl)-pyrazol-5-yl]pyridine (0.250 g, 0.124 mmol) in absolute ethanol (10.0 mL) was refluxed for 1 hour and left stirring at room temperature overnight. The mixture was reduced to approximately half its ethanol content under reduced pressure. The blue-green solution was left stationary at ambient conditions for 7 days to allow the ethanol to evaporate (slow evaporation method), whereafter clear blue-green square crystals had formed on the sides of the glass container, suitable for X-ray analysis. **IR (ATR, cm^{-1})** 3241 (N–H str), 3140 (aromatic C–H str), 2967 (aliphatic C–H str), 1572 (pyridine C=N str), 1561 (pyrazole C=N str), 1452 (–CH₃ bend). **EA calculated for $\text{C}_{12}\text{H}_{17}\text{CuN}_5\text{O}_7$ (%)** C, 35.43; H, 4.21; N, 17.21. **EA found (%)** C, 35.13; H, 4.11; N, 16.95.

4.3 Results and discussion

Crystal and molecular structure results supply invaluable information regarding the interaction of metal ions with bidentate aromatic amine ligands. In this study, crystals suitable for X-ray diffraction were grown by means of the slow evaporation method. For months on end we attempted to grow crystals of nickel(II) and copper(II) complexes with ligands **1–10**, meticulously following all of the aforementioned techniques (**Section 4.2.2, Chapter 4**), but to no avail. We knew that growing crystals of nickel(II) and copper(II) with ligands **3, 4, 8** and **10** would be particularly difficult, due to their long alkyl chain moieties preventing efficient packing and creating considerable disorder. Eventually we managed to grow suitable crystals from copper(II) nitrate trihydrate and 2-[3-(*tert*-butyl)-pyrazol-5-yl]pyridine (**9**).

The IR spectrum of the $[\text{Cu}(\text{H}_2\text{O})(\text{C}_{12}\text{H}_{15}\text{N}_3)(\text{NO}_3)_2]$ complex clearly shows a shift of the pyridyl- and pyrazolyl N–H stretching frequencies to lower wavenumbers. This is a powerful tool that indicates whether successful coordination to copper(II) has occurred (see IR spectra of ligand **9** and the $[\text{Cu}(\text{H}_2\text{O})(\text{C}_{12}\text{H}_{15}\text{N}_3)(\text{NO}_3)_2]$ complex in **Supplementary information** on CD).

4.3.1 Crystal and molecular structure of the $[\text{Cu}(\text{H}_2\text{O})(\text{C}_{12}\text{H}_{15}\text{N}_3)(\text{NO}_3)_2]$ complex

The asymmetric unit cell contains $[\text{Cu}(\text{H}_2\text{O})(\text{C}_{12}\text{H}_{15}\text{N}_3)(\text{NO}_3)_2]$, with 2-[3-(*tert*-butyl)-pyrazol-5-yl]pyridine (**9**), two nitrate ions and one water molecule bound to copper(II) (**Figure 4.2**). The complex crystallised in the monoclinic crystal system, space group $P2_1/c$. The crystallographic data and structure refinement details are summarised in **Table 4.3** at the end of the **Results and discussion** section.

The molecular structure of $[\text{Cu}(\text{H}_2\text{O})(\text{C}_{12}\text{H}_{15}\text{N}_3)(\text{NO}_3)_2]$ with the appropriate atom numbering is shown in **Figure 4.3**, with selected bond lengths and angles listed in **Table 4.1**. According to Miessler and Tarr,⁷ very little energy is needed to convert between a trigonal bipyramidal and square pyramidal geometry, which often leads to incorrect geometry assessments of five-coordinate complexes. Trigonal bipyramidal complexes can also undergo Berry pseudorotation, whereby axial monodentate ligands rotate toward the equatorial positions and two equatorial monodentate ligands rotate toward the axial positions.⁸ Conventional NMR studies cannot distinguish between the axial and equatorial ligands due to the rapid pseudorotation,

which renders the ligands chemically equivalent. Therefore, low-temperature NMR studies are needed to slow down the rate of pseudorotation, upon which distinctive axial and equatorial signals will appear. In our case, however, the rapid pseudorotation is restricted due to the presence of a bidentate aromatic amine ligand. To determine whether a complex is either trigonal bipyramidal or square pyramidal, one must determine the geometric parameter, tau (τ), which is only applicable to five-coordinate structures and can be calculated as follows (**Equation 38**):⁹

$$\tau = (\beta - \alpha)/60 \quad \text{Equation 38}$$

where β is the largest angle between any of the five ligand coordinates and α is the second largest angle. When $\tau = 1$, an ideal trigonal bipyramidal geometry is implied, while $\tau = 0$ implies an ideal square pyramidal structure. A tau value of $0 < \tau < 0.5$ signifies a pseudo square pyramidal structure, while $0.5 < \tau < 1$ signifies a pseudo trigonal bipyramidal geometry.⁹ We calculated τ and obtained the following result (**Equation 39**):

$$\tau = (178.19 - 150.01)/60 = 0.47 \quad \text{Equation 39}$$

This borderline tau value tends toward the square pyramidal geometry, which makes our complex a pseudo square pyramidal complex with ample trigonal bipyramidal character. One of these characteristic features is the elongated Cu1–O6 bond length at 2.217(2) Å, which is significantly longer than either of the other two Cu1–O bonds. The Cu1–O6 bond would be in the axial position and is slightly elongated due to Jahn-Teller distortion. In our case, having a short and long Cu1–O bond to two distinct nitrate ions, proves that our structure has square pyramidal character and gives credence to Jahn-Teller distortion.

The pseudo square pyramidal geometry of the [Cu(H₂O)(C₁₂H₁₅N₃)(NO₃)₂] complex, has the oxygen atom of the nitrate molecule (O6) occupying the axial position. The pyridyl and pyrazolyl nitrogen atoms (N1 and N2) along with the oxygen atoms of the second nitrate molecule and water molecule (O1 and O7) occupy the equatorial positions, forming the base of the pyramidal structure.

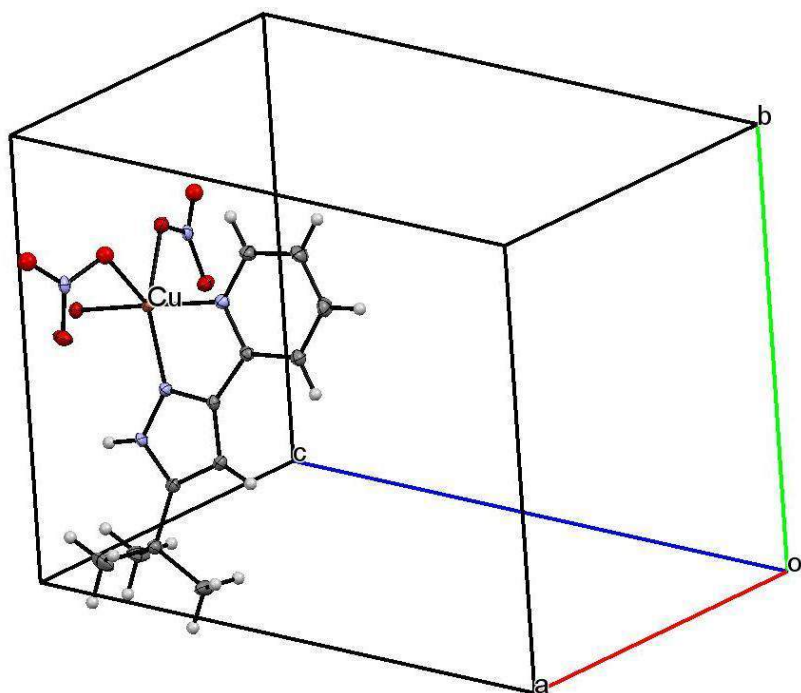


Figure 4.2: Asymmetric unit cell diagram of the $[\text{Cu}(\text{H}_2\text{O})(\text{C}_{12}\text{H}_{15}\text{N}_3)(\text{NO}_3)_2]$ complex (50% thermal ellipsoids).

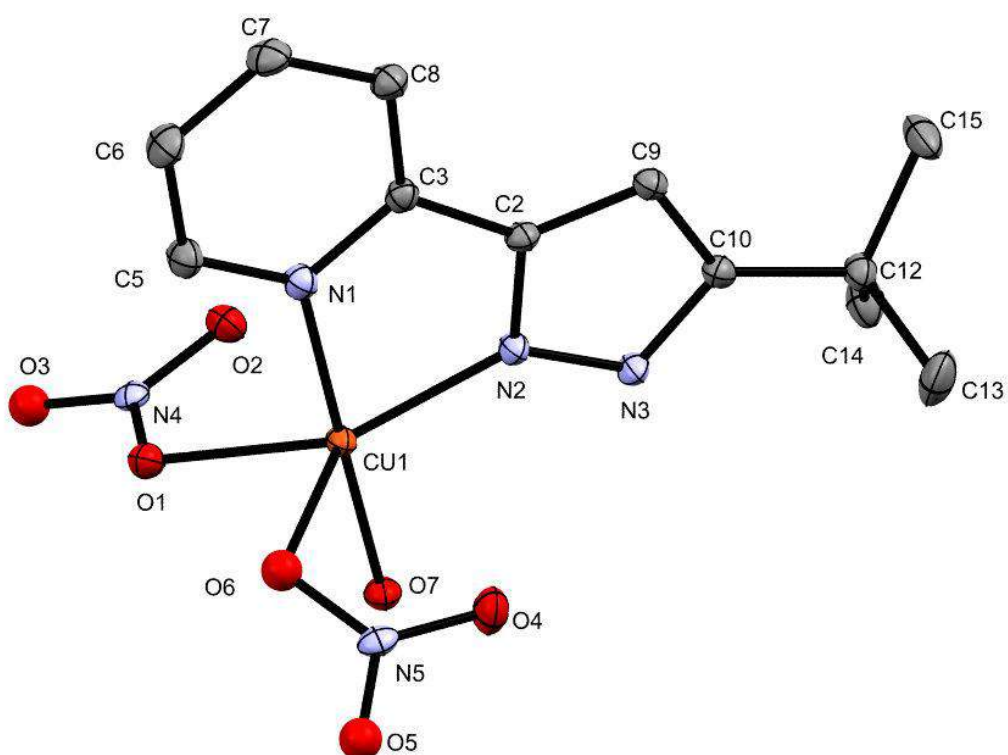


Figure 4.3: ORTEP diagram of the $[\text{Cu}(\text{H}_2\text{O})(\text{C}_{12}\text{H}_{15}\text{N}_3)(\text{NO}_3)_2]$ complex. Hydrogen atoms have been omitted for the sake of clarity (50% thermal ellipsoids).

Table 4.1: Selected bond lengths and angles for the $[\text{Cu}(\text{H}_2\text{O})(\text{C}_{12}\text{H}_{15}\text{N}_3)(\text{NO}_3)_2]$ complex.

Bond lengths (Å)		Bond angles (°)	
Cu1–N1	1.988(2)	N1–Cu1–N2	80.96(8)
Cu1–N2	1.987(2)	N1–Cu1–O1	91.90(7)
Cu1–O1	2.068(2)	N1–Cu1–O6	90.43(7)
Cu1–O6	2.217(2)	N1–Cu1–O7	178.19(7)
Cu1–O7	1.954(2)	N2–Cu1–O1	150.01(7)
		N2–Cu1–O6	125.10(8)
		N2–Cu1–O7	98.07(7)
		O1–Cu1–O6	83.75(7)
		O1–Cu1–O7	88.20(7)
		O6–Cu1–O7	91.37(7)

The pyridyl and pyrazolyl nitrogen atoms (N1 and N2), along with C2, C3 and Cu1 form a five-membered chelate ring. The bond lengths and angles are compared to the ideal bond lengths and angles of ethylenediamine in **Figure 4.4**.

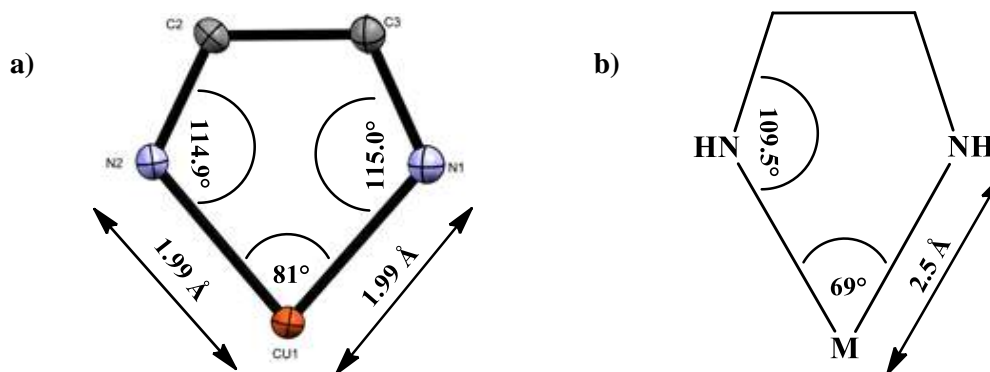


Figure 4.4: The bond lengths and angles of the five-membered chelate ring for **a)** $[\text{Cu}(\text{H}_2\text{O})(\text{C}_{12}\text{H}_{15}\text{N}_3)(\text{NO}_3)_2]$ compared to the idealised bond lengths and angles of **b)** ethylenediamine.

The C–N–Cu bond angles of the pyridyl pyrazolyl complex (**Figure 4.4a**) are slightly larger (114.9 and 115.0°) than the idealised bond angles of ethylenediamine (109.5°), which is somewhat surprising since the N–Cu–N bond angle is enlarged to 81°.⁵ Additionally, The Cu–N bond length is much shorter (1.99 Å) than the M–N bond of ethylenediamine (2.5 Å).⁵ This indicates that strong coordination bonds have formed between the pyridyl and pyrazolyl nitrogen atoms and the copper centre, which in turn forced the bond angles to be slightly larger compared to the idealised bond angles of ethylenediamine. Moreover, the bond angles and lengths of the pyridyl pyrazolyl complex accommodates the smaller copper(II) ion more efficiently, while the bond angles and lengths of ethylenediamine are better suited to fit larger metal ions. It

must also be noted that the carbon-nitrogen bonds of the pyridyl pyrazolyl complex have double bond character, while the carbon-nitrogen bonds of ethylenediamine have single bond character.

In this investigation, the average Cu–N bond distance of the complex was 1.99 Å. The average Cu–N bond distances reported by Zhilina *et al.*¹⁰ for similar complexes are 1.98 Å, while Henkelis *et al.*¹¹ reported average bond distances of 2.04 Å. The N1–Cu1–N2 bond angle (or bite angle) in this investigation is 80.96°, and compares well with the average bond angles of 79.35 and 78.52° reported by Zhilina *et al.*¹⁰ and Henkelis *et al.*¹¹ respectively. This shows that our findings are similar to those found in literature.

There are four symmetry elements present in the packing of this crystal lattice: an identity, a two-fold screw axis (green), an inversion centre (yellow) and a glide plane (purple) (**Figure 4.5**). See **Table 4.2** for more detailed information regarding the symmetry elements.

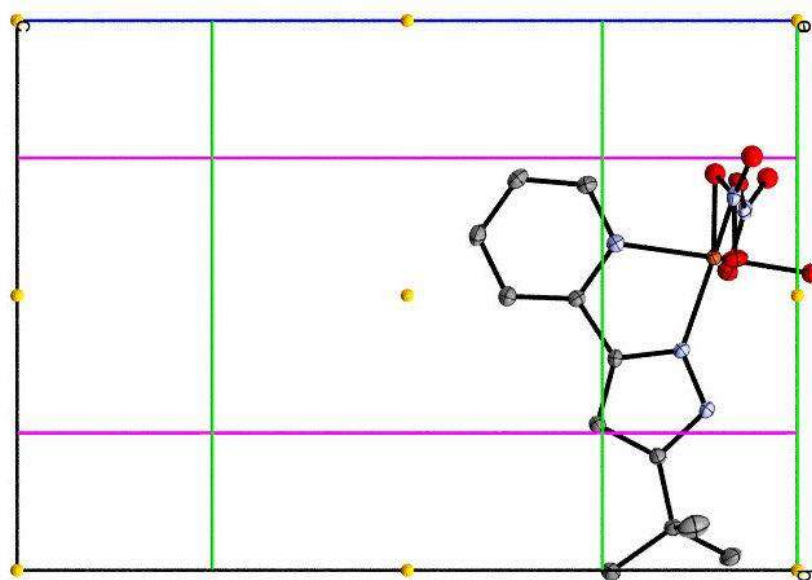


Figure 4.5: Symmetry elements present in an asymmetric unit cell along the a-axis. Green = two-fold screw axis, yellow = inversion centre and purple = glide plane.

Table 4.2: Detailed information regarding the symmetry elements and operators of the crystal structure of the $[\text{Cu}(\text{H}_2\text{O})(\text{C}_{12}\text{H}_{15}\text{N}_3)(\text{NO}_3)_2]$ complex. [Complimentary to **Figure 4.5** below]

Colour	Symmetry operation	Description	Detailed description	Order	Type
–	x, y, z	Identity	Identity	1	1
Green	$-x, \frac{1}{2}+y, \frac{1}{2}-z$	2-Fold screw axis	2-Fold screw axis with direction $[0, 1, 0]$ at $0, y, \frac{1}{4}$ with screw component $[0, \frac{1}{2}, 0]$	2	2
Yellow	$-x, -y, -z$	Inversion centre	Inversion at $[0, 0, 0]$	2	-1
Purple	$x, \frac{1}{2}-y, \frac{1}{2}+z$	Glide plane	Glide plane perpendicular to $[0, 1, 0]$ with glide component $[0, 0, \frac{1}{2}]$	2	-2

The crystal is held together by a network of intermolecular hydrogen bonds involving the oxygens of the nitrate ions and the hydrogens bound to the pyrazolyl nitrogen atoms (**Figure 4.6**). The packing diagram of the $[\text{Cu}(\text{H}_2\text{O})(\text{C}_{12}\text{H}_{15}\text{N}_3)(\text{NO}_3)_2]$ complex is represented by **Figures 4.7** and **4.8**.

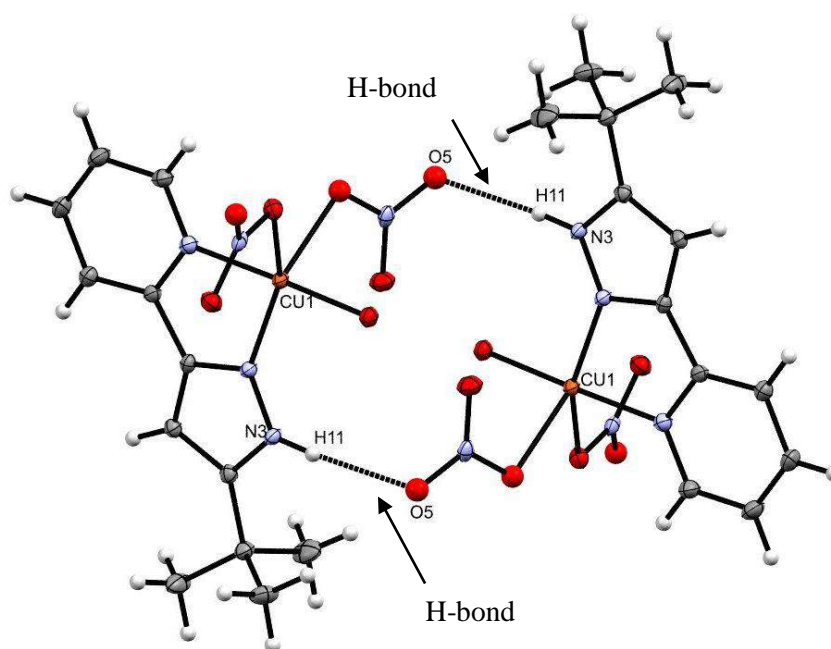


Figure 4.6: ORTEP diagram of the $[\text{Cu}(\text{H}_2\text{O})(\text{C}_{12}\text{H}_{15}\text{N}_3)(\text{NO}_3)_2]$ complex (50% thermal ellipsoids) showing a network of intermolecular hydrogen bonds.

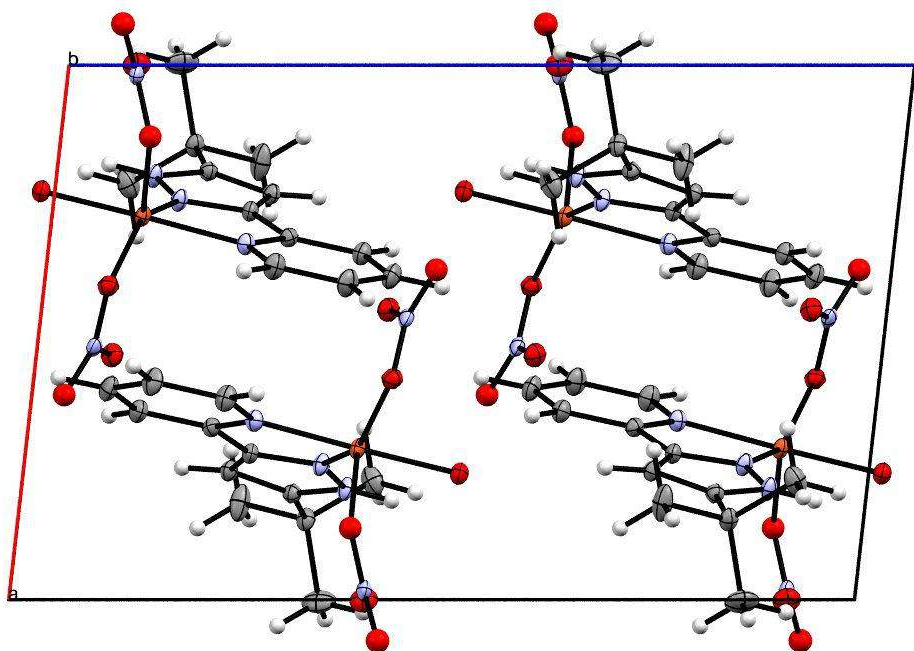


Figure 4.7: The packing diagram of the $[\text{Cu}(\text{H}_2\text{O})(\text{C}_{12}\text{H}_{15}\text{N}_3)(\text{NO}_3)_2]$ complex (50% thermal ellipsoids) along the a-axis.

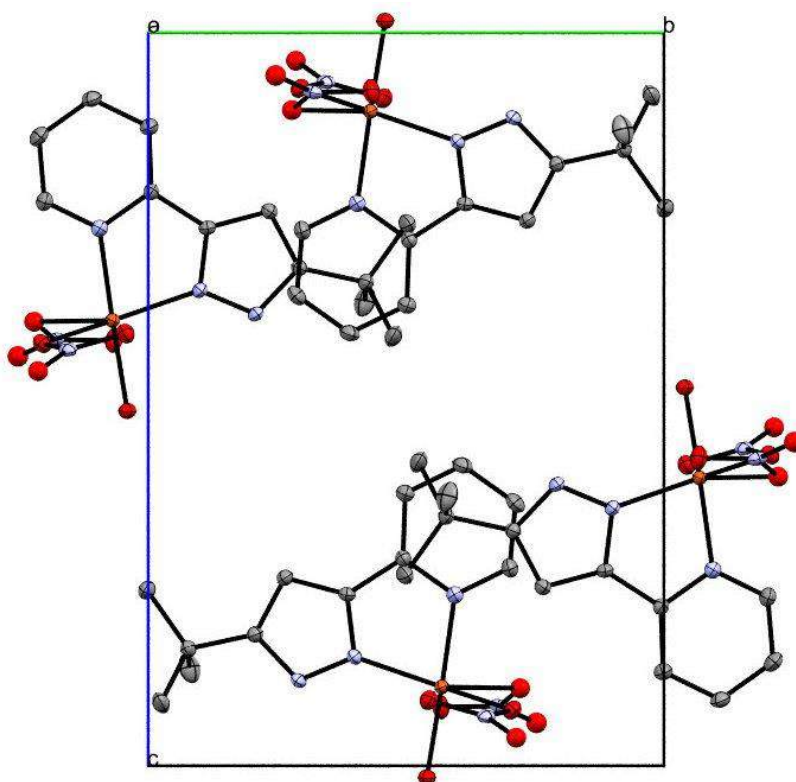


Figure 4.8: The packing diagram of the $[\text{Cu}(\text{H}_2\text{O})(\text{C}_{12}\text{H}_{15}\text{N}_3)(\text{NO}_3)_2]$ complex (50% thermal ellipsoids) along the b-axis. Hydrogen atoms have been omitted for the sake of clarity.

Table 4.3: Crystallographic data and structure refinement of the $[\text{Cu}(\text{H}_2\text{O})(\text{C}_{12}\text{H}_{15}\text{N}_3)(\text{NO}_3)_2]$ complex.

Compound	$[\text{Cu}(\text{H}_2\text{O})(\text{C}_{12}\text{H}_{15}\text{N}_3)(\text{NO}_3)_2]$
Empirical formula	$\text{C}_{12}\text{H}_{17}\text{CuN}_5\text{O}_7$
M_r ($\text{g}\cdot\text{mol}^{-1}$)	406.84
Temperature (K)	100
Crystal habit	Block
Crystal dimension (mm)	$0.16 \times 0.15 \times 0.11$
Crystal system	Monoclinic
Space group	$P 2_1/c$
a (\AA)	9.918(4)
b (\AA)	10.907(5)
c (\AA)	15.594(7)
α ($^\circ$)	90.00
β ($^\circ$)	96.428(6)
γ ($^\circ$)	90.00
μ (Mo $K\alpha$) (mm^{-1})	1.349
V (\AA^3)	1676.3(13)
Z , D_c (M , $\text{g}\cdot\text{m}^{-3}$)	4, 1.620
Index ranges	$-11 \leq h \leq 13, -13 \leq k \leq 14, -18 \leq l \leq 20$
Reflections collected	10402
Independent reflections	3624
Absorption correction	Multi-scan
Max/min. transmission	0.890/0.850
Refinement method	Full matrix least squares on F^2
Data/restraints/parameters	3889/0/214
$F(000)$	844
Final R indices [$I > 2\sigma(I)$]	0.0363, 0.1021
R indices (all data) R_1 , wR_2	0.0385, 0.1037
Goodness of fit on F^2	1.069

4.4 Conclusions

The crystal and molecular structure of the $[\text{Cu}(\text{H}_2\text{O})(\text{C}_{12}\text{H}_{15}\text{N}_3)(\text{NO}_3)_2]$ complex was successfully determined by single-crystal X-ray diffraction. Unfortunately, we only managed to grow crystals of this unique complex and still need to find alternative ways of growing nickel(II) and copper(II) crystals with ligands **1–10**. Ligand **9**, in conjunction with one water molecule and two nitrate ions, coordinated to copper(II) in a pseudo square pyramidal fashion, with an elongated axial bond and distorted equatorial bond angles that can be attributed to

the steric bulk of ligand **9**. Copper complexes often exhibit axial bond distortions (Jahn-Teller distortion), but in this case, it was not highly emphasised. One important aspect gained from this investigation is the fact that one ligand molecule coordinates to one copper(II) ion, denoting a ligand to metal ratio of 1:1, as we theorised in the extraction results (**Section 3.3, Chapter 3**).

Finally, we recognise that solvent extraction studies are “liquid studies”, while single-crystal X-ray diffractions are “solid state studies”, but since X-ray diffraction studies indicate the thermodynamically most stable arrangements, we expect the method of coordination to be present in solvent extraction studies as well.

4.5 References

- Schmidt, G. M. J. Photodimerization in the solid state. *Pure Appl. Chem.* **1971**, *27*, 647-678.
- Desiraju, G. R. *Crystal engineering: the design of organic solids*; Materials science monographs; Elsevier: Amsterdam, 1989; Vol. 54, pp 312.
- Wang, Q.; Yan, S.; Liao, D.; Jiang, Z.; Cheng, P.; Leng, X.; Wang, H. A novel three-dimensional cobalt (III) complex via hydrogen bonds: [Co(tacn)₂] (ClO₄)₃ (tacn = 1,4,7-triazacyclononane). *J. Mol. Struct.* **2002**, *608*, 49-53.
- Sumani, J. E. Y. *Synthesis and characterisation of macrocyclic ligands with hydroxyalkyl and thiol pendant arms tethered on 1,5,9-triazacyclododecane and their complex formation chemistry*, Stellenbosch University, Stellenbosch, South Africa, 2010.
- Martell, A. E.; Hancock, R. D. *Metal Complexes in Aqueous Solutions*; Modern Inorganic Chemistry; Plenum Press: New York, 1996, pp 253.
- Jahn, H. A.; Teller, E. Stability of Polyatomic Molecules in Degenerate Electronic States. I. Orbital Degeneracy. *Proc R Soc Lond A Math Phys Sci* **1937**, *161*, 220-235.
- Miessler, G. L.; Tarr, D. A. *Inorganic Chemistry*; Pearson Education, Inc.: USA, 2011; Vol. 1, p 350.
- Berry, S. R. Correlation of rates of intramolecular tunneling processes, with application to some group V compounds. *J. Chem. Phys.* **1960**, *32*, 933-938.
- Addison, A. W.; Rao, T. N.; Reedijk, J.; Van Rijn, J.; Verschoor, G. C. Synthesis, structure, and spectroscopic properties of copper(II) compounds containing nitrogen-sulphur donor ligands; the crystal and molecular structure of aqua[1,7-bis(N-methylbenzimidazol-2'-yl)-2,6-dithiaheptane]copper(II) perchlorate. *Journal of the Chemical Society, Dalton Transactions* **1984**, 1349-1356.
- Zhilina, E. F.; Chizhov, D. L.; Sidorov, A. A.; Aleksandrov, G. G.; Kiskin, M.; Slepukhin, P. A.; Fedin, M.; Starichenko, D. V.; Korolev, A. V.; Shvachko, Y. N.; Eremenko, I. L.; Charushin, V. N. Neutral tetranuclear Cu(II) complex of 2,6-di(5-trifluoromethylpyrazol-3-yl)pyridine: Synthesis, characterization and its transformation with selected aza-ligands. *Polyhedron* **2013**, *53*, 122-131.
- Henkelis, J. J.; Jones, L. F.; De Miranda, M. P.; Kilner, C. A.; Halcrow, M. A. Two heptacopper(II) disk complexes with a [Cu₇((μ-3-OH)₄(μ-OR)₂)⁸⁺ core. *Inorg. Chem.* **2010**, *49*, 11127-11132.

Chapter 5

Chapter summaries, concluding remarks and future work

5.1 Chapter summaries and concluding remarks

Chapter 1 initially informed the reader of the historic provenance of extractive metallurgy, which included both pyro- and hydrometallurgy. Important historical hydrometallurgical processes, such as the cyanidation- and Bayer processes, were mentioned with the focus on modern hydrometallurgical means for separating base metal ions from one another. Strong emphases were placed on the various types of extractants and the roles they played within a solvent extraction setup. This led to an intense study on ligand design for the sole purpose of optimising ligand-metal compatibility. Numerous factors that influence ligand-metal compatibility, such as the chelate effect and donor atom selection, were studied in depth. This ultimately led us to study the selective extraction of nickel(II) and copper(II) by means of bidentate aromatic amine ligands within a solvent extraction setup.

Chapter 2 gave a comprehensive outline regarding the synthesis of the imidazole- (**1–4**), methylpyrazole- (**5–7/7'**) and pyrazole-based pyridine ligands (**8–10**), complete with the appropriate characterisations. The characterisation techniques included FTIR (ATR), ¹H and ¹³C NMR, mass spectrometry and elemental analyses. The classic Debus-Radziszewski and Knorr mechanisms were studied in depth to explain the formation of unwanted side-products, whereafter certain reaction conditions were modified in an attempt to curb the formation of those side-products. This, however, was unsuccessful and led to the inevitable purification of the pyrazolyl ligands (**8–10**) by means of silica-based gravitational column chromatography. Ligands **7/7'** yielded interesting NMR spectra as a result of tautomerism and could not be separated by conventional separating techniques. Finally, for the first time we reported the synthesis of 2-(3-octyl-pyrazol-5-yl)pyridine (**10**), which to the best of our knowledge, is novel.

Chapter 3 represented the bulk of the laboratory work done for this thesis. At first, the reader was introduced to the term *synergism* and its significance in modern-day hydrometallurgy. This led to the justification of the use of a sulfonic acid synergist (SDBS) in this investigation by referring to studies done by Flett¹, Osseo-Asare and Keeney² and Okewole *et al.*³ The solvent extraction procedure was explained in great detail, followed by a study that determined the optimum synergist concentration for nickel(II) extractions. The optimum concentration was found to be 0.05 M, five times the metal ion concentration in solution. Ligands **1–10**, in conjunction with SDBS, exhibited excellent nickel(II) extraction results in the low to mid-70% range. The reader was subsequently introduced to competitive extraction studies – the principal focus point of this thesis. These studies showed that ligands **8** and **10** were exceptional copper(II) extractants in a competitive metal ion environment without the use of SDBS as synergist. Moreover, selectivity studies corroborated these findings with ligand **10** extracting 90.0 (± 0.4)% of copper(II) with a concentration a hundred times less than the other base metal ions present. In addition to competitive and selectivity studies, the reader was introduced to time-dependent studies, metal stripping studies as well as pH isotherm studies,

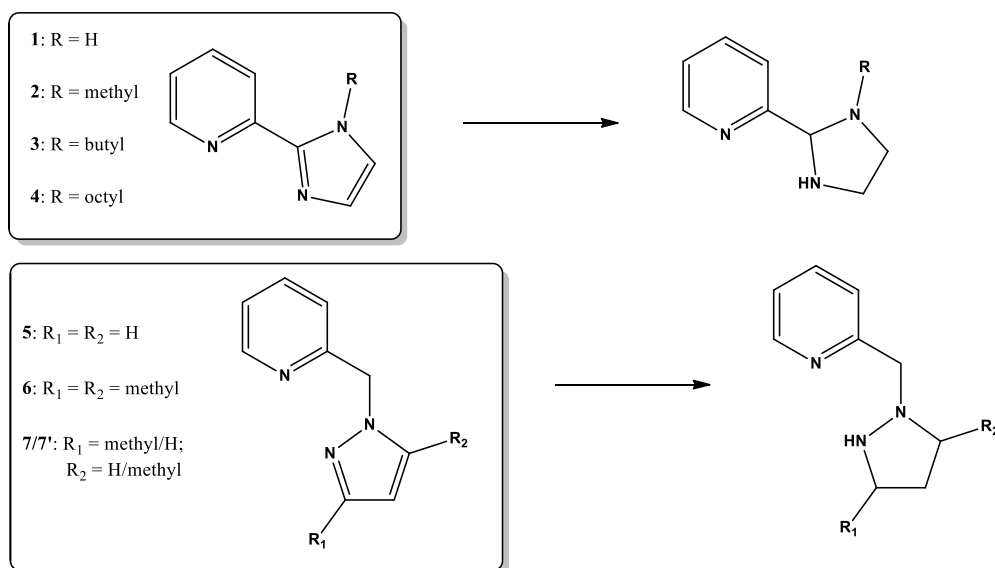
all of which provided valuable information regarding the extractive and stripping abilities of pyrazolyl ligands **8–10**.

Chapter 4 presented and discussed the crystal and molecular structure of the $[\text{Cu}(\text{H}_2\text{O})(\text{C}_{12}\text{H}_{15}\text{N}_3)(\text{NO}_3)_2]$ complex, which was prepared by refluxing 2-[3-(*tert*-butyl)-pyrazol-5-yl]pyridine (**9**) and copper(II) nitrate trihydrate in ethanol. Suitable crystals for X-ray diffraction analysis were obtained by means of slow solvent evaporation. The results clearly showed one ligand **9** molecule, one water molecule and two nitrate ions coordinating to copper(II) in a pseudo square pyramidal fashion. An elongated axial bond and distorted equatorial bond angles and lengths were observed, which was attributed to Jahn-Teller distortion and the ample trigonal bipyramidal character of the complex. It was also shown that the crystal structure of the $[\text{Cu}(\text{NO}_3)_2(\text{H}_2\text{O})(\text{C}_{12}\text{H}_{15}\text{N}_3)]$ complex was held together by a network of intermolecular hydrogen bonds. Most importantly, however, we learned that ligand **9** coordinated to copper(II) in a 1:1 ratio, thereby supporting our theory (**Section 3.3, Chapter 3**) that the solvent extraction of copper(II) occurred in a 1:1 metal-to-ligand ratio.

5.2 Future work

5.2.1 Structural modifications to enhance metal ion extractability

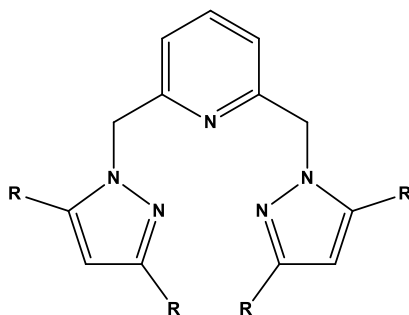
Upon observing the excellent copper(II) extraction results for ligands **8–10**, we propose that ligands **1–7/7'** be structurally modified to include an acidic/labile proton (**Scheme 5.1**). It should be noted, however, that the presence of an acidic proton would strip the imidazolyl- and pyrazolyl moieties of their aromaticity, resulting in the formation of non-flat imidazolidine and pyrazolidine moieties that have many more single bonds which allows the structures to be more flexible. The loss of aromaticity could have a negative impact on the extractive ability of the ligands, but still warrants further investigation none the less.



Scheme 5.1: Modification of ligands **1–7/7'** to include an acidic proton to strengthen the coordination bond to nickel(II) and copper(II).

Ligands **8–10** showed that an increase in the alkyl chain length increases the percentage extraction of both copper(II) and nickel(II). This can be exploited even further by substituting the current alkyl chains with alkyl chains containing between nine and fifteen consecutive carbons (C₉–C₁₅). Moreover, these hydrophobic alkyl chains can be altered in terms of their position on the imidazolyl- and pyrazolyl moieties as well to determine the effect it might have on the extractive ability of these ligands.

In 2006, Bouabdallah *et al.*⁴ reported the extraction of copper(II) by means of tripodal *N*-donor pyrazole ligands. By following their lead, ligands **5–7/7'** can structurally be modified to incorporate an additional pyrazole moiety tethered to the pyridine moiety (**Scheme 5.2**). This means the pyridine moiety will be flanked on either side by a pyrazole moiety, possibly resulting in an increase in metal ion extraction. Strong electron donating R-groups, such as alcohols (–OH), ethers (–OR) or amines (–NH₂) can impart electron density into the pyrazole ring and increase the extractive ability of such ligands, however, it is important to note that polar R-groups might impart hydrophilicity to the ligand.



Scheme 5.2: The suggested methylpyrazolyl tripodal extractant with possible electron donating R-groups.

5.2.2 Modifications to the solvent extraction setup

In conjunction with SDBS, ligands **1–7/7'** exhibited impressive extractive abilities for nickel(II) and copper(II), which warrants further investigation into varying the ligand concentrations. Ligands **8–10**, in the presence of SDBS, did not yield satisfactory results, however, and should be used as ligands on their own and not in conjunction with a sulfonic acid synergist. Another possible point of difference for future studies could include the change of sulfonic acid synergists to synergists with less of a surfactant-like nature to prevent the formation of micelles within a solvent extraction setup.

Competitive extraction studies were rather successful in pointing out the selectivity of ligands **8** and **10** for copper(II) in a mixed base metal ion environment. The expansion of the base metal ion library to include divalent metal ions such as Cr²⁺, Mn²⁺ and Fe²⁺ can particularly be insightful regarding the true selectivity of ligands **8** and **10** toward copper(II).

Metal stripping studies can greatly be improved by lowering the pH to approximately 0. This will ensure that cationic competition for the ligand binding site is fierce, resulting in the release of metal ions into the aqueous phase and thereby facilitating the process of metal ion recovery.

5.2.3 Extraction of nickel(II) and copper(II) using imidazolyl- and pyrazolyl ligands on resin, silica-based and nanofibrous polymeric supports.

The use of resin, silica-based and nanofibrous polymeric supports for the selective extraction of metal ions is a relatively new development in the hydrometallurgy arena.

The selective extraction of nickel(II) and copper(II) by means of pyrazolyl- and imidazolyl ligands tethered to a nanofibrous polymeric backbone is a feasible modern hydrometallurgical novelty worth pursuing. We suggest the use of poly(acrylonitrile) (PAN) as the backbone due to its excellent stability at low pH. This is important since the PAN nanofibrous support must be able to withstand extremely acidic environments during metal ion stripping studies. It is also important that PAN nanofibers be recyclable. To the best of our knowledge, pyrazolyl ligands have not yet been tethered to nanofibers, however, a sole example in literature of 2-(2'-pyridyl)imidazole tethered to PAN nanofibers have been reported,⁵ indicating a possible gap in the discipline of hydrometallurgy. We suggest the expansion of the imidazolyl- and pyrazolyl ligand library with the ultimate aim of tethering them to PAN nanofibers for the selective extraction of copper(II) and nickel(II).

The extraction of nickel(II) and copper(II) by means of resin systems has not been fully explored either. Leinonen *et al.*⁶ and Zainol *et al.*⁷ did, however, use iminodiacetic acid chelating resins, *Chelex 100* and *Amberlite IRC 748* respectively, for the purification of aqueous streams containing base metal ions. For future work we suggest these examples to be used as references to synthesise novel resin systems for the selective extraction of copper(II) and nickel(II).

The use of silica supported chelating adsorbents for the removal of heavy atoms from aqueous solutions is somewhat of an under-researched discipline. Sirola *et al.*⁸ studied the removal of copper(II) and nickel(II) from concentrated zinc sulfate solutions using two different silica-supported chelating adsorbents (WP-1 and CuWRAM). The WP-1 adsorbent contained branched poly(ethyleneimine) anchored to silica, while CuWRAM had anchored polyamine that was further functionalized with 2-(aminomethyl)pyridine groups. We suggest the use of such systems as future blue-prints to develop novel systems to improve the extraction of nickel(II) and copper(II).

5.2.4 Computational modelling methods

To further probe the metal-ligand interaction, density functional theory (DFT) calculations can be carried out to determine, by means of quantum analyses, whether a metal-ligand combination is likely to form a complex or not. This can be achieved by calculating the binding energies (ΔU_b) of the metal-ligand system which will give us insight into the strength of the coordination bonds.⁹ Thermodynamic considerations must be included as well to ensure that the results are accurate and trustworthy.

5.3 References

1. Flett, D. S. SOLVENT EXTRACTION. *Chem Ind (London)* **1977**, 223-224.
2. Osseo-Asare, K.; Keeney, M. E. Sulfonic acids: Catalysts for the liquid-liquid extraction of metals. *Sep. Sci. Technol.* **1980**, *15*, 999-1011.
3. Okewole, A. I.; Magwa, N. P.; Tshentu, Z. R. The separation of nickel(II) from base metal ions using 1-octyl-2-(2'-pyridyl)imidazole as extractant in a highly acidic sulfate medium. *Hydrometallurgy* **2012**, *121-124*, 81-89.
4. Bouabdallah, I.; Zidane, I.; Hacht, B.; Touzani, R.; Ramdani, A. Liquid-liquid extraction of copper(II), cadmium(II) and lead(II) using tripodal *N*-donor pyrazole ligands. *Arkivoc* **2006**, *2006*, 59-65.
5. Ndayambaje, G.; Laatikainen, K.; Laatikainen, M.; Beukes, E.; Fatoba, O.; van der Walt, N.; Petrik, L.; Sainio, T. Adsorption of nickel(II) on polyacrylonitrile nanofiber modified with 2-(2'-pyridyl)imidazole. *Chem. Eng. J.* **2016**, *284*, 1106-1116.
6. Leinonen, H.; Lehto, J. Ion-exchange of nickel by iminodiacetic acid chelating resin Chelex 100. *React Funct Polym* **2000**, *43*, 1-6.
7. Zainol, Z.; Nicol, M. J. Ion-exchange equilibria of Ni²⁺, Co²⁺, Mn²⁺ and Mg²⁺ with iminodiacetic acid chelating resin Amberlite IRC 748. *Hydrometallurgy* **2009**, *99*, 175-180.
8. Sirola, K.; Laatikainen, M.; Lahtinen, M.; Paatero, E. Removal of copper and nickel from concentrated ZnSO₄ solutions with silica-supported chelating adsorbents. *Separation and Purification Technology* **2008**, *64*, 88-100.
9. Carson, I.; MacRuary, K. J.; Doidge, E. D.; Ellis, R. J.; Grant, R. A.; Gordon, R. J.; Love, J. B.; Morrison, C. A.; Nichol, G. S.; Tasker, P. A.; Wilson, A. M. Anion Receptor Design: Exploiting Outer-Sphere Coordination Chemistry to Obtain High Selectivity for Chloridometalates over Chloride. *Inorg. Chem.* **2015**, *54*, 8685-8692.